PB89-159032

Validation Testing of New Mechanisms with Outdoor Chamber Data. Volume 1 Comparison of CB4 and CAL Mechanisms

North Carolina Univ. at Chapel Hill

Prepared for

Environmental Protection Agency
Research Triangle Park, NC

Jan 89

U.S. Department of Commerce
National Technical Information Service
NTIS

TECHNICAL REPORT DATA
(Please read Instructions on the reverse before completing)

1. REPORT NO. EPA/600/3-89/010a	**2.**	**3. RECIPIENT'S ACCESSION NO.** PB89 159032/AS
4. TITLE AND SUBTITLE VALIDATION TESTING OF NEW MECHANISMS WITH OUTDOOR CHAMBER DATA, VOLUME 1: COMPARISON OF CB4 AND CAL MECHANISMS		**5. REPORT DATE** January 1989 **6. PERFORMING ORGANIZATION CODE**
7. AUTHOR(S) H. E. Jeffries, K. G. Sexton, J. R. Arnold, J. L. Li		**8. PERFORMING ORGANIZATION REPORT NO.**
9. PERFORMING ORGANIZATION NAME AND ADDRESS School of Public Health University of North Carolina Chapel Hill, North Carolina 27514		**10. PROGRAM ELEMENT NO.** A101/B/63/20/6031 (FY-88) **11. CONTRACT/GRANT NO.** Cooperative Agreement 813107
12. SPONSORING AGENCY NAME AND ADDRESS Atmospheric Research & Exposure Assessment Lab. Office of Research and Development U.S. Environmental Protection Agency Research Triangle Park, North Carolina 27711		**13. TYPE OF REPORT AND PERIOD COVERED** Final (4/86 - 9/88) **14. SPONSORING AGENCY CODE** EPA 600/09

15. SUPPLEMENTARY NOTES

16. ABSTRACT

The UNC smog chamber data base was used to compare the performance of two state of the science photochemical mechanisms: the Carbon Bond four Mechanism (CB4) and the Carter, Atkinson, Lurmann Mechanism (CAL). Although the mechanism behaved differently, both mechanisms showed good agreement with ozone and oxides of nitrogen chamber data. The agreement for other products such as formaldehyde and peroxyacetylnitrate were not as good. Neither mechanism, however, was overall superior to the other in fitting chamber data. The two mechanisms predicted very similar VOC control requirements for the standard SIP-type cases. In SIP-like sensitivity analyses, CB4 was more sensitive to decreasing hydrocarbon and ozone aloft and to decreasing the temperature, giving somewhat lower control requirements than CAL at the extreme conditions. Although problems remain in the performance of both mechanisms, we do not believe that it is possible to choose between them on the basis of performance in either fitting chamber data or in predicting control calculations.

the authors

17. KEY WORDS AND DOCUMENT ANALYSIS

a. DESCRIPTORS	b. IDENTIFIERS/OPEN ENDED TERMS	c. COSATI Field/Group

18. DISTRIBUTION STATEMENT RELEASE TO PUBLIC	**19. SECURITY CLASS** *(This Report)* UNCLASSIFIED	**21. NO. OF PAGES** 298
	20. SECURITY CLASS *(This page)* UNCLASSIFIED	**22. PRICE** MF PC$28.95/$6.95

EPA Form 2220-1 (9-73)

PB89-159032

EPA/600/3-89/010a
January 1989

Validation Testing of New Mechanisms with Outdoor Chamber Data

Volume 1: Comparison of CB4 and CAL Mechanisms

H. E. Jeffries,K. G. Sexton,
J. R. Arnold, and J.L. Li

Department of Environmental Sciences
and Engineering
School of Public Health
University of North Carolina
Chapel Hill, N.C. 27514

Cooperative Agreement 813107

Project Officer
Marcia Dodge

Atmospheric Chemistry and Physics Division
Atmospheric Sciences Research Laboratory
Research Triangle Park, N.C. 27711

ATMOSPHERIC RESEARCH AND EXPOSURE ASSESSMENT LABORATORY
OFFICE OF RESEARCH AND DEVELOPMENT
U.S. ENVIRONMENTAL PROTECTION AGENCY
RESEARCH TRIANGLE PARK, NC 27711

REPRODUCED BY
U.S. DEPARTMENT OF COMMERCE
NATIONAL TECHNICAL INFORMATION SERVICE
SPRINGFIELD, VA. 22161

DISCLAIMER

This report has been reviewed by the U. S. Environmental Protection Agency, and approved for publication. Approval does not signify that the contents necessarily reflect the views and policies of the U. S. Environmental Protection Agency, nor does mention of trade names or commercial products constitute endorsement or recommendation for use.

Abstract

The UNC smog chamber data base was used as a basis to compare the performance of two state of the science photochemical mechanisms: Carbon Bond Four Mechanism (CB4) and the Carter, Atkinson, Lurmann Mechanism (CAL). A number of tasks had to be performed before such comparisons could be conducted. These included: comparing and reconciling the thermal rate constants used in the two mechanisms; re-assessing the photolytic rates for the UNC chamber and producing a new radiation transfer model; performing new experiments with new instrumentation for formaldehyde and hydrogen peroxide to confirm older test data; and analyzing three years of ambient speciated hydrocarbon data to determine the default composition for use in EKMA comparisons. A series of side- by-side chamber experiments were modeled with both mechanisms to assess their performance for specific chemistry. Then a series of State Implementation Plan EKMA calculations were performed for a range of conditions with both mechanisms.

The rate constant comparison task and the new experiments for formaldehyde are reported in Volume 1; the hydrocarbon analysis task is reported in Volume 2; and the radiation transfer model and photolytic rate calculations are reported in Volumes 3 and 4. Chamber comparisons and EKMA calculations are reported in Volume 1.

Although there were differences between them, both mechanisms showed good agreement with ozone and oxides of nitrogen chamber data and in most cases, with the new photolytic rates, showed fits better than those in the original development efforts. The agreement for other products such as formaldehyde and peroxyacetylnitrate were not as good. Neither mechanism, however, was overall superior to the other in fitting chamber data.

The two mechanisms predicted very similar VOC control requirements for the standard SIP-type cases. In SIP-like sensitivity analyses, CB4 was more sensitive to decreasing hydrocarbon and ozone aloft and to decreasing the temperature, giving somewhat lower control requirements than CAL at the extreme conditions.

Although problems remain in the performance of both mechanisms, we do not believe that it is possible to choose between them on the basis of performance in either fitting chamber data or in predicting control calculations.

Contents

1 Introduction 1

Background 1

Purpose and Work Performed 2

Mechanism Testing 4

The Rest of Volume 1 7

2 Mechanisms 10

Mechanism Sources 10

Implementation of Mechanisms 11

3 ICRS Reconciliation 33

Procedure 33

Simulations Using Original Rates 35

Comparison of Rates 38

Comparison of Mass Throughput 41

Arrhenius and Other Rate Expressions 44

Simulations Using New Rates 46

Responses from Model Developers 56

4 Chamber Simulations 70

Developer's Fits to Experimental Data 70

Factors that Effect Chamber Fits 76

Demonstration Using Dual Experiments 78

Summary 200

Tables

1. The Carter, Atkinson, Lurmann Mechanism Used in Chamber Simulations 13
2. The Carter, Atkinson, Lurmann Mechanism Used in OZIPM Simulations 20
3. The Carbon Bond Four, Version One Mechanism Used in Chamber Simulations 24
4. The Carbon Bond Four, Version Two Mechanism Used in Chamber Simulations . . . 27
5. CAL Inorganic and HCHO Mechanism 35
6. CBX Inorganic and HCHO Mechanism 36
7. Comparison of Rate Constants 37
8. Integrated Rates and Ratio for 1.0 ppm HCHO and 0.3 ppm NO_x 40
9. Mass Balance for 1.0 ppm HCHO, Original Rates 42
10. Reactant Mass Flow for 1.0 ppm HCHO, Original Rates. 43
11. Integrated Reaction Rates for 1.0 ppm HCHO, Modified Rates 48
12. Mass Balance for 1.0 ppm HCHO, Modified Rates 49
13. Reactant Mass Flow for 1.0 ppm HCHO, Modified Rates 50
14. Integrated Reaction Rates for 1.0 ppm HCHO, Reduced Reactions 53
15. Mass Balance for 1.0 ppm HCHO, Reduced Reactions 54
16. Reactant Mass Flow for 1.0 ppm HCHO, Reduced Reactions 55
K. Comparison of Rate Constants 57
17. Order of Presentation of Experiments 80
18. A Network Ordering of Experiments 81
19. Common initial condition input files. 81
20. July 8, 1986 CB4 Initial Condition Simulation File 84
21. August 4, 1979 Initial Condition Simulation File 92
22. August 23, 1978 Initial Condition Simulation File 100
23. July 9, 1986 Initial Condition Simulation File 105
24. July 30, 1978 Initial Condition Simulation File 112
25. July 13, 1986 Initial Condition Simulation File 118
26. October 11, 1984 Initial Condition Simulation File 127
27. September 27, 1983 Initial Condition Simulation File 136
28. June 27, 1984 Initial Condition Simulation File 141
29. June 26, 1984 Initial Condition Simulation File 147
30. August 31, 1981 Initial Condition Simulation File 152
31. August 5, 1984 Initial Condition Simulation File 158
32. August 6, 1984 Initial Condition Simulation File 164
34. August 8, 1984 Initial Condition Simulation File 173
37. August 22, 1984 Initial Condition Simulation File 185
38. September 1, 1984 Initial Condition Simulation File 192
39. September 2, 1984 Initial Condition Simulation File 197
40. SIP Cases: Basic Meteorological Input Conditions 211
41. SIP Cases: Basic Chemical Input Conditions 213
42. SIP Cases: Control Predicted 214
43. Conditions in the SIP Sensitivity Cases. 230
44. Reactivity Variations on a SIP Case. 230
45. Temperature Variations on a SIP Case. 231
46. July 2 Intercomparison of Calibration Sources. 259

47. July 16 Multi-Group Measurements of Four Calibration Sources. 263
48. Non-linear Correction Curve for Texas Data. 266
49. HCHO Measurements in July 16 Dual Experiment. 270

Figures

1. Ozone Maximum Scatter Diagram for CAL Mechanisms. 6
2. Schematic examples of run networks. 8
3. Comparison of Predictions from UNC Version of Mechanisms With Author's OZIPM Outputs 12
4. Comparison of CAL and CBX, Original Rates. 39
5. Comparison of CBX and CAL, Modified Rates 47
6. Comparison of CBX and CAL, Reduced Reactions 52
7. Errors in Mechanisms Predictions 71
8. Comparison of Side-to-Side Ozone. 74
9. Comparison of Side-to-Side Ozone Differences (3D). 75
10. July 8, 1986 0.5 ppm and 1.0 ppm Formaldehyde, Data 83
11. July 8, 1984, Standard Carter Wall Model 85
12. July 8, 1984, Standard Carter Wall Model 86
13. July 8, 1984, No Wall Model 87
14. July 8, 1984, No Wall Model 88
15. July 8, 1984, Killus Wall Model 89
16. August 4, 1979 0.88 ppmC Ethylene and 0.5 ppm Formaldehyde, Data 91
17. Aug. 4, 1979, Standard Carter Wall Model 93
18. Aug. 4, 1979, Standard Carter Wall Model 94
19. Aug. 4, 1979, HONO and Carter Wall Model 95
20. Aug. 4, 1979, HONO and Carter Wall Model 96
21. Aug. 4, 1979, Integrated HO from Walls 97
22. August 23, 1978, Matched Ethylene, Data 99
23. August 23, 1978, Standard Carter Wall Model. 101
24. August 23, 1978, Standard Carter Wall Model. 102
25. July 9, 1986 Delta Ethylene, Data 104
26. July 9, 1986, Delta ethylene 106
27. July 9, 1986, Delta ethylene 107
28. July 9, 1986, Delta ethylene 108
29. July 9, 1986, Delta ethylene 109
30. July 30, 1978 Ethylene vs Propylene, Data 111
31. July 30, 1978, Standard Carter Wall Model 113
32. July 30, 1978, Standard Carter Wall Model 114
33. July 30, 1978, 1.7 times Carter Wall Model 115
34. July 30, 1978, 1.7 times Carter Wall Model 116
35. July 13, 1986 Ethylene vs Propylene, Data 117b
36. July 13, 1986, Standard Carter Wall Model 119
37. July 13, 1986, Standard Carter Wall Model 120
38. July 13, 1986, No Wall Model 121
39. July 13, 1986, No Wall Model 122
40. July 13, 1986, Half Carter Wall Model 123
41. July 13, 1986, Half Carter Wall Model 124
42. October 11, 1984 2.9 ppmC Ethylene and 2.3 ppmC Propylene, Data 126
43. October 11, 1984, Standard Carter Wall Model 128

44. October 11, 1984, Standard Carter Wall Model 129
45. October 11, 1984, Standard Carter Wall Model 130
46. October 11, 1984, Standard Carter Wall Model 131
47. October 11, 1984, Standard Carter Wall Model 132
48. October 11, 1984, Standard Carter Wall Model 133
49. September 27, 1983 1-Butene vs. T-2-butene, Data 135
50. September 27, 1983, Standard Carter Wall Model 137
51. September 27, 1983, Standard Carter Wall Model 138
52. June 27, 1984 m-Xylene vs. Toluene, Data 140
53. June 27, 1984, Standard Carter Wall Model 142
54. June 27, 1984, Standard Carter Wall Model 143
55. June 27, 1984, Standard Carter Wall Model 144
56. June 26, 1984 o-Xylene and 2.95 ppmC m-Xylene, Data 146
57. June 26, 1984, Standard Carter Wall Model 148
58. June 26, 1984, Standard Carter Wall Model 149
59. June 26, 1984, Standard Carter Wall Model 150
60. August 31, 1981 SIMMIX vs. UNCMIX, Data 151a
61. August 31, 1981, Standard Carter Wall Model 154
62. August 31, 1981, Standard Carter Wall Model 155
63. August 5, 1984 Delta HC SYNAUTO, Data 157
64. August 5, 1984, Standard Carter Wall Model 160
65. August 5, 1984, Standard Carter Wall Model 161
66. August 6, 1984 Delta HC SYNAUTO, Data 163
67. August 6, 1984, Standard Carter Wall Model 166
68. August 6, 1984, Standard Carter Wall Model 167
69. August 7, 1984 SynAuto vs. SynAuto/SynMeth, Data 169
70. August 7, 1984, Standard Carter Wall Model 170
71. August 8, 1984 SynAuto vs. SynAuto/SynMeth, Data 172
72. August 8, 1984, Standard Carter Wall Model 175
73. August 8, 1984, Standard Carter Wall Model 176
74. August 9, 1984 SynAuto vs. SynAuto/SynMeth, Data 178
75. August 9, 1984, Standard Carter Wall Model 179
76. June 26, 1985, Delta HC SynUrban, Data 181
77. June 26, 1985, Standard Carter Wall Model 182
78. August 22, 1984, SynUrban vs. SynUrban/SynMeth, Data 184
79. August 22, 1984, Standard Carter Wall Model 187
80. August 22, 1984, Standard Carter Wall Model 188
81. August 22, 1984, Standard Carter Wall Model 189
82. September 1, 1984, SynUrban vs. SynUrban/SynMeth Data 191
83. September 1, 1984, Standard Carter Wall Model 194
84. September 2, 1984, Delta HC SynUrban, Data 196
85. September 2, 1984, Standard Carter Wall Model 199
86. Base Case Philadelphia SIP Trajectory Calculation. 204
87. CB4 and CAL Ozone Surfaces 205
88. CB4 and CAL Isopleths (bottom) and CB4-CAL (top). 206
89. Ozone As A Function Of HC For CB4 and CAL For Three HC Compositions. 208
90. SIP Cases: Surface Temperature Profiles 212
91. Comparison of VOC Controls in Selected SIP Scenarios 215

92a. Ozone Isopleth for Nashville. 217
92b. NO_x Isopleth for Nashville. 218
92c. PAN and HCHO Isopleth for Nashville. 219
93a. Ozone Isopleth for Tulsa. 220
93b. NO_x Isopleth for Tulsa. 221
93c. PAN and HCHO Isopleth for Tulsa. 222
94a. Ozone Isopleth for Washington. 223
94b. NO_x Isopleth for Washington. 224
94c. PAN and HCHO Isopleth for Washington. 225
95a. Ozone Isopleth for New York. 226
95b. NO_x Isopleth for New York. 227
95c. PAN and HCHO Isopleth for New York. 228
96. Reactivity Variations on a SIP Case. 232
97. Temperature Variations on a SIP Case. 233
98. Differences in Control Predictions vs. 1400 LDT Temperature 236
99. Helicopter soundings above St. Louis 240
100. Average Temperature profiles over Oak Ridge. 241
101. Washington DC SIP Temperature Profile and Average Box Temperature. 243
102. CEA Calibration Factors from Three UNC Sources 252
103. Separate Calibration Factors from Three UNC Sources. 253
104. NCAR determinations of standard HCHO stock solution concentration. 254
105. NCAR calibration curves for selected days in the UNC study. 256
106. Effect of small changes in fitted non-linear calibration curve on NCAR HCHO measurements. 257
107. July 2 intercomparison of calibration sources. 260
108. Unisearch calibration and group averaged calibration applied to July 8 HCHO data. 262
109. Measurements of Four Calibration Sources 264
111. NO_x, O_3, and Ethylene Profiles For Dual Experiment. 268
112. Formaldehyde Profiles For Dual Experiment. 269
113. Measurements at key events in July 16 dual experiment. 270
114. July 8, 1986 Chamber Data. 273
115. Chamber Data. 274
116. Chamber Data 275
117. Chamber Data. 276
118. Hydrogen Peroxide Chamber Data. 279
119. Hydrogen Peroxide Chamber Data. 280

Acknowledgements

We are indebted to William Carter, University of California, Riverside and Mike Gery, System Applications, Inc. for their time and cooperation in sharing their mechanisms development work. Without this contribution, this project would not have been possible. We also thank Jim Killus for discussions on wall effects.

We thank Robert Arnts at EPA for making available a carbon monoxide monitor during the experimental portion of this project.

We thank Richard Kamens for many helpful discussions and suggestions.

We also thank Ken Daisy, student at UNC, for his careful efforts in performing quality assurance activities on all of our data files.

1

Introduction

Background

Photochemical kinetics models, which integrate diverse kinetics information into a unified description of urban atmospheric chemistry, are central components in the U.S. Environmental Protection Agency's (EPA) method for computing control requirements for organic emissions needed to meet Federal Air Quality Standards for ozone[1]

The EPA has a long standing program (about 10 years) to develop accurate chemical mechanisms for use in these urban models. One part of this program produced kinetics data needed to specify rate constants for critical reactions in the mechanisms. One part of the program produced smog chamber data from several chambers, both indoors and outdoors, needed to determine how the individual kinetic data pieces fitted together. Another part of the program, using experimental information from the other program elements, theory, and model construction techniques, produced the actual mechanisms.

Over the life of this program, two basic mechanism construction approaches have evolved: the Carbon Bond approach,[2,3,4] with its emphasis on conservation of carbon mass, and the surrogate approach[5,6,7] with its emphasis on quasi-explicit chemistry. Neither approach has a clear theoretical advantage. As stated by Carter,[8]

> "Because of the large numbers of species and chemical reactions occurring in real atmospheres, and because of computer constraints and data limitations, any practical chemical mechanism to be used for control strategy evaluation must necessarily contain approximations and condensations of species and reactions in order to make the mechanism and its data input requirements of manageable size."

Both mechanism development approaches require that choices be made between detail and accuracy, and both may have very definite individual advantages.

Having two mechanisms based on different design principles and constructed by different groups is a distinct advantage. Each mechanism is so complex, and involves so many interconnected feedback paths, that it is sometimes very difficult to understand why a mechanism predicts a certain result. Occasionally the predictions are even "counter-intuitive." Having a second mechanism that is based upon a different principle of simplification helps determine if the unexpected result might be an artifact of the simplification process and therefore calling for more work or simulations, or if it might be more associated with fundamentals of complex chemistry, thus calling for consideration in policy making.

Having two mechanism, however, immediately invites comparison. The comparison process can show that some assumptions made by one development group are better than other assumptions made by the other developer. Or it might reveal that differences in predictions between the two mechanisms are due to mistakes made by the developers. This is not to fault the developers: the process of mechanism development and testing is extremely complex and many parts require tedious attention to a myriad of details. Sometimes what might be learned is that chamber data were not correctly transferred or were inadequately documented or are just plain wrong. Because different assumptions have been made, one mechanism approach might be superior to the other in certain circumstances, *e.g.*, urban, high ozone cases might be better handled by one, while low level rural cases might be better handled by the other.

Purpose and Work Performed

The primary purpose of this co-operative agreement was to conduct an intercomparison of two independently developed photochemical kinetics mechanisms for oxidants: the Carbon Bond Mechanism-Version IV (CB4) and the Carter, Atkinson, Lurmann Mechanism (CAL). In addition to comparing the mechanisms' predictions with each other, they were to be compared with outdoor smog chamber data to access, by some measure, the "goodness of fit" between the mechanisms and experimental measurements. It was not the purpose of this work to repeat the chamber testing programs that had been conducted by each mechanism developer, but rather, as time allowed, to examine (and perhaps to reconcile) issues that prevented direct comparison, or that resulted in prediction differences between the two EPA-funded mechanisms. It was already clear from the developers own testing that there was a "good" quality of overall fit of the mechanism predictions to the chamber data as measured by simple statistics. In assessing the performance of his own mechanism, one factor that each developer had neglected, however, was the side-to-side nature of the UNC chamber data base. In our comparison work, we will emphasize this side-to-side factor.

The sensitivity and accuracy of response to input parameters including thermal and photolytic rates of reaction, HC composition, and various treatments of wall radicals were domains for investigation. Of particular concern for control applications were the mechanisms' responses for $\Delta O_3/\Delta HC$ and O_3 production as a function of HC composition. In the latter case, the two mechanism developers each suggested a default urban composition. Further, the Office of Air Quality Planning and Standards had produced a default urban composition for CB4.[9] We found these to be sufficiently different (and inconsistent) so as to result in different predictions. During our project a new urban hydrocarbon (HC) speciated data base became available,[10] and we performed an analysis of these data and developed new mechanism HC speciations that were consistent. These results are reported in Volume 2 of this report.

In addition to the model testing, approximately two months of outdoor chamber experiments were conducted during the first summer of the program. The primary purpose of the chamber experiments was to provide a test situation for the intercomparison of five formaldehyde (HCHO) and four hydrogen peroxide (H_2O_2) measurement methods in typical smog chamber conditions. These chamber experiments were also designed to determine the accuracy of previous chamber results for HCHO and H_2O_2 that had been used by the model developers in testing the mechanisms. The developers had questioned the validity of both kinds of measurements in a range of chamber experiments. The new HCHO and H_2O_2 results are reported in Volume 1.

Finally, this program provided for the measurement of the solar irradiance spectrum outside and inside the UNC outdoor chamber using a precision, computer-based, portable spectroradiometer. These measurement were in response to modelers' complaints that the photolytic rates were inadequately characterized to allow further refinement in testing mechanisms using outdoor data.[11] As part of this task we examined in detail the methods used by both model development groups to compute the in-chamber photodissociation rates for their mechanism. These methods were quite different, and they used different data bases for the absorption cross sections and quantum yields.

For this task, we experimentally characterized the spectral optical properties of TFE Teflon film, as well as investigated the effect that clouds had on the solar irradicance spectrum. We also found that the older, commonly used Peterson actinic fluxes[12] provided an inadequate description of the solar irradiance at the

UNC site, especially with regard to the effects of aerosols. We therefore developed a new simple, surface radiation transmission model which predicts spectra in excellent agreement with a large series of spectroradiometer measurements over the range 300–850 nm and for various meteorological conditions. Using this model as a basis, we developed predictions of site tower total solar irradiance and ultraviolet irradiance for all 282 days in the current UNC chamber data base. From these and the Teflon and chamber geometry models, we developed predictions of in-chamber actinic flux every 16 minutes of each of the 282 days and computed in-chamber photolysis rates for up to 20 reactions. This work is described in Volumes 3 and 4 of this report.

Mechanism Testing

Three factors influenced the direct testing of the two mechanisms in this program. The first was that the CB4 mechanism was still under development throughout most of the lifetime of this project. That is, the mechanism was changing on a month-by-month basis. Such changes, except for historical reasons, render much of the early comparison testing useless from the viewpoint of the policy maker. We were in continual contact with Micheal Gery, the primary CB4 author, however, and our testing and comparison work influenced the development of CB4 and focused attention on the real differences between the two mechanisms. The second factor was that in the second year of our project, William Carter undertook a mechanism testing program for the Regional Acid Deposition Model (RADM) mechanism using the same approach and data base that had been used for testing CAL. We were sub-contracted to the University of California at Riverside (UCR) to supply a new photolytic rate calculation process and to perform quality assurance tasks for the UNC chamber conditions. Because the previous light treatment used by Carter in testing CAL was so different than our new in-chamber flux model, there were major changes in the way CAL fits the UNC data. In addition, Carter has up-dated the CAL mechanism as part of the comparison process. Again, the comparison work we have performed has had an influence.[13]

The third factor that influenced the type of comparison testing we did was the EPA Workshop on Evaluation/Documentation of Chemical Mechanisms held in Raleigh NC in December 1987. This workshop was necessary to resolve or reach accord on how mechanisms that were to be used by EPA in regulatory applications should be developed and tested. Part of our early efforts in this project supplied evidence that such a workshop would be useful and the results of this workshop had an impact on our actions in this project. To quote from the proceedings abstract:[14]

> Participants agreed that smog chamber data provide the most unambiguous test of urban atmospheric photochemistry mechanisms. They also agreed, however, that there are uncertainties associated with the representation of chamber radical sources and of photolytic rates in outdoor chambers, with smog chamber measurement errors, and with the representation of as yet unknown reaction pathways. The participants recommended that task forces and/or review groups be established to discuss and resolve existing smog chamber methodology issues, to assemble a required smog chamber data base for mechanisms testing, and to review/evaluate relevant kinetic and smog chamber data and mechanism testing results.

A definitive mechanism comparison can not be conducted in the eyes of the modeling community until these review and task groups have reached a consensus. The support of these task forces and review groups is planned by EPA over the next two years.

There remains in our minds major questions about how to assess the "goodness of fit" between mechanism predictions and chamber data. The approach taken by Carter is rather remote from the data, reached apparently from his experience with his own evacuable chamber (EC) data. In general, Carter feels that, because of large run-to-run variation, he must model a large number of experiments, using very simple *and uniform* assumptions, and then measure goodness of fit by statistical techniques such as the average error in predicting ozone maximum value, or the error in predicting the timing parameter $(d([O_3]-[NO])/dt)$, and by scatter diagrams like the one in Figure 1. In carrying out his modeling, Carter uses a single simple model for wall radical sources, a single model for initial HONO, a single model for background hydrocarbon, a single dilution rate, and he performs no run-to-run adjustments. He believes that such adjustments, in the presence of high run-to-run variability, would hide systematic errors in his mechanism. Therefore, he rarely examines or accounts for fits to individual experiments.

Whitten, Killus, and Gery, the researchers from SAI who developed the Carbon Bond mechanisms, tend to be more concerned with the individual experiment. They examine each simulation of each experiment and explore the sensitivity of the mechanisms to "reasonable" assumptions of initial radical sources such as HONO, and to different wall radical models. They give tables giving the run-to-run choices of these parameters. They use large numbers of plots to demonstrate the quality of the model fits to the data. In the last report, Gery *et al.*[4] also added statistical tables and scatter diagram plots.

As Carter has pointed out,[13] "With over 400 runs, I do not have time to look at every run." How to comprehend the information that is present in 400 to 1000 plots of model verses data is certainly an issue.

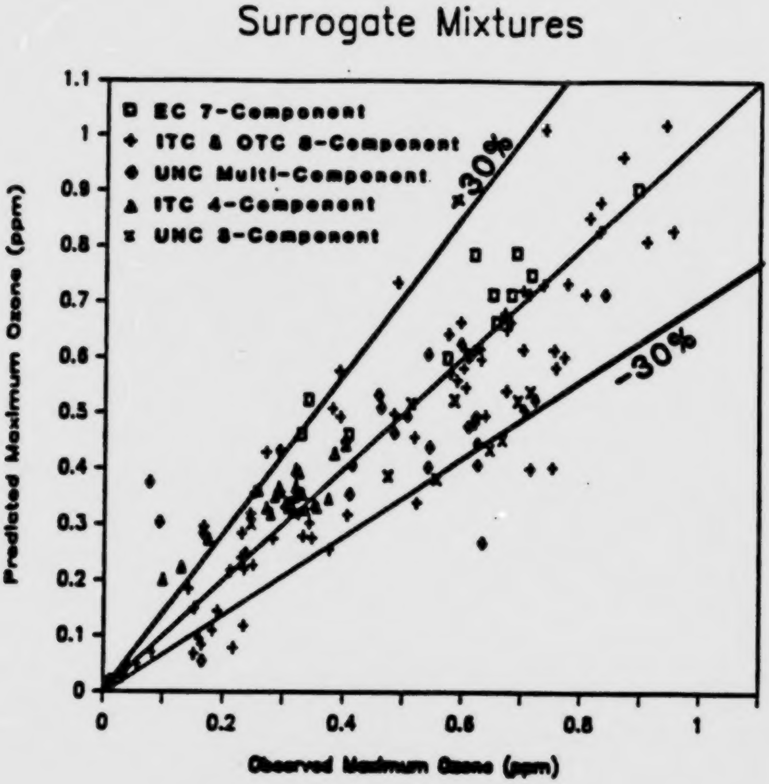

Figure 1. Predicted and observed ozone concentrations for irradiations of complex organic mixtures and NO_x, carried out in the SAPRC evacuable (EC), indoor Teflon (ITC), and outdoor Teflon (OTC), and in the UNC outdoor dual chambers (UNC).[7]

Unlike either the SAI or UCR group, we tend to focus attention on the nature of the dual side-to-side comparison of models with data. Much of the variability that Carter is concerned about is not present in this situation. The same instruments, with the same calibration were used to make both sets of measurements at the same time. The same sun was shining on both halves. It requires a lot of justification to choose different wall assumptions or different initial HONO for these conditions. Much of the freedom that Carter is concerned about is removed in these side-to-side cases, especially when these are combined into "networks," that is, paring of similar sides across different days and examining the quality of fit on the other two sides. Such networks were described by Pua and Jeffries[15] and a schematic example is shown in Figure 2.

In any case, new software that allows easier access to both the UCR and UNC smog chamber data for simulations and comparisons is needed to reduce the highly labor intensive testing. This is presently under EPA funding.

The Rest of Volume 1

Chapter 2 describes the mechanisms that were compared in this study and demonstrates that we implemented the mechanisms correctly.

Chapter 3 reports on a detailed intercomparison of inorganic and carbonyl reaction and rate constants that was conducted early in the study. The developers did re-examine their choices of rate constants and made some changes.

The fourth chapter reports on an intercomparison conducted in the last year of the project using the mechanism authors' own fitting statistics. The is followed by a "demonstration" of goodness of fit we performed for selected UNC experiments using the new photolytic rates and various assumptions of wall radical sources. The performances of the mechanisms are shown to be very good, even though there clearly are remaining problems, especially with aromatics and the predictions of secondary products other than ozone, such as HCHO.

The fifth chapter reports on an intercomparison for EKMA applications and for selected real SIP cases. These tests make use of the new HC composition "splits" determined as part of this project, use comparable photolytic rates, and identical physical conditions. The two mechanisms are shown to be very similar.

The sixth chapter reports on the HCHO and H_2O_2 intercomparison experiments from the first year of this project. These results show that HCHO measurement systems can perform nearly identically, if the calibration sources are reconciled.

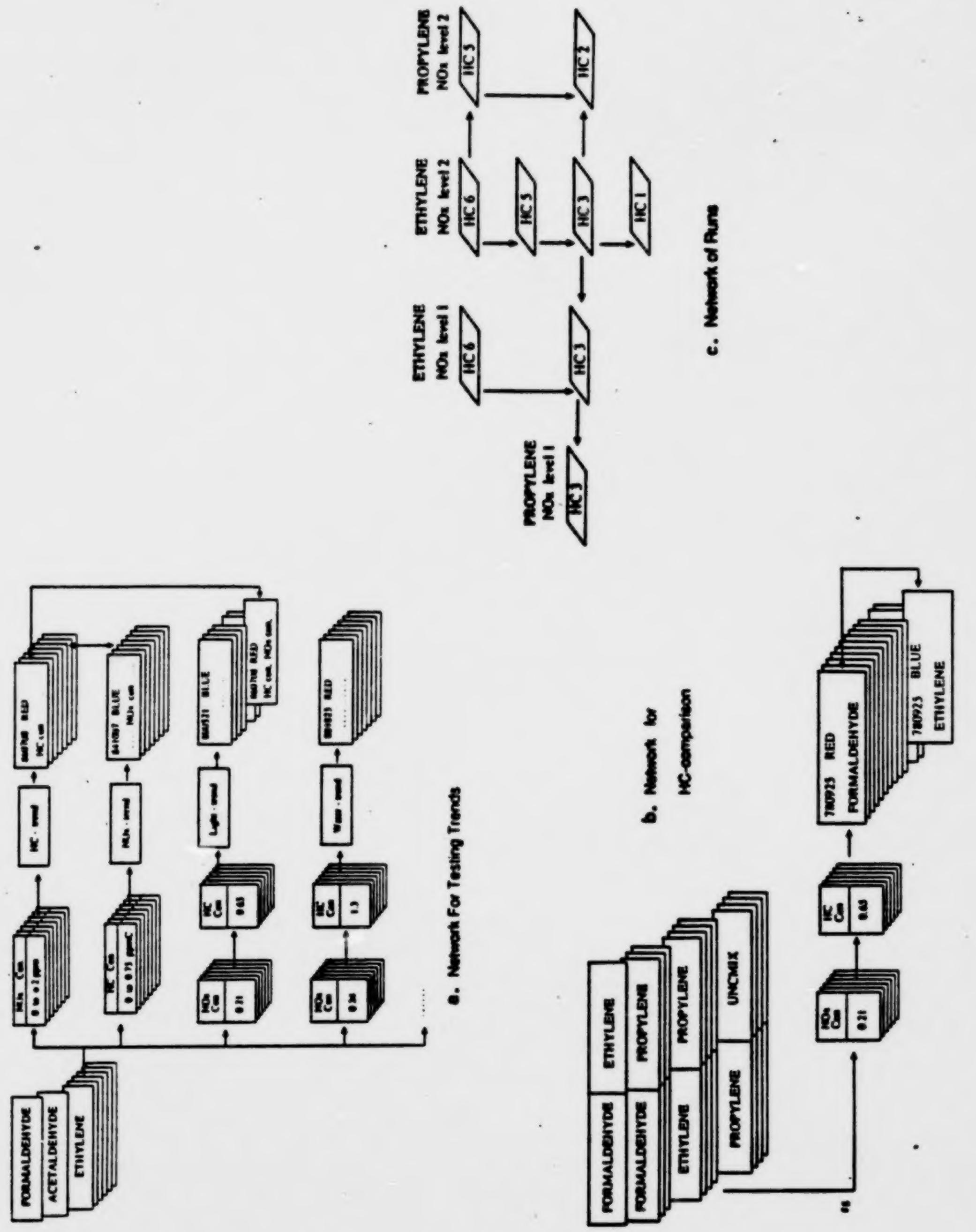
ETHYLENE
NOx level 1
HC 6
HC 3
ETHYLENE
NOx level 2
HC 6
HC 5
HC 3
HC 1
PROPYLENE
NOx level 2
HC 5
HC 2
PROPYLENE
NOx level 1
HC 3
c. Network of Runs
FORMALDEHYDE
ACETALDEHYDE
ETHYLENE
NOx Con
HC Con
HC - trend
NOx - trend
Light - trend
Water - trend
RED
BLUE
NOx Con 0.21
HC Con 0.65
a. Network For Testing Trends
b. Network for HC-comparison
FORMALDEHYDE
ETHYLENE
PROPYLENE
UNCMIX
780923 RED FORMALDEHYDE
780923 BLUE ETHYLENE

Figure 2. Schematic examples of run networks.[15]

All methods at one time or another in the two week testing period had problems, but there were frequent conditions under which several methods simultaneously agreed. All H_2O_2 instruments agreed very well. The biggest problem was that in the UNC chambers, injected H_2O_2 not only had a short half life, even in the dark, its half life was dramatically decreased by the addition of CO. The same was not true in newly manufactured Teflon bags tested at the same time. The H_2O_2 concentrations measured in smog chamber experiments were very much below expected values, suggesting that the same process that caused injected H_2O_2 to disappear also occurred for *in situ* produced H_2O_2. It is speculated that this process involves the aged chamber walls.

In a brief summary, the magnitude, temporal characteristics, and chemistry responsible for the production of radicals from "wall-sources" and for the wall off-gasing of various forms of NO_x, and the presence of loss processes, apparently to the walls, for products such as nitric acid and H_2O_2, even in the large UNC chamber remain the largest areas of uncertainty in the chamber data. On the theoretical side, the mechanism and kinetics of aromatics oxidation and the lack of kinetics data for the full ambient temperature range are limitations to the certainty of predictions especially for secondard products other than ozone.

2

Mechanisms

Mechanism Sources

For the CAL mechanism, we had three "official" sources:

1) an IBM PC diskette from Fred Lurmann[16] with the 20-NOV- 86 version of the CAL mechanism set up for OZIPM3; this input deck was translated by a computer program to the listing style show here.
2) the November 26, 1986 letter from Fred Lurmann[17] to Marcia Dodge (and copied to Jeffries and Carter) describing changes in the Arrhenius versions of the rate expressions for eight inorganic reactions; these rates superseded those in the diskette listing in item 1.
3) Table 3-2 (page 3-3) which lists the SAPRC/ERT OZIPM Chemical Mechanism in the March 1987 EPA report "Adaptation of the Mechanism"[7]; this listing is considered the final official source for the mechanism with one exception: the rate constant for reaction two is incorrect in the listing. Other rate constants in this version also differ with those given in step 2; see Chapter 3 for discussion.

The version of the CAL mechanism used in chamber simulations in this report is given in Table 1. The version of the CAL mechanism used in OZIPM4 simulations is given in Table 2.

For the CB4/X mechanism, we have five "official" sources:

1) Table 3 (page 21) of the November 1985 final report, "Development of CBM-X Mechanism for Urban and Regional AQSMs" by Whitten and Gery.[2]
2) an original OZIPM4 printout (with CB4 as the built-in mechanism) produced in December 1986 and send by Mike Gery.

3) the February 1987 source code listings for OZIPM4 with the CB4 mechanism "coded" into data statements;
4) an April 10, 1987 letter from Mike Gery to us listing the inorganic section that he intended to use in the newer versions of Carbon Bond mechanisms including numbered sources of the rate constants.
5) an October, 1987 IBM PC diskette sent by Mike Gery with version 4.2 of the Carbon Bond IV mechanism.[18] This is the same version that appeared in the final report.[4] and therefore this listing is considered the final official source for the mechanism.

The CB4 mechanisms described in sources 1–3 are now referred to as the "Carbon Bond Four point One" mechanism. The CB4 mechanism described in sources 4 and 5 are now referred to as the "Carbon Bond Four point Two" mechanism. CB4.2 is the mechanism internally coded into the OZIPM4 program for use with the EKAM technique. The CB4.1 mechanism was used in the early part of our work and it is listed in Table 3. The CB4.2 mechanism was used in all simulations since October 1987 and the version we use is listed in Table 4. When we used the OZIPM4 program, we used the built-in version of the CB4.2 mechanism.

Implementation of Mechanisms

Even when mechanisms are exchanged by magnetic media, there is the possibility that they might not be implemented correctly. In our case, we also acquired hard copy computer printouts of example cases. We then duplicated these example results using our own computer codes and methods. The "duplications" are shown in Figure 3.

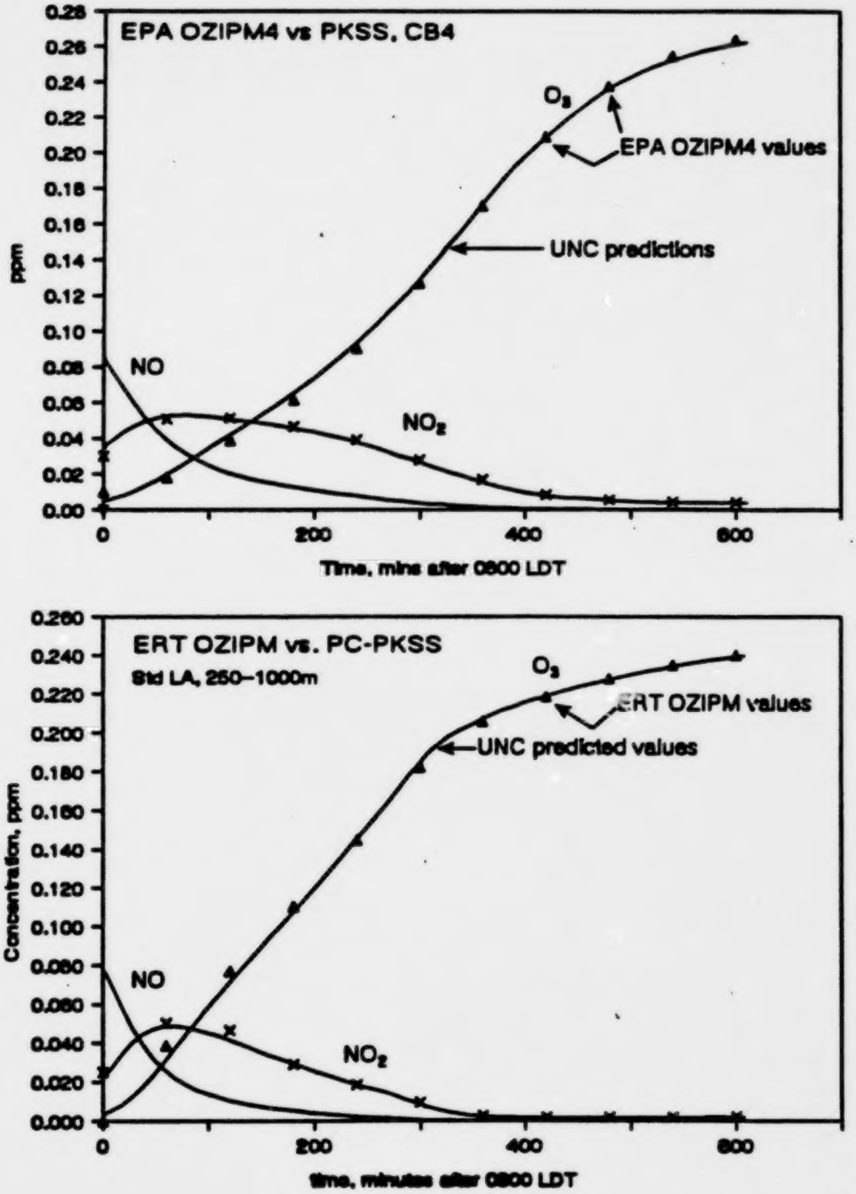

Figure 3. Comparison of Predictions from UNC Version of Mechanisms With Author's OZIPM Outputs

Table 1. The Carter, Atkinson, Lurmann Mechanism Used in Chamber Simulations

```
Carter, Atkinson, Lurman, Chamber Version 3.2(K&C)
!*****************************************************************
!Adopted from BASELINE CASE sent by Lurmann on diskette
!Revised per March 87 final report
!rxn 79  OH + MEK  ROR2 changed to R2O2
!rxn 125 OH + PHENOL , MGLY changed to GLYX
!
!Modified June 26, 1988 to use new in-chamber photolysis rates:
!Five PhotoRate Tables
!L1 = NO2        L2 = HCHO,Rx1000  L3 = HCHO,Sx1000  L4 = O1Dx1000
!L5 = RCHOx1000  L6 = O3Px1000
!The rest are based on ratios derived from JL0986.WK1
!
!******************************************************************

(* Inorganic Chemistry *)
(  1)        NO2  = NO   + O            # 1.00/L1;
(  2)        O    = O3                  # 6.3E+4@ 1282;
(  3) O    + NO2  = NO                  # 1.37E+04;
(  4) O    + NO2  = NO3                 # 164.06@ 894;
(  5) NO   + O3   = NO2                 # 2.57877E+03@ -1370;
(  6) NO2  + O3   = NO3                 # 1.67980E+02@ -2450;
(  7) NO   + NO3  = 2.*NO2              # 1.18720E+04@ 252;
(  8) NO   + NO   = 2.*NO2              # 2.45205E-05@ 529;
(  9) NO2  + NO3  = N2O5                # 6.902E+2@ 270;
( 10)        N2O5 = NO2  + NO3          # 1.11E+16 @ -10790;
( 11)        N2O5 = 2.*HNO3             # 1.4E-5/W;
                                          (^changed from E-6 for chamber)
( 12) NO2  + NO3  = NO   + NO2          # 3.59634E+01@ -1229;
( 13)        NO3  = NO                  # 0.043/L6;
( 14)        NO3  = NO2  + O            # 0.385/L6;
( 15)        O3   = O                   # 0.001/L6;
( 16)        O3   = O1D                 # 0.001/L4;
( 17)        O1D  = 2.*OH               # 3.260(1E+5)/W;
( 18)        O1D  = O                   # 4.32E+5(1E+5);
( 19) NO   + OH   = HONO                # 1.06528E+03@ 670;
( 20)        HONO = NO   + OH           # 0.171/L1;

( 21)        NO2  = HONO + -1.*NO2  + HNO3   #1.17E-04;

( 22) NO2  + OH   = HNO3                # 2.18674E+03@ 617;
( 23) HNO3 + OH   = NO3                 # 1.41316E+01@ 778;
( 24) CO   + OH   = HO2                 # 3.22E+02;
( 25) O3   + OH   = HO2                 # 2.31039E+03@ -942;
```

Table 1 The CAL Mechanism, Chamber Version, cont.

```
( 26) NO   + HO2  = NO2  + OH            # 5.48181E+03@ 240;
( 27) NO2  + HO2  = HNO4                 # 2.49368E+02@ 632;
( 28)        HNO4 = NO2  + HO2           # 4.2E+15@ -10240;
( 29) HNO4 + OH   = NO2                  # 5.91E+03;

( 30) O3   + HO2  = OH                   # 2.03930E+01@ -579;
( 31) HO2  + HO2  = H2O2                 # 3.41349E+02@ 771;
( 32) HO2  + HO2  = H2O2                 # 2.52539E-01@ 2971;
( 33) NO3  + HO2  = HNO3                 # 3.41349E+02@ 771;
( 34) NO3  + HO2  = HNO3                 # 2.52539E-01@ 2971;
( 35)        H2O2 = 2.*OH                # 0.293E-3/L2;
( 36) H2O2 + OH   = HO2                  # 4.56958E+03@ -187;

(* Generalized RO2 Chemistry *)
   (-- the loss steps --)
( 37) RO2  + NO   = NO                   # 6.25645E+03@ 180;
( 38) RCO3 + NO   = NO                   # 6.25645E+03@ 180;
( 39) RCO3 + NO2  = NO2                  # 4.15450E+03@ 180;
( 40) RO2  + HO2  = HO2                  # 4.43E+03;
( 41) RCO3 + HO2  = HO2                  # 4.43E+03;
( 42) RO2  + RO2  =                      # 1.48E+00;
( 43) RO2  + RCO3 =                      # 4.43E+03;
( 44) RCO3 + RCO3 =                      # 3.69E+03;


   (-- the oxidation steps --)
( 45) RO2R + NO   = NO2  + HO2           # 6.25645E+03@ 180;
( 46) RO2R + HO2  = ROOH                 # 4.43E+03;
( 47) RO2R + RO2  = .5*HO2  + RO2        # 1.48E+00;
( 48) RO2R + RCO3 = .5*HO2  + RCO3       # 4.43E+03;
( 49)        ROOH = HO2  + OH            # 0.294E-3/L2;


(* Carbonyl Chemistry *)
     (-- Formaldehyde --)
( 50)        HCHO = 2.*HO2  + CO         # 0.001/L2;
( 51)        HCHO = CO                   # 0.001/L3;
( 52) HCHO + OH   = HO2  + CO            # 1.50E+04 (1.33E+04);
( 53) HCHO + NO3  = HNO3 + HO2  + CO     # 8.46494E+02@ -2060;
( 54) HCHO + HO2  = FROX                 # 1.48E+01;
( 55)        FROX = HCHO + HO2           # 90.0;
( 56) FROX + NO   = (FACID+) NO2 + HO2   # 6.25645E+03@ 180;

(Original reaction was ...
     HCHO + HO2  = RO2R + RO2            # 1.48E+01;
.... which omitted the back reaction and overestimated pathway )
```

Table 1 The CAL Mechanism, Chamber Version, cont.

```
   (-- Acetaldehyde --)
( 58)        ALD2 = CO   + HCHO + HO2  +
                    RO2R + RO2            # 0.001/L5;
( 59) ALD2 + OH   = MCO3 + RCO3           # 1.02565E+04@ 250;
( 60) ALD2 + NO3  = HNO3 + MCO3 + RCO3   # 4.29359E+02@ -1427;
( 61) MCO3 + NO   = NO2  + HCHO + RO2R +
                    RO2                   # 6.25645E+03@ 180;
( 62) MCO3 + NO2  = PAN                   # 4.15450E+03@ 180;
( 63) MCO3 + HO2  = ROOH + HCHO           # 4.43E+03;
( 64) MCO3 + RO2  = .5*HO2  + HCHO + RO2 # 4.43E+03;
( 65) MCO3 + RCO3 = HO2  + HCHO + RCO3   # 3.69E+03;
( 66)        PAN  = MCO3 + NO2  + RCO3  # 1.2014926E+18@ -13550;

   (-- Higher Aldehyde --)
( 67)        RCHO = ALD2 + HO2  + CO   +
                    RO2R + RO2            # 0.0037/L5;
                                            (^was 0.0023)
( 68) RCHO + OH   = RCO3 + PCO3           # 1.26468E+04@ 250;
( 69) RCHO + NO3  = HNO3 + PCO3 + RCO3   # 4.29359E+02@ -1427;
( 70) PCO3 + NO   = NO2  + ALD2 + RO2R +
                    RO2                   # 6.25645E+03@ 180;
( 71) PCO3 + NO2  = PPN                   # 4.15450E+03@ 180;
( 72) PCO3 + HO2  = ROOH + ALD2           # 4.43E+03;
( 73) PCO3 + RO2  = .5*HO2  + ALD2 + RO2 # 4.43E+03;
( 74) PCO3 + RCO3 = NO2  + ALD2 + RCO3   # 3.69E+03;
( 75)        PPN  = PCO3 + NO2  + RCO3  # 8.87304E+17@ -13550;

   (-- Acetone --)
( 76)        ACET = MCO3 + HCHO + RCO3 +
                    RO2R + RO2            # 0.2E-3/L1;
( 77) ACET + OH   = MGLY + RO2R + RO2    # 1.44146E+04@ -1125;
   (-- Ketones --)
( 78)        MEK  = MCO3 + ALD2 + RCO3 +
                    RO2R + RO2            # 3.5E-3/L5;
( 79) MEK  + OH   = 1.5*R2O2 + 1.5*RO2  + .5*MCO3 +
                    .5*ALD2 + .5*HCHO + .5*PCO3 + RCO3
                                          # 1.74925E+04@ -745;
   (-- glyoxal --)
( 80)        GLYX = .13*HCHO + 1.87*CO   # 0.011/L1;
( 81) GLYX + OH   = .63*HO2  + 1.26*CO   + .37*GCO3 +
                    .37*RCO3              # 1.70E+04;
( 82) GLYX + NO3  = HNO3 + .63*HO2  + 1.26*CO   +
                    .37*GCO3 + .37*RCO3  # 8.46494E+02@ -2060;
( 83) GCO3 + NO2  = GPAN                  # 4.15450E+03@ 180;
( 84) GCO3 + NO   = NO2  + HO2  + CO     # 6.25645E+03@ 180;
( 85)        GPAN = GCO3 + NO2  + RCO3   # 8.87304E+17@ -13550;
( 86) GCO3 + HO2  = ROOH + CO             # 4.43E+03;
( 87) GCO3 + RO2  = .5*HO2  + CO   + RO2 # 4.43E+03;
( 88) GCO3 + RCO3 = HO2  + CO   + RCO3   # 3.69E+03;
   (-- methyl glyoxal --)
( 89)        MGLY = MCO3 + HO2  + CO   +
                    RCO3                  # 0.021/L1;
( 90) MGLY + OH   = MCO3 + CO   + RCO3   # 2.51E+04;
( 91) MGLY + NO3  = HNO3 + MCO3 + CO   +
                    RCO3                  # 4.29359E+02@ -1427;
```

Table 1 The CAL Mechanism, Chamber Version, cont.

```
(* Paraffin chemistry *)

( 92) ALK4 + OH   = .19*HCHO + .31*ALD2 + .17*RCHO +
                    .34*ACET + .44*MEK  + .07*RO2N +
                    .93*RO2R + .6*R2O2  + 1.6*RO2
                                        # 1.54257E+04@ -354;
( 93) ALK7 + OH   = .02*HCHO + .03*ALD2 + .25*RCHO +
                    .36*ACET + .88*MEK  + .18*RO2N +
                    .82*RO2R + .84*R2O2 + 1.84*RO2
                                        # 2.37934E+04@ -289;

( 94) ALKN + OH   = NO2  + .15*MEK  + 1.05*RCHO +
                    .48*ALD2 + .16*HCHO + 1.39*R2O2 +
                   1.39*RO2             # 3.18782E+04@ -711;

( 95) RO2N + NO   = ALKN                # 6.25645E+03@ 180;
( 96) RO2N + HO2  = ROOH + MEK          # 4.43E+03;
( 97) RO2N + RO2  = RO2  + .5*HO2  + MEK # 1.48E+00;
( 98) RO2N + RCO3 = RCO3 + .5*HO2  + MEK # 4.43E+03;

( 99) R2O2 + NO   = NO2                 # 6.25645E+03@ 180;
(100) R2O2 + HO2  = ROOH                # 4.43E+03;
(101) R2O2 + RO2  = RO2                 # 1.48E+00;
(102) R2O2 + RCO3 = RCO3                # 4.43E+03;
```

Table 1 The CAL Mechanism, Chamber Version, cont.

```
(* Olefin Chemistry *)
   (- ethylene -)
(103) ETHE + OH   = RO2R + RO2  + 1.56*HCHO +
                    .22*ALD2             # 3.20175E+03@ 411;
(104) ETHE + O3   = HCHO + .12*HO2  + .42*CO
                                          # 1.67124E+01@ -2634;
(105) ETHE + O    = HCHO + HO2  + CO   +
                    RO2R + RO2           # 1.51343E+04@ -792;
(106) ETHE + NO3  = NO2  + 2.*HCHO + R2O2 +
                    RO2                  # 2.76183E+03@ -2925;
   (- propylene -)
(107) PRPE + OH   = RO2R + HCHO + ALD2 +
                    RO2                  # 7.24995E+03@ 504;
(108) PRPE + O3   = .64*HCHO + .5*ALD2  + .28*CO   +
                    .06*OH   + .17*HO2  + .13*RO2R +
                    .13*RO2              # 1.86216E+01@ -2105;
(109) PRPE + O    = .6*ACET + .4*HCHO + .2*ALD2 +
                    .2*HO2  + .6*RO2R + .4*CO   +
                    .6*RO2               # 1.73147E+04@ -324;
(110) PRPE + NO3  = NO2  + HCHO + ALD2 +
                    R2O2 + RO2           # 7.08627E+03@ -1935;

   (- trans-2-butene -)
(111) TBUT + OH   = RO2R + 2.*ALD2 + RO2    # 1.51110E+04@ 549;
(112) TBUT + O3   = ALD2 + .15*CO   + .27*RO2R +
                    .12*OH   + .21*HO2  + .27*RO2  +
                    .30*HCHO                # 1.30999E+01@ -1137;
(113) TBUT + O    = MEK  + .4*HO2           # 3.33690E+04@ 10;
(114) TBUT + NO3  = NO2  + 2.*ALD2 + R2O2 +
                    RO2                     # 1.44684E+04@ -975;
```

Table 1 The CAL Mechanism, Chamber Version, cont.

```
(* Aromatics Chemistry *)
   (- toluene -)
(115) TOLU + OH   = .16*CRES + .16*HO2  + .84*RO2R +
                   .4*DIAL + .84*RO2  + .144*MGLY +
                  .114*GLYX                  # 3.12492E+03@ 320;
(116) DIAL + OH   = PCO3 + RCO3              # 4.43E+04;
(117)        DIAL = HO2  + CO   + MCO3 +
                   RCO3                      # 0.060/L1(8.4E-3/L3);
   (- xylene -)
(118) XYLE + OH   = .17*CRES + .17*HO2  + .83*RO2R +
                   .83*RO2  + .65*DIAL + .316*MGLY +
                  .095*GLYX                  # 2.45913E+04@ 116;

   (- tri methyl benzene -)
(119) TMBZ + OH   = .17*CRES + .17*HO2  + .83*RO2R +
                   .83*RO2  + .49*DIAL + .86*MGLY
                                             #9.16E+04;
   (- cresol -)
(120) CRES + OH   = .2*MGLY + .15*RO2P + .85*RO2R +
                   RO2                       # 5.91E+04;
(121) CRES + NO3  = HNO3 + BZO               #3.25E+04;
(122) BZO  + NO2  = NPHE                     #2.22E+04;
(123) BZO  + HO2  = PHEN                     #4.43E+03;
(124)        BZO  = PHEN                     #6.00E-02;
   (- phenol -)
(125) PHEN + OH   = .2*GLYX + .15*RO2P + .85*RO2R +
                   RO2                       #4.14E+04;
(126) PHEN + NO3  = HNO3 + BZO               #5.62E+03;
   (- nitro phenols -)
(127) NPHE + NO3  = HNO3 + BZN2              #5.62E+03;
(128) BZN2 + NO2  =                          #2.22E+04;
(129) BZN2 + HO2  = NPHE                     #4.43E+03;
(130)        BZN2 = NPHE                     #6.00E-02;

   (- generalized phenolic RO2 -)
(131) RO2P + NO   = NPHE                     # 6.25645E+03@ 180;
(132) RO2P + HO2  = ROOH                     # 4.43E+03;
(133) RO2P + RO2  = .5*HO2  + RO2            # 1.48E+00;
(134) RO2P + RCO3 = .5*HO2  + RCO3           # 4.43E+03;

(135) OH   + MEOH = HCHO + HO2               # 1.98E+04@-805;

! include the model independent standard wall model
@stdcham.rxn

! include the model dependent Killus and Carter
!  chamber wall radical models
@WalModC.rxn
```

Table 1 The CAL Mechanism, Chamber Version, cont.

```
! This is WalModC.rxn file
! Mechanism specific Wall models for CAL

! Killus's model for CAL mechanism based upon SAI report
! and personal communication with Killus.  .
! The Killus Model is initially turned off
$1: ( Background HC brought in with dilution air...0.038 ppmC NMOC )
      = 0.005*HCHO + 0.0025*ALD2 + 0.00062*ALK4 +
        0.001*ETHE + 0.0005*PRPE + 0.0008*TOLU    #(1.0)  0.0/D;
                     = HONO                      #(0.11E-3) 0.0/L1;
                     = HCHO                      #(0.22E-3) 0.0/L1;
! Carter Model based upon telephone conversation with Carter August, 1988
! This model is initially turned on.
$2:
                  OH = HO2                       #250.0;
                     = OH                          #0.30E-3/L1;
                     = HO2                         #0.110E-3/L1;


! This is StdCham.Rxn file:
! Mechanism independent chamber and wall reactions

    ( ENTRAINED WITH DILUTION AIR)
                = 0.50*CO + 0.07*O3          #1.0/D;
    ( WALL REACTIONS )
        NO2     = 0.21 * HONO + 0.79 * HNO3 #1.6E-4;
        O3      =                           #1.8E-4;
```

Table 2. The Carter, Atkinson, Lurmann Mechanism Used in OZIPM Simulations

```
! CAL Standard Mechanism
!  from Table 3-2 March 1987 Adaptation Report
!  with R2 rate fixed (lower by factor of 10)
!  and with R133 (OH+CH4) added
!  Requires 17 photolytic rates and has 12 VOC species
MECH              133.       17.        12.        0.       303.
        1.         13.       14.        15.       16.        20.       35.
       42.         46.       47.        52.       61.        69.       71.
       73.         82.      114.
ALK4       ALK7        ETHE       PRPE       TBUT       TOLU       XYLE
TMBZ       HCHO        ALD2       RCHO       NRHC
 4.5       7.0         2.0        3.0        4.0        7.0        8.0
 9.0       1.0         2.0        3.0        1.0
NO2         HV       1   1.NO       1. O                         1.00        0.
O                    2   1.O3                                    4.87E+06 -1282.
O     NO2            3   1.NO                                    1.37E+04    0.
O     NO2            4   1.NO3                                   3.29E+03  -894.
NO    O3             5   1.NO2                                   2.68E+01  1370.
NO2   O3             6   1.NO3                                   4.77E-02  2450.
NO    NO3            7   2.NO2                                   2.75E+04  -252.
NO    NO             8   2.NO2                                   1.50E-04  -529.
NO2   NO3            9   1.N2O5                                  1.71E+03  -273.
N2O5                10   1.NO2      1. NO3                       2.08E+00 11379.
N2O5                11   2.HNO3                                  3.00E-02    0.
NO2   NO3           12   1.NO       1. NO2                       5.98E-01  1229.
NO3         HV      13   1.NO                                    1.00        0.
NO3         HV      14   1.NO2      1. O                         1.00        0.
O3          HV      15   1.O                                     1.00        0.
O3          HV      16   1.O*SD                                  1.00        0.
O*SD                17   2.OH                                    6.54E+09    0.
O*SD                18   1.O                                     4.32E+10    0.
NO    OH            19   1.HONO                                  9.75E+03  -833.
HONO        HV      20   1.NO       1. OH                        1.00        0.
NO2                 21   1.HONO    -1. NO2     1. HNO3           1.17E-04    0.
NO2   OH            22   1.HNO3                                  1.68E+04  -737.
HNO3  OH            23   1.NO3                                   1.89E+02  -778.
CO    OH            24   1.HO2                                   3.22E+02    0.
O3    OH            25   1.HO2                                   1.00E+02   942.
NO    HO2           26   1.NO2      1. OH                        1.22E+04  -240.
NO2   HO2           27   1.HNO4                                  2.02E+03  -773.
HNO4                28   1.NO2      1. HO2                       4.93E+00 10103.
HNO4  OH            29   1.NO2                                   5.91E+03    0.
O3    HO2           30   1.OH                                    2.96E+00   579.
HO2   HO2           31   1.H2O2                                  4.46E+03  -771.
HO2   HO2           32   1.H2O2                                  5.05E+03 -2971.
NO3   HO2           33   1.HNO3                                  4.46E+03  -771.
NO3   HO2           34   1.HNO3                                  5.05E+03 -2971.
```

Table 2 The CAL Mechanism, OZIPM Version, cont.

```
H2O2      HV   35  2.OH                                1.00       0.
H2O2 OH        36  1.HO2                               2.45E+03  187.
RO2  NO        37  1.NO                                1.14E+04 -180.
RCO3 NO        38  1.NO                                1.14E+04 -180.
RCO3 NO2       39  1.NO2                               7.57E+03 -180.
RO2  HO2       40  1.HO2                               4.43E+03   0.
RCO3 HO2       41  1.HO2                               4.43E+03   0.
ROOH      HV   42  1.HO2     1. OH                     1.00       0.
RO2  RO2       43                                      1.48E+00   0.
RO2  RCO3      44                                      4.43E+03   0.
RCO3 RCO3      45                                      3.69E+03   0.
HCHO      HV   46  2.HO2     1. CO                     1.00       0.
HCHO      HV   47  1.CO                                1.00       0.
HCHO OH        48  1.HO2     1. CO                     1.33E+04   0.
HCHO NO3       49  1.HNO3    1. HO2     1. CO          8.82E-01 2060.
HCHO HO2       50  1.RO2R    1. RO2                    1.48E+01   0.
ALD2 OH        51  1.MCO3    1. RCO3                   2.36E+04 -250.
ALD2      HV   52  1.CO  *    1. HCHO   1. HO2         1.00       0.
  1. RO2R    1. RO2
ALD2 NO3       53  1.HNO3    1. MCO3    1. RCO3        3.69E+00 1427.
MCO3 NO        54  1.NO2 *    1. HCHO   1. RO2R        1.14E+04 -180.
  1. RO2
MCO3 NO2       55  1.PAN                               7.57E+03 -180.
MCO3 HO2       56  1.ROOH    1. HCHO                   4.43E+03   0.
MCO3 RO2       57  .5HO2     1. HCHO    1. RO2         4.43E+03   0.
MCO3 RCO3      58  1.HO2     1. HCHO    1. RCO3        3.69E+03   0.
PAN            59  1.MCO3    1. NO2     1. RCO3        2.21E-02 13542.
RCHO OH        60  1.RCO3    1. PCO3                   2.93E+04 -252.
RCHO      HV   61  1.ALD2*    1. HO2    1. CO          1.00       0.
  1. RO2R    1. RO2
RCHO NO3       62  1.HNO3    1. PCO3    1. RCO3        3.63E+00 1427.
PCO3 NO        63  1.NO2 *    1. ALD2   1. RO2R        1.14E+04 -180.
  1. RO2
PCO3 NO2       64  1.PPN                               7.57E+03 -180.
PCO3 HO2       65  1.ROOH    1. ALD2                   4.43E+03   0.
PCO3 RO2       66  .5HO2     1. ALD2    1. RO2         4.43E+03   0.
PCO3 RCO3      67  1.HO2     1. ALD2    1. RCO3        3.69E+03   0.
PPN            68  1.PCO3    1. NO2     1. RCO3        2.21E-02 13542.
ACET      HV   69  1.MCO3*    1. HCHO   1. RCO3        1.00       0.
  1. RO2R    1. RO2
ACET OH        70  1.MGLY    1. RO2R    1. RO2         3.39E+02 1125.
MEK       HV   71  1.MCO3*    1. ALD2   1. RCO3        1.00       0.
  1. RO2R    1. RO2
MEK  OH        72 1.5R2O2*   1.5 RO2    .5 MCO3        1.46E+03  745.
  .5 ALD2    .5 HCHO    .5 PCO3    1. RCO3
```

Table 2 The CAL Mechanism, OZIPM Version, cont.

```
GLYX       HV     73  .13HCHO   1.87 CO                  1.00        0.
GLYX  OH          74  .63HO2 *  1.26 CO      .37 GCO3    1.70E+04    0.
  .37 RCO3
GLYX  NO3         75   1.HNO3*   .63 HO2    1.26 CO     8.88E-01  2058.
  .37 GCO3     .37 RCO3
GCO3  NO2         76   1.GPAN                           7.57E+03  -180.
GCO3  NO          77   1.NO2      1. HO2      1. CO     1.14E+04  -180.
GPAN              78   1.GCO3     1. NO2      1. RCO3   2.21E-02 13542.
GCO3  HO2         79   1.ROOH     1. CO                 4.43E+03    0.
GCO3  RO2         80   .5HO2      1. CO       1. RO2    4.43E+03    0.
GCO3  RCO3        81   1.HO2      1. CO       1. RCO3   3.69E+03    0.
MGLY       HV     82   1.MCO3*     1. HO2     1. CO     1.00        0.
   1. RCO3
MGLY  OH          83   1.MCO3     1. CO       1. RCO3   2.51E+04    0.
MGLY  NO3         84   1.HNO3*     1. MCO3    1. CO     3.69E+00  1427.
   1. RCO3
ALK4  OH          85  .19HCHO*   .31 ALD2    .17 RCHO    4.76E+03   353.
  .34 ACET     .44 MEK    .07 RO2N    .93 RO2R    .6 R2O2    1.6 RO2
ALK7  OH          86  .02HCHO*   .03 ALD2    .25 RCHO    9.11E+03   288.
  .36 ACET     .88 MEK    .18 RO2N    .82 RO2R    .84 R2O2  1.84 RO2
ALKN  OH          87   1.NO2 *   .15 MEK    1.05 RCHO    3.00E+03   709.
  .48 ALD2     .16 HCHO   1.39 R2O2   1.39 RO2
RO2N  NO          88   1.ALKN                           1.14E+04  -180.
RO2N  HO2         89   1.ROOH     1. MEK                4.43E+03    0.
RO2N  RO2         90   1.RO2     .5 HO2       1. MEK    1.48E+00    0.
RO2N  RCO3        91   1.RCO3    .5 HO2       1. MEK    4.43E+03    0.
R2O2  NO          92   1.NO2                            1.14E+04  -180.
R2O2  HO2         93   1.ROOH                           4.43E+03    0.
R2O2  RO2         94   1.RO2                            1.48E+00    0.
R2O2  RCO3        95   1.RCO3                           4.43E+03    0.
RO2R  NO          96   1.NO2      1. HO2                1.14E+04  -180.
RO2R  HO2         97   1.ROOH                           4.43E+03    0.
RO2R  RO2         98   .5HO2      1. RO2                1.48E+00    0.
RO2R  RCO3        99   .5HO2      1. RCO3               4.43E+03    0.
ETHE  OH         100   1.RO2R*     1. RO2    1.56 HCHO    1.26E+04  -411.
  .22 ALD2
ETHE  O3         101   1.HCHO    .12 HO2     .42 CO     2.57E-03  2634.
ETHE  O          102   1.HCHO*    1. HO2      1. CO     1.08E+03   792.
   1. RO2R     1. RO2
ETHE  NO3        103   1.NO2 *    2. HCHO     1. R2O2   1.62E-01  2923.
   1. RO2
PRPE  OH         104   1.RO2R*    1. HCHO     1. ALD2   3.89E+04  -504.
   1. RO2
PRPE  O3         105  .64HCHO*    .5 ALD2    .28 CO     1.67E-02  2105.
  .06 OH       .17 HO2     .13 RO2R    .13 RO2
PRPE  O          106   .6ACET*    .4 HCHO    .2 ALD2    5.88E+03   324.
   .2 HO2      .6 RO2R     .4 CO       .6 RO2
PRPE  NO3        107   1.NO2 *    1. HCHO     1. ALD2   1.12E+01  1935.
   1. R2O2     1. RO2
```

Table 2 The CAL Mechanism, OZIPM Version, cont.

```
TBUT  OH       108  1.RO2R     2. ALD2     1. RO2     9.42E+04  -549.
TBUT  O3       109  1.ALD2*    .15 CO     .27 RO2R    2.96E-01  1137.
  .12 OH      .21 HO2     .27 RO2     .30 HCHO
TBUT  O        110  1.MEK      .4 HO2                 3.45E+04   -10.
TBUT  NO3      111  1.NO2 *    2. ALD2     1. R2O2    5.61E+02   975.
   1. RO2
TOLU  OH       112  .16CRES*   .16 HO2    .84 RO2R    9.14E+03  -322.
   .4 DIAL    .84 RO2     .144 MGLY   .114 GLYX
DIAL  OH       113  1.PCO3     1. RCO3                4.43E+04     0.
DIAL      HV   114  1.HO2 *    1. CO       1. MCO3    1.00         0.
   1. RCO3
XYLE  OH       115  .17CRES*   .17 HO2    .83 RO2R    3.62E+04  -116.
  .83 RO2     .65 DIAL    .316 MGLY   .095 GLYX
TMBZ  OH       116  .17CRES*   .17 HO2    .83 RO2R    9.16E+04     0.
  .83 RO2     .49 DIAL    .86 MGLY
CRES  OH       117  .2MGLY*    .15 RO2P    .85 RO2R    5.91E+04    0.
   1. RO2
RO2P  NO       118  1.NPHE                            1.14E+04  -180.
RO2P  HO2      119  1.ROOH                            4.43E+03     0.
RO2P  RO2      120  .5HO2      1. RO2                 1.48E+00     0.
RO2P  RCO3     121  .5HO2      1. RCO3                4.43E+03     0.
CRES  NO3      122  1.HNO3     1. BZO                 3.25E+04     0.
BZO   NO2      123  1.NPHE                            2.22E+04     0.
BZO   HO2      124  1.PHEN                            4.43E+03     0.
BZO            125  1.PHEN                            6.00E-02     0.
PHEN  OH       126  .2GLYX*    .15 RO2P    .85 RO2R    4.14E+04    0.
   1. RO2
PHEN  NO3      127  1.HNO3     1. BZO                 5.62E+03     0.
NPHE  NO3      128  1.HNO3     1. BZN2                5.62E+03     0.
BZN2  NO2      129                                    2.22E+04     0.
BZN2  HO2      130  1.NPHE                            4.43E+03     0.
BZN2           131  1.NPHE                            6.00E-02     0.
NRHC           132  1.NRHC                            6.00E+01     0.
OH             133  1.HCHO     1. RO2R     1. RO2     2.10E+01  1710.
! R133 (OH+CH4) added by Jeffries to match reactivity of CB4
! end of mechanism
```

Table 3. The Carbon Bond Four, Version One Mechanism Used in Chamber Simulations

```
Carbon Bond Four, Chamber Version
(*********************************************************************
Obtained from Mike Gery's PrintOut, December, 1986.
Verified with OAQPS's PrintOut of Example 1, December, 1986.
NOTE: includes the ROR species in PAR + OH
Five PhotRate Tables are Required.
L1=NO2; L2=HCHO,RAD; L3=HCHO,STA; L4=O3->O1D; L5=RCHO;
*********************************************************************)
(1)       NO2  = NO + O                         # 1.0/L1;
(2)         O  = O3                             # 4.59E+05 @ 690;
(3)  O3  + NO  = NO2                            # 3.228E+03  @-1430. ;

(4)   O  + NO2 = NO                             # 1.38E+04;
(5)   O  + NO  = NO2                            # 785.6 @411;

   ( NO3 CHEMISTRY )
(6)   O  + NO2 = NO3                            # 309.8 @600;
(7)  O3  + NO2 = NO3                            # 176.3 @-2450;
(8)        NO3 = 0.85*NO2 + 0.85*O + 0.15*NO  # 30.6/L1;
(9)  NO3 + NO  = 2.0 * NO2                      # 12144 @250;
(10) NO3 + NO2 = NO + NO2                       # 36.59 @-1230;
(11) NO3 + NO2 = N2O5                           # 2177 @-60;
(12)      N2O5 = NO3 + NO2                      # 1.96E16 @-10840;
(13)      N2O5 = 2.0 * HNO3                     # 1.9E-5/W ;
           (above rate has been increased by 10 for chamber)
(14)       O3  = O                              # 0.042/L1;
(15)       O3  = O1D                            # 0.001/L4;
(16)       O1D = O                              # 3.067E+5 (1E+5) @100.;
(17)       O1D = 2 * OH                         # 3.260(1E+5)/W;
              (above rates multiplied by 1E-5 to lower stiffness)

(18) O3  + OH  = HO2                            # 2343.8 @-940;
(19) O3  + HO2 = OH                             # 21 @-580;

   ( THERMAL DARK OXIDATION )
(20)   NO + NO   = 2.0 * NO2                    # 2.57E-5 @530;

   ( HONO CHEMISTRY )
(21)   NO + NO2  = 2.0 * HONO                   # 2.4E-7;
(22) HONO + HONO = NO + NO2                     # 1.5E-5;
(23)  OH  + NO   = HONO                         # 2331 @427;
(24)        HONO = NO + OH                      # 0.18/L1;
(25)  OH  + HONO = NO2                          # 9770;

   ( HO2 CHEMISTRY )
(26)  HO2 + NO  = OH + NO2                      # 5497 @240;

(27) HO2 + HO2  = H2O2                          # 87.4 @1150;
(28) HO2 + HO2  = H2O2                          # 1.153E-5 @5800;
(29)       H2O2 = 2.0 * OH                      # 0.321/L2;
                          (0.321 is ave ratio H2O2/HCHO rate vs za)
(30)  OH  + H2O2 = HO2                          # 4719.8 @-187;

(31)  OH  + NO2  = HNO3                         # 2489 @560;
(32)  OH  + HNO3 = NO3                          # 14.11 @778;
```

```
(33) OH  + CO  = HO2                              # 400;
(34) OH (+CH4) = XO2 + HCHO + HO2                 # 21;

 ( FORMALDHYDE CHEMISTRY )

(35) HCHO      = 2 * HO2 + CO                     # 0.001/L2;
(36) HCHO      = CO                               # 0.001/L3;

(37) HCHO + OH  = HO2 + CO                        # 15000;
(38) HCHO + O   = OH + HO2 + CO                   # 43019.2 @-1550;
(39) HCHO + NO3 = HNO3 + HO2 + CO                 # 0.93;

 ( HIGHER ALDEHYDE CHEMISTRY )
(40)       RCHO = XO2 + 2.0 * HO2 + CO + HCHO # 0.001/L5;

(41) RCHO + O   = RCO3 + OH                       # 17394.7 @-986;
(42) RCHO + OH  = RCO3                            # 10372.2 @250;
(43) RCHO + NO3 = RCO3 +HNO3                      # 3.7;
(44) RCHO + HO2 = XO2 + 2.0 * HCHO + HO2          # 5.;

 ( DICARBONYL CHEMISTRY )
(45) MGLY      = RCO3 + HO2 + CO                  # 0.02/L1;
(46) MGLY + OH = XO2 + RCO3                       # 26000;

 ( PAN CHEMISTRY )
(47) RCO3 + NO  = NO2 + XO2 + HCHO + HO2          # 7130.9 @250;
(48) RCO3 + NO2 = PAN                             # 3889.6 @250;
(49)        PAN = RCO3 + NO2                      # 5.616E18 @-14000;

(50) RCO3+ RCO3= 2.0 * XO2 + 2.0 * HCHO + 2.0 * HO2  # 3700;
(51) RCO3+ HO2 =                                  # 9600;

 ( RO2-TYPE CHEMISTRY )
(52) XO2 + NO   = NO2                             # 12000;
(53) XO2 + HO2  =                                 # 63.8 @1300;
(54) XO2 + RCO3 = XO2 + 2.0 * HO2 + HCHO          # 2400;
(55) XO2N+ NO  =                                  # 1000;

 ( PARAFFIN CHEMISTRY )
(56) PAR + OH = 0.92 * XO2 + 0.067* XO2N + 0.13 * HO2 + 0.13 * RCHO +
                0.80 * ROR +  -0.13 * PAR         # 1150.0;
(57)    ROR = 1.3 * RCHO + XO2 + HO2 + -2.3 * PAR  # 1.4315E+15 @-7000 ;
(58)    ROR = 0.615 * XO2 + HO2 + 0.185 * RCHO
              + -0.415 * PAR                      # 3.9E+5 ;

 ( ETHYLENE CHEMISTRY )
(59) O   + ETH = HCHO + XO2 + CO + 2.0 * HO2          # 15824 @-800;
(60) OH  + ETH = XO2 + 1.56 * HCHO + HO2 + 0.22 * RCHO # 3330.2 @382;
(61) O3  + ETH = HCHO + 0.37 * CO + 0.13 * HO2        # 37.2 @-2840;

 ( OLEFIN CHEMISTRY )
(62) O   + OLE = 0.95* RCHO + 0.35 * HO2 + 0.20 * XO2 + 0.15 * CO +
                0.05* HCHO + 0.05 * RCO3 + -0.35 * PAR
                                                      # 17559.3 @-324;
(63) OH  + OLE = HCHO + RCHO + XO2 + HO2 + -1.0 * PAR
                                                      # 6928.6 @537;
```

```
(64) O3  + OLE = 0.5 * RCHO + 0.66 * HCHO + 0.212 * CO + 0.28 * HO2 +
               0.144 * XO2 + 0.08 * OH + -1.0 * PAR
                                                        # 10.5 @-1897;
(65) NO3 + OLE = 0.91 * XO2 + 0.91 * HO2 + 0.09 * XO2N # 11.4;

( OMIT FOR NOW ....
 ( ISOPRENE CHEMISTRY )
(66) ISOP+ O   = HO2 + 0.8 * RCHO + 0.55 * OLE + 0.5 * XO2 +  0.5 * CO +
                 0.45 * ETH + -0.1 * PAR                # 28000;
(67) ISOP+ OH  = 0.87 * XO2 + 0.87 * HCHO + 0.87 * HO2 + 0.29 * PAR +
                 0.29 * OLE + 0.58 * ETH + 0.29 * RCHO   # 126000;
(68) ISOP+ O3  = HCHO + 0.45 * RCHO + 0.55 * ETH + 0.98 * HO2 +
                 0.1* OLE + 0.06* CO + -0.45* PAR       # 0.018;
(69) ISOP+ NO3 = XO2N                          # 165;
 ... END OF OMIT )


 ( TOLUENE CHEMISTRY )
(66) TOL + OH  = HO2 + 0.64 * XO2 + 1.13 * HCHO + 0.56 * MGLY +
               0.36 * PHEN + 0.36 * PAR + 1.13 * CO  # 9750;

 ( XYLENE CHEMISTRY )
(67) XYL + OH  = HO2 + 0.72 * XO2 + 0.67 * CO + 1.33 * MGLY +
              0.28 * PHEN + 0.56 * PAR + 0.06 * TLA + 0.67 * HCHO
                                               # 36000;
(68) TLA + OH  = XO2 + PHO + 2.0 * PAR         # 20000;

(69) PHEN+ NO3 = PHO + HNO3                    # 14000;
(70) PHO + NO2 =                               # 20000;

$0: ( Background HC, CO, O3 brought in with dilution air... )
    = 0.50*CO + 0.07*O3 + 0.005*HCHO + 0.0025*RCHO +
      0.0028*PAR + 0.001*ETH + 0.0005*OLE + 0.0008*TOL #1.0/D;

 ( WALL REACTIONS )
             NO2      = 0.21 * HONO + 0.79 * HNO3 #1.6E-4;
             NO2WALL  = NO2                      #0.01/L1;
             HCHOWALL = HCHO                     #0.02/L1;
!  ( Do not dilute the wall species ... )
NO2WALL/N
HCHOWALL/N
```

Table 4. The Carbon Bond Four, Version Two Mechanism Used in Chamber Simulations

```
Carbon Bond 4.2, Chamber Version, Sub 3.2(K&C)
!*********************************************************************
!This file obtained from Mike Gery on floppy October 1987.
! CB4.1 is from January Report, EPA-600/3-86-012 (Whitten and Gery)
! Changes to CB4.1 get CB4.2:
!  1. New inorganic rates added based upon UNC mech comparison report
!  2. Rates marked with (*) are further updates made by Gery
!       and may be changed upon final agreement.
!  3. Explicit O1D chemistry added
!  4. Rxn #41 removed (HO2 + RCHO)
!  5. New PAR chemistry with explicit ROR
!  6. New ETH and OLE splits and rates.
!  7. New species OPEN, TO2 from TOL and XYL to make HCHO explicit again
!  8. Rename PHEN and PHO to CRES and CRO and increase rates
!  9. New TOL and XYL chemistries
! 10. New XO2 chemistry and disproportionation products from
!       HO2 reactions
! 11. New ISOP chemistry
! 12. new PAN formation rate
!
! Rates assume [O2]=209000 PPM [M]=1000000 PPM at 1 atm, 298 K
!
!Emission and Aloft Fractions from UNC's HC composition report
!
!Converted to in-chamber Jspectra rates June 12, 1988.
!Six PhotRate Tables are Required.
!L1:NO2 L2:HCHO=HO2x1000 L3:HCHO=H2x1000 L4:O3=O1Dx1000 L5:RCHO=RADx1000
!L6:O3=O3Px1000
!Ratios of other photolysis reactions based on JL0986 comparison of
!all rates with these six (see JL0986.WK1).
!Photolysis ratios last updated: June 25, 1988
!***************************************************************************)

   ( INORGANIC CHEMISTRY )

(  1)              NO2   = NO   + O          # 1.0  /L1     ;
(  2)  O  (+ O2   + M   ) = O3  (+ M   )     # (*)83830.     @ 1175.        ;
(  3) O3   + NO           = NO2 (+ O2  )     # (*)2.643E+03  @-1370.        ;

(  4)  O   + NO2          = NO  (+ O2  )     # 1.375E+04                    ;
(  5)  O   + NO2 (+ M   ) = NO3 (+ M   )     # (*)230.284    @ 687.         ;
(  6)  O   + NO  (+ M   ) = NO2 (+ M   )     # (*)323.31     @ 602.         ;
!
```

Table 4 The CB4.2 Mechanism, Chamber Version, cont.

```
    ( NO3 CHEMISTRY )
(  7) O3   + NO2          = NO3 (+ O2  )      # 176.00        @-2450.       ;
(  8)        NO3          = 0.90*NO2 + 0.90*O + 0.10*NO
                                              # 0.428/L6;
(  9) NO3  + NO           = 2.0*NO2           # (*)19086      @ 250.        ;
( 10) NO3  + NO2          = NO    + NO2       # 36.6          @-1230.       ;
( 11) NO3  + NO2 (+ M   ) = N2O5 (+ M      )  # (*)784.88     @ 256.        ;
( 12) N2O5 (+ M        ) = NO3 + NO2 (+M   )  # 2.11E+16      @-10897.      ;
( 13) N2O5 (+ H2O      ) = 2.0*HNO3           # (*)1.4E-5/W     ;
                                                (^changed from 1.9E-6)
(... following two rxns are omitted for now...
      NO3  + HO2          = HNO3              # 341.35        @ 771.        ;
      NO3  + HO2          = HNO3              # 0.25254       @ 2971.       ;
 ... end of omit )

( 14) O3                  = O   (+ O2  )      # 0.001/L6 ;
( 15) O3                  = O1D (+ O2  )      # 0.001/L4 ;
( 16) O1D (+ M         ) = O   (+ O2  )       # (*)1.147E5(1E+5)@ 390.        ;
( 17) O1D (+ H2O       ) = 2.0*OH             # 3.26(1E+5)/W     ;
                (above rates were multiplied by 1E-5 to lower stiffness)

( 18) O3   + OH           = HO2 (+ O2  )      # 2343.8        @-940.        ;
( 19) O3   + HO2          = OH  (+ 2O2 )      # 21.0          @-580.        ;

( 20) NO   + NO  (+ O2  ) = 2.0*NO2           # 2.60E-5       @ 530.        ;

    ( HONO CHEMISTRY )
( 21) NO   + NO2 (+ O2  ) = 2.0*HONO          # 1.6E-11/W ;
( 22) HONO + HONO         = NO   + NO2 (+H2O) # 1.5E-5                      ;
( 23) OH   + NO  (+ M   ) = HONO (+ M      )  # 655.44        @ 806.        ;
( 24)        HONO         = OH   + NO         # 0.171/L1 ;
( 25) OH   + HONO         = NO2  (+ H2O    )  # 9770.                       ;

( 26) HO2  + NO           = OH   + NO2        # 5482.1        @ 242.        ;

( 27) HO2  + NO2 (+ M   ) = PNA (+ M       )  # 164.0         @ 749.        ;
( 28) PNA  (+ M        ) = HO2 + NO2 (+M   )  # 2.876E+15     @-10121.      ;
( 29) OH   + PNA          = NO2 (+H2O  + O2 ) # 1909.         @ 380.        ;

( 30) OH   + NO2 (+ M   ) = HNO3              # 1536.78       @ 713.        ;
( 31) OH   + HNO3         = NO3               # (*)7.6        @ 1000.       ;

( 32) HO2  + HO2          = H2O2 (+ O2)       # 87.39         @ 1150.       ;
( 33) HO2  + HO2 (+ H2O ) = H2O2 (+ O2 + H2O) # 7.69E-10      @ 5800.  /W   ;
( 34)              H2O2   = 2*OH              # 0.293E-3/L2     ;

( 35) OH   + H2O2         = HO2  (+ H2O    )  # 4719.8        @-187         ;

( 36) OH   + CO  (+ M   ) = HO2  (+ CO2    )  # 322.0                       ;
( 37) OH  (+ CH4)         = XO2 + HCHO + HO2  # 6521          @-1710        ;
```

Table 4 The CB4.2 Mechanism, Chamber Version, cont.

```
 ( FORMALDHYDE CHEMISTRY )
( 38)        HCHO = 2*HO2 + CO                # 0.001/L2 ;
( 39)        HCHO = CO                        # 0.001/L3 ;
( 40) HCHO + OH   = HO2   + CO                # 15000                          ;
( 41) HCHO + O    = OH   + HO2 + CO           # 43019.2      @-1550            ;
( 42) HCHO + NO3  = HNO3 + HO2 + CO           # 0.93                           ;

 ( HIGHER ALDEHYDE CHEMISTRY )
( 43)        RCHO = XO2  + 2*HO2 + CO + HCHO  # 0.001/L5 ;

( 44) RCHO + O    = C2O3 + OH                 # 17394.7      @-986             ;
( 45) RCHO + OH   = C2O3                      # 10372.2      @ 250             ;
( 46) RCHO + NO3  = C2O3 + HNO3               # 3.7                            ;

 ( DICARBONYL CHEMISTRY )
( 47)        MGLY = C2O3 + HO2 + CO           # 0.021/L1 ;
                                               (^Gery uses 9.64/L2)
( 48) OH   + MGLY = XO2 + C2O3                # 26000.                         ;

 ( PAN CHEMISTRY )
( 49) C2O3 + NO   = NO2  + XO2 + HCHO + HO2   # 7915.0       @ 250             ;
( 50) C2O3 + NO2  = PAN                       # 0.000118     @ 5500            ;
( 51)        PAN  = C2O3 + NO2                # 5.616E18     @-14000 ;

( 52) C2O3+ C2O3  = 2*XO2 + 2*HCHO + 2*HO2     # 3700                          ;
( 53) C2O3+ HO2   = 0.79*HCHO + 0.79*XO2
                  + 0.79*HO2 + 0.79*OH        # 9600                           ;

 ( PARAFFIN CHEMISTRY )
( 54) OH  + PAR   = 0.87*XO2 + 0.13*XO2N + 0.11*HO2 + 0.11*RCHO
                  + 0.76*ROR + -0.11*PAR       # 1203.0                          ;
( 55)       ROR   = 1.1*RCHO + 0.96*XO2 + 0.94*HO2 + -2.1*PAR
                  + 0.04*XO2N + 0.02*ROR       # 6.2495E+16   @-8000           ;
( 56)       ROR   = HO2 (+ KET)               # 95455.                         ;
( 57) ROR + NO2   = (NTR)                     # 22000.                         ;
```

Table 4 The CB4.2 Mechanism, Chamber Version, cont.

```
 ( ETHYLENE CHEMISTRY )
( 58)  O  + ETH   = HCHO + 0.70*XO2 + CO + 1.70*HO2+ 0.30*OH
                                      # 15400       @-792        ;
( 59) OH  + ETH   = XO2 + 1.56*HCHO + HO2 + 0.22*RCHO
                                      # 3000        @ 411        ;
( 60) O3  + ETH   = HCHO + 0.42*CO + 0.12*HO2 # 18.56   @-2633   ;

 ( OLEFIN CHEMISTRY )
( 61)  O  + OLE   = 0.63*RCHO + 0.38*HO2 + 0.28*XO2 + 0.30*CO
                 + 0.20*HCHO + 0.02*XO2N + 0.22*PAR + 0.20*OH
                                      # 17560.0     @-324        ;
( 62) OH  + OLE   = HCHO + RCHO + XO2 + HO2 + -1*PAR
                                      # 7740.0      @ 504        ;
( 63) O3  + OLE   = 0.5*RCHO + 0.74*HCHO + 0.33*CO + 0.44*HO2
                 + 0.22*XO2 + 0.10*OH + -1.0*PAR
                                        # 21.04     @-2105       ;
( 64) NO3 + OLE   = 0.91*XO2 + 0.09*XO2N + HCHO + RCHO + -1*PAR
                 + NO2                # 11.35                    ;

 ( ISOPRENE CHEMISTRY--CONDENSED )
(**** omit isoprene chemistry for now...
( 65) O    + ISOP = 0.6*HO2 + 0.80*RCHO + 0.55*OLE + 0.50*XO2
                 + 0.50*CO + 0.45*ETH + 0.9*PAR
                                        # 27000.                 ;
( 66) OH   + ISOP = XO2 + HCHO(+ 0.05*PAR) + 0.67*HO2 + 0.13*XO2N
                 + 1.0*ETH + 0.4*MGLY + 0.2*C2O3 + 0.2*RCHO
                                      # 142000.                  ;
( 67) O3   + ISOP = HCHO + 0.4*RCHO + 0.55*ETH + 0.2*MGLY
                 + 0.10*PAR + 0.06*CO + 0.44*HO2 +0.1*OH
                                      # 0.018                    ;
( 68) NO3  + ISOP = XO2N              # 470.                     ;
... end of omit )
```

Table 4 The CB4.2 Mechanism, Chamber Version, cont.

```
 ( TOLUENE CHEMISTRY )
( 65) OH   + TOL  = 0.08*XO2 + 0.36*CRES + 0.44*HO2 + 0.56*TO2
                                           # 3105.6       @322.            ;
( 66) TO2  + NO   = 0.90*NO2 + 0.90*HO2 + 0.90*OPEN
                                           # 12000.                        ;
( 67) TO2         = CRES + HO2             # 250                           ;
( 68) OH   + CRES = 0.4*CRO + 0.60*XO2 + 0.60*HO2 + 0.30*OPEN
                                           # 61000                         ;
( 69) NO3  + CRES = CRO + HNO3             # 32500                         ;
( 70) CRO  + NO2=                          # 20000                         ;
( 71) OPEN        = C2O3 + HO2 + CO        # 0.021/L1 ;
( 72) OPEN + OH = XO2 + 2.0*CO + 2.0*HO2 + C2O3 + HCHO
                                           # 44000.                        ;
( 73) OPEN + O3 = 0.03*RCHO + 0.62*C2O3 + 0.70*HCHO + 0.03*XO2
                + 0.69*CO + 0.08*OH + 0.76*HO2 + 0.2*MGLY
                                           # 0.0803       @-500.           ;

 ( XYLENE CHEMISTRY )
( 74) OH   + XYL = 0.70*HO2 + 0.50*XO2 + 0.20*CRES + 0.80*MGLY
                + 1.10*PAR + 0.30*TO2      # 24527.56     @ 116.           ;

 (Operator Chemistry)
( 75) XO2  + NO   = NO2                    # 12000.0                       ;
( 76) XO2N + NO   = (NTR)                  # 1000.0                        ;
( 77) XO2  + XO2  =                        # 25.5          @ 1300.         ;

( 78) OH   + MEOH = HCHO + HO2             # 1.98E+04@-805.;

! Include the Mechanism Independent Chamber Wall reactions
@stdcham.rxn

! Include the Mechanism Specific Wall Models (Killus and Std Carter)
@WalMod4.Rxn
|
```

Table 4 The CB4.2 Mechanism, Chamber Version, cont.

```
! This is WalMod4.Rxn file
! Mechanism specific Wall models for CB4.2
! Killus's model for CAL mechanism based upon SAI report
! and personal communication with Killus.
! The Killus Model is initially turned off
$1: ( Background HC brought in with dilution air...0.038 ppmC NMOC )
     = 0.005*HCHO + 0.0025*RCHO + 0.0028*PAR +
       0.001*ETH + 0.0005*OLE + 0.0008*TOL        #0.0 (1.0)/D;
                      = HONO                      #0.0 (0.11E-3)/L1;
                      = HCHO                      #0.0 (0.22E-3)/L1;

! Carter Model based upon telephone conversation with Carter August, 1988
! This model is initially turned on.
$2:
                   OH = NO2                       #250.0;
                      = OH                          #0.30E-3/L1;
                      = NO2                         #0.11E-3/L1;


! This is StdCham.Rxn file:
! Mechanism independent chamber and wall reactions

    ( ENTRAINED WITH DILUTION AIR)
                 = 0.50*CO + 0.07*O3          #1.0/D;
    ( WALL REACTIONS )
        NO2      = 0.21 * HONO + 0.79 * HNO3 #1.6E-4;
        O3       =                            #1.8E-4;
```

3

ICRS Reconciliation

This chapter first describes work we did at the beginning of the project to compare the reactions and rate constants that were selected by each development group. Later it describes some of the subsequent changes made by the developers.

ICRS is a term used by SAI for *Inorganic and Carbonyl Reaction Set* and these reactions represent the most basic part of a chemical mechanism. The kinetics information sources that supports these parts of both mechanisms are supposed to be so well understood and agreed upon that essentially no differences should be expected between the two mechanisms.[19,20,21,22,23,24] As we shall see there were small, but nevertheless important, differences between the two mechanisms that caused differences between their predictions in even the most simple of simulations. Resolving these differences was important for subsequent testing of the mechanisms.

Procedure

The CAL OZIPM mechanism has 36 inorganic reactions, the CB4 mechanism has 34 inorganic reactions, and the CBX mechanism has 36 inorganic reactions. CB4.1 has some "lumped" inorganic reactions that CBX does not. We decided to use the inorganic and formaldehyde set from CBX as being more closely comparable with CAL for the tests described herein. Later we will show what was changed between CBX and CB4.1.

Both the CAL and the CBX ICRS's were sorted into the same order. The sorted mechanism listings appear in Tables 5 through 7. There were five reactions that appeared in the CBX mechanism that did not appear in the CAL mechanism (6, 27, 28, 44, 49) and there were six reactions that appeared in the CAL mechanism that did not appear in CBX mechanism (15,16,32,46,47,48). The five CBX reactions were added to the CAL set, but with a zero rate, and the six CAL reactions were added to the CBX set, also with a zero rate. Of the fifty reactions in the intercomparison, 39 were inorganic and 11 were for HCHO (The three $RO_2^{\cdot}$ balancing reactions in the CAL mechanism are not counted). Thus one item that needs reconciliation is how important are the reactions that were not included in both mechanisms, and should these have been included in both, or could they be dropped from both.

There is one reaction omitted from the CAL mechanism that could have a large impact on the simulations of certain experiments as was discussed by Carter *et al.*[6]. The reaction is (44). The reaction sequence is

$$HO_2^{\cdot} + HCHO \longrightarrow HOCH_2O_2^{\cdot} \qquad (43)$$

$$HOCH_2O_2^{\cdot} \longrightarrow HO_2^{\cdot} + HCHO \qquad (44)$$

$$HOCH_2O_2^{\cdot} + NO \longrightarrow NO_2 + HO_2^{\cdot} + HOCHO \qquad (45)$$

where the rate constants are

(43)	14.8	ppm^{-1}-min^{-1}	in both
(44)	90.0	min^{-1}	in CBX
(44)	0.0	min^{-1}	in CAL
(45)	11,000	ppm^{-1}-min^{-1}	in both

The $HOCH_2O_2^{\cdot}$ radical is formed by isomerization of the $HO_2CH_2O^{\cdot}$ radical. Carter's original discussion of this reaction (page II-49 of reference 6) consisted of a single sentence in which he stated that reaction 44 would be "negligible under atmospheric conditions" and thus he ignored the reaction. In none of the three papers cited in his discussion of the rate constant for reaction 43, (*i.e.*, Su *et al.*[25], Vegret, *et al.*[26] and Barnes *et al.*[27]) was reaction 44 considered to be negligible. In fact, its rate was given by Su *et al.* as being 90.0/min, the rate used by Whitten and Gery, and the 1985 Barnes paper suggested that reaction 43's rate was a factor of 10 higher and reaction 44's rate was a factor of 13 higher than the Su *et al.* values. A large rate for reaction 44 makes the significance of reaction 45 much less, and invalidates the modeling tests Carter showed on pages II-51–53 of his report. Further, it conflicts with the peroxy radical generalization used by Carter in that he used the generalized species RO2R to represent $HOCH_2O_2^{\cdot}$ which can only work if reaction 44 is ignored. If reaction 44 has a non-zero rate, then an explicit representation for the unique chemistry of $HOCH_2O_2^{\cdot}$ must be included, and at least one additional species would be needed. Thus, for comparison purposes here, we have replaced Carter's RO2R species with FROX in the CAL ICRS. For initial testing purposes, however, we have set the rate of reaction 44 to 0.0 as did Carter.

Table 5. CAL Inorganic and HCHO Mechanism

```
Carter, Atkinson, Lurman, Mechanism -- Chamber HCHO Only Version
  1)        NO2  -HV1--> NO      + O                           1.00E+00
  2)        O    ------> O3                                    6.30E+04*EXP(  1282/T)
  3) O3   + NO   ------> NO2                                   2.57E+03*EXP( -1370/T)
  4) O    + NO2  ------> NO                                    1.37E+04
  5) O    + NO2  ------> NO3                                   1.64E+02*EXP(   894/T)
  6) O    + NO   ------> NO2                                   0.00E+00
  7) O3   + NO2  ------> NO3                                   1.67E+02*EXP( -2450/T)
  8)        NO3  -HV1--> NO                                    4.59E+00
  9)        NO3  -HV1--> NO2     + O                           2.60E+01
 10) NO3  + NO   ------>  2.00NO2                              1.18E+04*EXP(   252/T)
 11) NO3  + NO2  ------> NO      + NO2                         3.59E+01*EXP( -1229/T)
 12) NO3  + NO2  ------> N2O5                                  6.90E+02*EXP(   270/T)
 13)        N2O5 ------> NO2     + NO3                         1.11E+16*EXP(-10790/T)
 14)        N2O5 ------>  2.00HNO3                       (H2O)*1.90E-05
 15) NO3  + HO2  ------> HNO3                                  3.41E+02*EXP(   771/T)
 16) NO3  + HO2  ------> HNO3                                  2.52E-01*EXP(  2971/T)
 17)        O3   -HV1--> O                                     4.20E-02
 18)        O3   -HV4--> O1D                                   1.00E-03
 19)        O1D  ------>  2.00OH                         (H2O)*3.26E+00
 20)        O1D  ------> O                                     4.32E+05
 21) O3   + OH   ------> HO2                                   2.31E+03*EXP(  -942/T)
 22) O3   + HO2  ------> OH                                    2.03E+01*EXP(  -579/T)
 23) NO   + NO   ------>  2.00NO2                              2.45E-05*EXP(   529/T)
 24)        NO2  ------> HONO    + -1.00NO2     + HNO3
                                                               1.17E-04
 25) OH   + NO   ------> HONO                                  5.92E+02*EXP(   833/T)
 26)        HONO -HV1--> NO      + OH                          1.80E-01
 27) OH   + HONO ------> NO2                                   0.00E+00
 28) HONO + HONO ------> NO      + NO2                         0.00E+00
 29) HO2  + NO   ------> NO2     + OH                          5.48E+03*EXP(   240/T)
 30) HO2  + NO2  ------> HNO4                                  2.49E+02*EXP(   632/T)
 31)        HNO4 ------> NO2     + HO2                         4.20E+15*EXP(-10240/T)
 32) OH   + HNO4 ------> NO2                                   5.91E+03
 33) OH   + NO2  ------> HNO3                                  2.18E+03*EXP(   617/T)
 34) OH   + HNO3 ------> NO3                                   1.41E+01*EXP(   778/T)
 35) HO2  + HO2  ------> H2O2                                  3.41E+02*EXP(   771/T)
 36) HO2  + HO2  ------> H2O2                                  2.52E-01*EXP(  2971/T)
 37)        H2O2 -HV2-->  2.00OH                               3.21E-04
 38) OH   + H2O2 ------> HO2                                   4.56E+03*EXP(  -187/T)
 39) OH   + CO   ------> HO2                                   3.22E+02
 40)        HCHO -HV2-->  2.00HO2     + CO                     1.00E-03
 41)        HCHO -HV3--> CO                                    1.00E-03
 42) OH   + HCHO ------> HO2     + CO                          1.33E+04
 43) HO2  + HCHO ------> FROX    + RO2                         1.48E+01
 44)        FROX ------> HO2     + HCHO                        0.00E+00
 45) FROX + NO   ------> FACID   + NO2     + HO2               6.25E+03*EXP(   180/T)
 46) FROX + HO2  ------> ROOH                                  4.43E+03
 47) FROX + RO2  ------>  0.50HO2     + RO2                    1.48E+00
 48)        ROOH -HV2--> HO2     + OH                          3.21E-04
 49) O    + HCHO ------> OH      + HO2     + CO                0.00E+00
 50) NO3  + HCHO ------> HNO3    + HO2     + CO                8.46E+02*EXP( -2060/T)
 51) RO2  + NO   ------> NO                                    6.25E+03*EXP(   180/T)
 52) RO2  + HO2  ------> HO2                                   4.43E+03
 53) RO2  + RO2  ------>                                       1.48E+00
```

Table 6. CB4 Inorganic and HCHO Mechanism

```
CBX Mechanism, Chamber HCHO-Only Version
 1)        NO2  -HV1--> NO      + O                       1.00E+00
 2)        O    ------> O3                                4.60E+05*EXP(   690/T)
 3) O3   + NO   ------> NO2                               3.22E+03*EXP( -1430/T)
 4) O    + NO2  ------> NO                                1.38E+04
 5) O    + NO2  ------> NO3                               3.09E+02*EXP(   600/T)
 6) O    + NO   ------> NO2                               7.85E+02*EXP(   411/T)
 7) O3   + NO2  ------> NO3                               1.76E+02*EXP( -2450/T)
 8)        NO3  -HV1--> NO                                4.59E+00
 9)        NO3  -HV1--> NO2     + O                       2.60E+01
10) NO3  + NO   ------>  2.00NO2                          1.21E+04*EXP(   250/T)
11) NO3  + NO2  ------> NO      + NO2                     3.66E+01*EXP( -1230/T)
12) NO3  + NO2  ------> N2O5                              8.31E+02*EXP(   226/T)
13)        N2O5 ------> NO3     + NO2                     1.96E+16*EXP(-10840/T)
14)        N2O5 ------>  2.00HNO3                    (H2O)*1.90E-05
15) NO3  + HO2  ------> HNO3                              0.00E+00
16) NO3  + HO2  ------> HNO3                              0.00E+00
17)        O3   -HV1--> O                                 4.20E-02
18)        O3   -HV4--> O1D                               1.00E-03
19)        O1D  ------>  2.00OH                      (H2O)*3.26E+00
20)        O1D  ------> O                                 4.32E+05
21) O3   + OH   ------> HO2                               2.34E+03*EXP(  -940/T)
22) O3   + HO2  ------> OH                                2.10E+01*EXP(  -580/T)
23) NO   + NO   ------>  2.00NO2                          2.60E-05*EXP(   530/T)
24) NO   + NO2  ------>  2.00HONO                    (H2O)*1.60E-11
25) OH   + NO   ------> HONO                              2.33E+03*EXP(   427/T)
26)        HONO -HV1--> OH      + NO                      1.80E-01
27) OH   + HONO ------> NO2                               9.77E+03
28) HONO + HONO ------> NO      + NO2                     1.50E-05
29) HO2  + NO   ------> OH      + NO2                     5.49E+03*EXP(   240/T)
30) HO2  + NO2  ------> PNA                               2.05E+02*EXP(   617/T)
31)        PNA  ------> HO2     + NO2                     7.85E+15*EXP(-10420/T)
32) OH   + PNA  ------> NO2                               0.00E+00
33) OH   + NO2  ------> HNO3                              2.48E+03*EXP(   560/T)
34) OH   + HNO3 ------> NO3                               1.41E+01*EXP(   778/T)
35) HO2  + HO2  ------> H2O2                              8.73E+01*EXP(  1150/T)
36) HO2  + HO2  ------> H2O2                         (H2O)*7.69E-10*EXP(  5800/T)
37)        H2O2 -HV2-->  2.00OH                           3.21E-04
38) OH   + H2O2 ------> HO2                               4.71E+03*EXP(  -187/T)
39) OH   + CO   ------> HO2                               4.00E+02
40)        HCHO -HV2-->  2.00HO2     + CO                 1.00E-03
41)        HCHO -HV3--> CO                                1.00E-03
42) OH   + HCHO ------> HO2     + CO                      1.50E+04
43) HO2  + HCHO ------> FROX                              1.48E+01
44)        FROX ------> HO2     + HCHO                    9.00E+01
45) FROX + NO   ------> FACID   + NO2     + HO2           1.04E+04
46) FROX + HO2  ------> ROOH                              0.00E+00
47) FROX + RO2  ------>  0.50HO2     + RO2                0.00E+00
48)        ROOH ------> HO2     + OH                      0.00E+00
49) O    + HCHO ------> OH      + HO2     + CO            4.30E+04*EXP( -1550/T)
50) NO3  + HCHO ------> HNO3    + HO2     + CO            9.30E-01
```

Table 7. Comparison of Rate Constants

	CAL Mechanism			CBX Mechanism			
Num	A	E	k, 298 K	A	E	k, 298 K	Rxn
1)	1.00E+00		1.00E+00	1.00E+00		1.00E+00	NO2=NO+O
2)	6.30E+04	1282	4.65E+06	4.60E+05	690	4.66E+06	O=O3
3)	2.57E+03	-1370	2.59E+01	3.22E+03	-1430	2.65E+01	O3+NO=NO2
4)	1.37E+04		1.37E+04	1.38E+04		1.38E+04	O+NO2=NO
5)	1.64E+02	894	3.29E+03	3.09E+02	600	2.32E+03	O+NO2=NO3
6)	0.00E+00		0.00E+00	7.85E+02	411	3.12E+03	O+NO=NO2
7)	1.67E+02	-2450	4.51E-02	1.76E+02	-2450	4.73E-02	O3+NO2=NO3
8)	4.59E+00		4.59E+00	4.59E+00		4.59E+00	NO3=NO
9)	2.60E+01		2.60E+01	2.60E+01		2.60E+01	NO3=NO2+O
10)	1.18E+04	252	2.76E+04	1.21E+04	250	2.80E+04	NO3+NO=2.00NO2
11)	3.59E+01	-1229	5.81E-01	3.66E+01	-1230	5.90E-01	NO3+NO2=NO+NO2
12)	6.90E+02	270	1.70E+03	8.31E+02	226	1.77E+03	NO3+NO2=N2O5
13)	1.11E+16	-10790	2.09E+00	1.96E+16	-10840	3.12E+00	N2O5=NO3+NO2
14)	(H2O)*1.90E-05		3.80E-01	(H2O)*1.90E-05		3.80E-01	N2O5=2.00HNO3
15)	3.41E+02	771	4.53E+03	0.00E+00		0.00E+00	NO3+HO2=HNO3
16)	2.52E-01	2971	5.39E+03	0.00E+00		0.00E+00	NO3+HO2=HNO3
17)	4.20E-02		4.20E-02	4.20E-02		4.20E-02	O3=O
18)	1.00E-03		1.00E-03	1.00E-03		1.00E-03	O3=O1D
19)	(H2O)*3.26E+00		6.52E+04	(H2O)*3.26E+00		6.52E+04	O1D=2.00OH
20)	4.32E+05		4.32E+05	4.32E+05		4.32E+05	O1D=O
21)	2.31E+03	-942	9.79E+01	2.34E+03	-940	9.99E+01	O3+OH=HO2
22)	2.03E+01	-579	2.92E+00	2.10E+01	-580	2.99E+00	O3+HO2=OH
23)	2.45E-05	529	1.44E-04	2.60E-05	530	1.53E-04	NO+NO=2.00NO2
24)	1.17E-04		1.17E-04	(H2O)*1.60E-11		3.20E-07	NO+NO2=2.00HONO
25)	1.06E+03	670	1.00E+04	2.33E+03	427	9.76E+03	OH+NO=HONO
26)	1.80E-01		1.80E-01	1.80E-01		1.80E-01	HONO=OH+NO
27)	0.00E+00		0.00E+00	9.77E+03		9.77E+03	OH+HONO=NO2
28)	0.00E+00		0.00E+00	1.50E-05		1.50E-05	HONO+HONO=NO+NO2
29)	5.48E+03	240	1.22E+04	5.49E+03	240	1.23E+04	HO2+NO=OH+NO2
30)	2.49E+02	632	2.07E+03	2.05E+02	617	1.63E+03	HO2+NO2=PNA
31)	4.20E+15	-10240	5.01E+00	7.85E+15	-10420	5.11E+00	PNA=HO2+NO2
32)	5.91E+03		5.91E+03	0.00E+00		0.00E+00	OH+PNA=NO2
33)	2.18E+03	617	1.73E+04	2.48E+03	560	1.62E+04	OH+NO2=HNO3
34)	1.41E+01	778	1.92E+02	1.41E+01	778	1.92E+02	OH+HNO3=NO3
35)	3.41E+02	771	4.53E+03	8.73E+01	1150	4.14E+03	HO2+HO2=H2O2
36)	2.52E-01	2971	5.39E+03	(H2O)*7.69E-10	5800	4.36E+03	HO2+HO2=H2O2
37)	3.21E-04		3.21E-04	3.21E-04		3.21E-04	H2O2=2.00OH
38)	4.56E+03	-187	2.43E+03	4.71E+03	-187	2.51E+03	OH+H2O2=HO2
39)	3.22E+02		3.22E+02	4.00E+02		4.00E+02	OH+CO=HO2
40)	1.00E-03		1.00E-03	1.00E-03		1.00E-03	HCHO=2.00HO2+CO
41)	1.00E-03		1.00E-03	1.00E-03		1.00E-03	HCHO=CO
42)	1.33E+04		1.33E+04	1.50E+04		1.50E+04	OH+HCHO=HO2+CO
43)	1.48E+01		1.48E+01	1.48E+01		1.48E+01	HO2+HCHO=FROX
44)	0.00E+00		0.00E+00	9.00E+01		9.00E+01	FROX=HO2+HCHO
45)	6.25E+03	180	1.14E+04	1.04E+04		1.04E+04	FROX+NO=NO2+HO2
46)	4.43E+03		4.43E+03	0.00E+00		0.00E+00	FROX+HO2=ROOH
47)	1.48E+00		1.48E+00	0.00E+00		0.00E+00	FROX+RO2=0.50HO2+RO2
48)	3.21E-04		3.21E-04	0.00E+00		0.00E+00	ROOH=HO2+OH
49)	0.00E+00		0.00E+00	4.30E+04	-1550	2.37E+02	O+HCHO=OH+HO2+CO
50)	8.46E+02	-2060	8.42E-01	9.30E-01		9.30E-01	NO3+HCHO=HNO3+HO2+CO
51)	6.25E+03	180	1.14E+04				RO2+NO=NO
52)	4.43E+03		4.43E+03				RO2+HO2=HO2
53)	1.48E+00		1.48E+00				RO2+RO2=

Simulations Using Original Rates

Comparison of Rates

Table 7 shows that although the rates at 298 K in both CAL and CBX are often very similar, the Arrhenius expressions are frequently not (for example see reaction 2 in which CAL has an E_a nearly twice that for CBX). These differences in Arrhenius expressions will be addressed in the next section. In addition to the Arrhenius expression differences, there are also some absolute differences at 298 K. Although these differences appear to be only about 5% (for example reaction 7), unless we know how important each reaction is to the overall transformation process, it is difficult to translate a difference in a rate constant to the impact such differences will have in a non-linear system. Therefore, to address this type of difference, we performed simulations.

Simple conditions were chosen for the simulation:

- one level of NO_X: 0.3 ppm (0.28 ppm NO, 0.02 ppm NO_2);
- two levels of HCHO: (1.0 ppm and 0.5 ppm);
- 298 K; same photolytic rate constants in both mechanisms; and
- no chamber effects; no entrainment; and minimal dilution.

Figure 4 shows the simulation results for NO_X, HNO_3, and O_3 for both mechanisms for both levels of HCHO. CBX had more NO_2 at the peak, made more O_3, and in the lower HCHO case, made less HNO_3. Table 8 compares the integrated reaction rates, that is, the total mass that passed through each reaction in the 600 minutes of the simulation for both mechanisms, and includes the ratio of CAL-to-CBX, as well as the reactions from the CAL listing. Whereas the rate constant for reaction 7 (O_3+ NO_2) only differed by 5%, the reaction's mass difference was 23%. Further, a significant amount of O_3 reacted by this pathway (0.28 vs. 0.37 ppm, a difference of about 0.08 ppm, approximately twice the final O_3 difference).

Other reaction differences that stand out in Table 8 are:

- R29: $HO_2^{\cdot} + NO \rightarrow NO_2 + HO^{\cdot}$, CAL had less mass (ratio of 0.94);
- R33: $HO^{\cdot} + NO_2 \rightarrow HNO_3$, both had same
- R39: $HO^{\cdot} + CO \rightarrow CO_2$, CAL had less mass (0.81)
- R42: $HO^{\cdot} + HCHO \rightarrow CO + HO_2^{\cdot}$, CAL had less mass (0.95)

In the last three cases, the differences are directly related to differences in the chosen rate constants. That is, the CAL mechanism has a slightly higher rate constant for R33 (17,000 vs. 16,300), a lower rate constant for R39 (320 vs. 400), and a lower

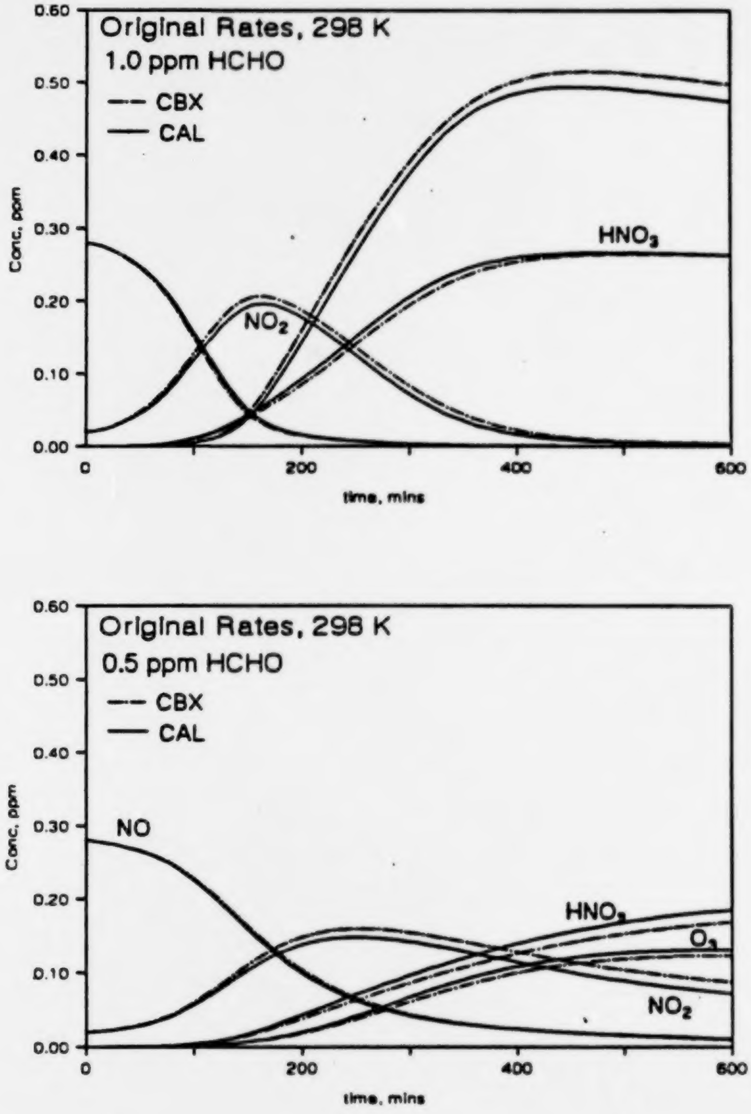

Figure 4. Comparison of CAL and CBX, Original Rates.

Table 8. Integrated Rates and Ratio for 1.0 ppm HCHO and 0.3 ppm NO_x.

Rxn	Ratio CAL/CBX	CAL HCHO--orig rates, 298 K ppm	CBX HCHO--orig rates, 298 K ppm	@ T=600.0, mins
1	0.899	13.47671	14.98976	NO2=NO+O
2	0.911	17.46750	19.17314	O=O3
3	0.900	12.63315	14.03768	O3+NO=NO2
4	0.854	0.005470	0.006409	O+NO2=NO
5	1.221	0.001315	0.001077	O+NO2=NO3
6		0	0.000274	O+NO=NO2
7	0.776	0.289178	0.372798	O3+NO2=NO3
8	0.786	0.007234	0.009205	NO3=NO
9	0.786	0.040978	0.052142	NO3=NO2+O
10	0.755	0.215606	0.285443	NO3+NO=2.00NO2
11	0.684	0.000076	0.000111	NO3+NO2=NO+NO2
12	0.667	0.223355	0.334901	NO3+NO2=N2O5
13	0.633	0.189008	0.298359	N2O5=NO2+NO3
14	0.946	0.034347	0.036315	N2O5=2.00HNO3
15		0.000992	0	NO3+HO2=HNO3
16		0.001180	0	NO3+HO2=HNO3
17	0.956	3.766557	3.940574	O3=O
18	0.958	0.217931	0.227490	O3=O1D
19	0.958	0.028586	0.029840	O1D=2.00OH
20	0.958	0.189404	0.197714	O1D=O
21	0.945	0.009707	0.010275	O3+OH=HO2
22	0.914	0.037032	0.040509	O3+HO2=OH
23	0.969	0.000927	0.000956	NO+NO=2.00NO2
24		0.004756	0.000000	NO2=HONO+-1.00NO2+HNO3
25	1.087	0.034256	0.031520	OH+NO=HONO
26	1.287	0.040723	0.031635	HONO=NO+OH
27		0	0.001639	OH+HONO=NO2
28		0	0.000000	HONO+HONO=NO+NO2
29	0.939	0.873693	0.930211	HO2+NO=NO2+OH
30	1.080	1.807902	1.674463	HO2+NO2=HNO4
31	1.079	1.806434	1.673473	HNO4=NO2+HO2
32		0.001000	0	OH+HNO4=NO2
33	0.996	0.218735	0.219617	OH+NO2=HNO3
34	1.035	0.010488	0.010130	OH+HNO3=NO3
35	1.050	0.009715	0.009254	HO2+HO2=H2O2
36	1.186	0.011555	0.009740	HO2+HO2=H2O2
37	1.187	0.001285	0.001082	H2O2=2.00OH
38	1.144	0.004092	0.003576	OH+H2O2=HO2
39	0.809	0.092552	0.114421	OH+CO=HO2
40	1.023	0.105601	0.103252	HCHO=2.00HO2+CO
41	1.022	0.162955	0.159464	HCHO=CO
42	0.951	0.640891	0.673748	OH+HCHO=HO2+CO
43	1.015	0.042254	0.041646	HO2+HCHO=FROX+RO2
44		0	0.026293	FROX=HO2+HCHO
45	2.693	0.041283	0.015328	FROX+NO=FACID+NO2+HO2
46		0.000903	0	FROX+HO2=ROOH
47		0.000000	0	FROX+RO2=0.50HO2+RO2
48		0.000067	0	ROOH=HO2+OH
49		0	0.000348	O+HCHO=OH+HO2+CO
50	0.745	0.000350	0.000470	NO3+HCHO=HNO3+HO2+CO

rate constant for R42, $HO^{\cdot} + HCHO$, (13,300 vs. 15,000). The rate constant for R29, $HO_2^{\cdot} + NO$, however, is nearly identical at 298 K and a reaction flow analysis must be used to understand this difference.

Comparison of Mass Throughput

Tables 9and 10 show the integrated mass balance and a reaction flow diagram for both mechanisms for the 1.0 ppm HCHO simulation. The CAL values are given above the CBX values in the flow diagram. At the top of the flow chart in Table 10, which traces the $HO^{\cdot}$ to $HO_2^{\cdot}$ and back to $HO^{\cdot}$ cycle, we see that CAL produced a total of 970 ppb of $HO^{\cdot}$ compared to 1032 ppb $HO^{\cdot}$ produced by CBX. The photolytic sources of radicals were nearly the same in the two simulations (*i.e.*, 266 vs. 268 ppb). A significant cause of this difference was that the radical yield of $HO^{\cdot}$ from $HO_2^{\cdot}$ was only 0.91 for CAL but was 0.95 for CBX. The major cause of the lower yield in CAL was the use of zero rate for reaction 44 in CAL which allowed reaction 45 to be a significant pathway. (The radical yield in this case is determined by the ratio of $HO^{\cdot}$ that comes out the bottom of the flowchart to the $HO_2^{\cdot}$ that is available to react, *e.g.*, for CAL:

$$\frac{913.3\text{ppb}}{995.6\text{ppb}} = 0.91$$

The O_3 mass balance is shown in column 5 of Table 9. As discussed above, the small difference (5%) in R7 and R10's rate constant does not explain the 23% difference in reaction mass throughput shown in Table 9a. The role of $NO_3^{\cdot}$ in the daylight can be viewed as a second pathway for O_3 to convert NO to NO_2 via $NO_3^{\cdot}$. That is, the combined effect of reactions 7 through 14 is

$$O_3 + NO \xrightarrow{(NO_3^{\cdot})} 0.89\ NO_2 + 0.11\ HNO_3 \quad \text{for CBX}$$

$$O_3 + NO \xrightarrow{(NO_3^{\cdot})} 0.86\ NO_2 + 0.14\ HNO_3 \quad \text{for CAL}$$

where the coefficients are computed from the ratios of mass throughput in R10 and R14 to that in R7. As indicated by the coefficients, CAL has a higher radical termination rate through this process than does CBX. So not only does less mass go this way in CAL, each cycle is less effective in producing NO_2 than it is in CBX.

Clearly several rates in both mechanisms that appear to be "close" are not close enough. The next step therefore is to examine the sources of the kinetic data and the subsequent calculations performed by each modeling group in producing the rates for some of the reactions in each mechanism.

Table 9. Mass Balance for 1.0 ppm HCHO, Original Rates.

```
         CAL Mass Balance--Orig rates
                NO2        NO         O        O3       NO3      N2O5        OH       HO2      HNO3
R1         -13.4767   13.4767   13.4767
R2                            -17.4675   17.4675
R3          12.6332  -12.6332            -12.6332
R4          -0.0055    0.0055   -0.0055
R5          -0.0013             -0.0013              0.0013
R17&R20                          3.9560   -3.9845                          0.0572
R21&R22                                   -0.0467                          0.0273   -0.0273
R7          -0.2892                       -0.2892    0.2892
R8&R9        0.0410    0.0072    0.0410             -0.0482
R10          0.4312   -0.2156                       -0.2156
R12&R13     -0.0343                                 -0.0343    0.0343
R14                                                           -0.0343                         0.0687
R34                                                  0.0105             -0.0105              -0.0105
R15&R16                                             -0.0022                       -0.0022    0.0022
R29&R45      0.9150   -0.9150                                            0.8737   -0.8737
R33         -0.2187                                                     -0.2187               0.2187
Others      -0.0048                                 -0.0004                                   0.0051
====================================================================================================
Sum        -0.01019  -0.27433  -0.00064   0.51394   0.00029  -0.00000   0.72897  -0.90319   0.28422
           -0.28422 =NOx loss            =Net O3                                          =Final NOx
```

```
         CBX Mass Balance--Orig rates
                NO2        NO         O        O3       NO3      N2O5        OH       HO2      HNO3
R1         -14.9898   14.9898   14.9898
R2                            -19.1731   19.1731
R3          14.0377  -14.0377            -14.0377
R4          -0.0064    0.0064   -0.0064
R5          -0.0011             -0.0011              0.0011
R17&R20                          4.1383   -4.1681                          0.0597
R21&R22                                   -0.0508                          0.0302   -0.0302
R7          -0.3728                       -0.3728    0.3728
R8&R9        0.0521    0.0092    0.0521             -0.0613
R10          0.5709   -0.2854                       -0.2854
R12&R13     -0.0365                                 -0.0365    0.0365
R14                                                           -0.0363                         0.0726
R34                                                  0.0101             -0.0101              -0.0101
R15&R16                                              0.0000                        0.0000    0.0000
R29&R45      0.9455   -0.9455                                            0.9302   -0.9302
R33         -0.2196                                                     -0.2196               0.2196
Others      -0.0000                                 -0.0005              0.0000               0.0005

====================================================================================================
Sum        -0.01996  -0.26328  -0.00044   0.54382   0.00020   0.00023   0.79038  -0.96045   0.28259
           -0.28304 =NOx loss            =Net O3                                          =Final NOx
```

Table 10. Reactant Mass Flow for 1.0 ppm HCHO, Original Rates.

```
CAL vs CBX, 1.0 ppm HCHO
                          ppb,CAL new
298 K, 1 ppm HCHO        ppb,CBX new

+-----------------------------> 913.30 ------->Tot [OH] <--O3hv 57.17
|                              972.89            970.47           59.68
|                                93.9%         1032.57
|                                                 94.0%
|                                                  |
|                                                  |
|            Fractional Loss of OH                 |
|        1.1%            22.5%             9.5%    |       66.0%            1.0% =  100.2%
|        1.0%            21.3%            11.1%    |       65.2%            1.0% =   99.6%
|               +------------------+---------------+------------------+----------------+
|              HNO3             NO2               CO              HCHO             O3
|                |               |                 |               |                |
|                |               |                 |               |                |
|              NO3             HNO3              NO2             HO2              HO2
|              10.49           218.74            92.55           640.89             9.71
|              10.13           219.62            114.42          673.75            10.28
|              103.5%            99.6%            80.9%           95.1%            94.5%
|                                                  |----------------+-----------------+
|                                          9.3%    |       64.4%            1.0%
|                                         11.2%    |       66.0%            1.0%
|                                                  |   Contribution to Tot [HO2]
|                                                  |
|                                                  |<---------------------------------+
|                                                  V                                 |
|                                              Tot [HO2]<-HCHOhv  211.20   21.2%     |
|                                                995.64          206.50    20.7%     |
|                                              1020.28            102.3%             |
|                    Fractional Loss HO2          97.6%                              |
|                                                  |                                 |
|                 4.3%    3.7%            87.8%    |        4.2%                     |
|                 3.7%    4.0%            91.2%    |        1.5%                     |
|                        +---------+----------------+-----------------+              |
|                       HO2      O3               NO              HCHO               |
|                        |        |                |               |                 |
|                        |        |                |               |                 |
|                      H2O2      OH               OH             FROX                |
|                       42.54    37.03          873.69            42.25              |
|                       37.99    40.51          930.21            15.35              |
|                       112.0%    91.4%           93.9%           275.2%             |
|                        |hv      |                |               |                 |
|                       OH        |                |               |+NO              |
|                        2.57     |                |              HO2                |
|                        2.17     |                |              41.28      4.1%    |
|                       118.7%    |                |              15.33      1.5%    |
|                         +-------+--------+--------+             269.3%             |
|                                         |                       +------------------+
|                                        OH
+---------------------------------------- 913.30       Total NO->NO2
                                        972.89          914.98
                                          93.9%         945.54
                                                           96.8%
```

Arrhenius and Other Rate Expressions

OZIPM (and other software) require that Troe-type expressions, often used in the kinetics literature for some reactions, be represented by Arrhenius approximation expressions. That is, expressions such as,

$$k = A(T/T^*)^B$$

and

$$k = \frac{k_0[M]}{(1 + (k_0[M]/k_\infty))} F^R$$

where

$$k_0 = A_0(T/T^*)^{B_0}$$
$$k_\infty = A_i(T/T^*)^{B_i}$$

and

$$R = \frac{1}{1 + (\log(k_0[M]/k_\infty)/N)^2}$$

(T^* is a reference temperature—often 300 K), must be converted to an Arrhenius form by a least squares fit, *i.e.*, to

$$k = A_a \exp(E_a/RT).$$

Carter's software accepts the non-Arrhenius expressions directly, with units of molecules/cc and seconds, and internally translates to ppm and minutes. That is, many of Carter's original rate constants were given as six parameters (k_o, B_o, k_i, B_i, F, N), so, in the testing phase, Carter actually used the literature value he had accepted. In the case of Gery's software, and for the "adaptation" of Carter's original mechanism for use in OZIPM, however, the kinetics database rate expressions had to be fitted with an Arrhenius-type expression to estimate a rate constant at 298 K in ppm-min units and to estimate an activation energy over a temperature range of 260–315 K. In the fitting process, however, there were possibilities for errors, or for making different implicit assumptions that do not show up in the final listing (*e.g.*, what is the value of T^*? or what was the temperature range used to do the fitting?). Such errors occurred in the first version of the CAL mechanism released by Lurmann and he sent out a letter with corrections.[28] Other rate constant calculation errors were made by SAI in the CBX and CB4.1 mechanisms; these will be described below. Considering how much difficulty each of us has had in using only the Arrhenius form, perhaps all EPA software should be changed to accept the full variety of rate expressions directly.

To compare the two sets of mechanisms rates, a spreadsheet was programmed to perform the calculations, do the regression, calculate the rates for the two mechanisms, document the assumptions, and plot the results. The simulation results given in Tables 7, 8, 9, and 10 were used to select the reactions to investigate.

The details of the intercomparisons are given as a series of tables and plots and these all appear at the end of this chapter in a single multi-page table (Table K). The reaction number and equation are given at the top of each page of the table. The "A" versions refer to the use of the "Adaptation Report" for CAL rates. A few highlights of these comparisons will be described here:

1) In performing a fit to rates such as

$$O + O_2 + M \rightarrow O_3 + M \qquad k = A(T/T^*)^B$$

which appear in the mechanism as first order reactions, *e.g.*,

$$O = O_3 \qquad k = [O_2][M]A\exp(E_a/RT)$$

Whitten *et al.*[2] did not take into account the temperature dependence of $[O_2]$ and $[M]$ in units of molecules/cc. This also effected the falloff calculations. Thus the CBX rates generally agree with those of Lurmann, and with the NASA85 document at 298 K, but not at any other temperature. Thus, the CBX fitted A and E_a are not correct. This happened in the case of reactions 2, 5, 12, 30, and 33 in Table 6. *For subsequent tests, we changed these rate constants in the* CBX *mechanism.*

2) In many cases, the values given by Lurmann in his November letter[28] are closer to our regression computed values than the rates later given in the "Adaptation Report".[7] In fact, the rate constant for R2 is too large by a factor of 10 in Table 3-2 of that report. For others, it is as if a slightly different set of conversion constants or assumptions had been programmed into whatever program produced Table 3-2 of the adaption report. In a few cases, the fits using both the values from the November letter and from the "Adaptation Report" are shown in Table K.

3) The CBX value of 400 ppm^{-1}-min^{-1} (2.7×10^{-13} molecules-cm^{-3}-sec^{-1}) for

$$HO^{\cdot} + CO \rightarrow CO_2 + HO_2^{\cdot}$$

is cited by Whitten *et al.*[2] as coming from their 1984 automobile exhaust modeling report.[29] The value of 322 ppm^{-1}-min^{-1} (2.2×10^{-13} molecules-cm^{-3}-sec^{-1}) used by Carter is from NASA85. We accepted the NASA value.

4) The CAL value of 13300 ppm^{-1}-min^{-1} (9.0×10^{-12} molecules-cm^{-3}-sec^{-1}) for

$$HO^{\cdot} + HCHO \rightarrow CO + HO_2^{\cdot} + H_2O$$

is the lowest value of those cited in Atkinson and Lloyd, 1984. Carter cites Atkinson[21] for the lower number. We accepted the more median recommendation of Baulch *et al.*[24] of 15000 ppm^{-1}-min^{-1} (1.0×10^{-11} molecules-cm^{-3}-sec^{-1})

5) The rate for reaction 44

$$FROX \rightarrow HO_2^{\cdot} + HCHO$$

was set at the same value used by CBX since Carter had used the same forward rate as CBX.

Simulations Using New Rates

The rates of the ten reactions discussed above were changed to be the same in both mechanisms, including the "merged" reactions from the other mechansism. Figure 5 compares predictions from the two mechanisms at 1.0 and 0.5 ppm formaldehyde. Table 11 gives the new integrated reaction rates, Table 12 gives the new mass balance and Table 13 gives the new mass flow.

Table 12 shows that the O_3 predicted by the two mechanisms with adjusted rates now agrees to within 5 ppb. Likewise, in Table 13, the total $HO^{\cdot}$ and $HO_2^{\cdot}$ production agrees to within 0.2%. There are still minor differences in H_2O_2 production and in a few termination steps. The adjustment of rates for R7–14 also resulted in improved agreement for the $NO_3^{\cdot}$ oxidation paths, *e.g.*,

$$O_3 + NO \xrightarrow{(NO_3^{\cdot})} 0.86\ NO_2 + 0.14\ HNO_3 \quad \text{for CBX.}$$
$$O_3 + NO \xrightarrow{(NO_3^{\cdot})} 0.86\ NO_2 + 0.14\ HNO_3 \quad \text{for CAL}$$

Note that is CBX that changed the most as a result of the rate changes and that the net result was to lower the amount of O_3 produced by CBX.

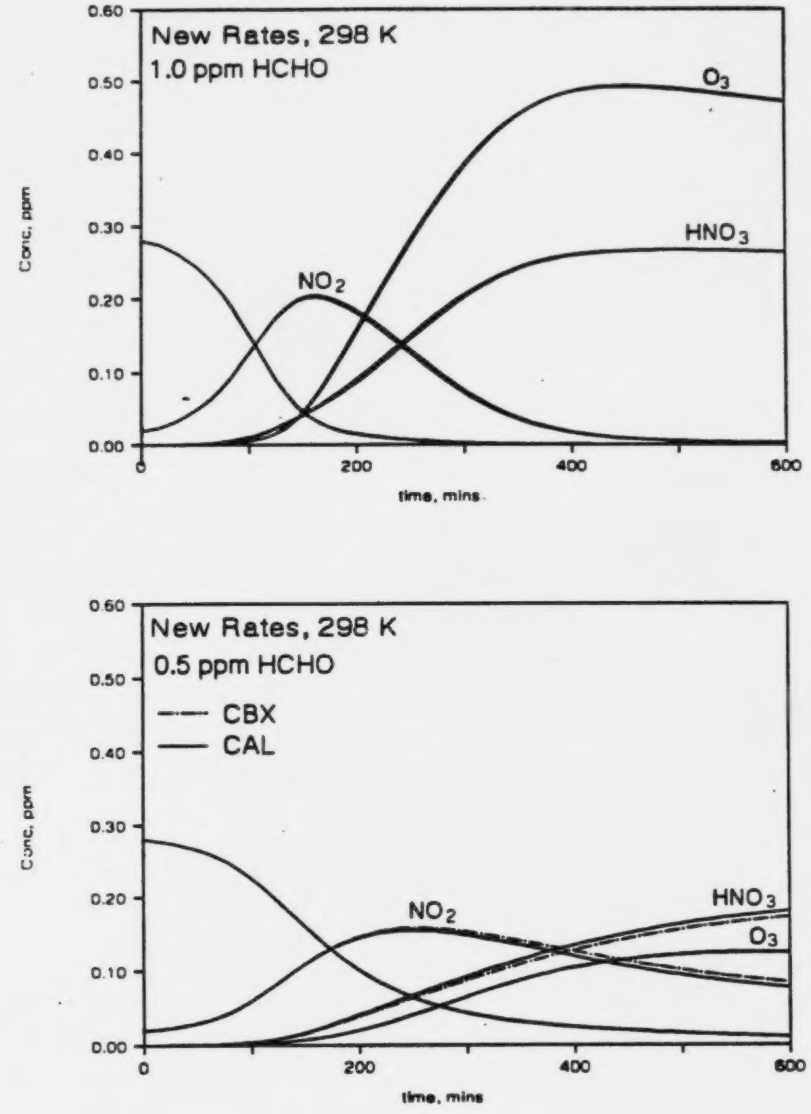

Figure 5. Comparison of CBX and CAL, Modified Rates

Table 11. Integrated Reaction Rates for 1.0 ppm HCHO, Modified Rates

```
             CAL vs CBX, 1.0 ppm HCHO
             CAL HCHO Only--Modified rates
                      CBX HCHO Only--Modified rates
             T=600.0  T=600.0
R1           13.76834 14.16858 NO2=NO+O
R2           17.78741 18.17826 O=O3
R3           12.90531 13.28153 O3+NO=NO2
R4           0.005759 0.006074 O+NO2=NO
R5           0.001385 0.001450 O+NO2=NO3
R6           0.000269 0.000277 O+NO=NO2
R7           0.321431 0.328585 O3+NO2=NO3
R8           0.007788 0.007885 NO3=NO
R9           0.044119 0.044666 NO3=NO2+O
R10          0.239923 0.244518 NO3+NO=2.00NO2
R11          0.000087 0.000092 NO3+NO2=NO+NO2
R12          0.261419 0.271090 NO3+NO2=N2O5
R13          0.222610 0.231061 N2O5=NO2+NO3
R14          0.038506 0.039968 N2O5=2.00HNO3
R15          0.001073 0.001122 NO3+HO2=HNO3
R16          0.001276 0.001334 NO3+HO2=HNO3
R17          3.791684 3.782471 O3=O
R18          0.218698 0.218391 O3=O1D
R19          0.028691 0.028646 O1D=2.00OH
R20          0.190100 0.189808 O1D=O
R21          0.009559 0.009925 O3+OH=HO2
R22          0.037589 0.039995 O3+HO2=OH
R23          0.000901 0.000963 NO+NO=2.00NO2
R24          0.004888 0.000000 NO2=HONO+-1.00NO2+HNO3
R25          0.031640 0.031389 OH+NO=HONO
R26          0.036375 0.031540 HONO=NO+OH
R27          0.001880 0.001606 OH+HONO=NO2
R28          0.000000 0.000000 HONO+HONO=NO+NO2
R29          0.902814 0.903176 HO2+NO=NO2+OH
R30          1.884156 1.931270 HO2+NO2=HNO4
R31          1.881544 1.929086 HNO4=NO2+HO2
R32          0.001004 0.001013 OH+HNO4=NO2
R33          0.209580 0.211335 OH+NO2=HNO3
R34          0.010255 0.010352 OH+HNO3=NO3
R35          0.009960 0.009830 HO2+HO2=H2O2
R36          0.011847 0.010346 HO2+HO2=H2O2
R37          0.001328 0.001191 H2O2=2.00OH
R38          0.004153 0.003970 OH+H2O2=HO2
R39          0.092256 0.093306 OH+CO=HO2
R40          0.102117 0.103793 HCHO=2.00HO2+CO
R41          0.157888 0.160288 HCHO=CO
R42          0.676147 0.672458 OH+HCHO=HO2+CO
R43          0.042622 0.043044 HO2+HCHO=FROX+RO2
R44          0.026708 0.027776 FROX=HO2+HCHO
R45          0.015806 0.015151 FROX+NO=FACID+NO2+HO2
R46          0.000082 0.000088 FROX+HO2=ROOH
R47          0.000000        0 FROX+RO2=0.50HO2+RO2
R48          0.000008 0.000008 ROOH=HO2+OH
R49          0.000333 0.000343 O+HCHO=OH+HO2+CO
R50          0.000379 0.000427 NO3+HCHO=HNO3+HO2+CO
```

Table 12. Mass Balance for 1.0 ppm HCHO, Modified Rates

```
          CAL Mass Balance--Modified rates
            NO2       NO        O        O3        NO3       N2O5      OH        HO2       HNO3
R1        -13.7683  13.7683  13.7683
R2                          -17.7874  17.7874
R3         12.9053 -12.9053          -12.9053
R4         -0.0058   0.0058  -0.0058
R5         -0.0014           -0.0014            0.0014
R17&R20                       3.9818  -4.0104                      0.0574
R21&R22                               -0.0471                      0.0280  -0.0280
R7         -0.3214                    -0.3214   0.3214
R8&R9       0.0441   0.0078   0.0441           -0.0519
R10         0.4798  -0.2399                    -0.2399
R12&R13    -0.0388                             -0.0388   0.0388
R14                                                     -0.0385                      0.0770
R34                                             0.0103            -0.0103           -0.0103
R15&R16                                        -0.0024                    -0.0024    0.0024
R29&R45     0.9186  -0.9186                                        0.9028  -0.9028
R33        -0.2096                                                -0.2096            0.2096
Others     -0.0049                             -0.0004                               0.0053
==================================================================================================
Sum       -0.00230 -0.28196 -0.00031  0.50314 -0.00030  0.00030  0.76839 -0.93320  0.28396
          -0.28456 =NOx loss          =Net O3                                       =Final NOx
```

```
          CBX Mass Balance--Modified rates
            NO2       NO        O        O3        NO3       N2O5      OH        HO2       HNO3
R1        -14.1686  14.1686  14.1686
R2                          -18.1783  18.1783
R3         13.2815 -13.2815          -13.2815
R4         -0.0061   0.0061  -0.0061
R5         -0.0015           -0.0015            0.0015
R17&R20                       3.9723  -4.0009                      0.0573
R21&R22                               -0.0499                      0.0301  -0.0301
R7         -0.3286                    -0.3286   0.3286
R8&R9       0.0447   0.0079   0.0447           -0.0526
R10         0.4890  -0.2445                    -0.2445
R12&R13    -0.0400                             -0.0400   0.0400
R14                                                     -0.0400                      0.0799
R34                                             0.0104            -0.0104           -0.0104
R15&R16                                        -0.0025                    -0.0025    0.0025
R29&R45     0.9183  -0.9183                                        0.9032  -0.9032
R33        -0.2113                                                -0.2113            0.2113
Others     -0.0000                             -0.0004             0.0000            0.0004

==================================================================================================
Sum       -0.02249 -0.26184 -0.00026  0.51736  0.00041  0.00006  0.76885 -0.93570  0.28380
          -0.28392 =NOx loss          =Net O3                                       =Final NOx
```

Table 13. Reactant Mass Flow for 1.0 ppm HCHO, Modified Rates

```
    CAL vs CBX, 1.0 ppm HCHO

                               ppb,CAL new
    298 K, 1 ppm HCHO         ppb,CBX new

+----------------------------->  943.06 -------->Tot [OH] <--O3hv 57.38
|                                945.56          1000.44          57.29
|                                  99.7%         1002.85
|                                                 99.8%
|                                                   |
|                                                   |
|            Fractional Loss of OH                  |
|        1.0%            20.9%             9.2%     |      67.6%             1.0% = 99.7%
|        1.0%            21.1%             9.3%     |      67.1%             1.0% = 99.5%
|               +-----------------+-----------------+----------------+----------------+
|              HNO3              NO2               CO              HCHO              O3
|               |                 |                 |                |                |
|               |                 |                 |                |                |
|               NO3             HNO3               HO2              HO2              HO2
|               10.26           209.58            92.26           676.15              9.56
|               10.35           211.34            93.31           672.46              9.93
|                99.1%            99.2%            98.9%           100.5%            96.3%
|                                                   |-----------------+-----------------+
|                                          9.2%     |      67.7%             1.0%
|                                          9.3%     |      67.4%             1.0%
|                                                   |   Contribution to Tot [HO2]
|                                                   |
|                                                   |<----------------------------------+
|                                                   V                                   |
|                                              Tot [HO2]<-HCHOhv  204.23     20.5%      |
|                                                998.00          207.59      20.8%      |
|                                                998.43            98.4%                |
|                    Fractional Loss HO2          100.0%                                |
|                                                   |                                   |
|                4.4%     3.8%             90.5%    |        1.6%                       |
|                4.0%     4.0%             90.5%    |        1.5%                       |
|                         +-------+-----------------+------------------+                |
|                        HO2      O3               NO               HCHO                |
|                         |       |                 |                |                  |
|                         |       |                 |                |                  |
|                       H2O2      OH               OH               FROX                |
|                        43.62    37.59          902.81              15.91              |
|                        40.35    40.00          903.18              15.27              |
|                        108.1%    94.0%           100.0%            104.2%             |
|                         |hv     |                 |                |                  |
|                        OH       |                 |                |+NO               |
|                         2.66    |                 |               HO2                 |
|                         2.38    |                 |               15.81      1.6%     |
|                        111.4%   |                 |               15.15      1.5%     |
|                                                                   104.3%              |
|                          +------+--------+--------+                +------------------+
|                                          |
|                                        OH
+-----------------------------------------  943.06       Total NO->NO2         =
                                         945.56          918.62
                                           99.7%         918.33
                                                          100.0%
```

The last and final step was to examine reactions that might be eliminated.

In compressing CBX to CB4.1, Whitten:

- lumped reactions 8 and 9 together
- ignored 15 and 16
- ignored 30,31, and 32
- ignored 43,44,45,46,47, and 48.

In compressing Carter's mechanism to the OZIPM version, Lurmann:

- ignored reaction 6
- ignored 27 and 28
- ignored reaction 49.

To determine how the mechanisms compared with these changes, the rates for reactions:

$$6, 15, 16, 30, 31, 32, 27, 28, 43, 44, 45, 46, 47, 48, 49$$

were set to zero.

Figure 6 compares the modified rate simulations and ignoring the 15 reactions above for both mechanisms at 1.0 ppm HCHO showed essentially no difference; there also were no differences in the 0.5 ppm HCHO simulations.

Tables 14, 15, and 16 are the integrated rates, mass balances, and mass flows for the modified rates, reduced reaction conditions. Comparing Tables 9 and 15, there is less than a 6 ppb change in O_3. The 15 ppb of $HO_2^{\cdot}$ that reacted with HCHO in Table 9 now reacts with NO directly and makes more $HO^{\cdot}$ This additional $HO^{\cdot}$ reacts with HCHO directly and with CO. In Table 16, the radical yields without the $HO_2^{\cdot}$ + HCHO reactions are 2%, or 18 ppb $HO^{\cdot}$ higher.

Under the lower 0.5 ppm HCHO conditions, the reaction $HO_2^{\cdot}$ + HCHO is even less important, and thus we believe that the whole FROX chemistry cycle can be ignored in both mechanisms as it was in CB4. The PNA (HNO4) reactions 30 and 31 should probably be kept in both mechanisms. Reaction 11 could also be deleted; since it will probably not compete effectively with 12.

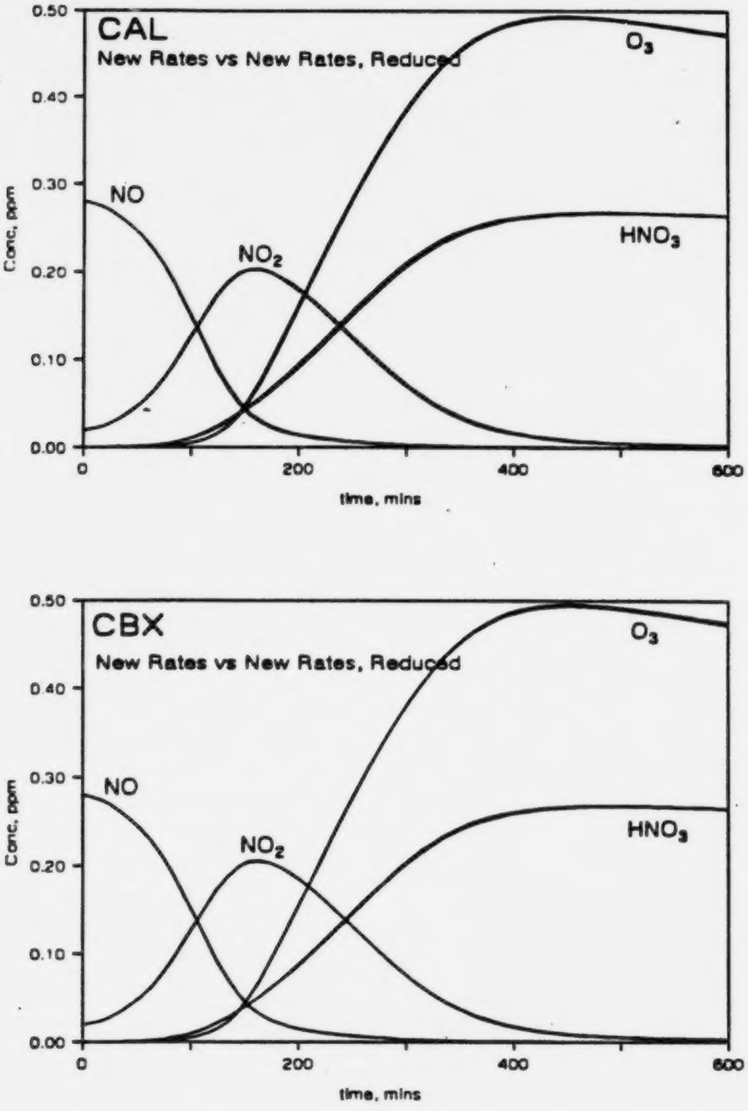

Figure 6. Comparison of CBX and CAL, Reduced Reactions

Table 14. Mass Balance for 1.0 ppm HCHO, Reduced Reactions

```
          CAL vs CBX, 1.0 ppm HCHO
          CAL HCHO Only--New rates
                   CBX HCHO Only--New rates
          T=600.0  T=600.0
R1        13.53791 14.11902 NO2=NO+O
R2        17.57900 18.14216 O=O3
R3        12.67227 13.23916 O3+NO=NO2
R4        0.005642 0.006060 O+NO2=NO
R5        0.001357 0.001447 O+NO2=NO3
R6               0        0 O+NO=NO2
R7        0.317873 0.326701 O3+NO2=NO3
R8        0.007954 0.008078 NO3=NO
R9        0.045055 0.045760 NO3=NO2+O
R10       0.237661 0.244328 NO3+NO=2.00NO2
R11       0.000087 0.000092 NO3+NO2=NO+NO2
R12       0.260328 0.270934 NO3+NO2=N2O5
R13       0.221768 0.230788 N2O5=NO2+NO3
R14       0.038360 0.039921 N2O5=2.00HNO3
R15              0        0 NO3+HO2=HNO3
R16              0        0 NO3+HO2=HNO3
R17       3.811143 3.794732 O3=O
R18       0.219643 0.219152 O3=O1D
R19       0.028817 0.028743 O1D=2.00OH
R20       0.190937 0.190447 O1D=O
R21       0.009734 0.010097 O3+OH=HO2
R22       0.039209 0.041534 O3+HO2=OH
R23       0.000893 0.000964 NO+NO=2.00NO2
R24       0.004839 0.000000 NO2=HONO+-1.00NO2+HNO3
R25       0.032021 0.031644 OH+NO=HONO
R26       0.038566 0.031762 HONO=NO+OH
R27              0 0.001631 OH+HONO=NO2
R28              0 0.000000 HONO+HONO=NO+NO2
R29       0.920644 0.920786 HO2+NO=NO2+OH
R30              0        0 HO2+NO2=HNO4
R31              0        0 HNO4=NO2+HO2
R32              0        0 OH+HNO4=NO2
R33       0.212669 0.214106 OH+NO2=HNO3
R34       0.010486 0.010538 OH+HNO3=NO3
R35       0.010756 0.010535 HO2+HO2=H2O2
R36       0.012793 0.011088 HO2+HO2=H2O2
R37       0.001455 0.001286 H2O2=2.00OH
R38       0.004586 0.004334 OH+H2O2=HO2
R39       0.094751 0.095442 OH+CO=HO2
R40       0.101422 0.104455 HCHO=2.00HO2+CO
R41       0.156839 0.161225 HCHO=CO
R42       0.694352 0.686433 OH+HCHO=HO2+CO
R43              0        0 HO2+HCHO=FROX+RO2
R44              0        0 FROX=HO2+HCHO
R45              0        0 FROX+NO=FACID+NO2+HO2
R46              0        0 FROX+HO2=ROOH
R47              0        0 FROX+RO2=0.50HO2+RO2
R48              0        0 ROOH=HO2+OH
R49              0        0 O+HCHO=OH+HO2+CO
R50       0.000386 0.000434 NO3+HCHO=HNO3+HO2+CO
```

Table 15. Mass Balance for 1.0 ppm HCHO, Reduced Reactions

CAL Mass Balance--New rates

	NO2	NO	O	O3	NO3	N2O5	OH	HO2	HNO3
R1	-13.5379	13.5379	13.5379						
R2			-17.5790	17.5790					
R3	12.6723	-12.6723		-12.6723					
R4	-0.0056	0.0056	-0.0056						
R5	-0.0014		-0.0014		0.0014				
R17&R20			4.0021	-4.0308			0.0576		
R21&R22				-0.0489			0.0295	-0.0295	
R7	-0.3179			-0.3179	0.3179				
R8&R9	0.0451	0.0080	0.0451		-0.0530				
R10	0.4753	-0.2377			-0.2377				
R12&R13	-0.0386				-0.0386	0.0386			
R14						-0.0384			0.0767
R34					0.0105		-0.0105		-0.0105
R15&R16					0.0000			0.0000	0.0000
R29&R45	0.9206	-0.9206					0.9206	-0.9206	
R33	-0.2127						-0.2127		0.2127
Others	-0.0048				-0.0004				0.0052
Sum	-0.00556	-0.27907	-0.00095	0.50912	0.00010	0.00020	0.78460	-0.95012	0.28413
	-0.28452	=NOx loss		=Net O3					=Final NOx

CBX Mass Balance--New rates

	NO2	NO	O	O3	NO3	N2O5	OH	HO2	HNO3
R1	-14.1190	14.1190	14.1190						
R2			-18.1422	18.1422					
R3	13.2392	-13.2392		-13.2392					
R4	-0.0061	0.0061	-0.0061						
R5	-0.0014		-0.0014		0.0014				
R17&R20			3.9852	-4.0139			0.0575		
R21&R22				-0.0516			0.0314	-0.0314	
R7	-0.3267			-0.3267	0.3267				
R8&R9	0.0458	0.0081	0.0458		-0.0538				
R10	0.4887	-0.2443			-0.2443				
R12&R13	-0.0401				-0.0401	0.0401			
R14						-0.0399			0.0798
R34					0.0105		-0.0105		-0.0105
R15&R16					0.0000			0.0000	0.0000
R29&R45	0.9208	-0.9208					0.9208	-0.9208	
R33	-0.2141						-0.2141		0.2141
Others	-0.0000				-0.0004		0.0000		0.0004
Sum	-0.01312	-0.27112	0.00029	0.51078	-0.00006	0.00022	0.78507	-0.95222	0.28385
	-0.28429	=NOx loss		=Net O3					=Final NOx

Table 16. Reactant Mass Flow for 1.0 ppm HCHO, Reduced Reactions

```
    CAL vs CBX, 1.0 ppm HCHO

                               ppb,CAL new
    298 K, 1 ppm HCHO         ppb,CBX new

+------------------------------> 962.76 --------->Tot [OH] <--O3hv 57.63
|                               964.90          1020.40            57.49
|                                 99.8%         1022.38
|                                                 99.8%
|                                                 |
|                                                 |
|           Fractional Loss of OH                 |
|        1.0%           20.8%            9.3%    |       68.0%             1.0%  = 100.2%
|        1.0%           20.9%            9.3%    |       67.1%             1.0%  =  99.4%
|              +------------------+---------------+-------------------+----------------+
|             HNO3              HO2              CO              HCHO              O3
|              |                 |                |                |                |
|              |                 |                |                |                |
|             NO3               HNO3             HO2              HO2              HO2
|             10.49             212.67           94.75            694.35            9.73
|             10.54             214.11           95.44            686.43           10.10
|              99.5%             99.3%            99.3%            101.2%           96.4%
|                                                 |-----------------+-----------------+
|                                         9.5%    |       69.3%             1.0%
|                                         9.5%    |       68.6%             1.0%
|                                                 |   Contribution to Tot [HO2]
|                                                 |
|                                                 |<----------------------------------+
|                                                 V                                 |
|                                             Tot [HO2]<-HCHOhv  202.85    20.3%    |
|                                              1001.68          208.91     20.9%    |
|                                              1000.88            97.1%             |
|                   Fractional Loss HO2         100.1%                              |
|                                                 |                                 |
|               4.7%    3.9%             91.9%    |        0.0%                     |
|               4.3%    4.1%             92.0%    |        0.0%                     |
|                       +--------+----------------+------------------+              |
|                      HO2     O3                NO             HCHO                |
|                       |       |                 |               |                 |
|                       |       |                 |               |                 |
|                     H2O2     OH                OH             FROX                |
|                      47.10   39.21          920.64              0.00              |
|                      43.25   41.53          920.79              0.00              |
|                      108.9%   94.4%           100.0%                              |
|                      |hv      |                 |               |                 |
|                     OH        |                 |               |+NO              |
|                       2.91    |                 |             HO2                 |
|                       2.57    |                 |               0.00     0.0%     |
|                     113.1%    |                 |               0.00     0.0%     |
|                       +-------+--------+--------+                                 |
|                                        |                        +-----------------+
|                                       OH
+--------------------------------------- 962.76        Total NO->NO2          =
                                       964.90            920.64
                                         99.8%           920.79
                                                          100.0%
```

Responses from Model Developers

The results presented above were sent to the model developers and project officer in early May 1987. In the case of CAL, the funding for the development effort ended in April 1987 and thus no changes were made to CAL. In subsequent work, however, Carter has made modifications to the inorganic and carbonyl reaction set in CAL based upon the new 1988 NASA review. He changed the rates of 18 reactions:

$$3, 4, 5, 7, 10, 13, 20, 22, 25, 30, 31, 32, 34, 38, 39, 42, 43, 44$$

and he deleted 4 reactions, 46, 47, 48, 49. In the case of the latter, he did add an explicit representation for $HOCH_2O_2^{\cdot}$, and, because of new data on the rates of its reactions, he deleted all but one its bimolecular reactions. Thus, the "official" version of CAL remains Table 3-2 of Lurmann *et al.* (*except for the rate of reaction 2 in that table*), and all subsequent work that used the CAL mechanism in this report was based upon this version.

In the case of CB4, development work continued until October 1987 and significant changes were made to this mechanism compared to the first version we used in May. The changes to the PAR, ETH, PAN, and aromatics chemistries were so significant that a sub-version number was given to the new mechanism: CB4.2.

In the ICRS part of CB4.2, Gery changed the rates of 11 reactions:

$$2, 3, 4, 5, 6, 10, 12, 13, 14, 20, 34$$

and he deleted the entire $HOCH_2O_2^{\cdot}$ set of 6 reactions.

Table K. Comparison of Rate Constants.

```
TEMPERATURE AND PRESSURE DEPENDENT RATE CONSTANTS--K2

Reaction:             O(+O2+M)=O3
Rate Constant:        (6.0E-34)*M*O2 (T/Tref)^-2.3
Source:               NASA85

Order (1,2,3) =                1
Falloff (0/1)?=                0 =No

    Ao          Bo        Eo                 ko=Ao*((T/Tref)^Bo) @ 298 K
7.627E+04      -2.3        0                 77452.143 /sec     4647128. /min

Best Regression Fit:
 Aa,c-m-s      Ea                            ka=Aa*exp(Ea/RT) @ 298 K
1.155E+03      2489                          77277.897 /sec     4636673. /min

Aa,ppm-min   Ea/R
69325.388     1252


----------Given CAL Values   ------------------
Aa,c-m-s       Ea                            ka,@ 298 K
1.050E+03      2548                          7.754E+04 /sec     4652444. /min

Aa,/ppm-min   Ea/R                           Ratio at 273K        1.0185
   63000      1282                           Ratio at 298K        1.0012
November Letter                              Ratio at 309K        1.0039

----------Given CBX Values   ------------------
Aa,c-m-s       Ea                            ka,@ 298K
7.671E+03      1371                          7.770E+04 /sec     4661998. /min

Aa,/ppm-min   Ea/R                           Ratio at 273K        0.8508
  460247       690                           Ratio at 298K        0.9965
O2IPM3 Source Code                           Ratio at 309K        1.0796
```

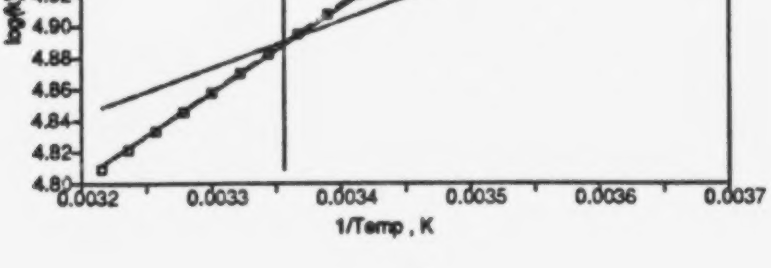

Table K. Comparison of Rate Constants, cont.

```
TEMPERATURE AND PRESSURE DEPENDENT RATE CONSTANTS--K5

Reaction:             O+NO2(+M)=NO3
Rate Constant:        (9.0E-32)*M (T/Tref)^-2.0
Source:               NASA85

Order (1,2,3) =             2
Falloff (0/1)?=             0 =No

    Ao          Bo          Eo              ko=Ao*((T/Tref)^Bo) @ 298 K
2.217E-12        -2          0               2.25E-12 c-m-s    3298.604 /ppm-min


Best Regression Fit:
 Aa,c-m-s      Ea                           ka=Aa*exp(Ea/RT) @ 298 K
1.195E-13      1736                          2.24E-12 c-m-s    3293.425 /ppm-min

Aa,ppm-min   Ea/R
175.45784      874


----------Given CAL Values   ------------------
Aa,c-m-s       Ea                           ka,@ 298 K
1.117E-13      1777                         2.244E-12 c-m-s    3295.233 /ppm-min

Aa,/ppm-min   Ea/R                          Ratio at 273K        1.0109
   164.06      894                          Ratio at 298K        0.9990
November Letter                             Ratio at 309K        1.0009

----------Given CBX Values   ------------------
Aa,c-m-s       Ea                           ka,@ 298K
2.110E-13      1192                         1.580E-12 c-m-s    2320.063 /ppm-min

Aa,/ppm-min   Ea/R                          Ratio at 273K        0.6503
   309.8       600                          Ratio at 298K        0.7010
02IPM3 Source Code                          Ratio at 309K        0.7299
```

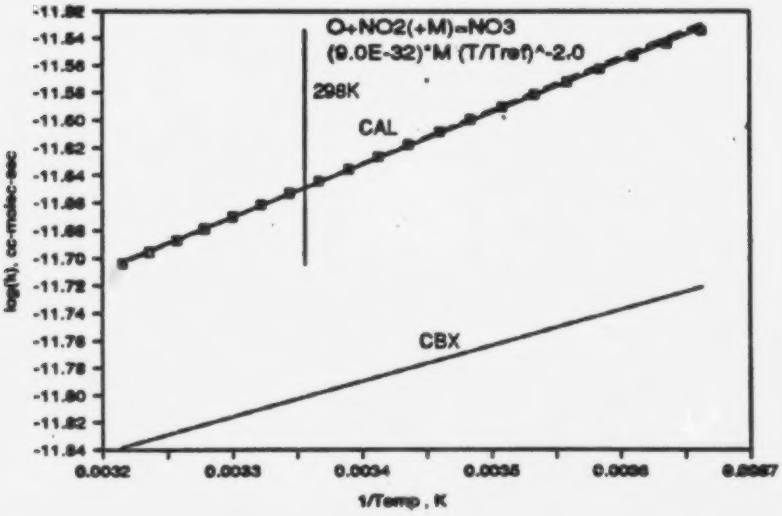

Table K. Comparison of Rate Constants, cont.

```
TEMPERATURE AND PRESSURE DEPENDENT RATE CONSTANTS--K7

Reaction:            O3+NO2=NO3
Rate Constant:       1.2E-13 exp(-4870/RT)
Source:              NASA85
Order (1,2,3) =            2
Falloff (0/1)?=            0 =No

   Ao          Bo       Eo                 ko=Ao*exp(Eo/RT) @ 298 K
1.200E-13         0    -4870                3.22E-17 c-m-s     0.047245 /ppm-min


Best Regression Fit:
 Aa,c-m-s      Ea                          ka=Aa*exp(Ea/RT) @ 298 K
1.200E-13     -4870                         3.22E-17 c-m-s     0.047245 /ppm-min

Aa,ppm-min   Ea/R
 176.1776     -2451


----------Given CAL Values    -------------------
Aa,c-m-s       Ea                          ka,@ 298 K
1.144E-13     -4869                        3.076E-17 c-m-s    0.045156 /ppm-min

Aa,/ppm-min   Ea/R                         Ratio at 273K        0.9560
    167.98    -2450                        Ratio at 298K        0.9558
                                           Ratio at 309K        0.9557

----------Given CBX Values    -------------------
Aa,c-m-s       Ea                          ka,@ 298K
1.201E-13     -4869                        3.228E-17 c-m-s    0.047392 /ppm-min

Aa,/ppm-min   Ea/R                         Ratio at 273K        1.0033
    176.3     -2450                        Ratio at 298K        1.0031
                                           Ratio at 309K        1.0030
```

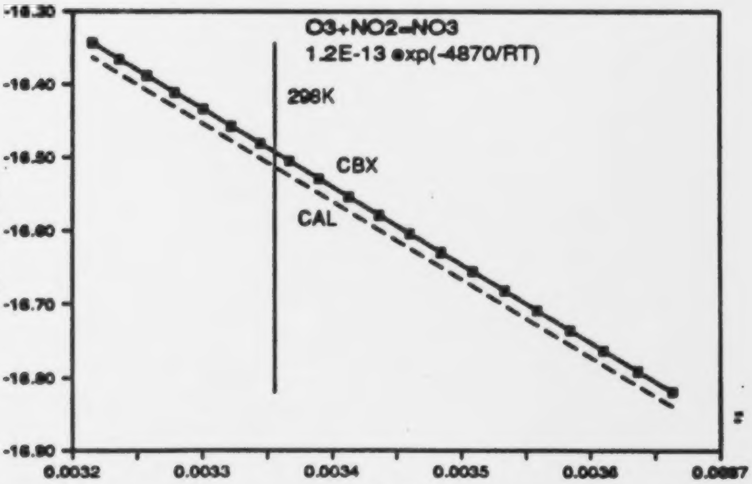

Table K. Comparison of Rate Constants, cont.

```
TEMPERATURE AND PRESSURE DEPENDENT RATE CONSTANTS--K12

Reaction:              NO2+NO3=N205
Rate Constant:         Falloff Expression
Source:                NASA85

Order (1,2,3) =               2
Falloff (0/1)?=               1 =Yes

   Ao         Bo        Eo               ko=Ao*((T/Tref)^Bo) @ 298 K
2.000E-30     -4.3        0               2.06E-30 c-m-s     3.0E-15 /ppm-min
   Ai         Bi        Ei               ki=Ai*((T/Tref)^Bi) @ 298 K
1.400E-12     -0.5                        1.40E-12 c-m-s =  2062.291 ppm-min
   F          N
     0.6      0.97                       k_falloff, @ 298 K, 1 atm =
                                          1.18E-12 m-c-s =  1738.978 /ppm-min
Best Regression Fit:
 Aa,c-m-s     Ea                         ka=Aa*exp(Ea/RT) @ 298 K
5.009E-13      509                        1.18E-12 c-m-s    1737.000 /ppm-min

Aa,ppm-min   Ea/R
735.38497      256


----------Given CAL Values   ------------------
Aa,c-m-s      Ea                         ka,@ 298 K
4.701E-13      537                       1.163E-12 c-m-s    1707.903 /ppm-min

Aa,/ppm-min   Ea/R                       Ratio at 273K        0.9902
    690.2      270                       Ratio at 298K        0.9821
November Letter                          Ratio at 309K        0.9836

----------Given CBX Values   ------------------
Aa,c-m-s      Ea                         ka,@ 298K
5.666E-13      449                       1.210E-12 c-m-s    1775.969 /ppm-min

Aa,/ppm-min   Ea/R                       Ratio at 273K        1.0158
    831.9      226                       Ratio at 298K        1.0208
OZIPM Source Code                        Ratio at 309K        1.0281
```

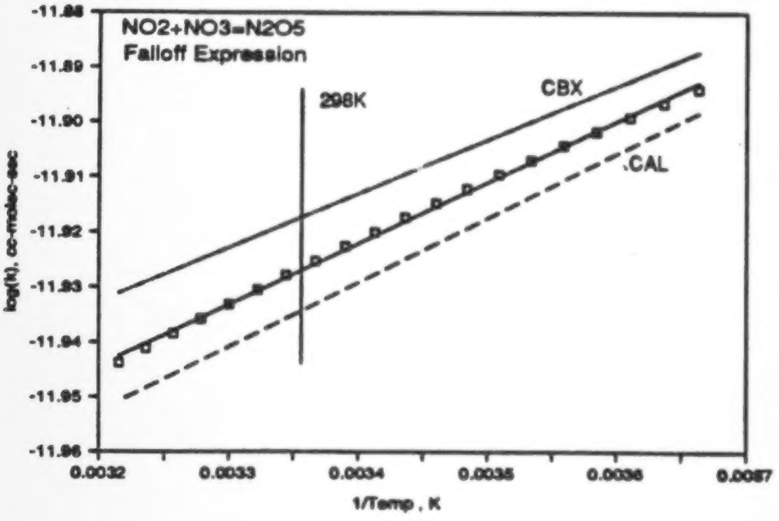

Table K. Comparison of Rate Constants, cont.

```
TEMPERATURE AND PRESSURE DEPENDENT RATE CONSTANTS--K12A

Reaction:            NO2+NO3=N2O5
Rate Constant:       Falloff Expression
Source:              NASA85

Order (1,2,3) =             2
Falloff (0/1)?=             1 =Yes

    Ao          Bo        Eo                ko=Ao*((T/Tref)^Bo) @ 298 K
2.000E-30      -4.3          0               2.06E-30 c-m-s     3.0E-15 /ppm-min
    Ai          Bi        Ei                ki=Ai*((T/Tref)^Bi) @ 298 K
1.400E-12      -0.5                          1.40E-12 c-m-s =  2062.291 ppm-min
    F           N
     0.6        0.97                        k_falloff, @ 298 K, 1 atm =
                                             1.18E-12 m-c-s =  1738.978 /ppm-min
Best Regression Fit:
 Aa,c-m-s      Ea                           ka=Aa*exp(Ea/RT) @ 298 K
5.009E-13        509                         1.18E-12 c-m-s    1737.000 /ppm-min

Aa,ppm-min    Ea/R
735.38497        256


----------Given CAL Values   ------------------
Aa,c-m-s        Ea                          ka,@ 298 K
4.625E-13        542                        1.156E-12 c-m-s    1697.188 /ppm-min

Aa,/ppm-min    Ea/R                         Ratio at 273K        0.9849
     679         273                        Ratio at 298K        0.9760
Adaption Report                             Ratio at 309K        0.9770

----------Given CBX Values   ------------------
Aa,c-m-s        Ea                          ka,@ 298K
5.666E-13        449                        1.210E-12 c-m-s    1775.969 /ppm-min

Aa,/ppm-min    Ea/R                         Ratio at 273K        1.0158
   831.9         226                        Ratio at 298K        1.0208
OZIPM Source Code                           Ratio at 309K        1.0281
```

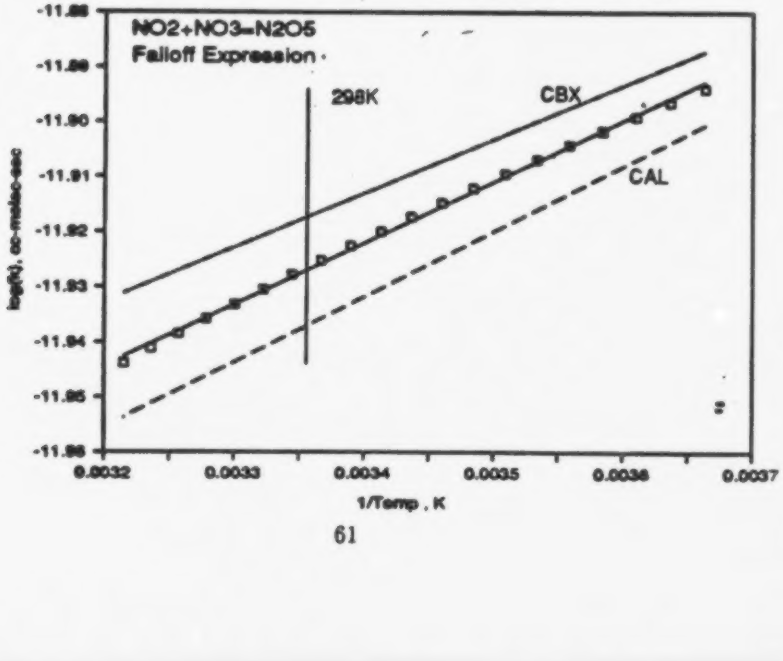

Table K. Comparison of Rate Constants, cont.

```
TEMPERATURE AND PRESSURE DEPENDENT RATE CONSTANTS--K13

Reaction:           N2O5=NO2+NO3
Rate Constant:      k12*1.06E27(T/Tref)^-1 exp(-22550/RT)
Source:             Carter86

Order (1,2,3) =             1
Falloff (0/1)?=             0 =No

    Ao          Bo         Eo               ko=Ao*((T/Tref)^Bo) @ 298 K
1.254E+15        -1    -22550               0.0365743 /sec      2.194463 /min


Best Regression Fit:
 Aa,c-m-s     Ea                            ka=Aa*exp(Ea/RT) @ 298 K
2.010E+14    -21462                         0.0365552 /sec      2.193314 /min

Aa,ppm-min   Ea/R
 1.21E+16    -10801


----------Given CAL Values   ------------------
Aa,c-m-s      Ea                            ka,@ 298 K
1.850E+14    -21442                         3.485E-02 /sec      2.091053 /min

Aa,/ppm-min   Ea/R                          Ratio at 273K        0.9578
 1.11E+16    -10790                         Ratio at 298K        0.9529
November Letter                             Ratio at 309K        0.9531

----------Given CBX Values   ------------------
Aa,c-m-s      Ea                            ka,@ 298K
3.267E+14    -21541                         5.203E-02 /sec      3.121978 /min

Aa,/ppm-min   Ea/R                          Ratio at 273K        1.4082
 1.96E+16    -10840                         Ratio at 298K        1.4219
OZIPM Source Code                           Ratio at 309K        1.4315
```

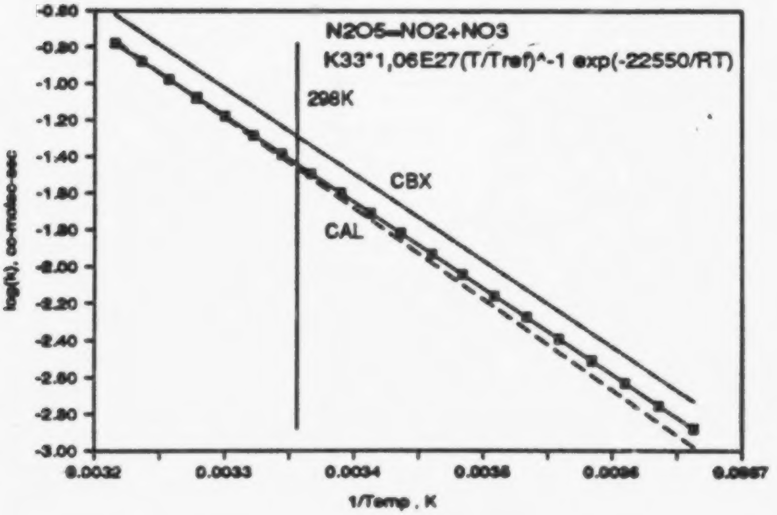

Table K. Comparison of Rate Constants, cont.

```
TEMPERATURE AND PRESSURE DEPENDENT RATE CONSTANTS--K13A

Reaction:            N2O5=NO2+NO3
Rate Constant:       K33*1.06E27(T/Tref)^-1 exp(-22550/RT)
Source:              Carter86

Order (1,2,3) =              1
Falloff (0/1)?=              0 =No

   Ao          Bo       Eo                  ko=Ao*((T/Tref)^Bo) @ 298 K
1.254E+15        -1   -22550                0.0365743 /sec      2.194463 /min



Best Regression Fit:
 Aa,c-m-s      Ea                           ka=Aa*exp(Ea/RT) @ 298 K
2.010E+14    -21462                         0.0365552 /sec      2.193314 /min

Aa,ppm-min   Ea/R
 1.21E+16    -10801


----------Given CAL Values    -------------------
Aa,c-m-s      Ea                            ka,@ 298 K
1.330E+15    -22612                         3.471E-02 /sec      2.082847 /min

Aa,/ppm-min   Ea/R                          Ratio at 273K         0.7961
 7.98E+16    -11379                         Ratio at 298K         0.9429
Adaption Report                             Ratio at 309K         1.0185

----------Given CBX Values    -------------------
Aa,c-m-s      Ea                            ka,@ 298K
3.267E+14    -21541                         5.203E-02 /sec      3.121978 /min

Aa,/ppm-min   Ea/R                          Ratio at 273K         1.4882
 1.96E+16    -10840                         Ratio at 298K         1.4219
OZIPM Source Code                           Ratio at 309K         1.4315
```

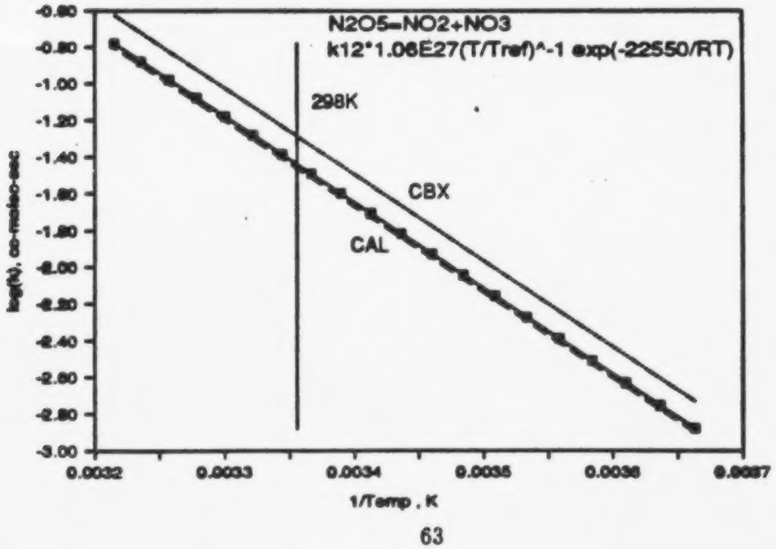

Table K. Comparison of Rate Constants, cont.

```
TEMPERATURE AND PRESSURE DEPENDENT RATE CONSTANTS--K30

Reaction:           HO2+NO2=HO2NO2
Rate Constant:      FallOff
Source:             AL84

Order (1,2,3) =            2
Falloff (0/1)?=            1 =Yes

   Ao          Bo        Eo              ko=Ao*((T/Tref)^Bo) @ 298 K
2.300E-31      -4.6        0              2.37E-31 c-m-s     3.5E-16 /ppm-min
   Ai          Bi        Ei              ki=Ai*((T/Tref)^Bi) @ 298 K
4.200E-12       0.2                       4.19E-12 c-m-s =  6157.972 /ppm-min
   F           N
    0.56       1.00                      k_falloff, @ 298 K, 1 atm =
                                          1.38E-12 m-c-s =  2031.123 /ppm-min
Best Regression Fit:
 Aa,c-m-s      Ea                        ka=Aa*exp(Ea/RT) @ 298 K
1.117E-13      1489                       1.38E-12 c-m-s    2026.361 /ppm-min

Aa,/ppm-min   Ea/R
164.04538      749


----------Given CAL Values    -------------------
Aa,c-m-s       Ea                        ka,@ 298 K
1.699E-13      1256                      1.416E-12 c-m-s    2079.209 /ppm-min

Aa,/ppm-min   Ea/R                       Ratio at 273K        0.9967
   249.37      632                       Ratio at 298K        1.0220
November Letter                          Ratio at 309K        1.0451

----------Given CBX Values    -------------------
Aa,c-m-s       Ea                        ka,@ 298K
1.400E-13      1226                      1.110E-12 c-m-s    1630.109 /ppm-min

Aa,/ppm-min   Ea/R                       Ratio at 273K        0.7779
   205.6       617                       Ratio at 298K        0.8011
OZIPM Source Code                        Ratio at 309K        0.8208
```

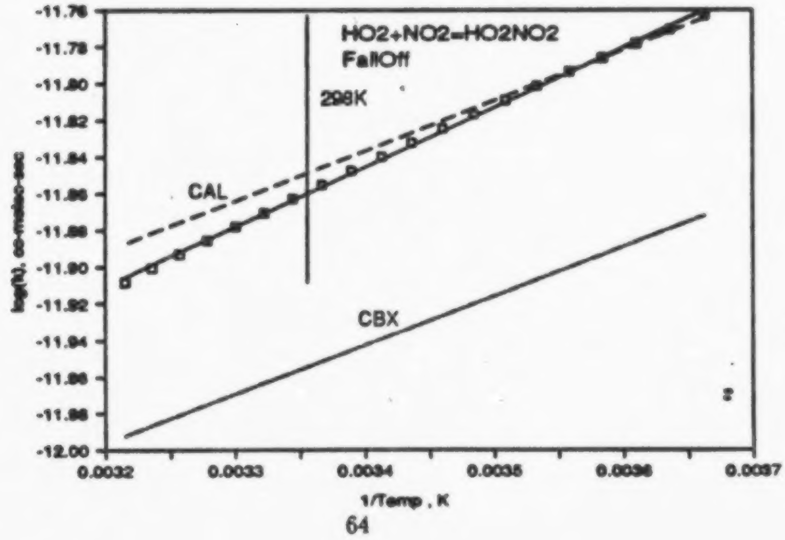

Table K. Comparison of Rate Constants, cont.

```
TEMPERATURE AND PRESSURE DEPENDENT RATE CONSTANTS--K30A

Reaction:            HO2+NO2=HO2NO2
Rate Constant:       FallOff
Source:              AL84

Order (1,2,3) =               2
Falloff (0/1)?=               1 =Yes

   Ao         Bo        Eo                 ko=Ao*((T/Tref)^Bo) @ 298 K
2.300E-31      -4.6        0                2.37E-31 c-m-s      3.5E-16 /ppm-min
   Ai         Bi        Ei                 ki=Ai*((T/Tref)^Bi) @ 298 K
4.200E-12       0.2                         4.19E-12 c-m-s =  6157.972 ppm-min
   F          M
    0.56      1.00                         k_falloff, @ 298 K, 1 atm =
                                            1.38E-12 m-c-s =  2031.123 /ppm-min
Best Regression Fit:
 Aa,c-m-s     Ea                           ka=Aa*exp(Ea/RT) @ 298 K
1.117E-13      1489                         1.38E-12 c-m-s    2026.361 /ppm-min

Aa,ppm-min   Ea/R
164.04538      749


----------Given CAL Values   -------------------
Aa,c-m-s       Ea                          ka,@ 298 K
1.022E-13      1536                        1.367E-12 c-m-s    2007.398 /ppm-min

Aa,/ppm-min   Ea/R                         Ratio at 273K        1.0049
     150       773                         Ratio at 298K        0.9882
Adaptation Report                          Ratio at 309K        0.9921

----------Given CBX Values   -------------------
Aa,c-m-s       Ea                          ka,@ 298K
1.658E-13      1262                        1.396E-12 c-m-s    2049.966 /ppm-min

Aa,/ppm-min   Ea/R                         Ratio at 273K        0.9836
   243.4       635                         Ratio at 298K        1.0076
Gery Letter                                Ratio at 309K        1.0306
```

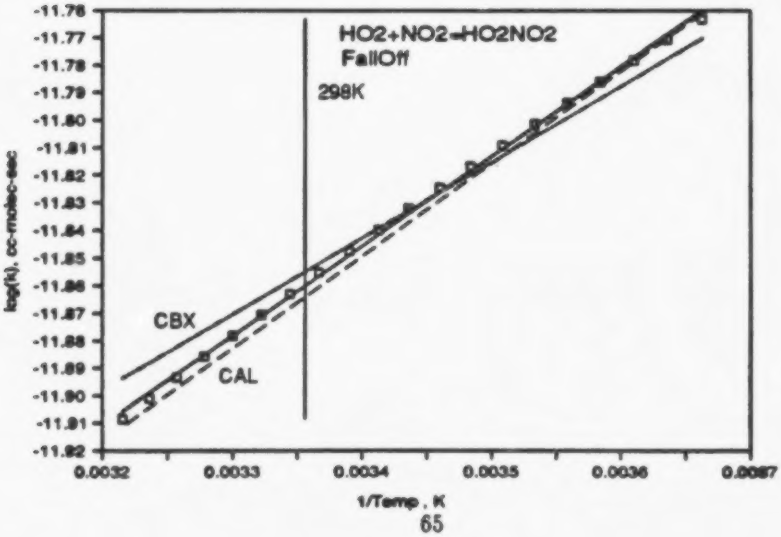

Table K. Comparison of Rate Constants, cont.

```
TEMPERATURE AND PRESSURE DEPENDENT RATE CONSTANTS--K31

Reaction:           HO2NO2=HO2+NO2
Rate Constant:      k30*(4.29E26)*exp(-21600/RT)
Source:             NASA85

Order (1,2,3) =              1
Falloff (0/1)?=              0 =No

   Ao          Bo      Eo              ko=Ao*exp(Eo/RT) @ 298 K
5.856E+14        0   -21600            0.0844203 /sec       5.065222 /min

Best Regression Fit:
 Aa,c-m-s      Ea                      ka=Aa*exp(Ea/RT) @ 298 K
4.376E+13    -20064                    0.0844203 /sec       5.065222 /min

Aa,ppm-min    Ea/R
 2.63E+15    -10097


----------Given CAL Values    -------------------
Aa,c-m-s      Ea                       ka,@ 298 K
7.000E+13    -20349                    8.350E-02 /sec       5.010044 /min

Aa,/ppm-min   Ea/R                     Ratio at 273K          0.9465
 4.20E+15    -10240                    Ratio at 298K          0.9875
November Letter                        Ratio at 309K          1.0062

----------Given CBX Values    -------------------
Aa,c-m-s      Ea                       ka,@ 298K
1.308E+14    -20706                    8.531E-02 /sec       5.118426 /min

Aa,/ppm-min   Ea/R                     Ratio at 273K          0.9149
 7.85E+15    -10420                    Ratio at 298K          1.0068
OZIPM3 Source Code                     Ratio at 309K          1.0503
```

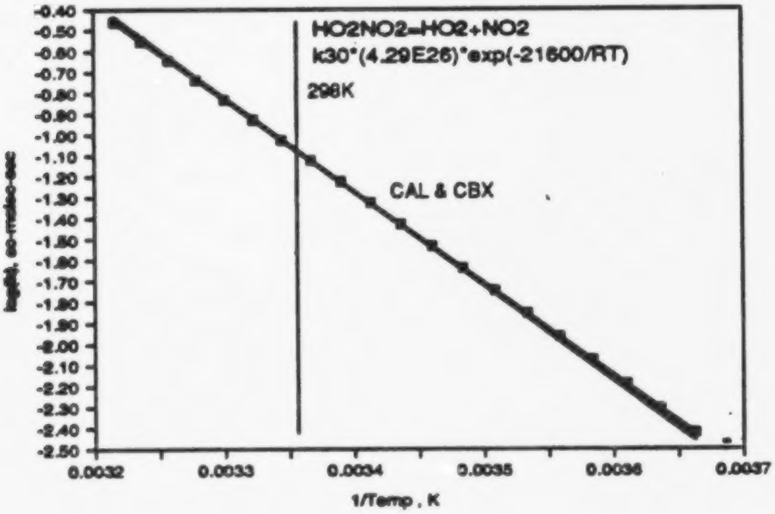

Table K. Comparison of Rate Constants, cont.

```
TEMPERATURE AND PRESSURE DEPENDENT RATE CONSTANTS-K33

Reaction:               OH+NO2=HNO3
Rate Constant:          Falloff Expression
Source:                 NASA85

Order (1,2,3) =                 2
Falloff (0/1)?=                 1 =Yes

    Ao          Bo        Eo                 ko=Ao*((T/Tref)^Bo) @ 298 K
2.600E-30      -3.2         0                 2.66E-30 c-m-s      3.9E-15 /ppm-min
    Ai          Bi        Ei                 ki=Ai*((T/Tref)^Bi) @ 298 K
2.400E-11      -1.3                           2.42E-11 c-m-s =  35543.25 ppm-min
    F           N
     0.6        1.00                         k_falloff, @ 298 K, 1 atm =
                                              1.15E-11 m-c-s =  16867.38 /ppm-min
Best Regression Fit:
 Aa,c-m-s      Ea                            ka=Aa*exp(Ea/RT) @ 298 K
1.047E-12       1418                          1.15E-11 c-m-s     16834.63 /ppm-min

Aa,ppm-min    Ea/R
1536.7787       713


-----------Given CAL Values    --------------------
Aa,c-m-s        Ea                           ka,@ 298 K
1.489E-12       1226                         1.181E-11 c-m-s     17337.67 /ppm-min

Aa,/ppm-min   Ea/R                           Ratio at 273K         1.0049
  2186.74       617                          Ratio at 298K         1.0265
November Letter                              Ratio at 309K         1.0454

-----------Given CBX Values    --------------------
Aa,c-m-s        Ea                           ka,@ 298K
1.695E-12       1113                         1.110E-11 c-m-s     16299.85 /ppm-min

Aa,/ppm-min   Ea/R                           Ratio at 273K         0.9284
   2489.2       560                          Ratio at 298K         0.9644
OZIPM Source Code                            Ratio at 309K         0.9805
```

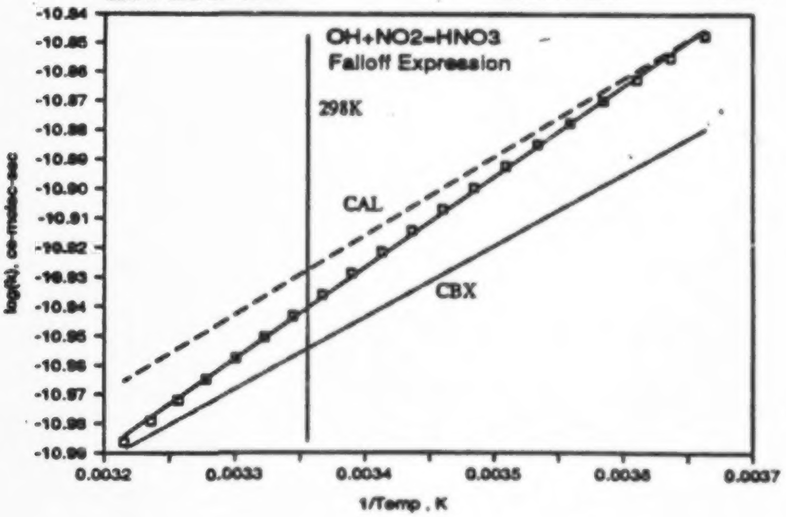

Table K. Comparison of Rate Constants, cont.

```
TEMPERATURE AND PRESSURE DEPENDENT RATE CONSTANTS-K33A

Reaction:               OH+NO2=HNO3
Rate Constant:          Falloff Expression
Source:                 NASA85

Order (1,2,3) =                2
Falloff (0/1)?=                1 =Yes

   Ao          Bo          Eo                  ko=Ao*((T/Tref)^Bo) @ 298 K
2.600E-30      -3.2           0                 2.66E-30 c-m-s     3.9E-15 /ppm-min
   Ai          Bi          Ei                  ki=Ai*((T/Tref)^Bi) @ 298 K
2.400E-11      -1.3                             2.42E-11 c-m-s =  35543.25 ppm-min
   F           N
    0.6        1.00                            k_falloff, @ 298 K, 1 atm =
                                                1.15E-11 m-c-s =  16867.38 /ppm-min
Best Regression Fit:
 Aa,c-m-s      Ea                              ka=Aa*exp(Ea/RT) @ 298 K
1.047E-12      1418                             1.15E-11 c-m-s    16834.63 /ppm-min

Aa,ppm-min    Ea/R
1536.7787      713


----------Given CAL Values  -------------------
Aa,c-m-s       Ea                              ka,@ 298 K
9.573E-13      1465                            1.135E-11 c-m-s    16668.94 /ppm-min

Aa,/ppm-min   Ea/R                             Ratio at 273K       1.0025
  1405.5       737                             Ratio at 298K       0.9882
Adaption Report                                Ratio at 309K       0.9908

----------Given CBX Values  -------------------
Aa,c-m-s       Ea                              ka,@ 298K
1.695E-12      1113                            1.110E-11 c-m-s    16299.85 /ppm-min

Aa,/ppm-min   Ea/R                             Ratio at 273K       0.9284
  2489.2       560                             Ratio at 298K       0.9644
OZIPM Source Code                              Ratio at 309K       0.9805
```

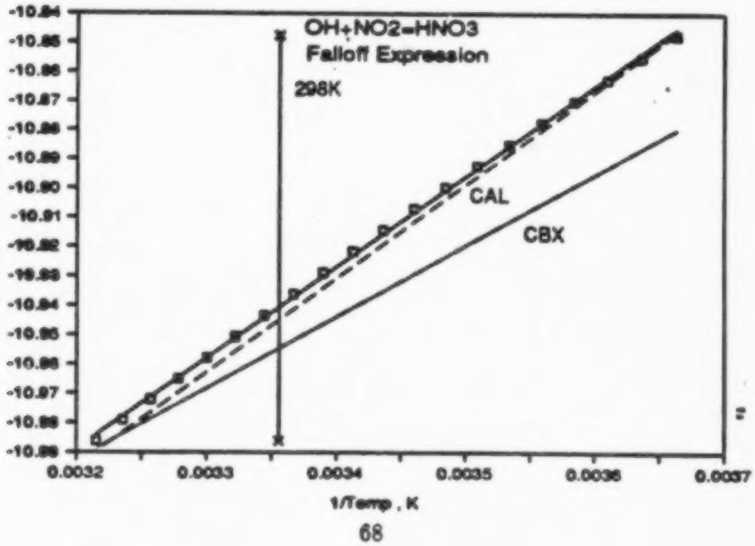

Table K. Comparison of Rate Constants, cont.

```
TEMPERATURE AND PRESSURE DEPENDENT RATE CONSTANTS--K39

Reaction:            OH+CO(+M,O2)=CO2+HO2
Rate Constant:       2.18E-13
Source:              Carter86

Order (1,2,3) =            2
Falloff (0/1)?=            0 =No

   Ao          Bo         Eo               ko=Ao*exp(Eo/RT) @ 298 K
2.180E-13        0          0               2.18E-13 c-m-s    320.0559 /ppm-min




Best Regression Fit:
 Aa,c-m-s     Ea                           ka=Aa*exp(Ea/RT) @ 298 K
2.180E-13        -0                         2.18E-13 c-m-s    320.0559 /ppm-min

Aa,ppm-min    Ea/R
320.05597        -0


----------Given CAL Values    -------------------
Aa,c-m-s        Ea                         ka,@ 298 K
2.193E-13        0                         2.193E-13 c-m-s          322 /ppm-min

Aa,/ppm-min   Ea/R                         Ratio at 273K       1.0061
     322         0                         Ratio at 298K       1.0061
October Baseline Run                       Ratio at 309K       1.0061

----------Given CB4 Values    -------------------
Aa,c-m-s        Ea                         ka,@ 298K
2.725E-13        0                         2.725E-13 c-m-s          400 /ppm-min

Aa,/ppm-min   Ea/R                         Ratio at 273K       1.2498
     400         0                         Ratio at 298K       1.2498
OZIPM4 Source Code                         Ratio at 309K       1.2498
```

4

Chamber Simulations

First we will discuss the developers' assessments of their mechanisms fit to the experimental data. Then we will demonstrate fits when using more uniform assumptions and the new photolytic rates for the UNC chamber.

Developer's Fits to Experimental Data

In their final report, Gery *et al.*[4] states that CB4 was tested with 170 experiments from three different chambers. Gery *et al.* found that for 68 different mixtures, the average prediction error in maximum ozone concentration was 2% (±22%). Similarly, Carter *et al.*[6] stated in their final report that they tested the CAL mechanism with 491 experiments done in four different chambers. They found that, "Although there were a number of experiments which were not well simulated by the model, the model simulated reasonably well the majority of the experimental data." For simple mixtures, they said that the CAL mechanism predicted the maximum O_3 within ±30% (except for some EC runs that had greater than 30% under-prediction), and that for the complex surrogate mixtures, the vast majority of the runs had a better than ±30% agreement for maximum O_3. Subsequently, Lurmann *et al.*[7] made several modifications to the CAL; the modifications were so significant that all the chamber data were re-modeled and new mechanism performance statistics were produced. These were reported as an appendix in reference 7. This appendix was the source of the values quoted below.

In Figure 7 we compare the average error of fits for O_3, formaldehyde (HCHO), and PAN obtained by each of the developers for single compounds in the UNC and EC chambers. The worst fits were for 1- butene (four UNC experiments and four EC experiments) and trans-2-butene (one UNC experiment and three EC experiments). For 1-butene, the O_3 errors were (here a negative number means an under-prediction, *e.g.*, the model was lower than the data, and the numbers after ± are standard

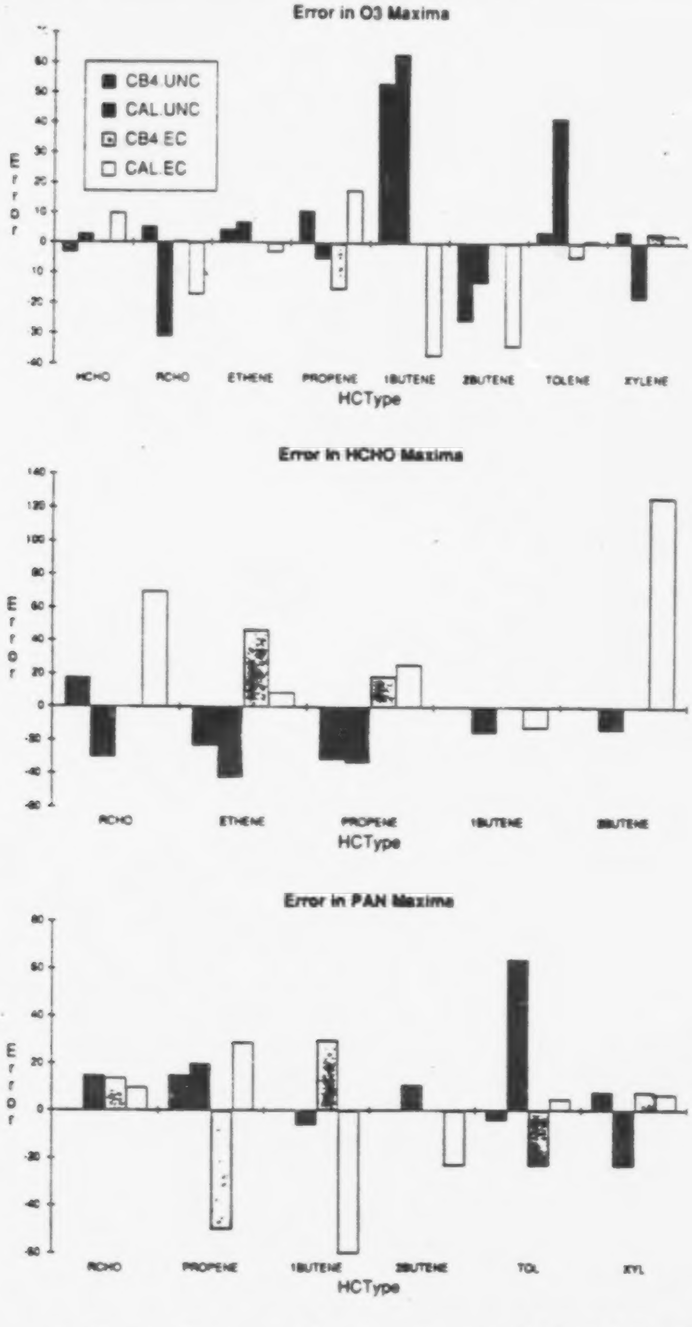

Figure 7. Errors Between Chamber Data and Model Predictions as Reported by Developers.

deviations):

	UNC	EC
CB4	53 ±17%	−28
CAL	63 ±39%	−37 ±13%

that is, the UNC data were greatly over-predicted and the EC data were largely under-predicted by both mechanisms. For trans-2-butene, however, the O_3 errors were all negative,

	UNC	EC
CB4	−30 ±0%	–
CAL	−13 ±0%	−33 ±8%

Both mechanisms under-predicted the UNC experiment and CAL under-predicted the EC experiments. The UNC trans-2-butene experiment was a same-day, side-by-side experiment with 1-butene at the same hydrocarbon and NO_x concentration as on the other side. Both mechanisms *over-predicted* the 1-butene side by about 50%, while at the same time they *under-predicted* the trans-2-butene side. The CAL mechanism also greatly over-predicted the HCHO maximum in this experiment. Finally, the CAL mechanism under-predicted the PAN in all the EC chamber butene experiments.

Another large problem was for the CAL mechanism applied to seven UNC toluene experiments:

	UNC	EC
CB4	4 ±8%	−5 ±8%
CAL	42 ±7%	−1 ±11%

The CB4 errors for these experiments were small. Note however that this part of both mechanisms was essentially an ad-hoc representation based on fitting chamber data and that CAL used a larger number of experiments than did CB4.

The average errors in O_3 maximum in propene experiments were:

	UNC	EC
CB4	11 ±25%	−5 ±21%
CAL	−5 ±12%	18 ±26%

The CAL mechanism's over-prediction of O_3 in propene experiments in the EC chamber was unexpected. In addition, the CAL mechanism *over-predicted* the PAN in the EC experiments by 29% (50% s.d.) and over-predicted the PAN in the UNC propene experiments by 20% (27% s.d.). The CB4 mechanism *under-predicted* the PAN in the EC propene experiments by about 50% (but there were only a few simulated) and *over-predicted* PAN by 15% (57% s.d.) in UNC propene experiments.

While at first the O_3 errors for ethene for both mechanisms for both chambers seem very good, further investigation shows that Carter *et al.* modeled only six EC ethene experiments: three were each over-predicted by about 25% and three were each under-predicted by about 25%. Likewise, only six UNC ethene experiments were modeled: two were each under-predicted by about 20% and four were over-predicted by about 25% depending upon the HC-to-NO_x ratio. Similarly, for the CB4 mechanism, eleven UNC (but no EC) ethene experiments were modeled: the errors in these ranged from +31% to -13%.

CAL, but not CB4, predicted the O_3 maxima in the UNC acetaldehyde experiments poorly, and both CB4 and the CAL mechanisms over-predicted the HCHO in the EC acetaldehyde experiments by 50–65% while at the same time under-predicting the HCHO in the UNC experiments.

For applications in which the mechanisms are being used to predict a *change* in O_3, as in EKMA, a more revealing test of the mechanisms' performance is to compare their relative performance for side-by-side, same-day experiments from the UNC dual chamber. That is, we can compare the relative change that occurred between the two sides of the UNC chamber with that predicted by the mechanisms for each side. Note that not all side-to-side pairs of UNC chamber experiments were simulated by the developers and only a limited set of comparisons using their own simulation results is possible. One dual set of experiments that were simulated by both SAI and UCR are the UNCMIX+mix1 verses UNCMIX+mix2 series where 'mix1' and 'mix2' were various aromatic mixtures or single compounds such as xylene or toluene. Figure 8a is a scatterplot of the models' predicted O_3 verses the observed O_3 for 17 dual UNC experiments with different hydrocarbon but same NO_x conditions on the two sides of the chamber. Most of the points fall within ±20% of a 1:1 ratio. In Figure 8b, c, and d, the data have been transformed as

$$\frac{O_3(\text{high side}) - O_3(\text{low side})}{O_3(\text{high side})}$$

expressed as a percentage. When the models' predicted differences are plotted against the observed side-to-side differences, the models' performances are seen to be worst than was first suggested by Figure 8a. Figure 9 shows that the CAL mechanism does worse than CB4 by this measure, having both predictions of large differences when small differences were observed, and predictions of small differences when

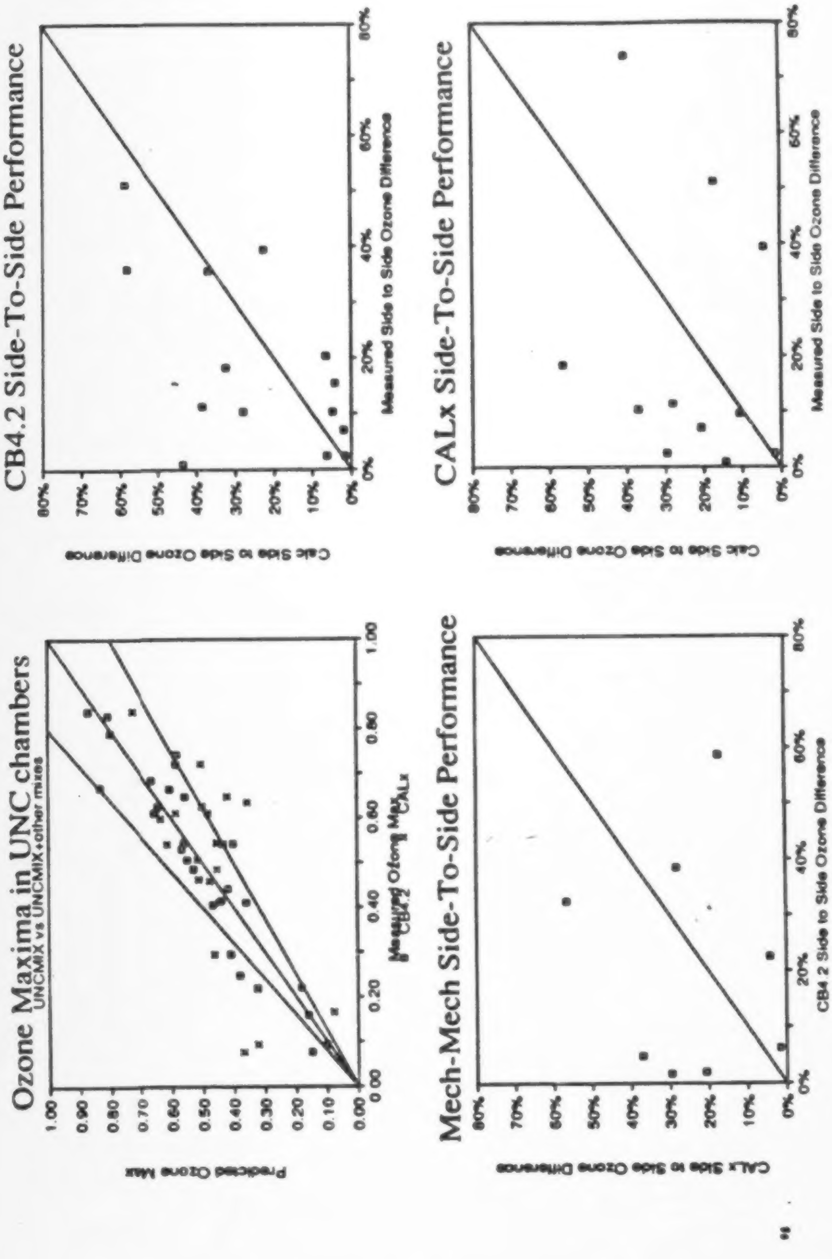

Figure 8. Comparison of Side-to-Side Ozone Predictions.

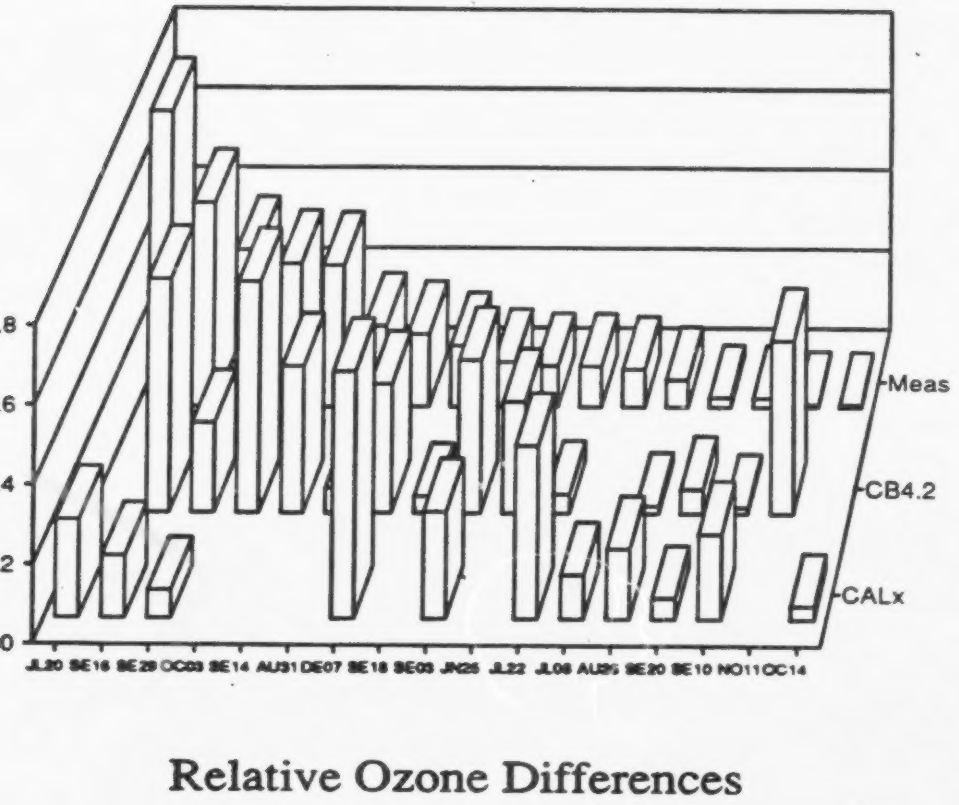

Figure 9. Comparison of Side-to-Side Ozone Predicted Differences.

large differences were observed. Finally, Figure 8d shows that the two mechanisms' predictions of differences are not related to each other in any systematic manner. This type of test suggests that more powerful tests of mechanism performance are possible and such tests may reveal weakness not easily seen in the usual scatter diagram.

Factors that Effect Chamber Fits

One factor that had an impact on the relative performance of the two mechanisms is the representation each modeler used for the photolytic rates. SAI and SAPRC not only used a different method to compute the actinic flux in the UNC chamber, they also used different molecular absorption cross-sections and quantum yields, and used different numerical algorithms to convert these data into photolysis rates. In Volume 3 of this report, we describe a new radiation transfer model, Teflon film transmission model, chamber geometry, and floor reflection model which are combined to compute the in-chamber actinic flux. Volume 3 also contains a detailed discussion of the numerical issues in evaluating photolysis rate expressions and describes new algorithms and a computer program to perform these calculations. In Volume 4 of this report, we describe the molecular absorption cross-sections and quantum yields that we believe are the present best values to use in modeling the UNC chamber. These data are a combination of data selected and used by Gery, *et al.*[4] and by Carter[13]. One important choice is that we, along with Gery, prefer the Bass cross sections for HCHO, whereas, Carter still uses an average of Bass and Moortgat values. Because the Moortgat values are larger than the Bass values at many wavelengths, the average values calculated by Carter result in a 16% higher rate of HCHO photolysis to radicals and a 37% higher rate of HCHO photolysis to stable products than are the rates we prefer (see the discussion on page 65 and following in Volume 3).

Another factor that affected the developers fits to the chamber data was the representation of the "chamber wall radical" process. Three kinds of wall models have been used:

- HONO and HCHO off-gasing from wall into gas phase, depleting the wall concentrations in the process (the Jeffries-Gery model);
- HONO and HCHO injected into the gas phase, proportional to light intensity only (the Killus model);
- $HO^{\cdot}$ and NO_2 injected into the gas phase, proportional to light intensity only (the Carter model).

These models are shown in the listings on page 19, 26, and 32 of this volume.

In addition to the "radicals," each modeler includes a a conversion of $HO^{\cdot}$ to $HO_2^{\cdot}$ which is supposed to be affected by ***background*** organic compounds. SAI and UNC generally include 0.038 ppmC of continental background HC with a composition estimated by Killus in the initial condition of the chamber (see page 32, under background HC) and include a similar amount in the dilution air (see page 32, under background HC). Carter uses a simple first order reaction

$$HO^{\cdot} \rightarrow HO_2^{\cdot} \quad 250\ \text{min}^{-1}$$

in which the rate constant was adjusted to reproduce aspects of chamber characterization experiments. (In the original testing with older light, Carter used 500 min^{-1}).

After a series of test simulations using all three "wall models" we have concluded that the Carter standard wall model is better than the HCHO and HONO off-gasing from the wall. It gives better fits, especially toward the end of the simulation. Therefore, we have adopted this model as the standard in the simulations to be presented below. If no wall model is cited, then you should assume that the Standard Carter wall model was used. It should be noted, however, that the standard Carter magnitudes are "average" values and individual experiments may be better simulated with more or less radical input than the standard model. This will be demonstrated below.

We have also adopted Carter's method for estimating initial HONO:

$$[HONO]_o = 0.07[NO_2]_o.$$

Demonstration Using Dual Experiments

Because we wished to investigate some of the differences suggested in the above analysis, we have modeled a set of UNC *dual* experiments with both mechanisms, taking care to assure we have duplicate conditions in the test inputs.

For each experiment to be shown,

- First, we show the chamber data with both sides on the same plot (solid lines are the RED chamber and dashed lines are the BLUE chamber. In the bottom plot we show tower TSR (solid line), tower UV (dash-dot line), chamber temperature, and (when available) dewpoint in both chamber halves.
- Second, we give the model input conditions for both chamber halves for both mechanisms in the form of standard PKSS initial condition files. These files, along with the photolytic rate file, the temperature, water, and dilution file, and the mechanism files as listed in Chapter 2 are sufficient to reproduce the simulation. The files document the assumptions needed to simulate the experiment. Because the data plot described above shows the temperature and dewpoint, we will not list the `*.twd` (temperature, water vapor, dilution) files here.
- Third, we show the data and model predictions for NO_x and O_3 plotted on the same graph. The top plot is always the RED side. Data are shown as solid lines and the model predictions are shown as dashed lines. CB4.2 is always represented by a dashed-dot-dot line and CAL by a dashed line.
- Fourth, in many cases, we show various HC species, HCHO, PAN, and others in the same manner as above.
- Fifth, for selected experiments, we show the effect of different choices of wall radical models or other such assumptions.

Table 17 shows the order of presentation of the experiments. The selected experiments have elements of both a species heirarchy and a network. A network-like diagram of experiments is given in Table 18.

Table 19 lists the contents of files that are common to all simulation initial conditions. These files can be "included" into a particular initial condition file by placing the filename after the character '@' in column 1 as for example,

```
@e:\path\filename
```

In addition the simulation program can be made to read different parts of the input file by defining symbolic names as the program is started. For example,

```
C:> peval  jl0986.ic/d:RED/d:CB4  jl0986.prn
```

will read normal statements and statements that appear between "conditional input" clauses, *e.g.*,

```
#if RED
 NO = 0.24,
#end
```

will only be read if '`RED`' has appeared in the input switches to the program. If a species name and concentration appear more than once, the new concentration is *added* to the existing species concentration.

Table 17. Order of Presentation of Experiments.

HCHO		
	July 8, 1986	Red, Blue
	Aug 4, 1979	Blue
Ethylene		
	Aug 4, 1986	Red
	July 9, 1986	Red, Blue
	Aug 23, 1978	Red, Blue
	July 30, 1978	Red
	July 13, 1986	Blue
	Oct 11, 1984	Red
Propylene		
	July 30, 1978	Blue
	July 13, 1986	Red
	Oct 11, 1984	Blue
1-Butene		
	Sept 27, 1983,	Red
t-2-butene		
	Sept 27, 1983,	Blue
Toluene		
	June 27, 1984	Blue
m-Xylene		
	June 27, 1984	Red
	June 26, 1984	Blue
o-Xylene		
	June 26, 1984	Red
SIMMIX		
	Aug 31, 1981	Red
UNCMIX		
	Aug 31, 1981	Blue
SYNAUTO-Delta HC		
	Aug 5, 1984	Red, Blue
	Aug 6, 1984	Red, Blue
SYNAUTO/SYNMETH		
	Aug 7, 1984	Red, Blue
	Aug 8, 1984	Red, Blue
	Aug 9, 1984	Red, Blue
SYNURB-Delta HC		
	June 26, 1985	Red, Blue
	Sept 2, 1984	Red, Blue
SYNURB/SYNMETH		
	Aug 22, 1984	Red, Blue
	Sept 1, 1984	Red, Blue
	Sept 3, 1984	Red, Blue

Table 18. A Network Ordering of Experiments.

```
HCHO------HCHO                                      JL0886
          HCHO--------Ethylene                      AU0479
                      Ethylene----Ethylene          JL0986, AU2378
          Propylene---Ethylene                      JL3078, JL1386, OC1184

1-butene--t-2-butene                                ST2783

Toluene---m-Xylene                                  JN2784
          m-Xylene----o-Xylene                      JN2684


SIMMIX----UNCMIX                                    AU3181

SYNAUTO---SYNAUTO                                   AU0584, AU0684
          SYNAUTO-----SYNAUTO/SYNMETH               AU0484, AU0884, AU0984

SYNURB----SYNURB                                    JN2685, ST0284
          SYNURB------SYNURB/SYNMETH                AU2284, ST0184, ST0384
```

Table 19. Common initial condition input files.

```
!file CBckCB4.icx
!Chamber Background for CB4 Mechanism
(Background NMHC = 0.038 ppmC)
PAR   =   0.0201,
ETH   =   0.0009,
OLE   =   0.0006,
TOL   =   0.0004,
XYL   =   0.0003,
HCHO  =   0.0038,
RCHO  =   0.0030,
```

```
!file CBckCAL.icx
!Chamber Background For CAL mechanism
(Surface NMHC = 0.0380 ppmC)
ALK4   =   0.0201,
ETHE   =   0.0009,
PRPE   =   0.0006,
TOLU   =   0.0004,
XYLE   =   0.0003,
HCHO   =   0.0038,
ALD2   =   0.0030,
```

July 8, 1986
Dual Formaldehyde Experiment

This experiment, shown in Figures 10 to 12, demonstrates that both models, using the new in-chamber actinic fluxes and the Bass absorption cross sections, agree *very* well with the measurements at two different, but simulataneous levels of HCHO. In Figure 10 note that the NO_x data are missing from just after cross over until 1230 EDT.

Figures 13 and 14 show the effect of using no wall radicals or sources of NO_x. Figure 15 shows the Killus wall model for this day.

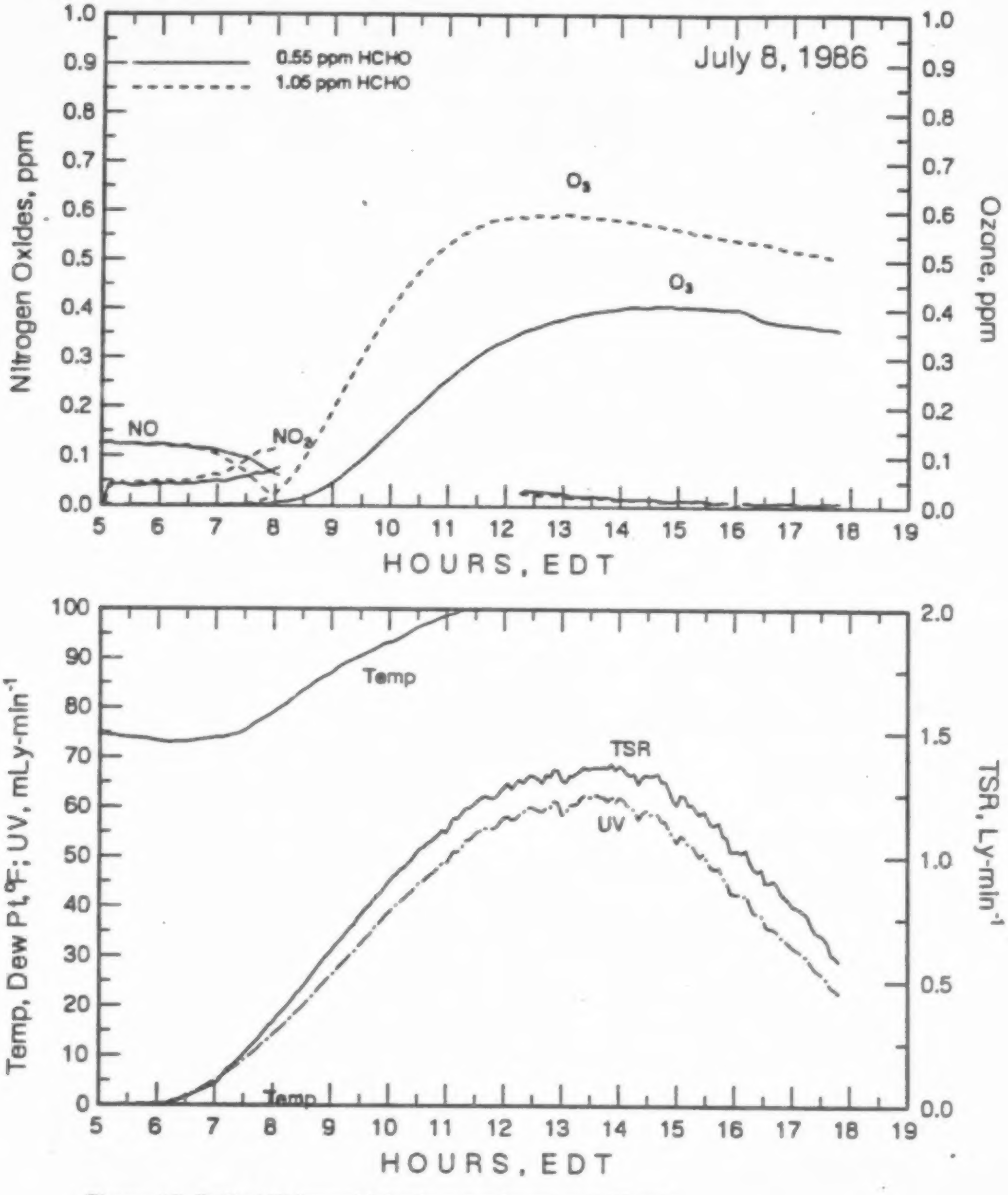

Figure 10. Delta-HC formaldehyde experiment at 0.20 NO_x.
Experimental data.

Table 20. July 8, 1986 CB4 Initial Condition Simulation File.

```
 #if RED
 July 8, 1986 (R) 0.55 ppmC HCHO
#end
 #if BLUE
 July 8, 1986 (B) 1.05 ppmC HCHO
#end
 #if CB4
c:\pkss\mech\CB42chm.pks
CONC=
@c:\pkss\mech\CBckCB4.icx
#end
 #if CAL
c:\pkss\mech\CALchm.pks
CONC=
@c:\pkss\mech\CBckCAL.icx
#end

 #if RED
  NO        =  0.121,
  NO2       =  0.045,
#end
 #if BLUE
  NO        =  0.125,
  NO2       =  0.045,
#end
 #if RED
 #if CB4
  HCHO      =  0.550,
#end
 #if CAL
  HCHO      =  0.550,
#end
#end
 #if BLUE
 #if CB4
  HCHO      =  1.05,
#end
 #if CAL
  HCHO      =  1.05,
#end
#end
  HONO  =         0.0031,
  CO    =         0.3;

@e:\segfiles\finalseg\86\jl0986.lix
@e:\segfiles\finalseg\86\jl0886.twd

FINISH;
```

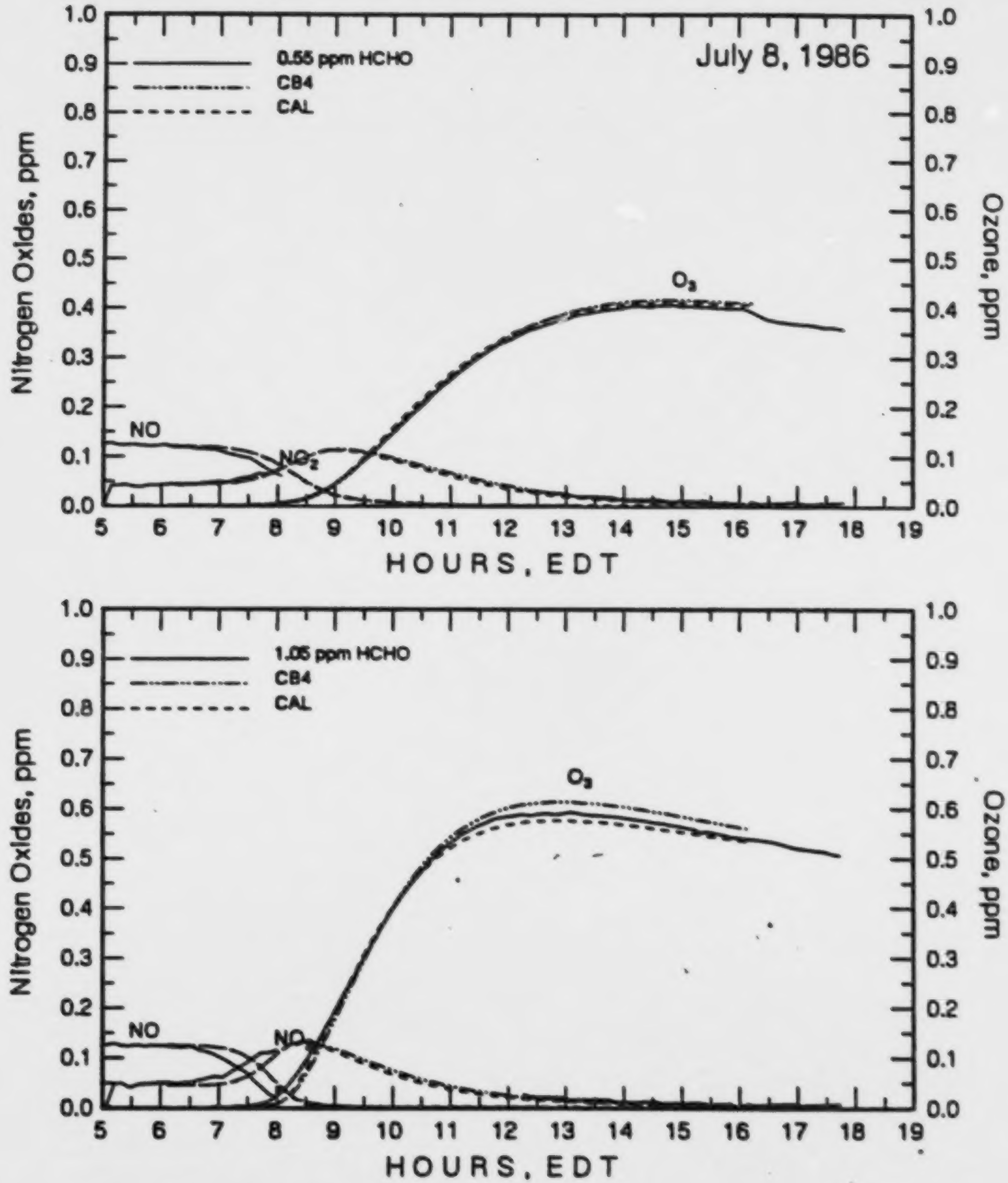

Figure 11. Standard Carter wall model.

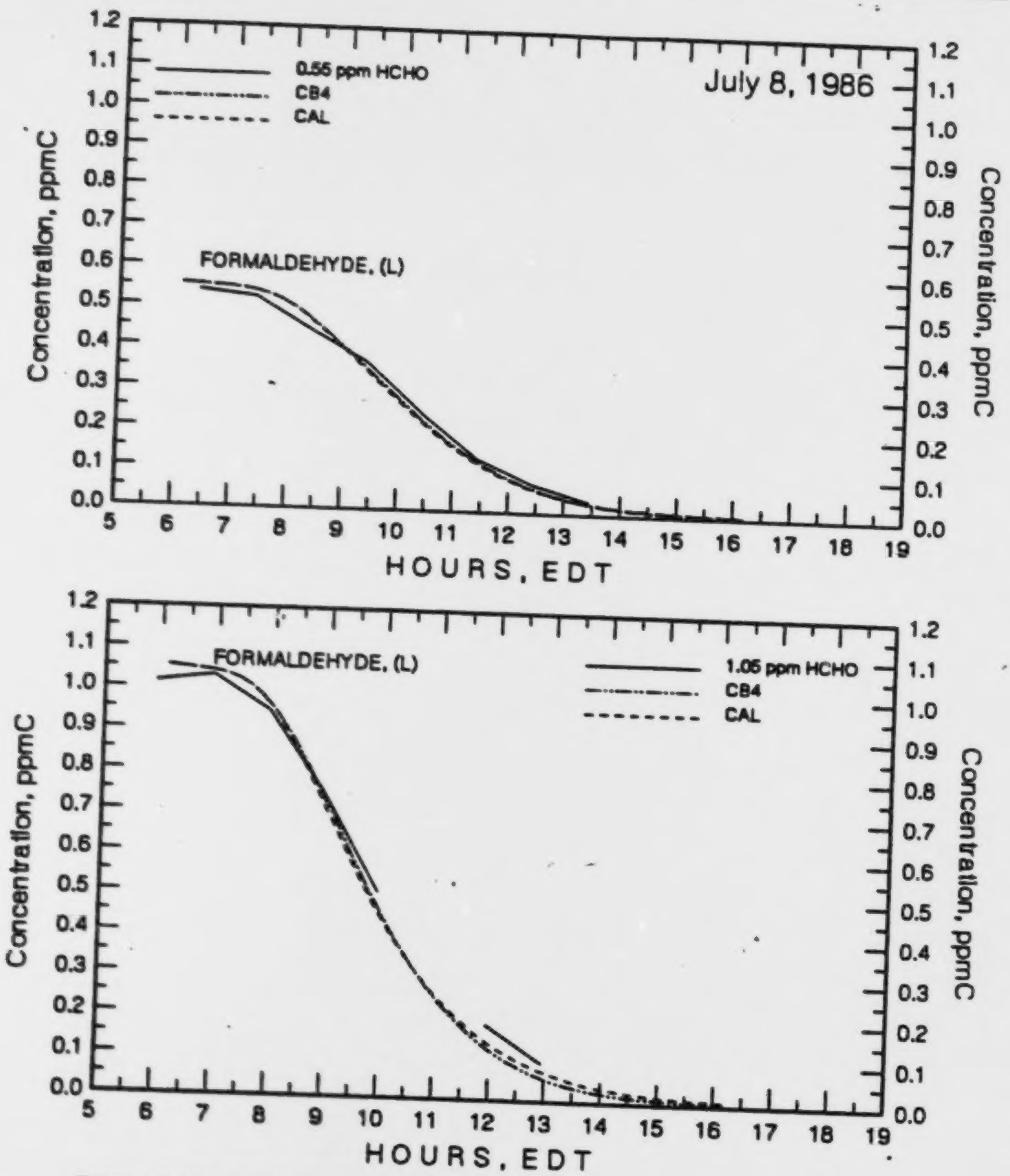

Figure 12. Standard Carter wall model.

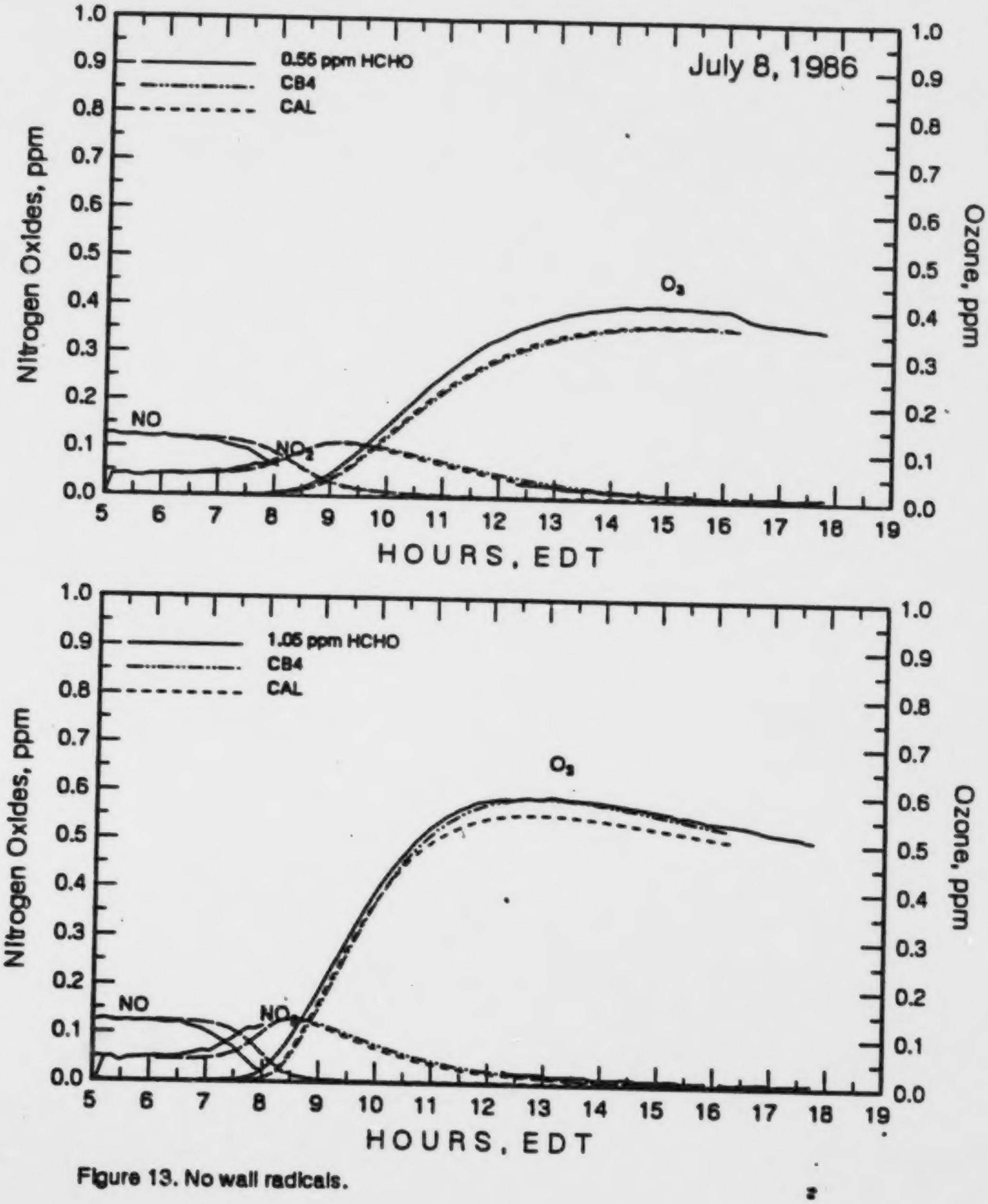

Figure 13. No wall radicals.

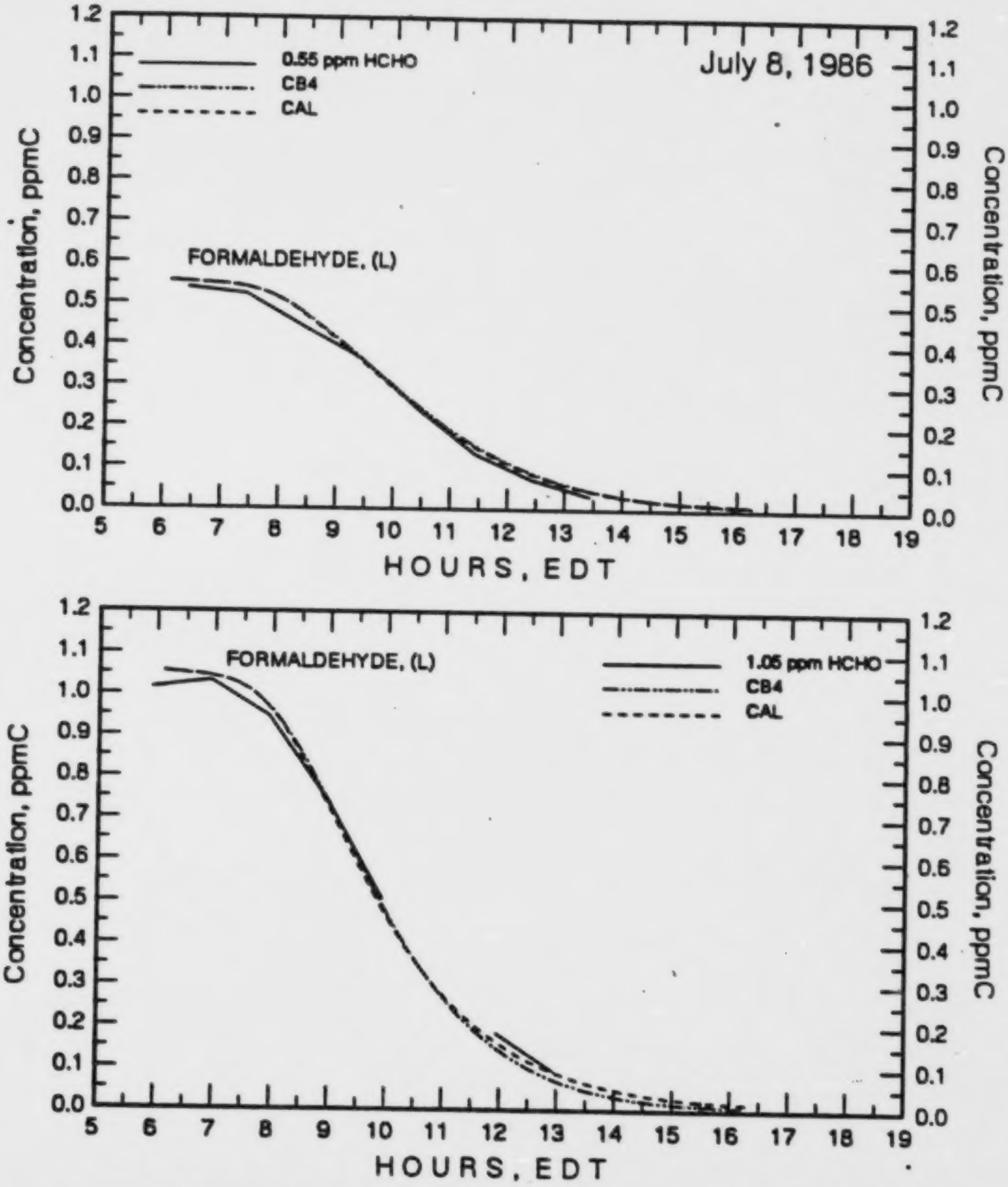

Figure 14. No wall radicals.

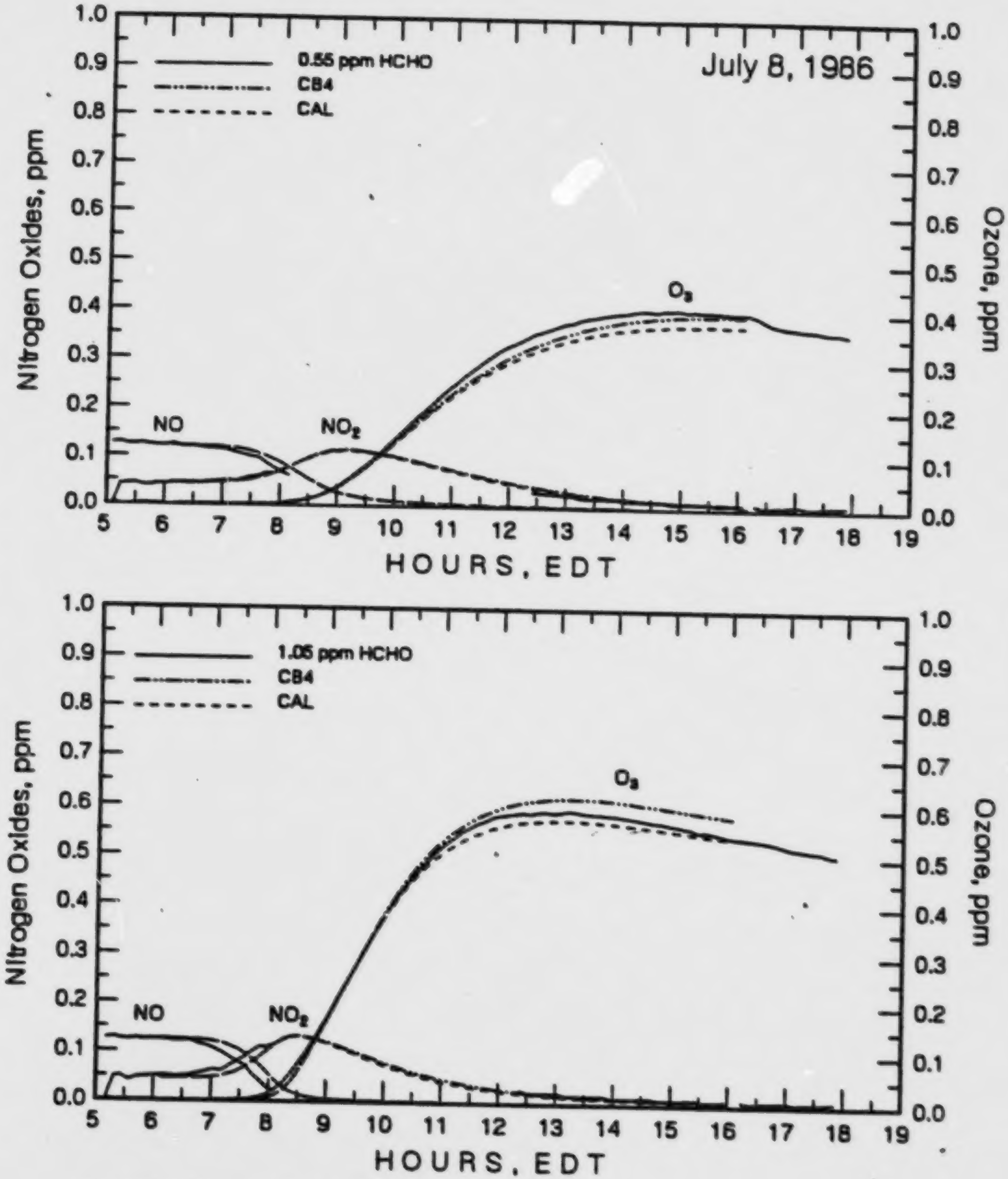

Figure 15. Standard Killus wall model.

August 4, 1979
Formaldehyde vs Ethylene

An ethylene–NO_x versus formaldehyde–NO_x experiment and model simulations with the standard wall model is shown in Figures 16 to 18. The formaldehyde side was dehumidified. Both models, using the new in-chamber actinic fluxes and the Bass absorption cross sections, agree well with the measurements of ozone and formaldehyde. Using the standard Carter wall model assumptions, the models do not simulate the early reactivity of this experiment. It appears that the ozone maximum would be correctly simulated if the early part of the experiment were simulated more correctly.

Figures 19 and 20 show a re-simulation with 40 ppb HONO evolving from the walls as the temperature rises just after sunset. This extra initial source results in excellent agreement for the ethylene decay. Figure 21 compares the integrated $HO^{\cdot}$ as a function of time for the two major radical sources in this simulation.

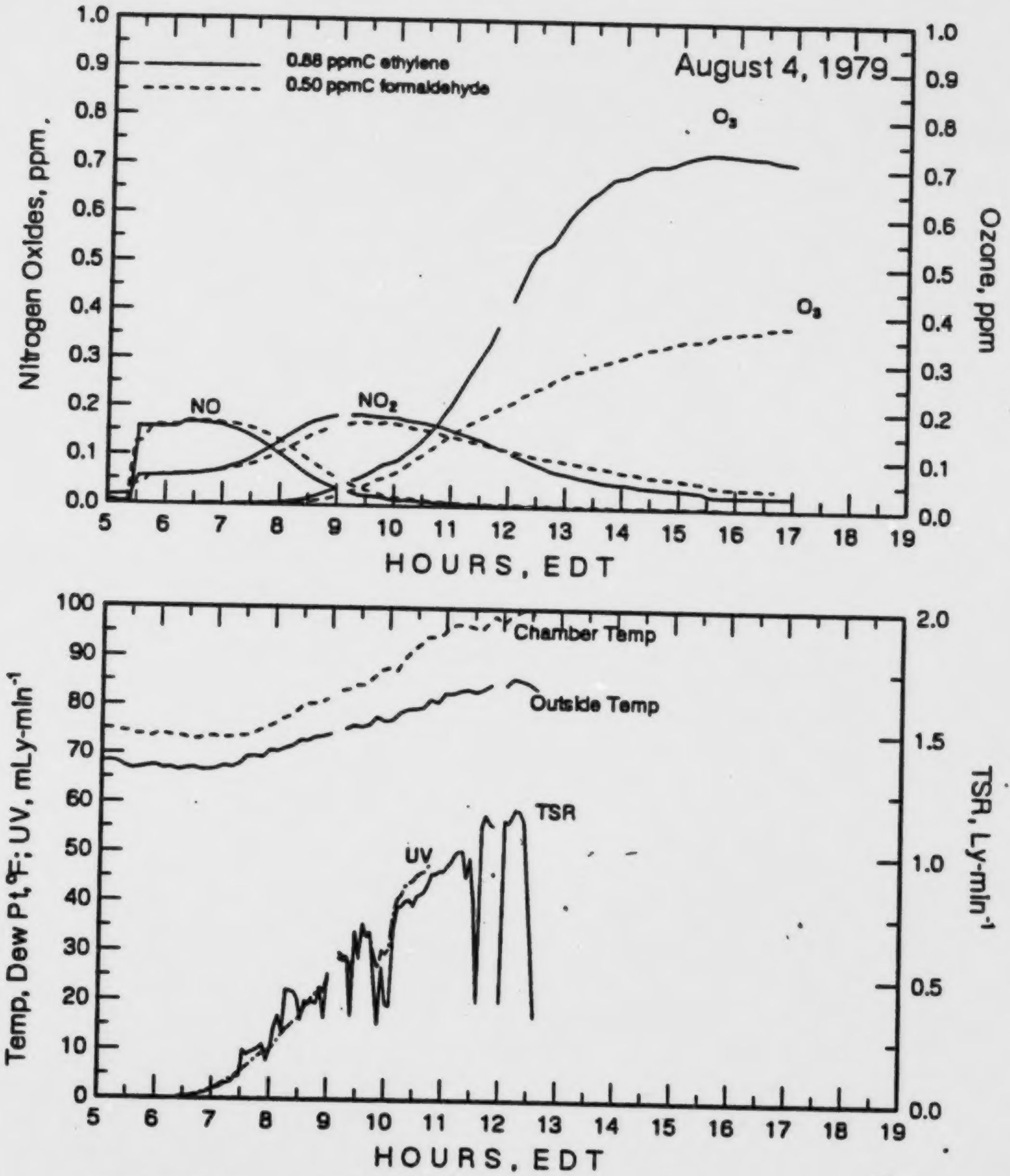

Figure 16. Relative HC reactivity experiment.

Table 21. August 4, 1979 Initial Condition Simulation File.

```
 #if RED
August 4, 1979 (R) 0.88 ppmC Ethylene
#end
 #if BLUE
August 4, 1979 (B) 0.50 ppmC HCHO
#end
 #if CB4
c:\pkss\mech\CB42chm.pks
CONC=
@c:\pkss\mech\CBckCB4.icx
#end
 #if CAL
c:\pkss\mech\CALchm.pks
CONC=
@c:\pkss\mech\CBckCAL.icx
#end

#if RED
 NO        =  0.167,
 NO2       =  0.060,
#end
#if BLUE
 NO        =  0.170,
 NO2       =  0.061,
#end

#if RED
#if CB4
 ETH       =  0.439,
#end

#if CAL
 ETHE      =  0.439,
#end
#end

#if BLUE
#if CB4
 HCHO      =  0.504,
#end

#if CAL
HCHO      =  0.504,
#end
#end

 HONO  =        0.004,
CO    =        0.45;

@e:\segfiles\finalseg\79\au0479.lix
@e:\segfiles\finalseg\79\au0479.twd
FINISH;
```

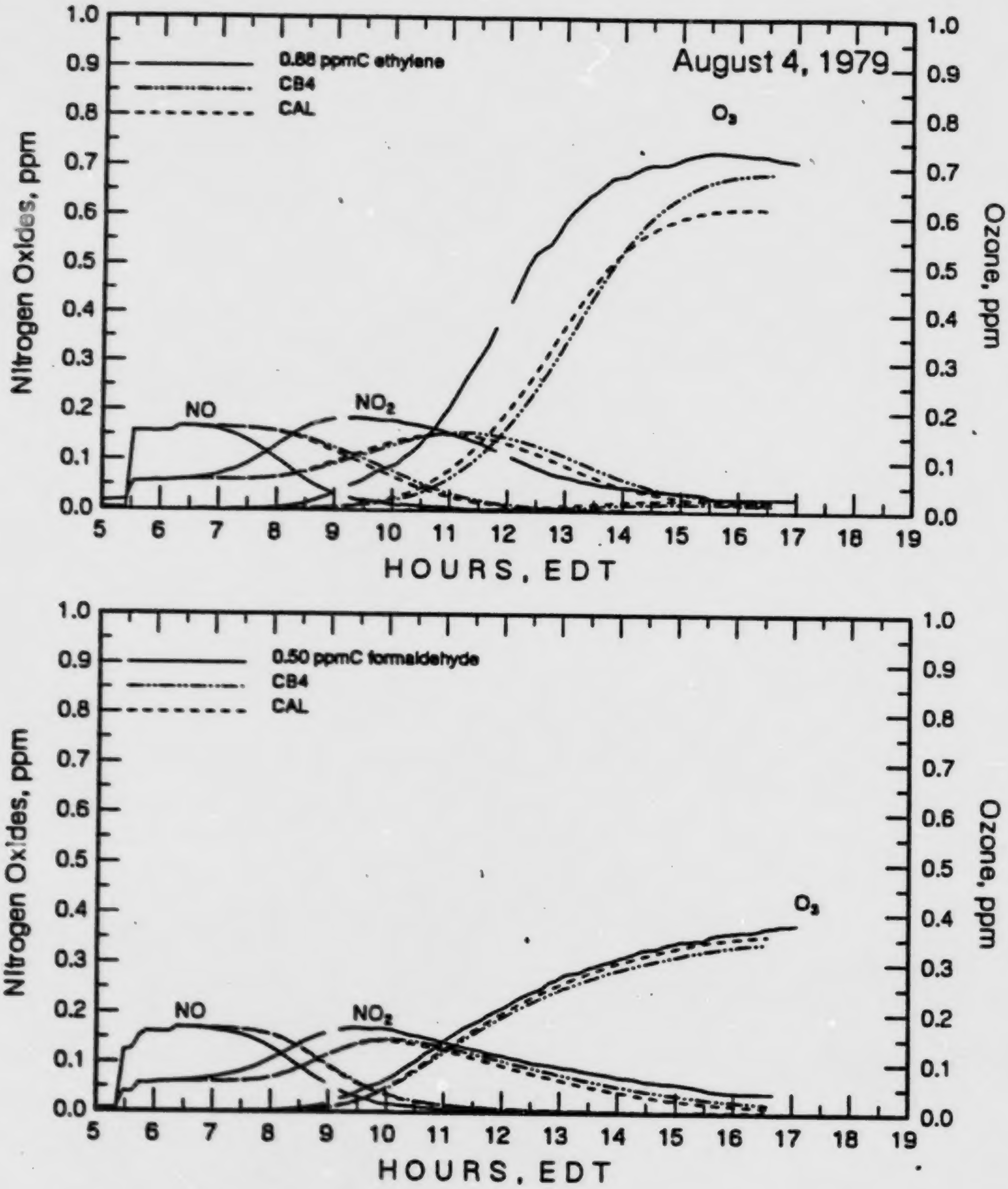

Figure 17. Standard Carter wall model.

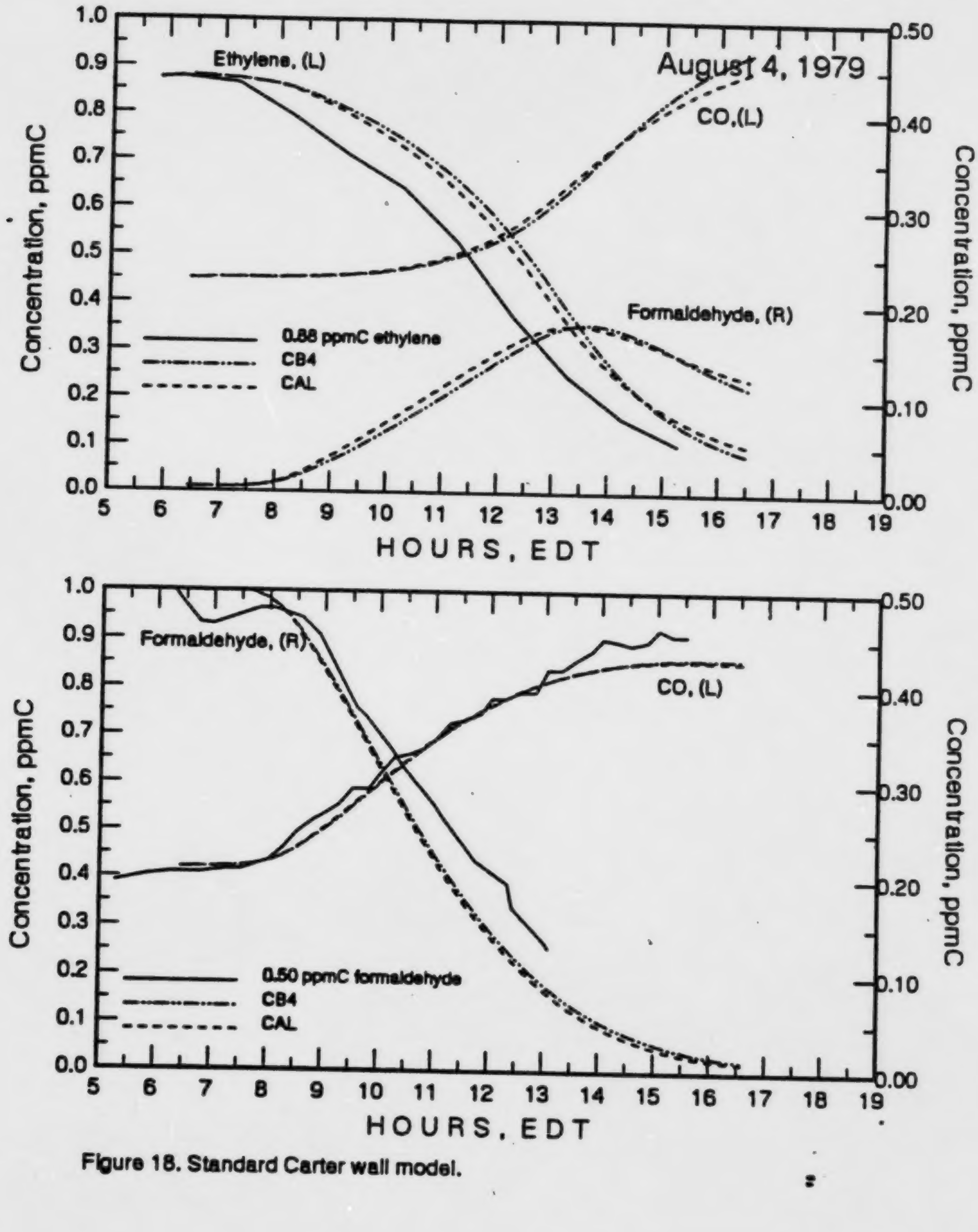

Figure 18. Standard Carter wall model.

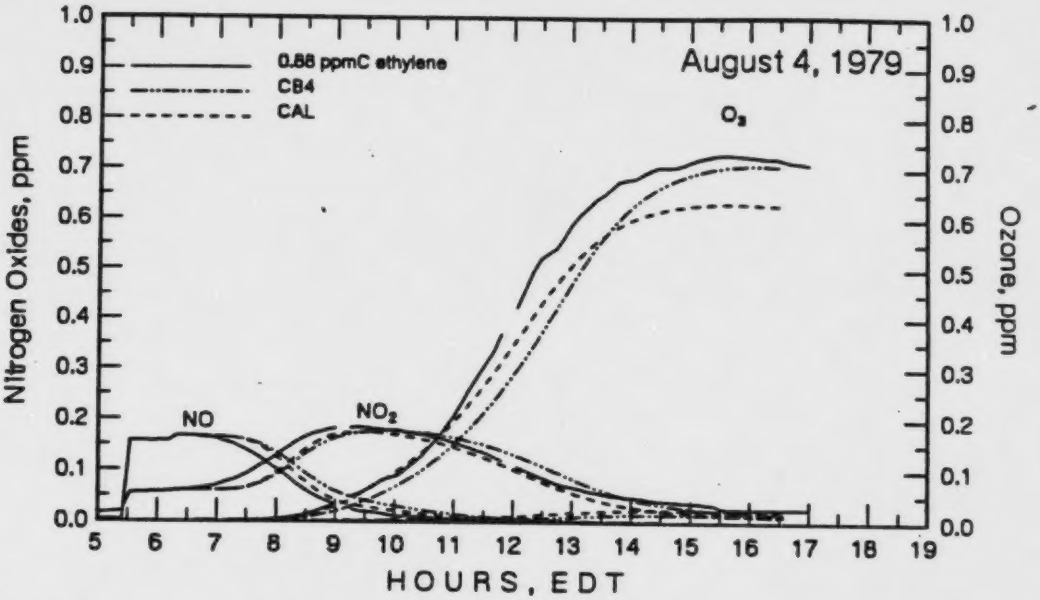

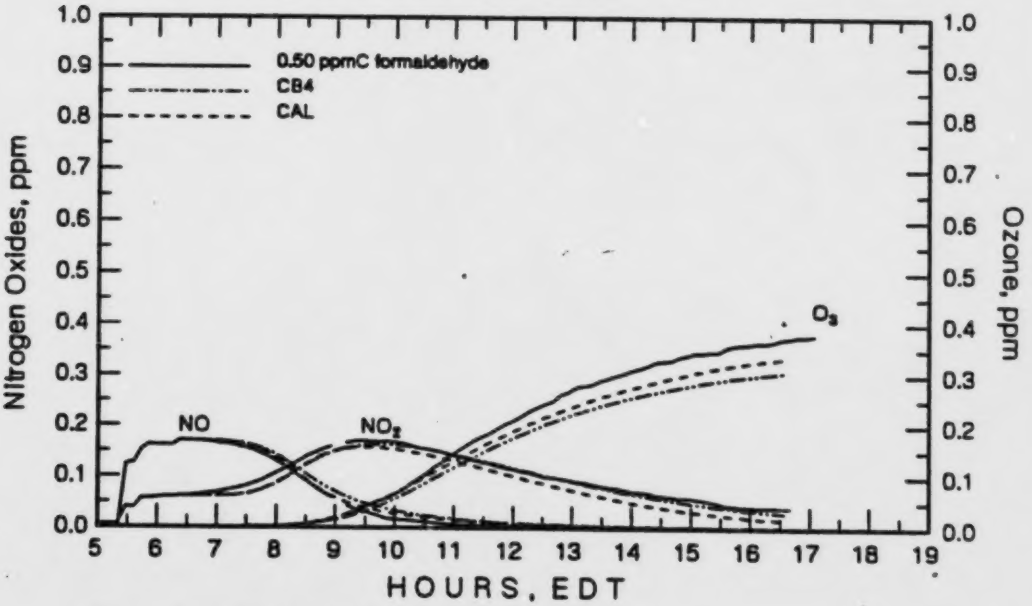

Figure 19. Wall HONO = 40 ppb, and Carter wall model.

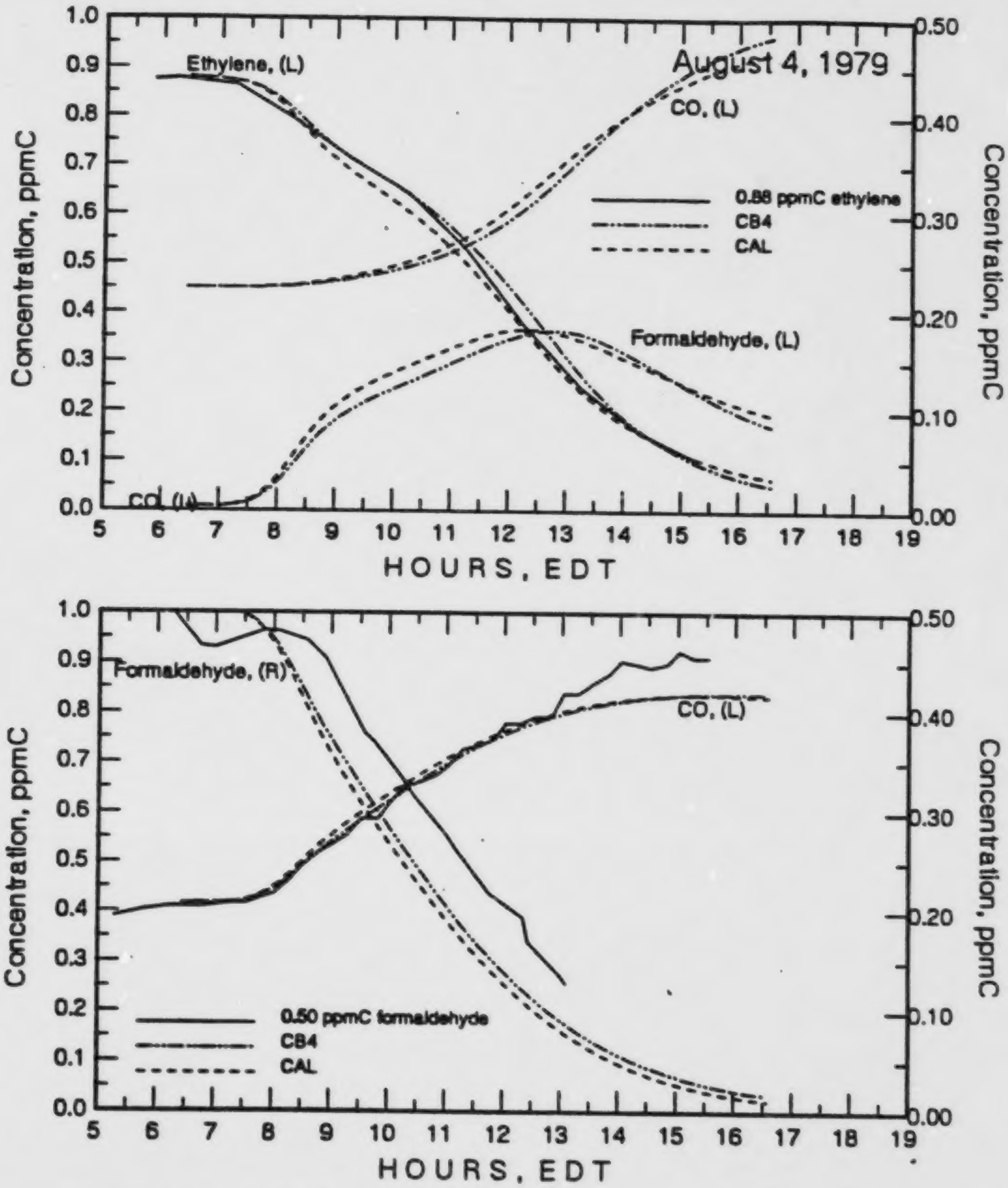

Figure 20. Wall HONO = 40 ppb, and Carter wall model.

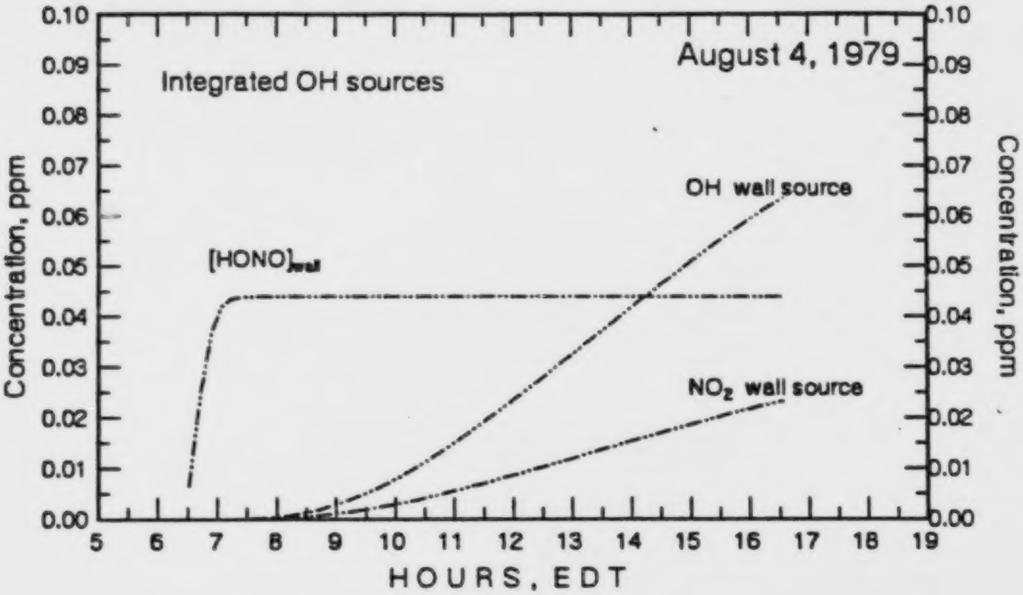

Figure 21. Total OH added by wall HONO (morning) and Carter OH source (afternoon), and additional NO_2 added by Carter NO_2 source.

August 23, 1978
Matched Ethylene at 0.5 NOx

Figure 22 shows a matched ethylene experiment at 0.50 ppm NO_x. Figures 23 and 24 show the simulation results. Although slightly too reactive in the beginning, both models are able to simulate this experiment well. The two mechanisms have nearly identical chemistry for ethylene:

For CB4:

```
OH   + C::C  = 1.56 HCHO +     HO2  + 0.22  RCHO  + XO2
XO2  + NO    =      HO2
O3   + C::C  =      HCHO + 0.12 HO2  + 0.42  CO
```

For CAL:

```
OH   + C::C  = 1.56 HCHO +          + 0.22  RCHO  + RO2R
RO2R + NO    =      HO2  +     HO2
O3   + C::C  =      HCHO + 0.12 HO2  + 0.42  CO
```

The difference in O_3 predictions at the end of the simulation, then is related to other chemistry than ethylene. Notice that CB4 correctly follows the ethylene decay at the end of the simulation (14-17 EDT in Figure 24, where as CAL does not. The termination chemistry is different in the two mechanisms, and it appears that CB4 has a better approximation of the correct reactivity.

There was no HCHO data for this day, but the fact that the CO data are under predicted is consistant with other simulations here that do have HCHO data and which are also under predicted.

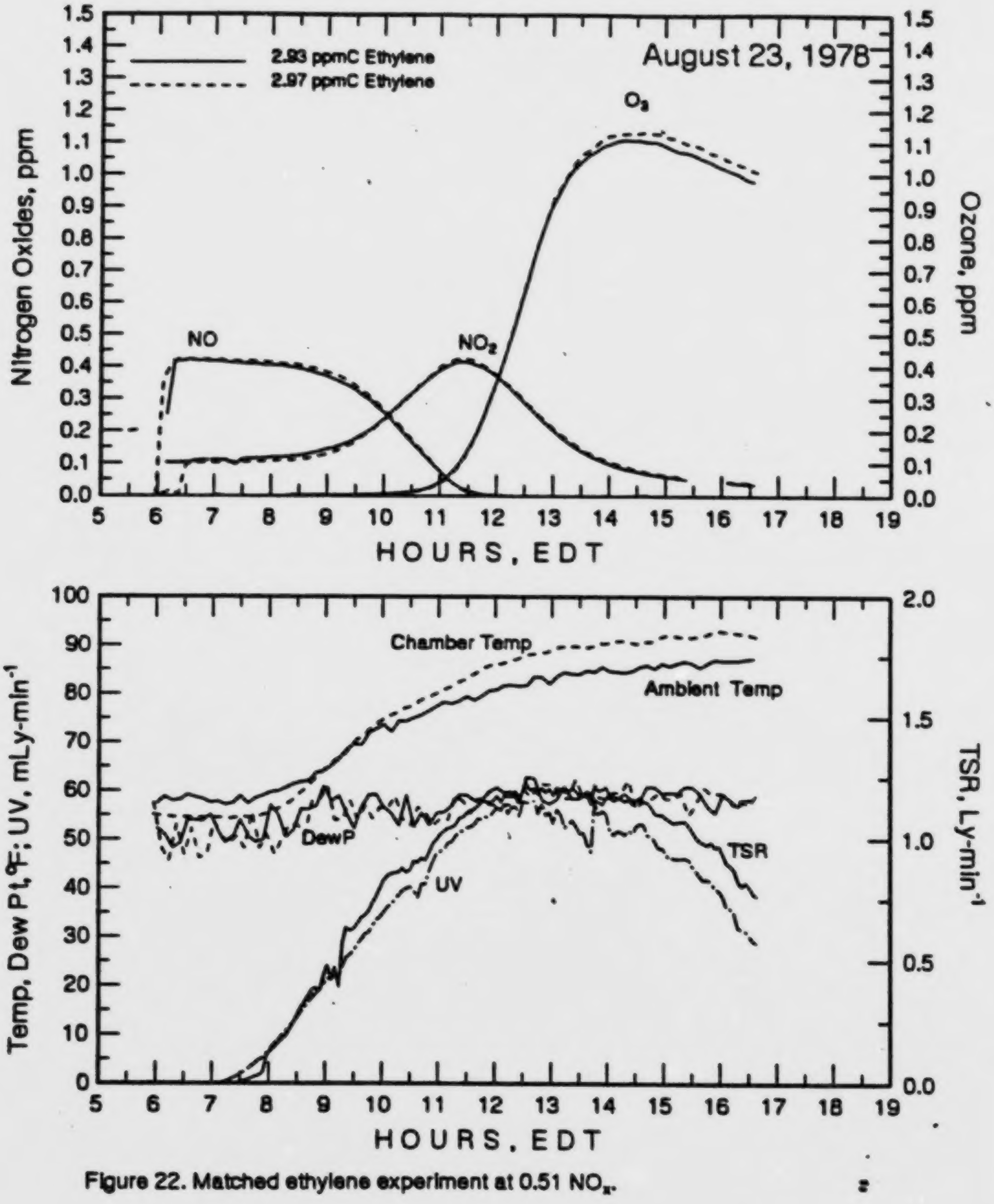

Figure 22. Matched ethylene experiment at 0.51 NO$_x$.

Table 22. August 23, 1978 Initial Condition Simulation File

```
#if RED
Aug 23, 1978 2.93 ppmC Ethylene (RED)
#end
#if BLUE
Aug 23, 1978 2.97 ppmC Ethylene (BLUE)
#end
#if CB4
c:\pkss\mech\CB42chm.pks
CONC=
@c:\pkss\mech\CBckCB4.icx
#end
#if CAL
c:\pkss\mech\CALchm.pks
CONC=
@c:\pkss\mech\CBckCAL.icx
#end

#if RED
 NO       =  0.412,
 NO2      =  0.095,
#end
#if BLUE
 NO       =  0.417,
 NO2      =  0.104,
#end

#if RED
#if CB4
 ETH  = 1.465,
#end
#if CAL
 ETHE = 1.465,
#end
#end
#if BLUE
#if CB4
 ETH    =  1.485,
#end
#if CAL
 ETHE   =  1.485,
#end
#end
 HONO  =          0.007,
CO     =          0.3;

@e:\segfiles\finalseg\B4\au2378.lix
@e:\segfiles\finalseg\B4\au2378.twd

FINISH;
```

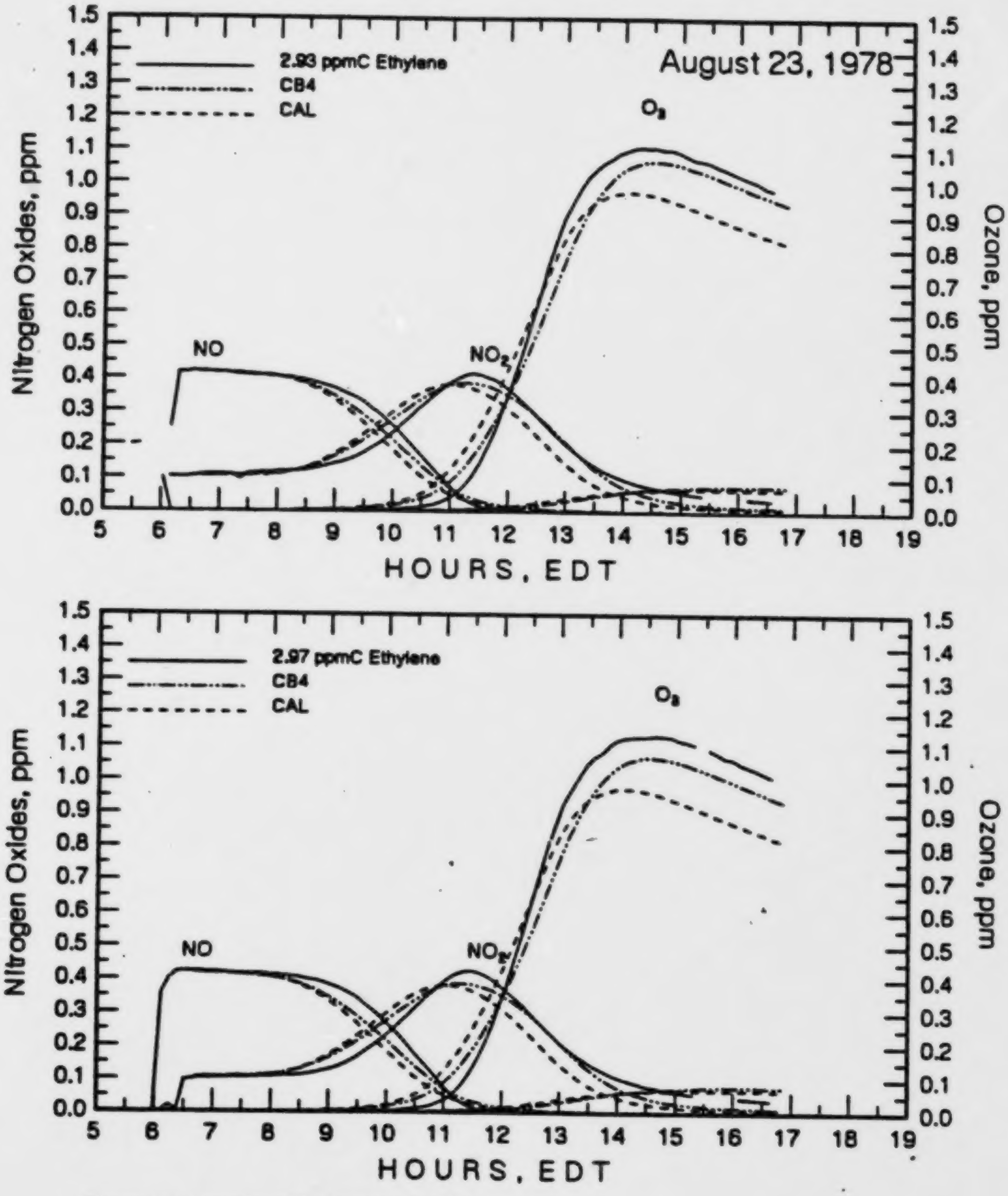

Figure 23. Standard Carter wall model.

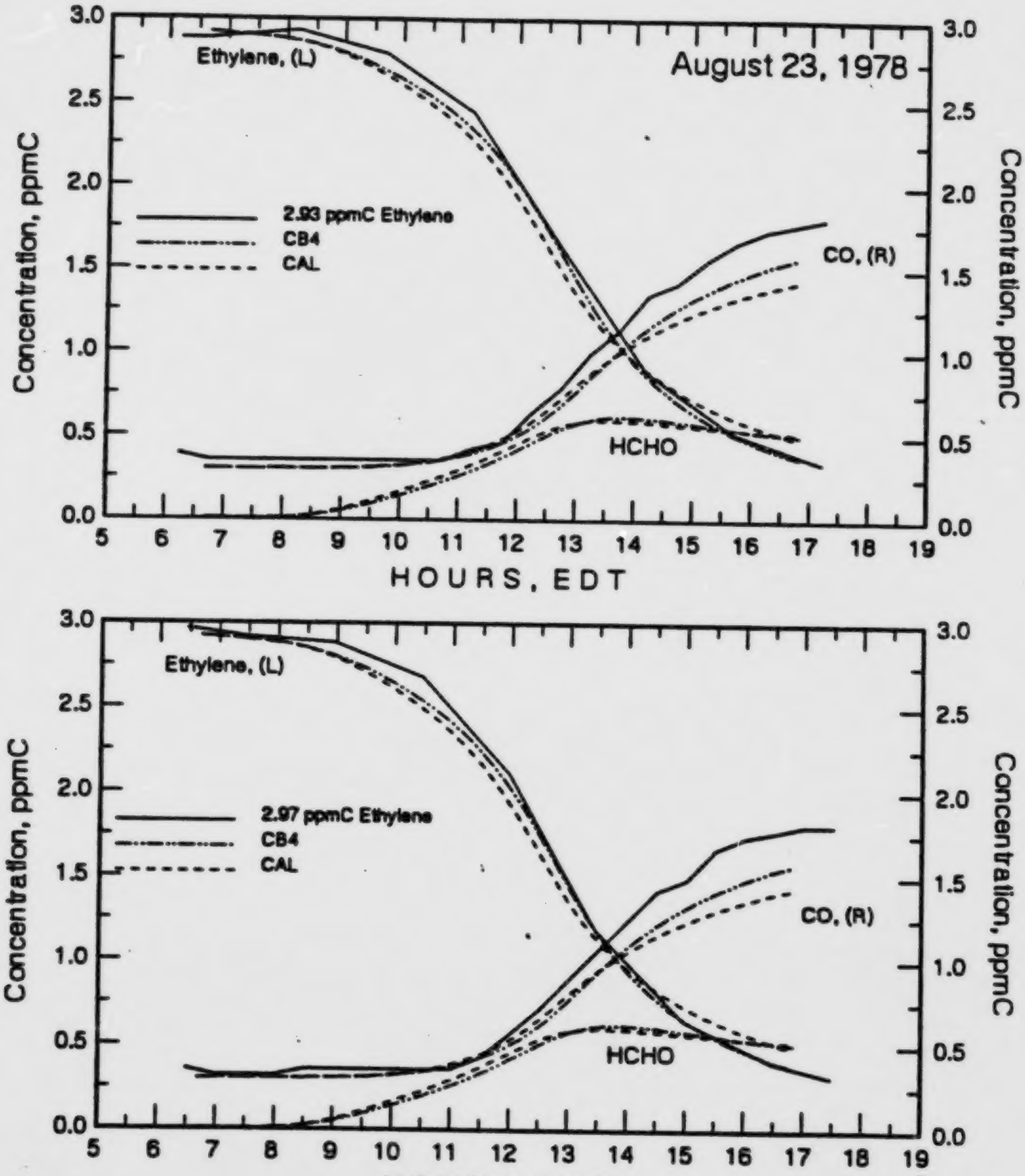

Figure 24. Standard Carter wall model.

July 9, 1986
Delta Ethylene

Figures 25 to 28 show the data and simulations for a delta HC experiment for ethylene. In Figure 26 two sets of model simulations are shown together: the standard Carter wall assumption and no wall radicals or wall NO_x. The difference at the lower 0.88 ppmC ethylene condition is remarkable, especially compared to the minimal effect this assumption has on the 1.87 ppmC ethylene side (simply delays simulation by about 1 hour). Figures 27 and 28 show that the ethylene decay is correctly reproduced for the standard wall assumption, but is very slow in the no wall radical case. Figure 29 shows the prediction using the Killus model, which because material is being depleted from the walls, shows a better fit to the morning conditions, but as the rate of injection of radicals falls off, the Killus model simulation of the lower side becomes worse, while the higher side merely slows down, but still achieves the peak O_3.

Again the two mechanisms separate at the end of the simulation, CB4 more accurately tracking the O_3 formation and the ethylene loss.

Likewise, both models fail to predict the HCHO in either side. As will be shown in Chapter 6, these HCHO data are probably very good and are consistent with a number of standards and with different analytical methods. In addition, they are similar to the HCHO yields from several ethylene experiments spread throughout the UNC data set.

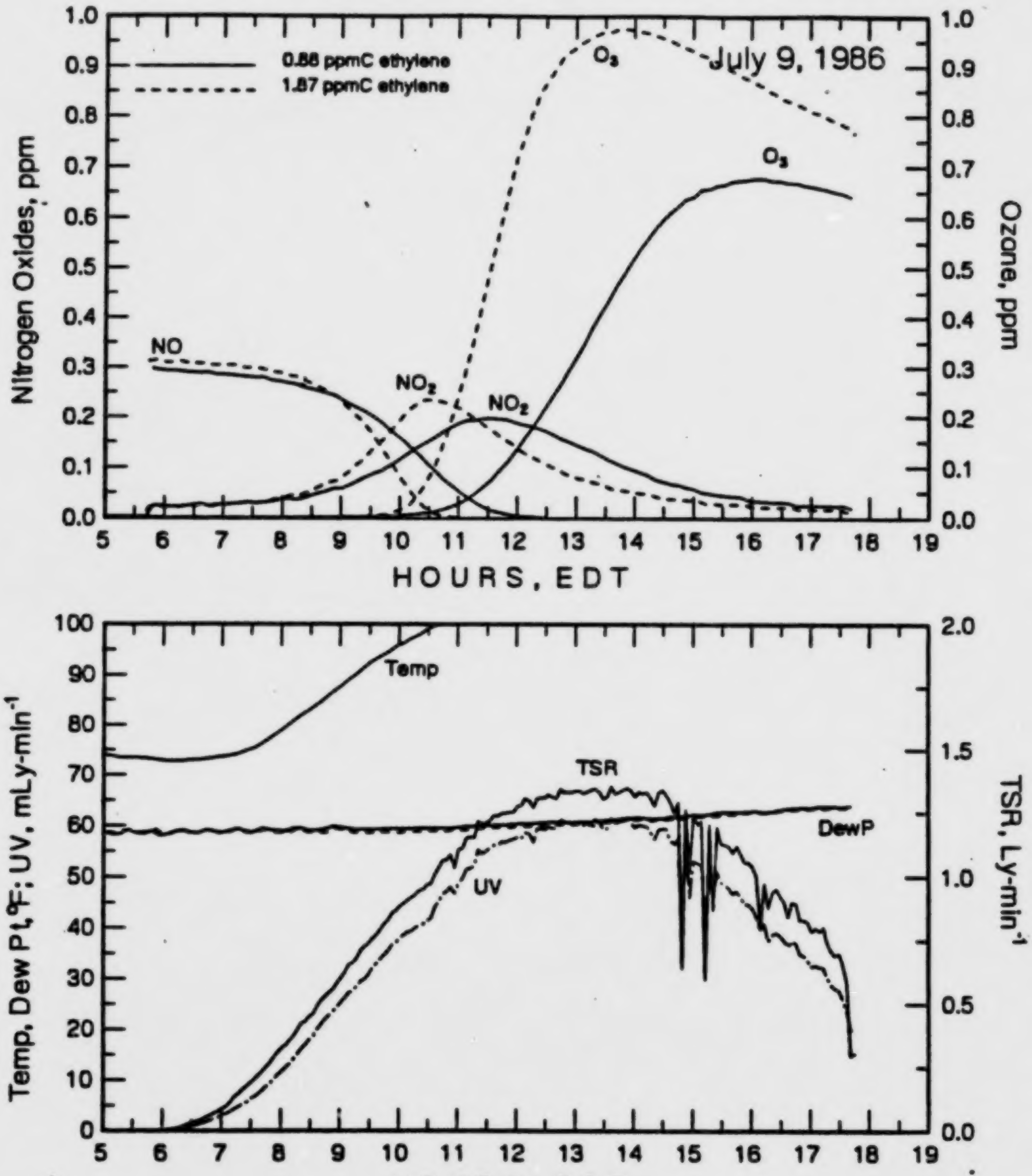

Figure 25. Delta-HC ethylene experiment at 0.33 ppm NO_x.

Table 23. July 9, 1986 Initial Condition Simulation File

```
#if RED
July 9, 1986 (R) 1.0 ppmC Ethylene
#end
#if BLUE
July 9, 1986 (B) 2.0 ppmC Ethylene
#end
#if CB4
c:\pkss\mech\CB42chm.pks
CONC=
@c:\pkss\mech\CBckCB4.icx
#end
#if CAL
c:\pkss\mech\CALchm.pks
CONC=
@c:\pkss\mech\CBckCAL.icx
#end
#if RED
 NO         =  0.291,
 NO2        =  0.023,
#end
#if BLUE
 NO         =  0.308,
 NO2        =  0.021,
#end

#if RED
#if CB4
 ETH        =  0.471,
#end

#if CAL
 ETHE       =  0.471,
#end
#end

#if BLUE
#if CB4
 ETH        =  0.989,
#end

#if CAL
 ETHE       =  0.989,
#end
#end

 HONO  =           0.001,
 CO    =           0.5;

@e:\segfiles\finalseg\86\jl0986.lix
@e:\segfiles\finalseg\86\jl0986.twd

FINISH;
```

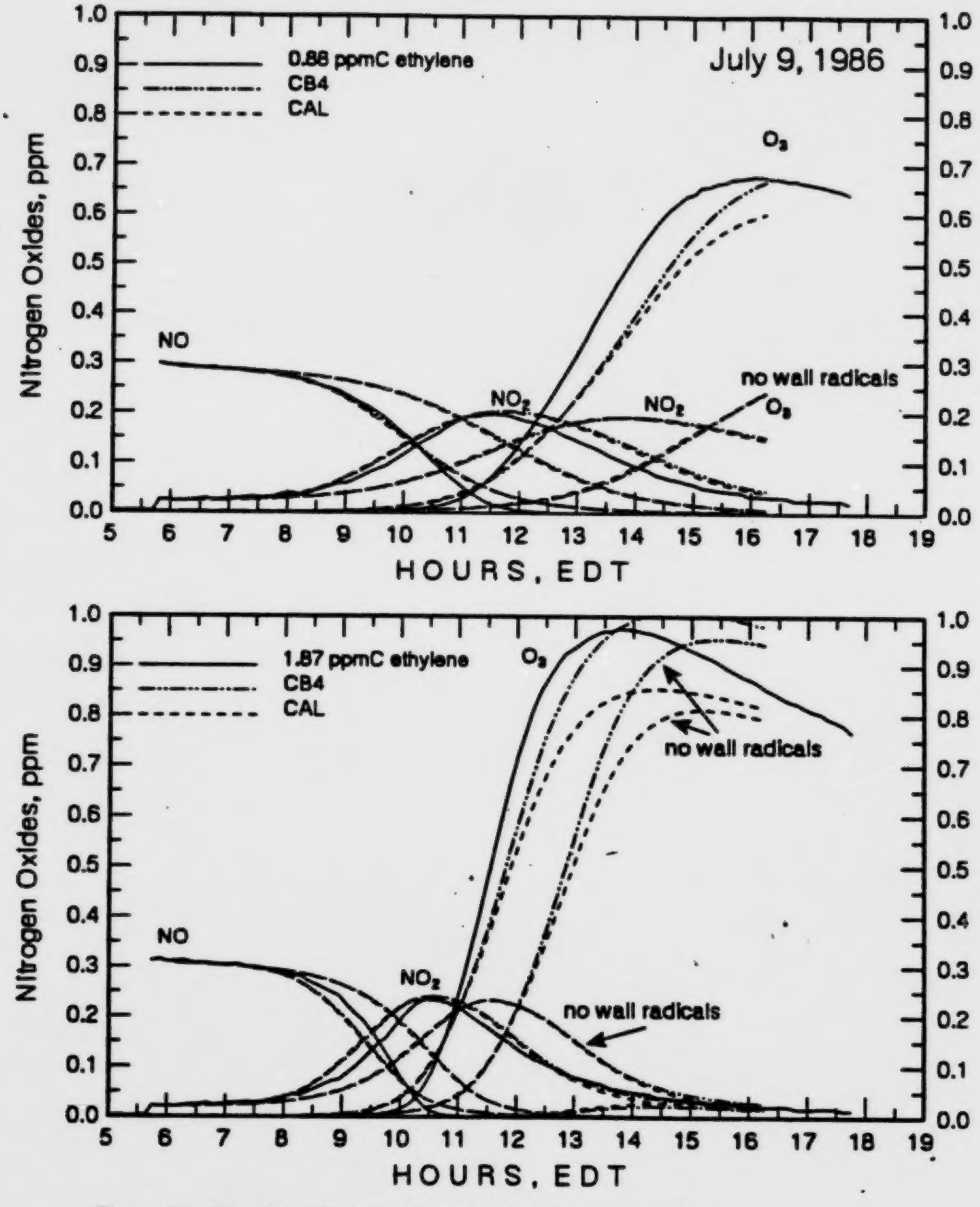

Figure 26. Standard Carter wall model and no wall radicals.

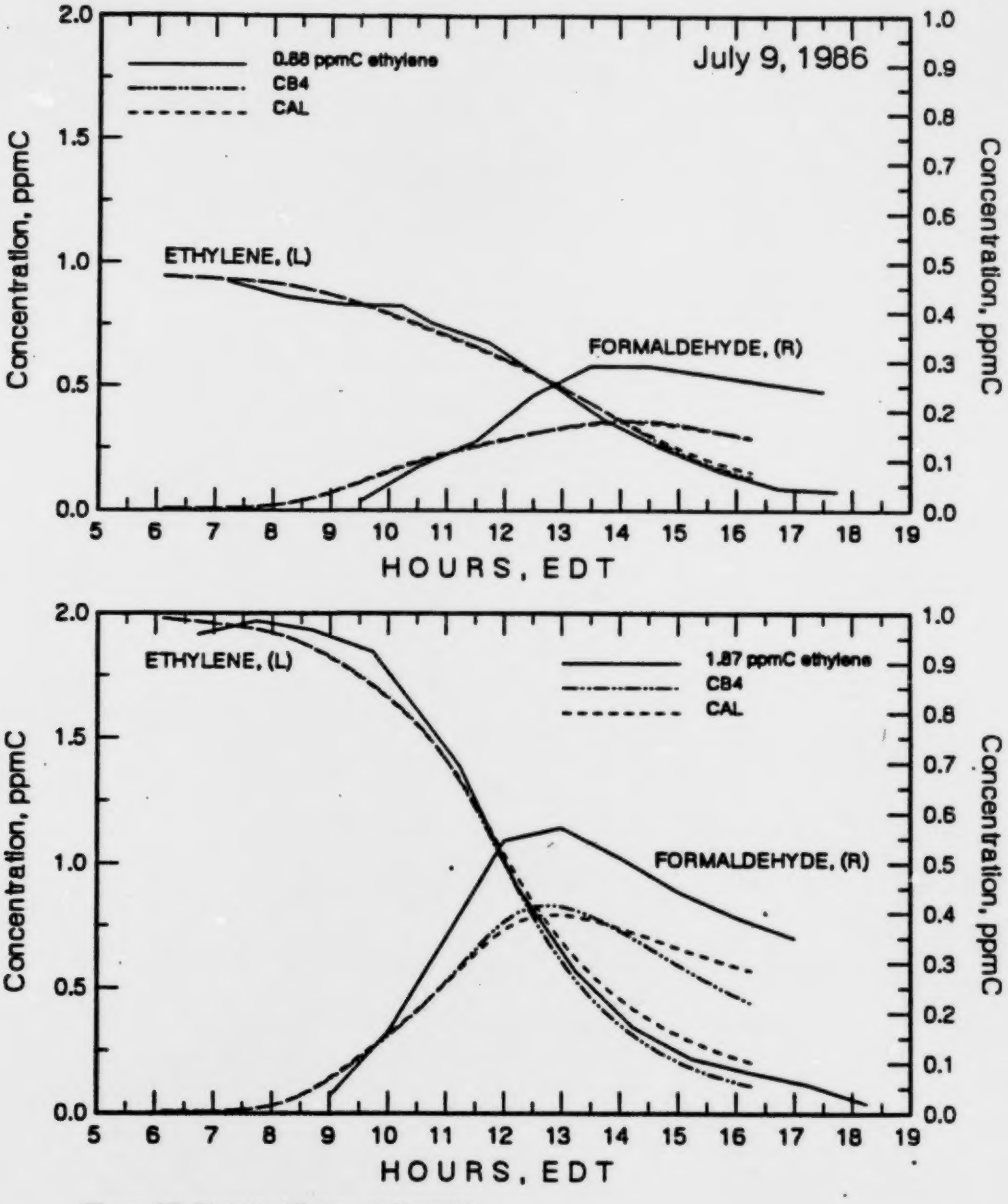

Figure 27. Standard Carter wall model.

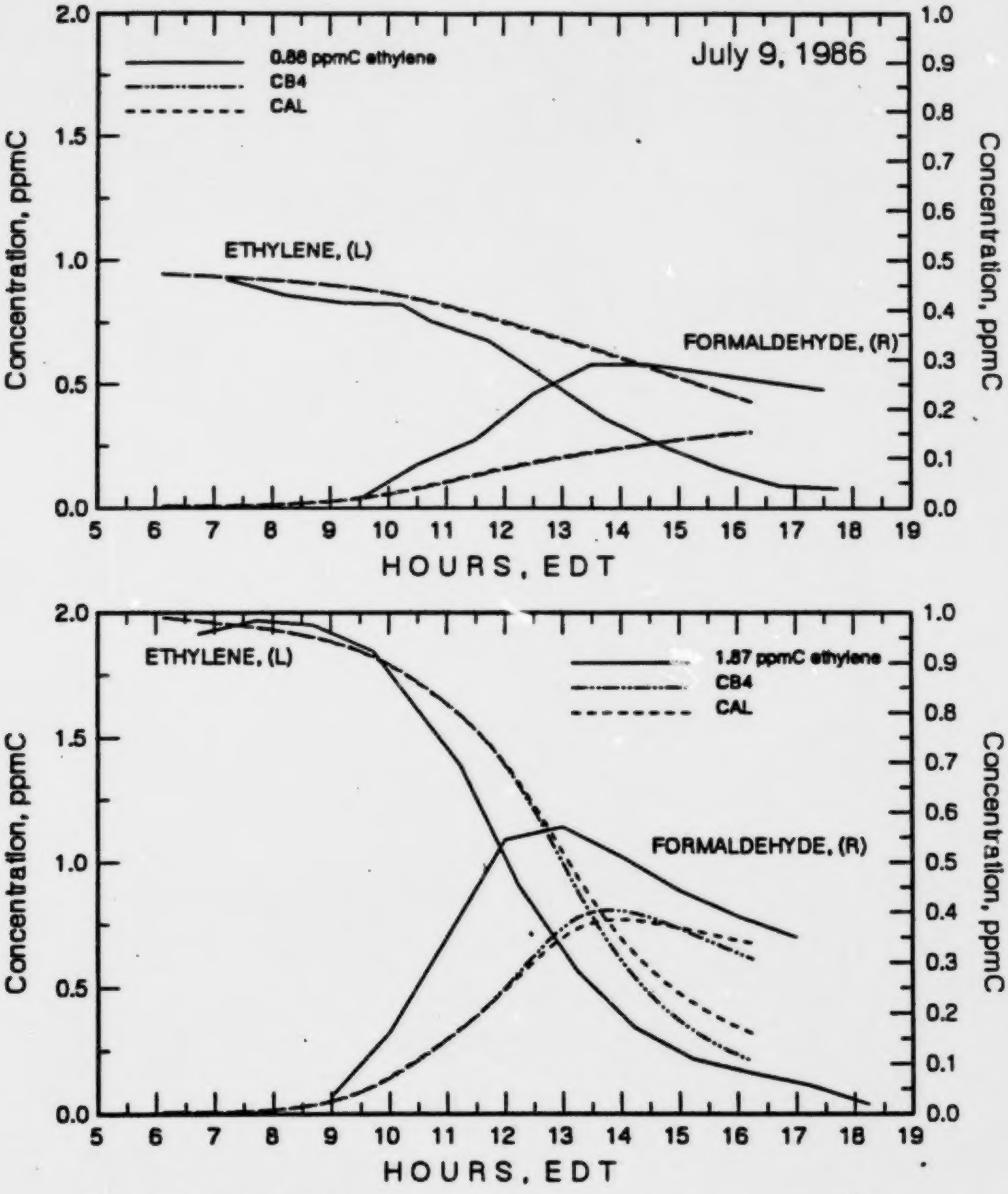

Figure 28. No wall model.

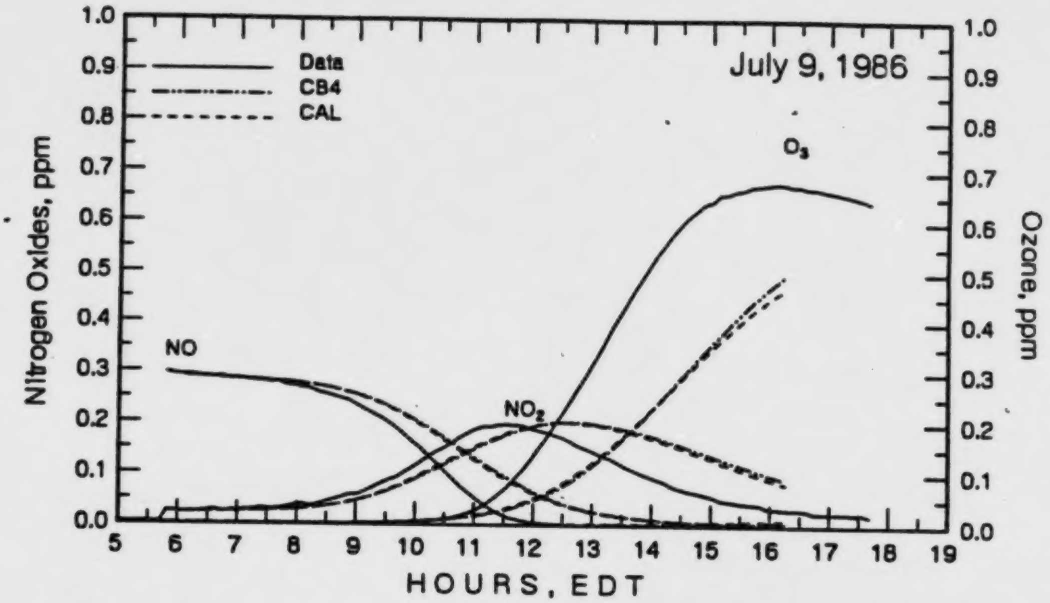

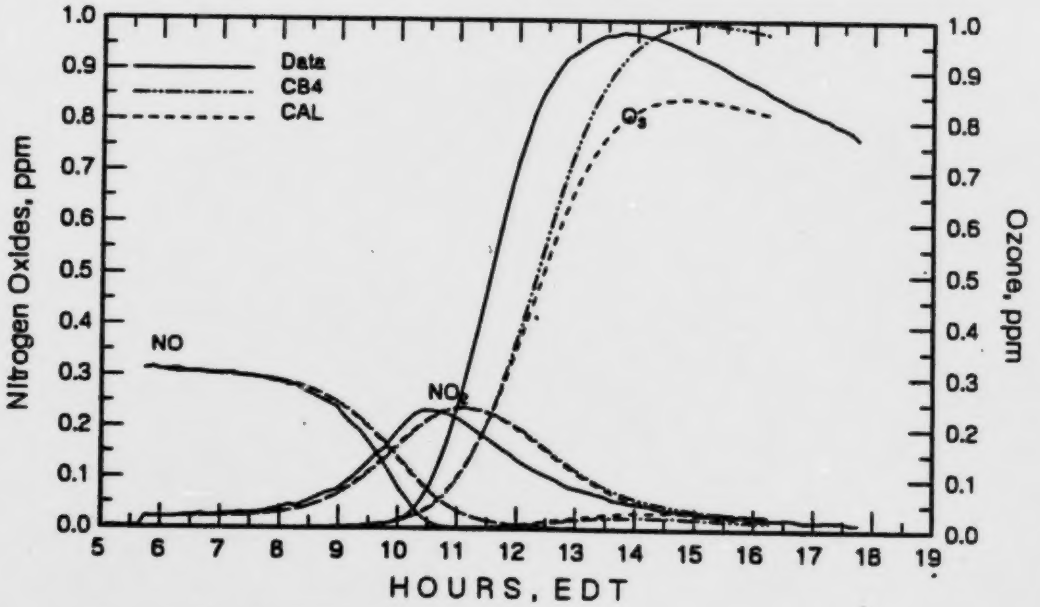

Figure 29. Standard Killus wall model.

July 30, 1978
Ethylene vs Propylene at 0.5 NOx

Figures 30 to 32 show the data and simulations for a relative reactivity experiment comparing ethylene and propylene.

The two mechanisms differ in the amount of radicals and stable products they predict for propylene,

For CB4:

```
OH   + OLE   =       HCHO +      ALD2 +       XO2  + NO2
XO2  + NO    =       NO2

O3   + OLE   =  0.74 HCHO + 0.50 ALD2 + 0.440 NO2  + 0.330 CO +
                0.10 OH   + 0.220 RO2 + 0.71 lost C
```

For CAL:

```
OH   + C::CC =       HCHO +      ALD2 +       RO2R
RO2R + NO    =       NO2  +      NO2

O3   + C::CC =  0.65 HCHO + 0.50  ALD2 + 0.165 NO2  + 0.285 CO +
                0.06 OH   + 0.135 RO2  + 0.92  lost C
```

The standard wall model is too low for this day. At first it appears from Figure 31 that CB4 for propylene is a good fit, but the hydrocarbon decay, the PAN production, and the CO production are all too low.

Figure 33 and 34 show simulations with 1.7 times the standard Carter Wall source. In these simulations, the ethylene side is well fitted by both mechanisms. The simultaneous fit to propylene, however, suggests that CB4 produces too many radicals—note that the propylene decay is well simulated by both.

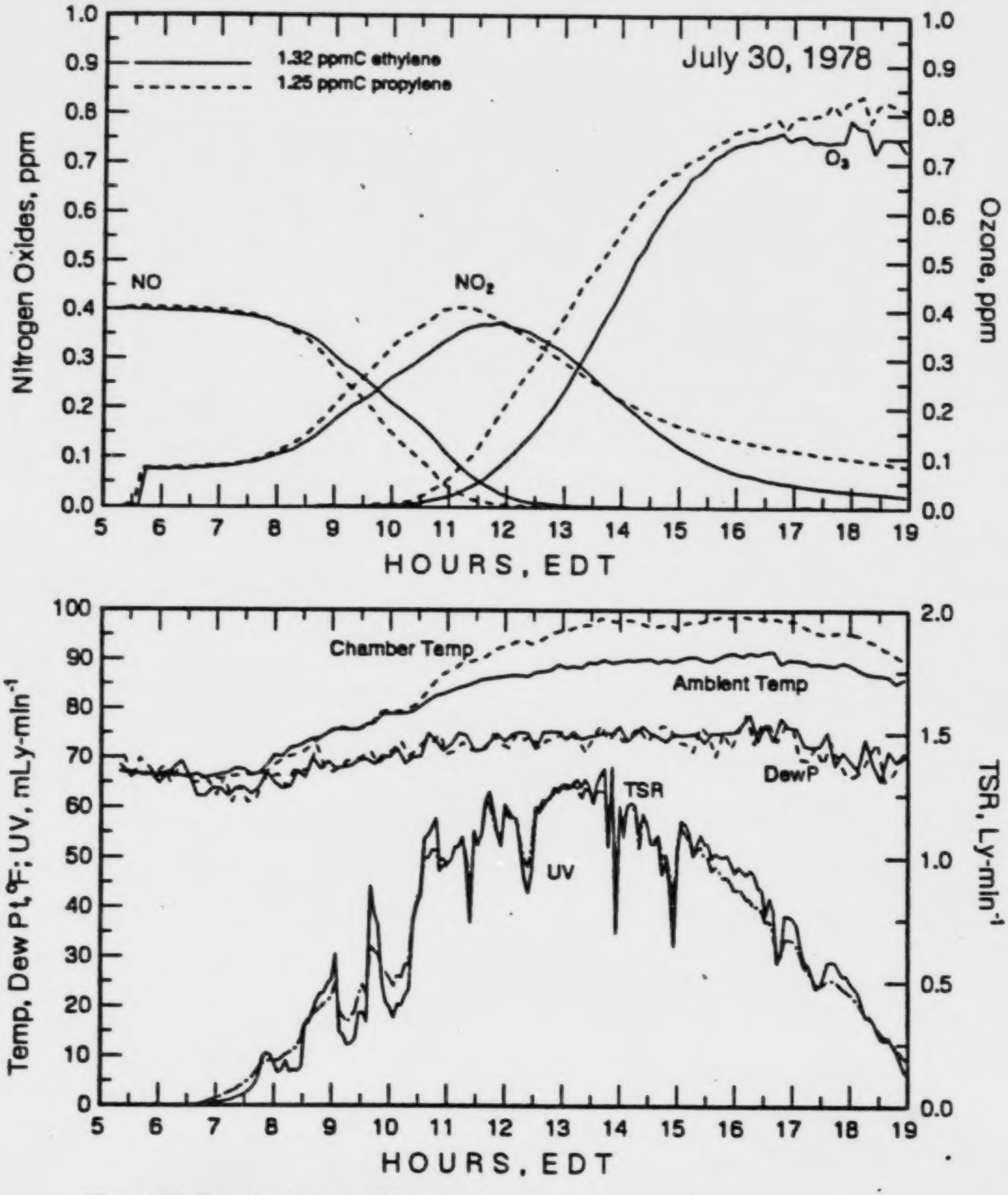

Figure 30. Relative HC reactivity experiment.

Table 24. July 30, 1978 Initial Condition Simulation File

```
#if RED
July 30, 1978 1.32 ppmC Ethylene (RED)
#end
#if BLUE
July 30, 1978 1.25 ppmC Propylene (BLUE)
#end
#if CB4
c:\pkss\mech\CB42chm.pks
CONC=
@c:\pkss\mech\CBckCB4.icx
#end
#if CAL
c:\pkss\mech\CALchm.pks
CONC=
@c:\pkss\mech\CBckCAL.icx
#end

#if RED
 NO       = 0.395,
 NO2      = 0.080,
#end
#if BLUE
 NO       = 0.405,
 NO2      = 0.078,
#end

#if RED
#if CB4
 ETH   = 0.66,
#end

#if CAL
 ETHE  = 0.66,
#end
 CO    = 0.45,
#end

#if BLUE
#if CB4
 OLE   = 0.4167,
 PAR   = 0.4167,
#end

#if CAL
 PRPE  = 0.4167,
#end
 CO    = 0.41,
#end

 HONO  = 0.0055;

@e:\segfiles\finalseg\78\jl3078.lix
@e:\segfiles\finalseg\78\Jl3078.twd

FINISH;
```

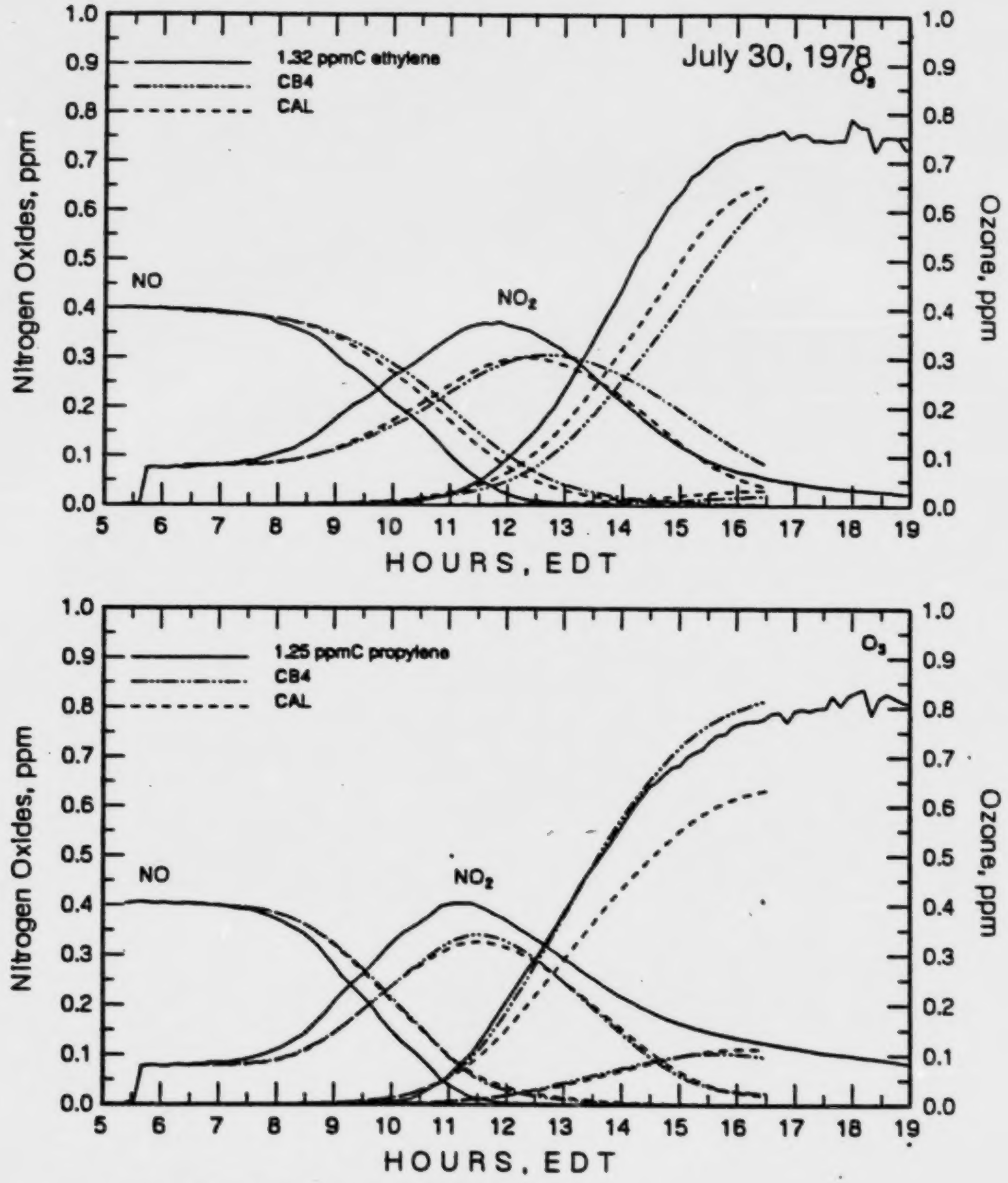

Figure 31. Standard Carter Wall Model.

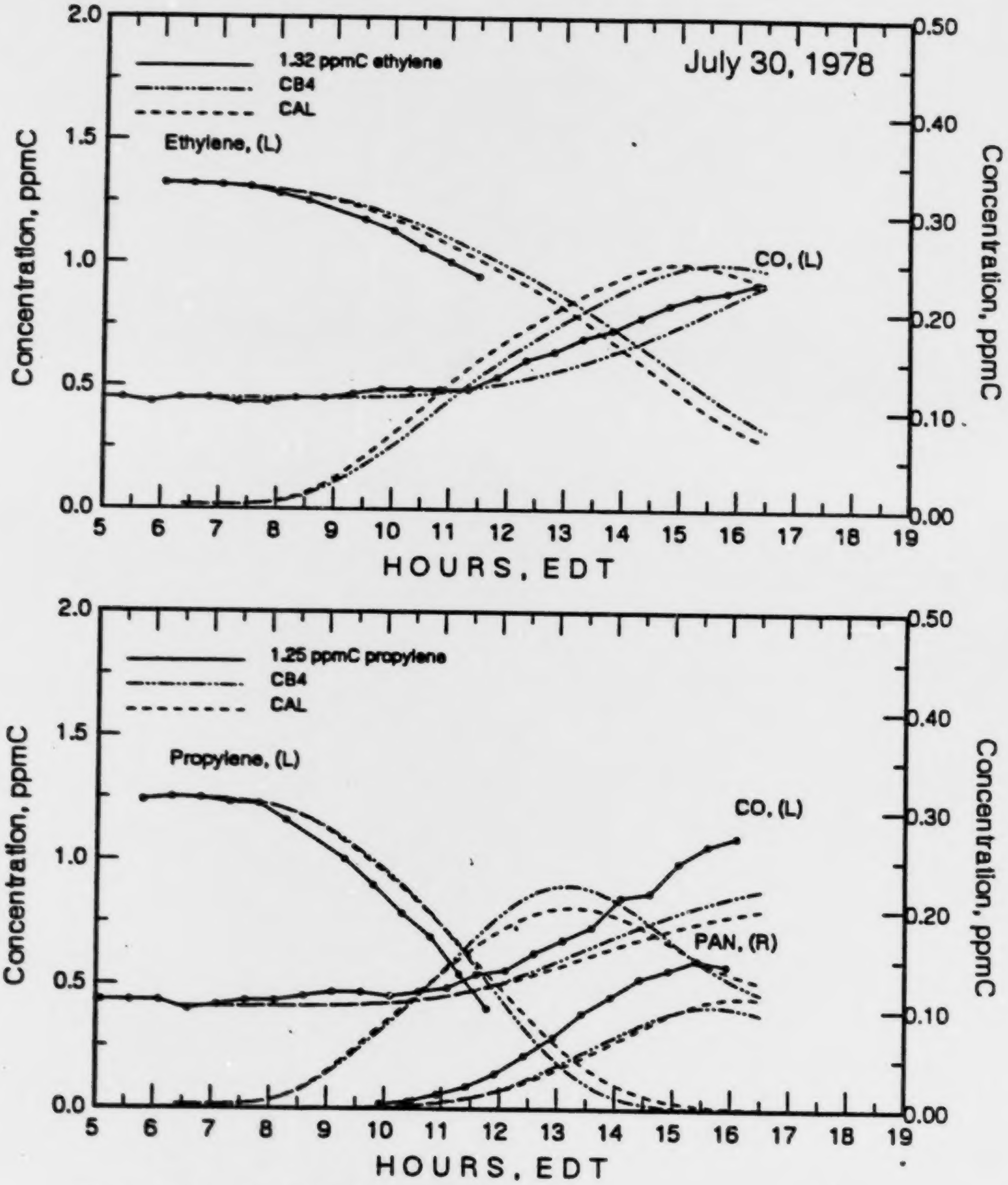

Figure 32. Standard Carter Wall Model.

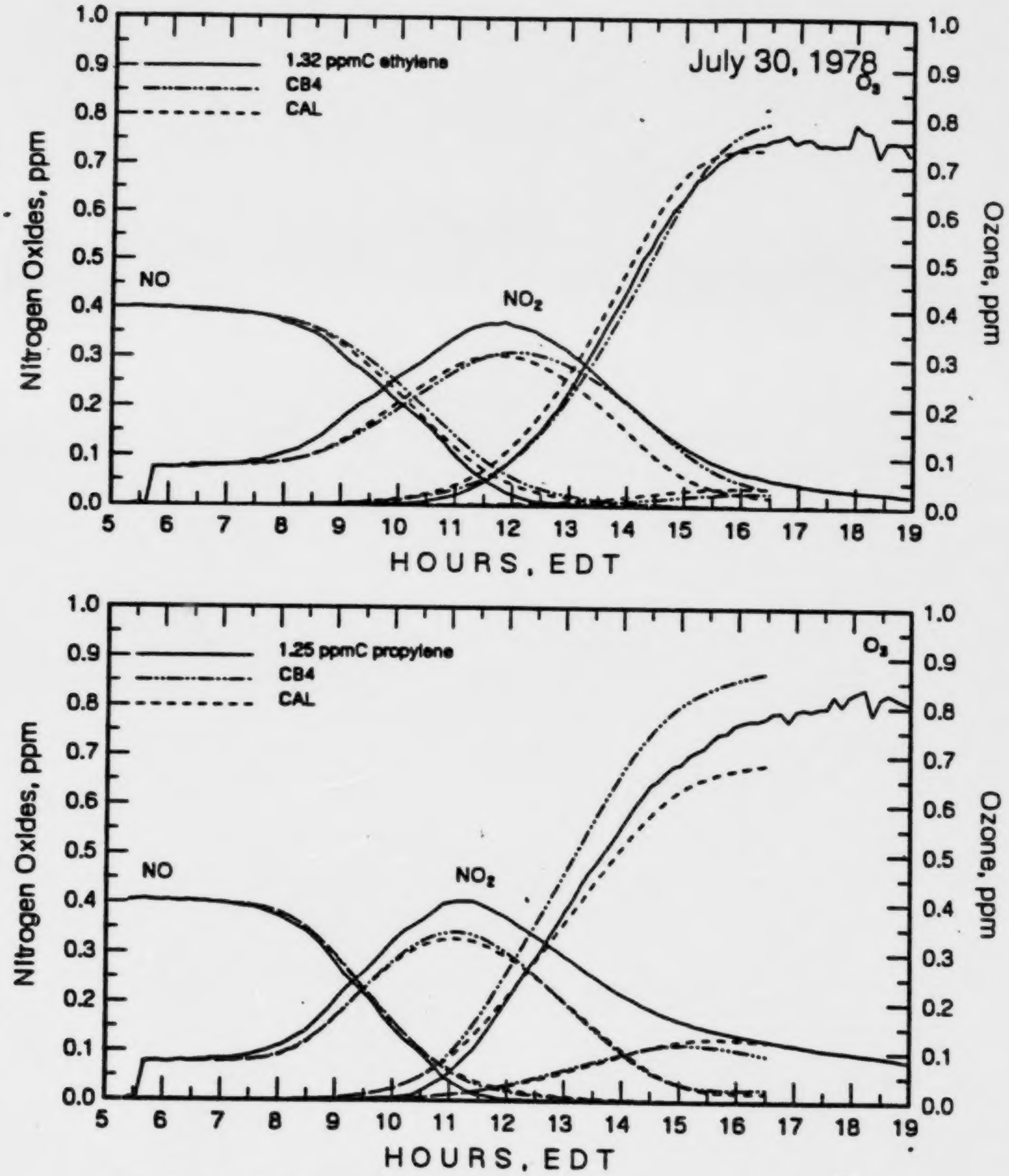

Figure 33. 1.7 times Carter Wall Model.

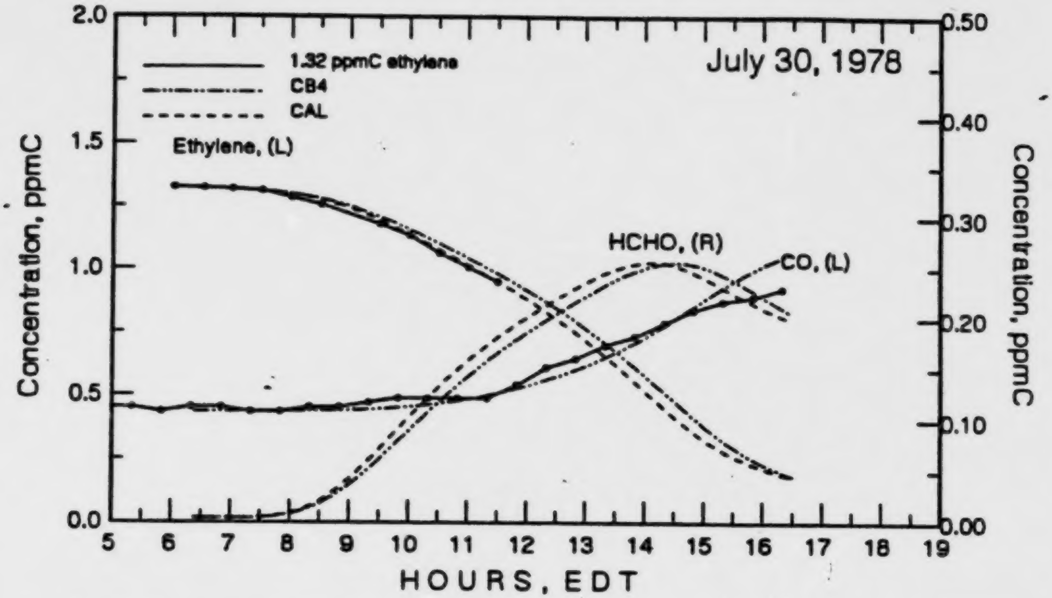

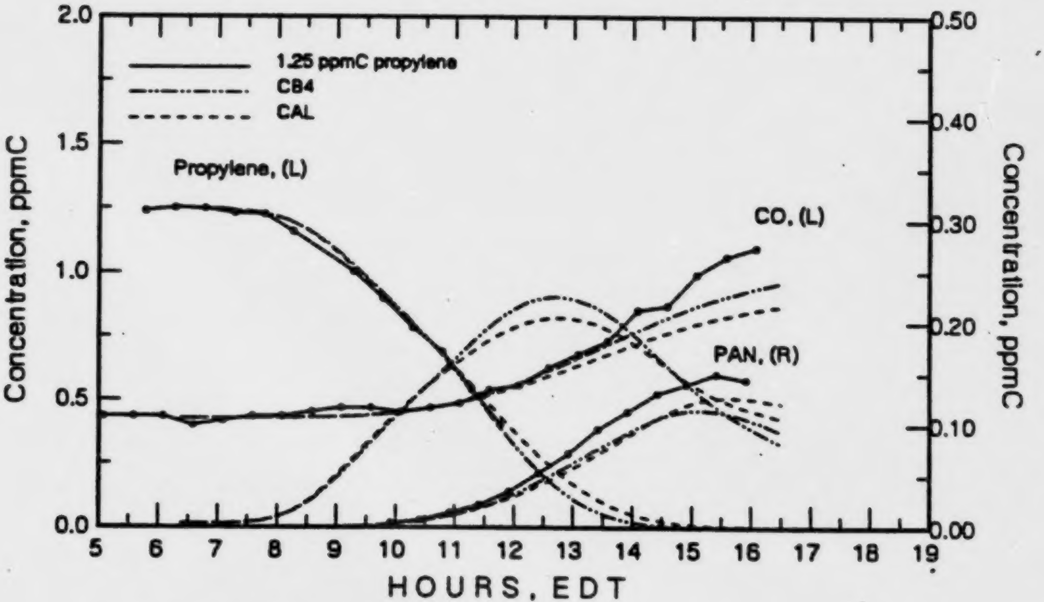

Figure 34. 1.7 times Carter Wall Model.

July 13, 1986
Ethylene vs Propylene at 0.3 NOx

Figures 35 to 37 show data and simulations for a relative reactivity experiment between ethylene and propylene.

The standard Carter Wall model is too reactive on this day. Ethylene is consumed too quickly, and propylene is consumed much too fast (Figure 37).

Figures 38 and 39 show simulations with no wall radicals. These are too slow for NO_x and show ethylene being consumed too slow. Note, however, that propylene appears to be correctly simulated here and CB4 almost fits the O_3 profile in the propylene experiment.

Figures 40 and 41 show simulations with one-half the standard wall model. Here the ethylene NO_x, O_3, and ethylene decays are well simulated. CB4 over predicts O_3 in the propylene side, CAL is a little low, and both over consume propylene.

As before, neither model comes close to fitting the HCHO data.

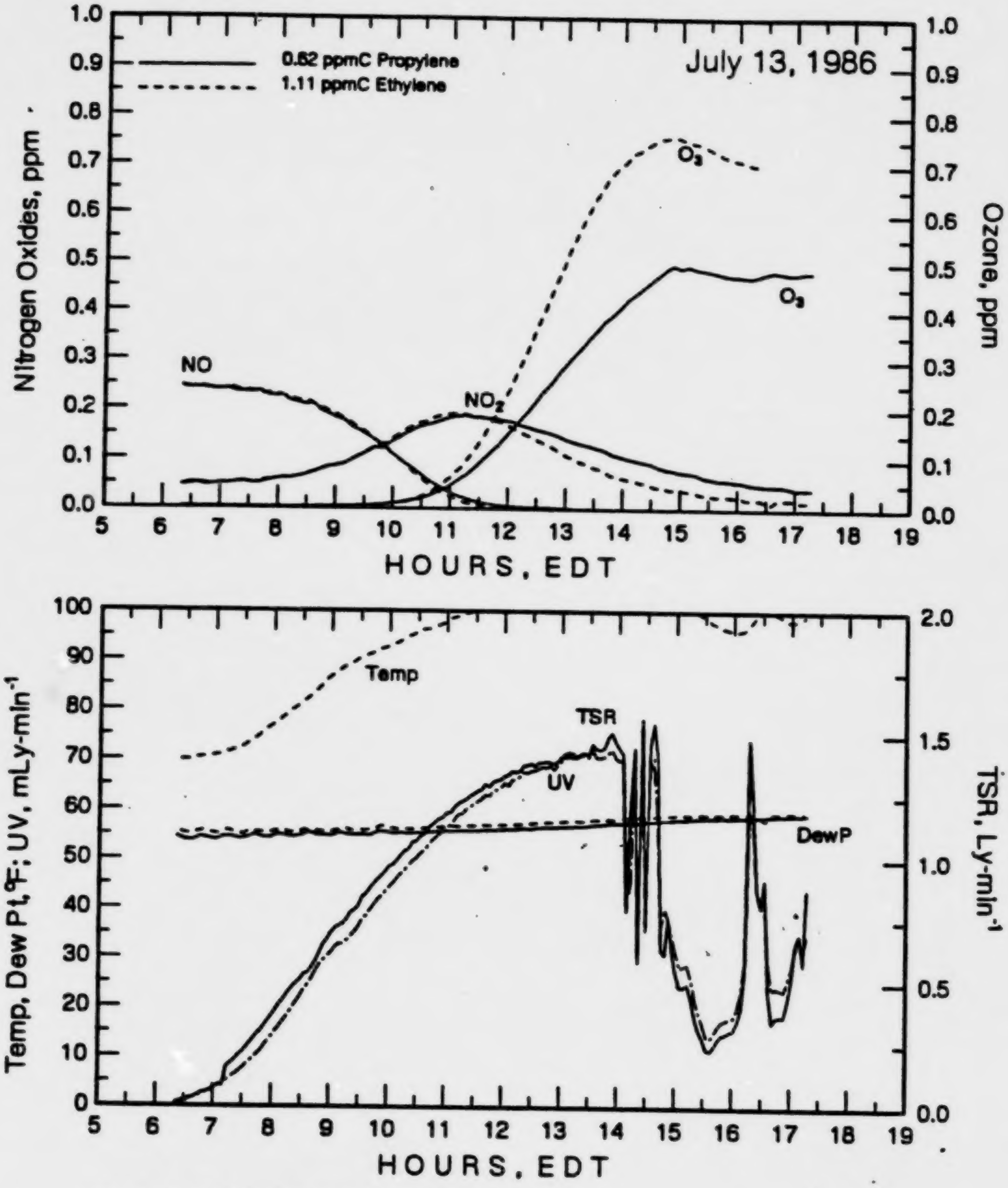

Figure 35. Relative HC reactivity experiment.

Table 25. July 13, 1986 Initial Condition Simulation File

```
#if RED
July 13, 1986 (R) 0.62 ppmC Propylene
#end
#if BLUE
July 13, 1986 (B) 1.11 ppmC ETHYLENE
#end
#if CB4
c:\pkss\mech\CB42chm.pks
CONC=
@c:\pkss\mech\CBckCB4.icx
#end
#if CAL
c:\pkss\mech\CALchm.pks
CONC=
@c:\pkss\mech\CBckCAL.icx
#end

#if RED
 NO        =  0.247,
 NO2       =  0.045,
#end
#if BLUE
 NO        =  0.243,
 NO2       =  0.047,
#end

#if RED
#if CB4
OLE       =  0.21,
PAR       =  0.21,
#end

#if CAL
PRPE      =  0.21,
#end
#end

#if BLUE
#if CB4
 ETH       =  0.555,
 PAR       =  0.0201,
#end

#if CAL
 ETHE      =  0.555,
#end
#end

 HONO  =         0.001,
 CO    =         0.3;

@e:\segfiles\finalseg\86\jl1386.lix
@e:\segfiles\finalseg\86\jl1386.twd

FINISH;
```

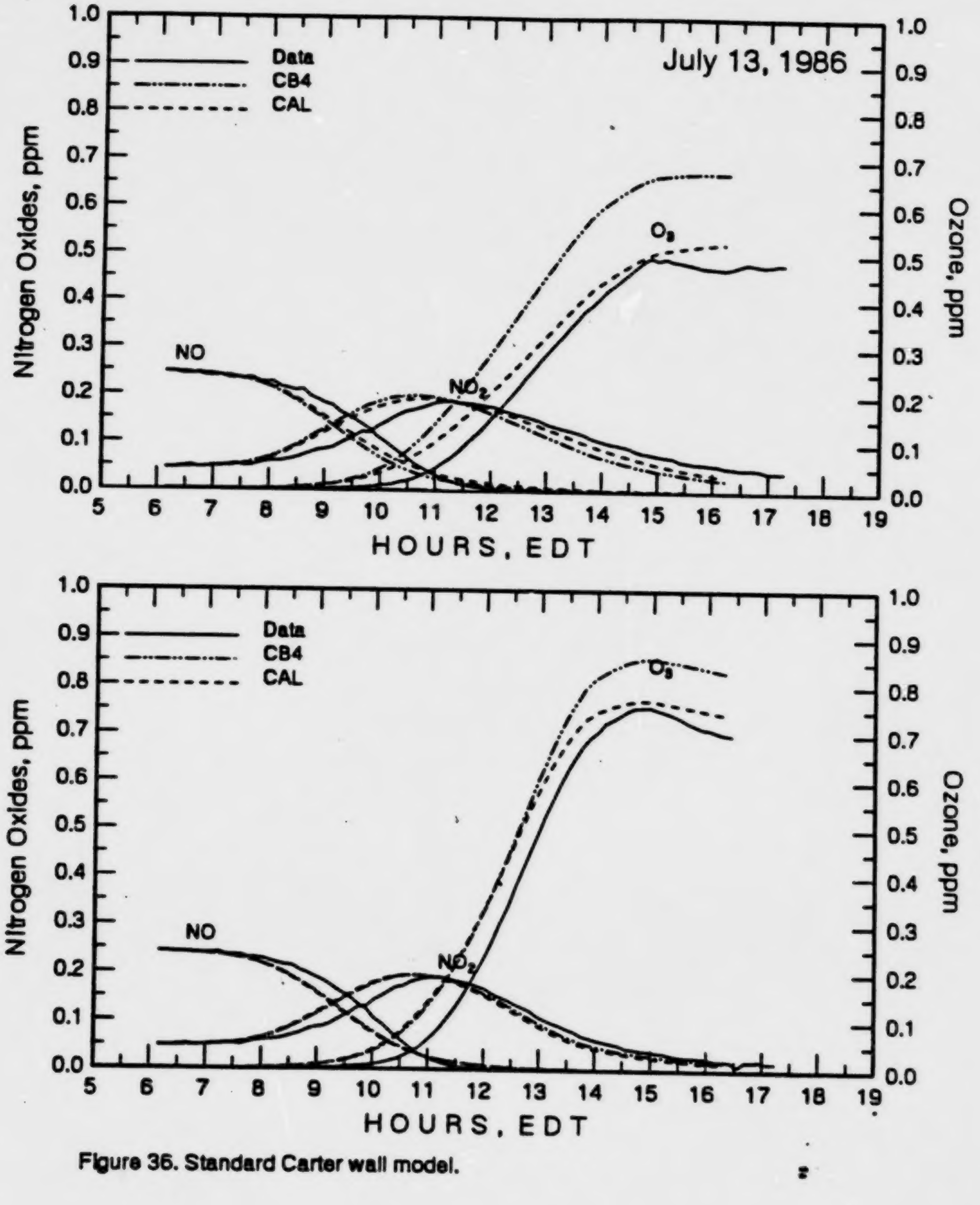

Figure 36. Standard Carter wall model.

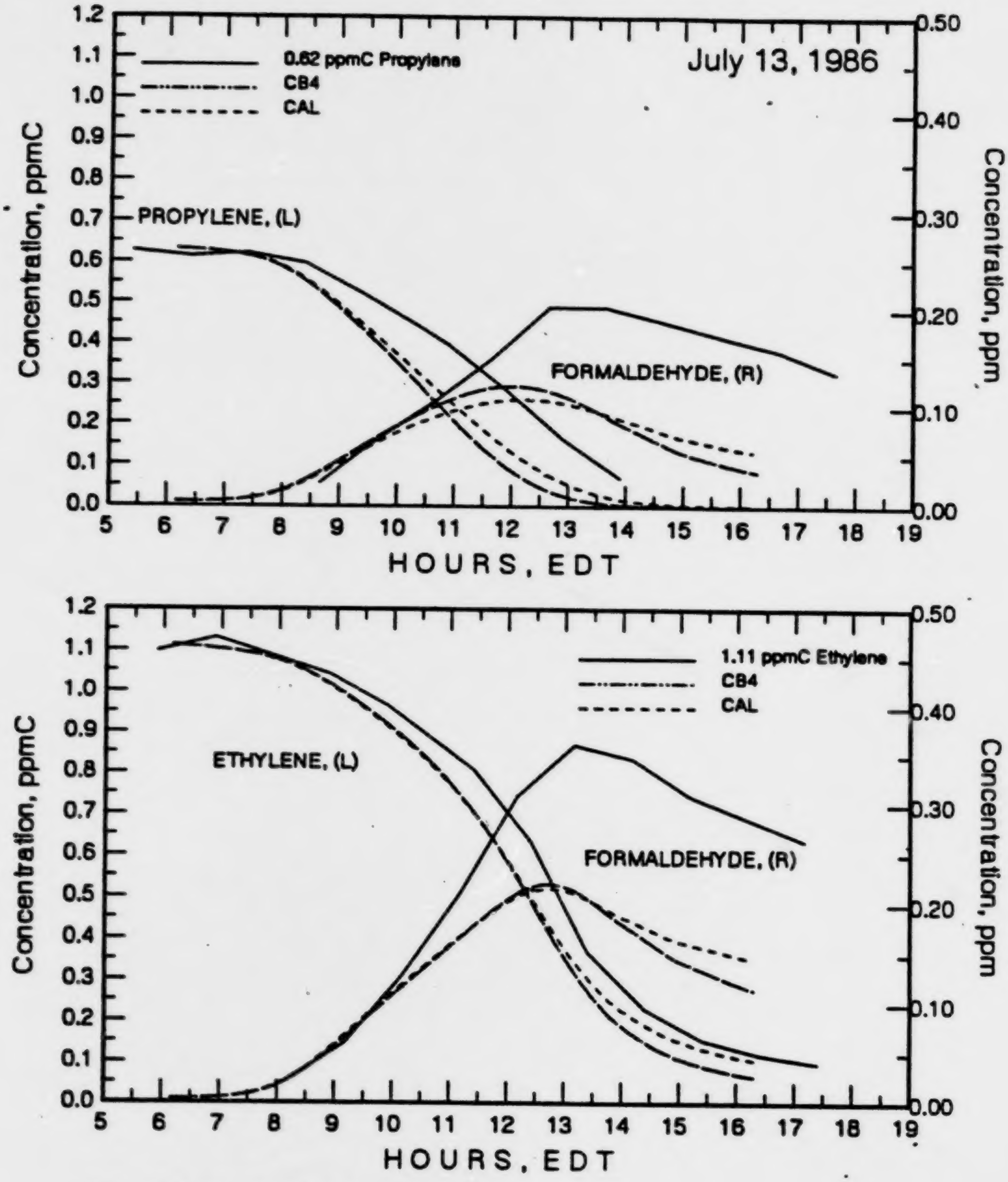

Figure 37. Standard Carter wall model.

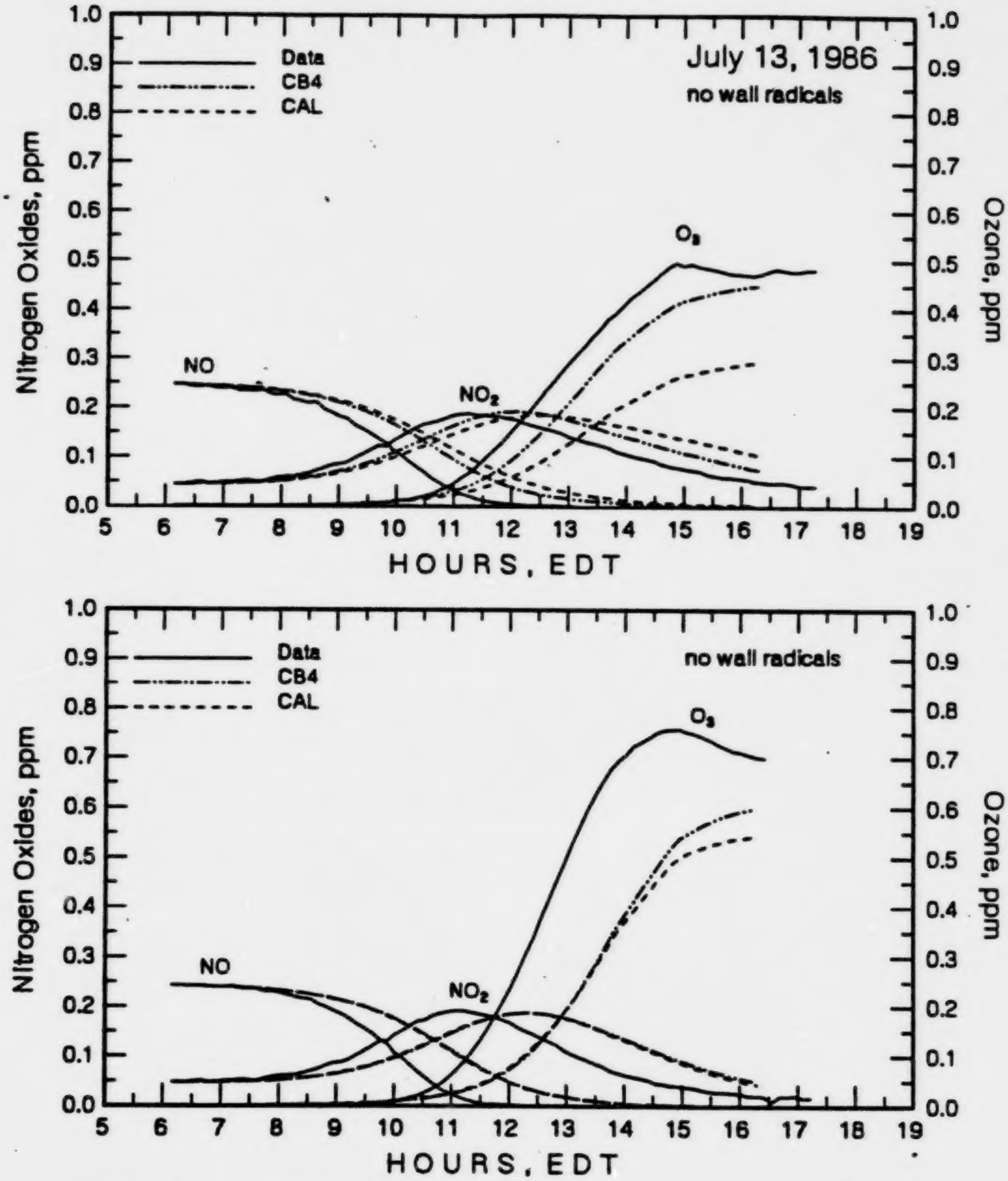

Figure 38. No wall model.

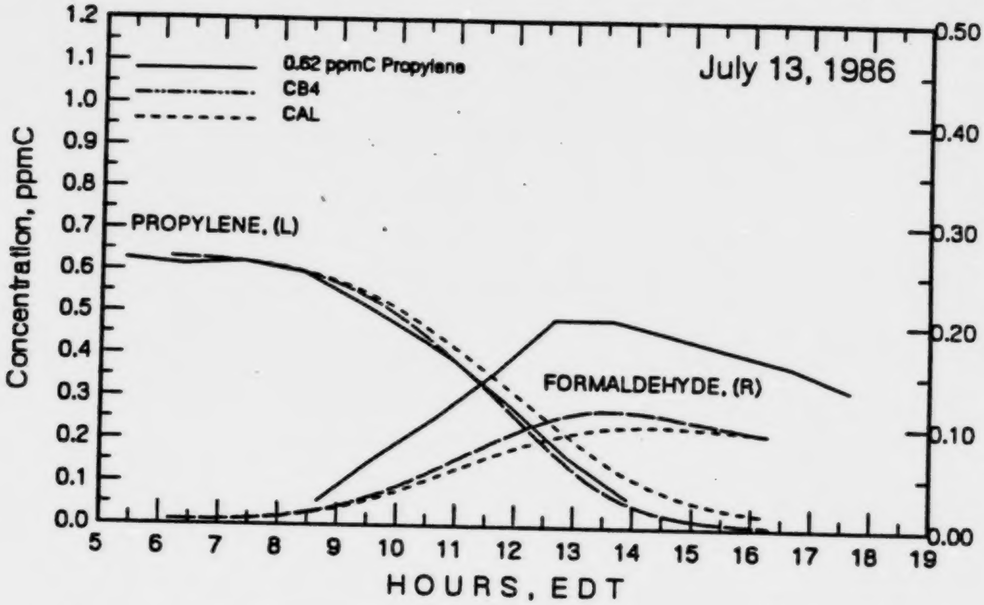

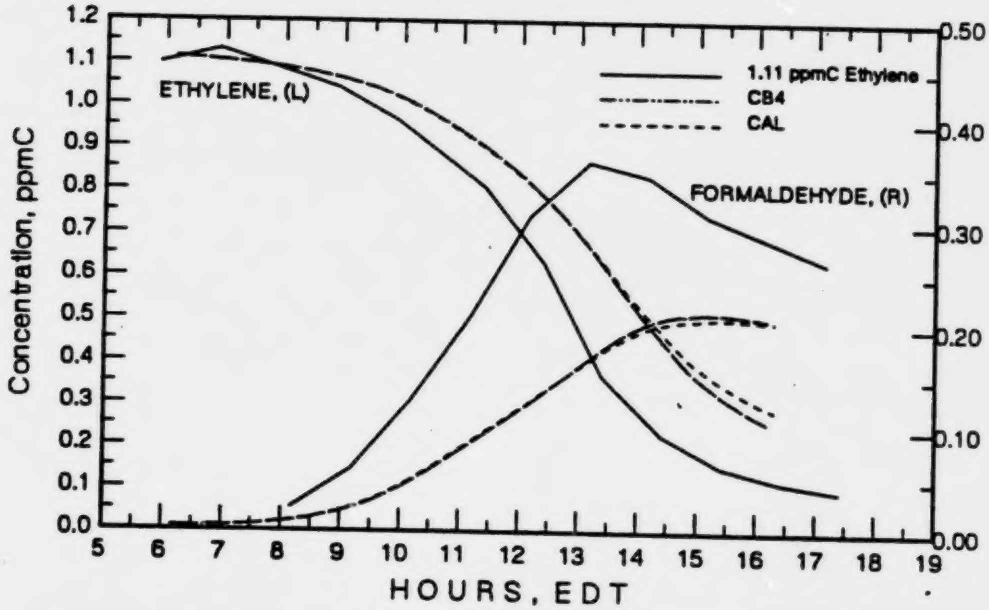

Figure 39. No wall model. No wall radicals.

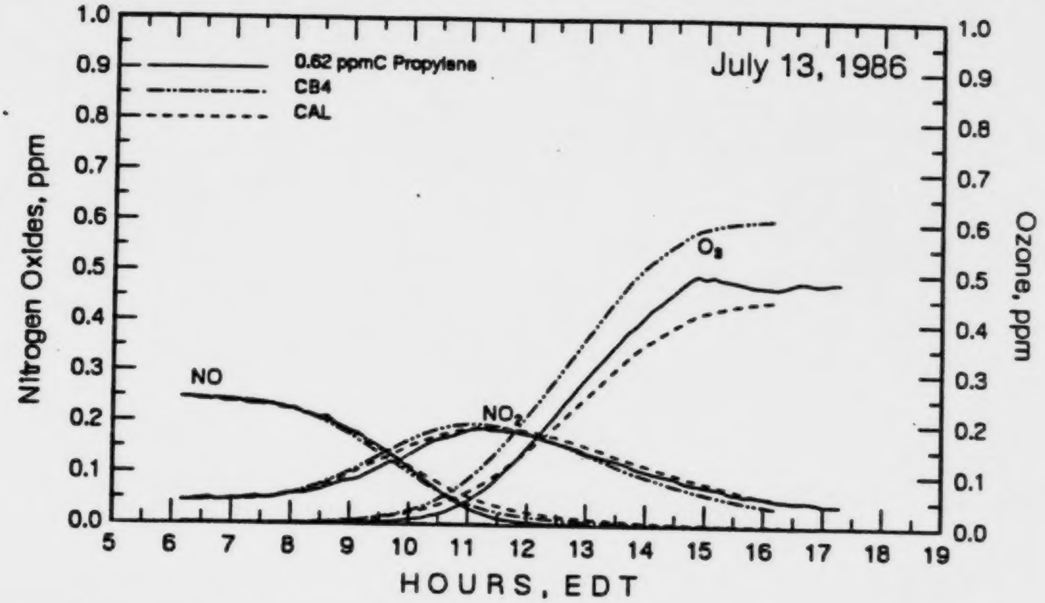

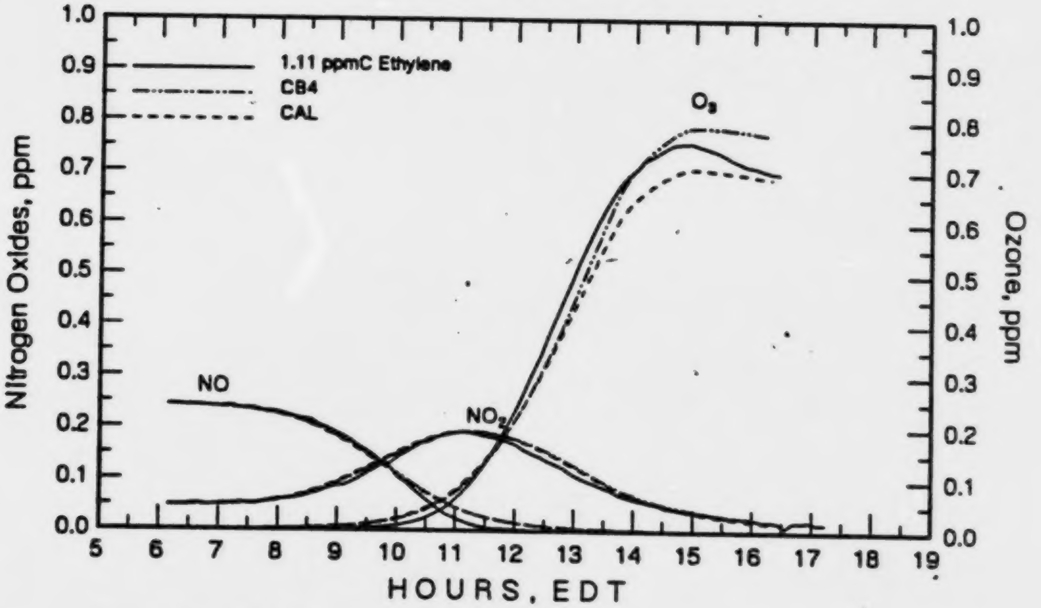

Figure 40. One half standard Carter wall model.

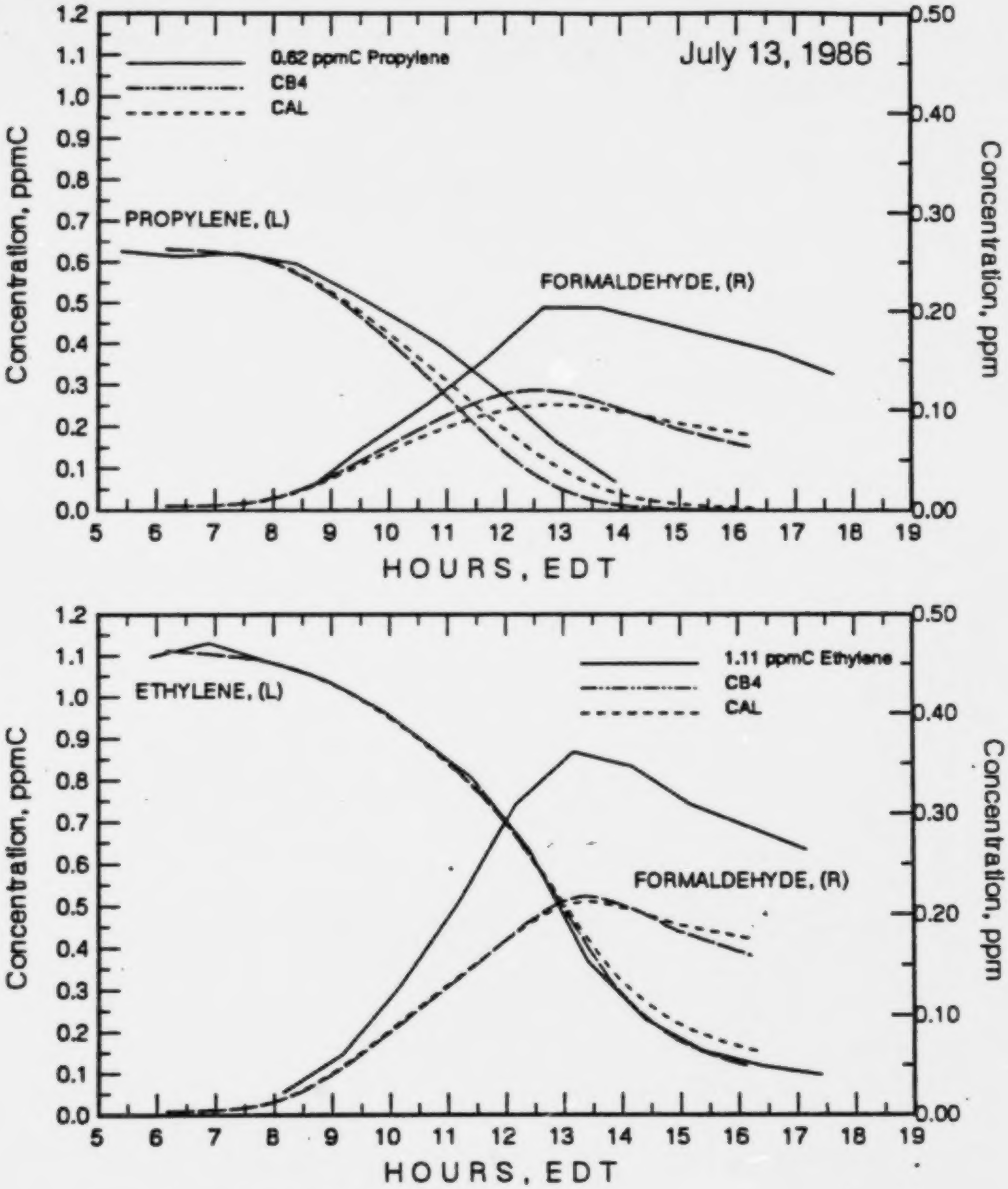

Figure 41. One half standard Carter wall model.

October 11, 1984
Ethylene vs Propylene

Figures 42 to 45 show the data and simulations for another ethylene vs. propylene experiment. This experiment was cool and dry (see Figure 42).

The standard Carter Wall model is too reactive on this day: cross over occurred nearly one hour too fast. The ozone production in the propylene system is approximately correct for both mechanisms, but CB4 over predicted the ozone in the ethylene system while CAL predicted the magnitude nearly perfectly. Since CAL had been below CB4 in all other ethylene simulations, however, this suggests that both mechanisms are too reactive for O_3 production in the ethylene case.

Figures 46 to 48 show simulations with no wall sources. The models are only a little slower than with the standard Carter wall model and are still too reactive. Ethylene decay is better fit, HCHO in ethylene is as close as the have been (Figure 47). For the propylene side, however, the propylene consumption is too rapid, and the production of acetaldehyde and HCHO is only about 60% of measured values. Notice in Figure 48 that we were able to measure methyl nitrate on this day, but the models do not predict this species.

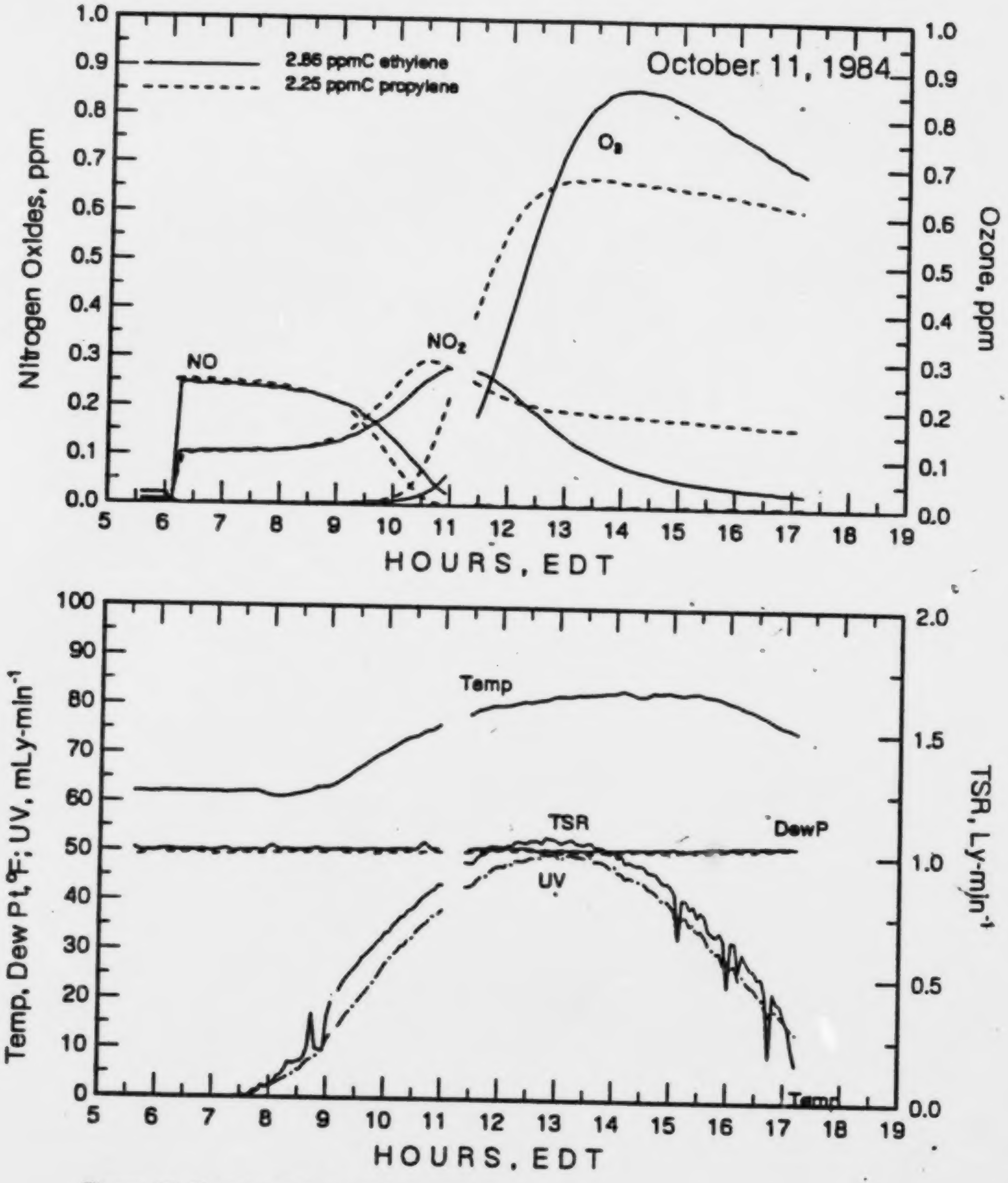

Figure 42. Relative HC reactivity experiment.

Table 26. October 11, 1984 Initial Condition Simulation File.

```
#if RED
October 11, 1984 (R) 2.856 ppmC ETHYLENE
#end
#if BLUE
October 11, 1984 (B) 2.252 ppmC Propylene
#end
#if CB4
c:\pkss\mech\CB42chm.pks
CONC=
@c:\pkss\mech\CBckCB4.icx
#end
#if CAL
c:\pkss\mech\CALchm.pks
CONC=
@c:\pkss\mech\CBckCAL.icx
#end

#if RED
 NO         = 0.243,
 NO2        = 0.108,
#end
#if BLUE
 NO         = 0.249,
 NO2        = 0.105,
#end

#if RED
#if CB4
 ETH        = 1.428,
#end

#if CAL
 ETHE       = 1.428,
#end
#end

#if BLUE
#if CB4
 OLE        = 0.7507,
 PAR        = 0.7507,
#end

#if CAL
 PRPE       = 0.7507,
#end
#end

 HONO  =        0.007,
 CO    =        0.3;

@e:\segfiles\finalseg\84\oc1184.lix
@e:\segfiles\finalseg\84\oc1184.twd
FINISH;
```

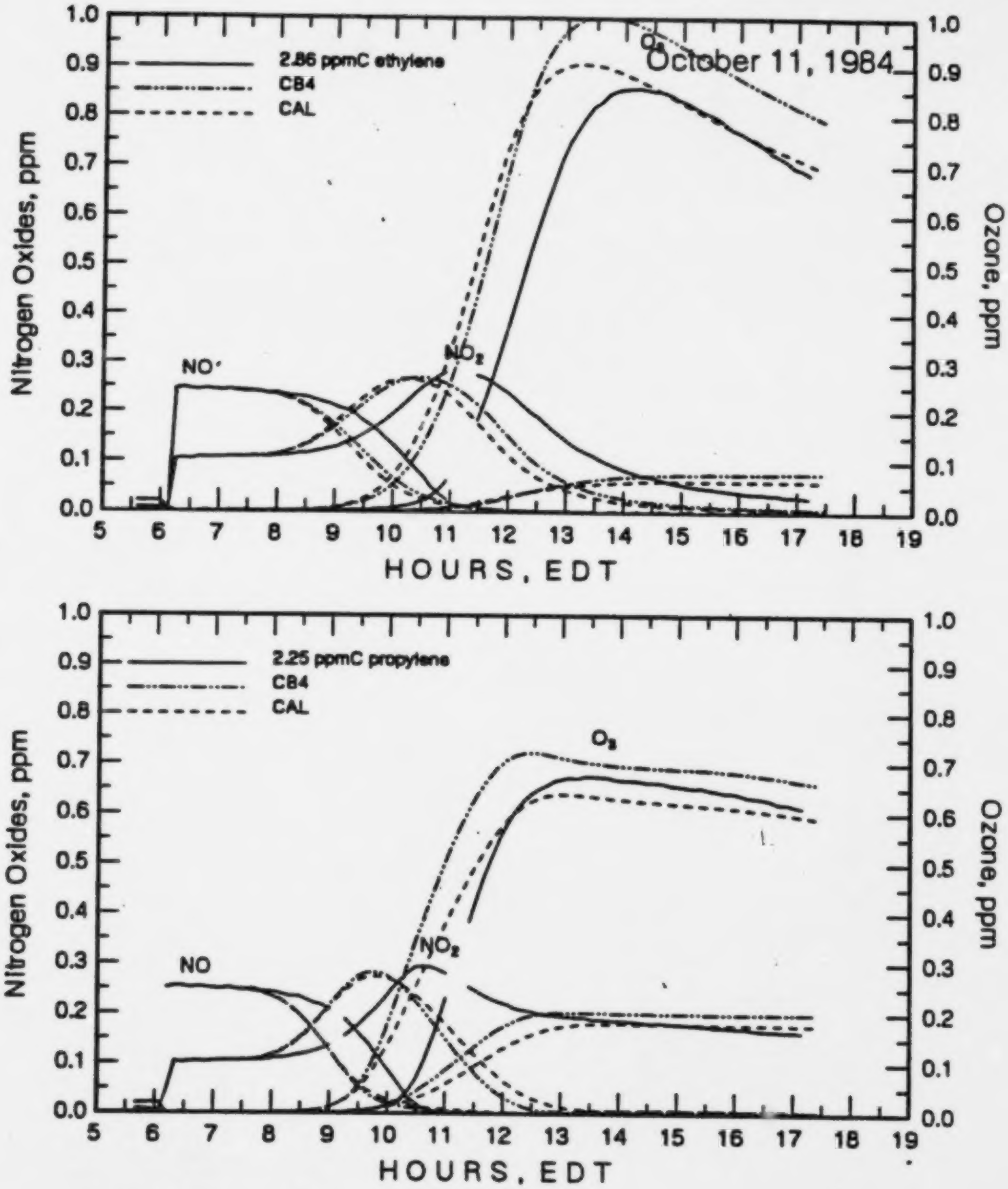

Figure 43. Standard Carter wall model.

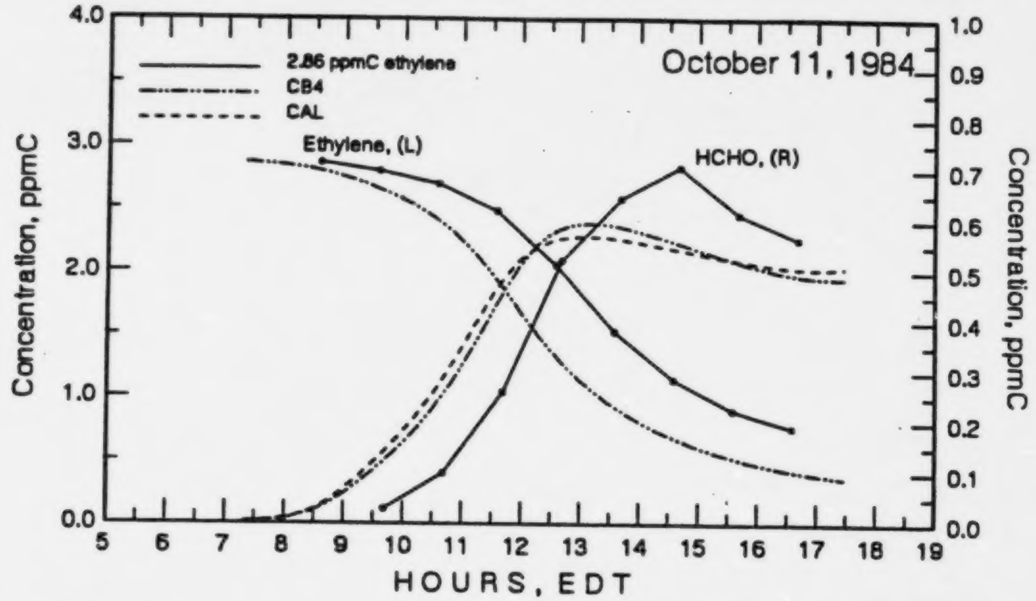

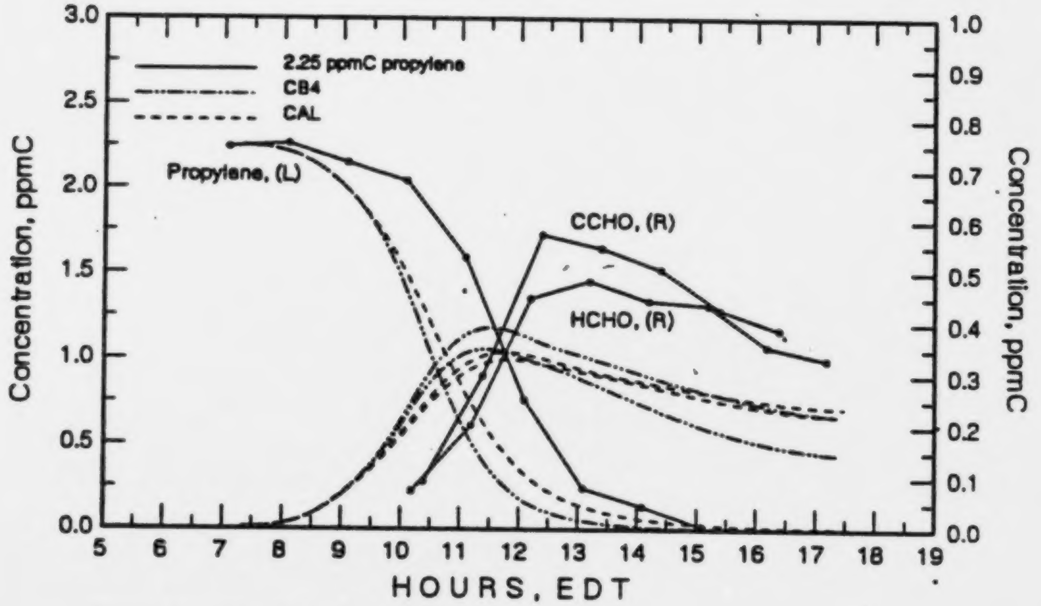

Figure 44. Standard Carter wall model.

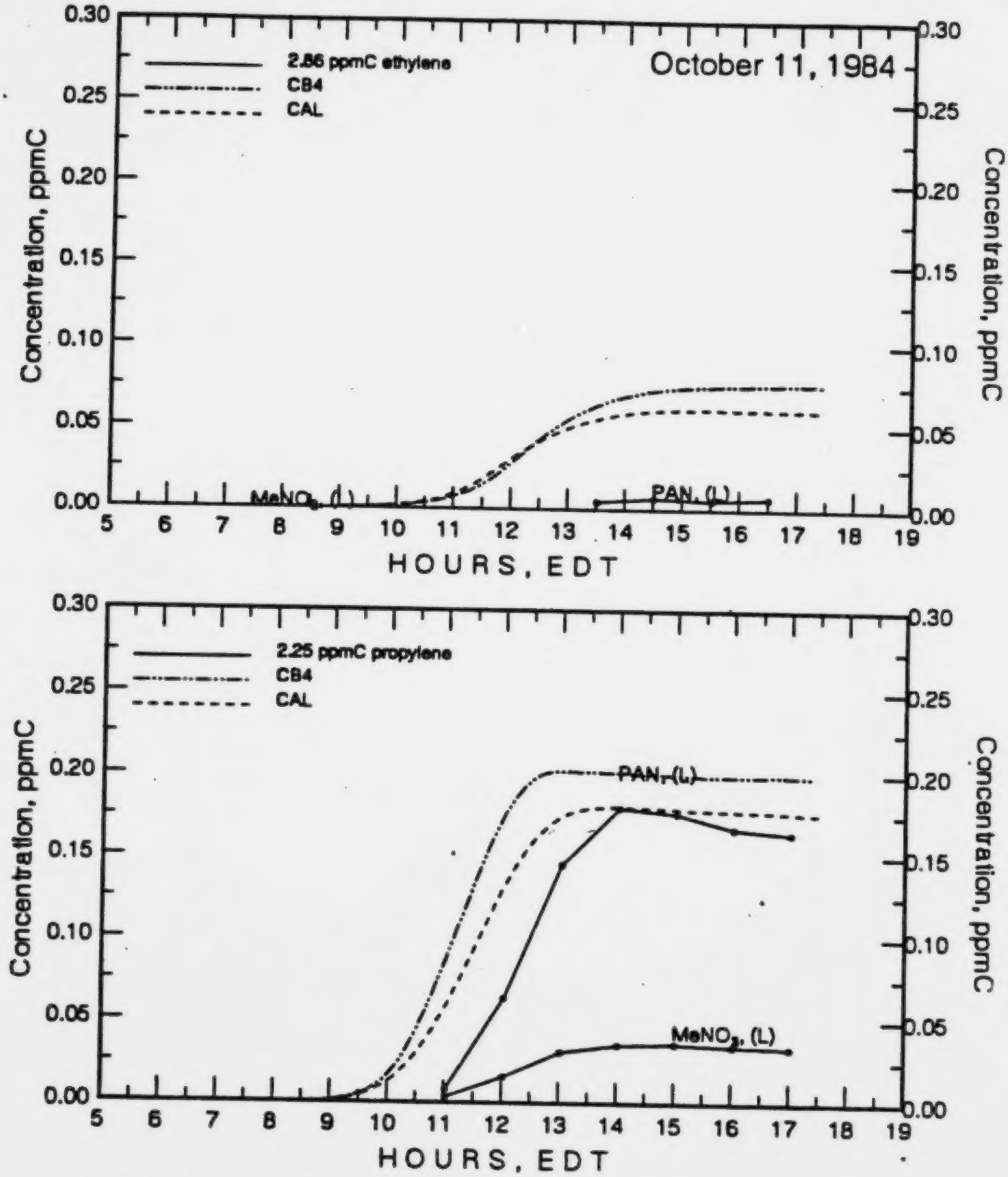

Figure 45. Standard Carter wall model.

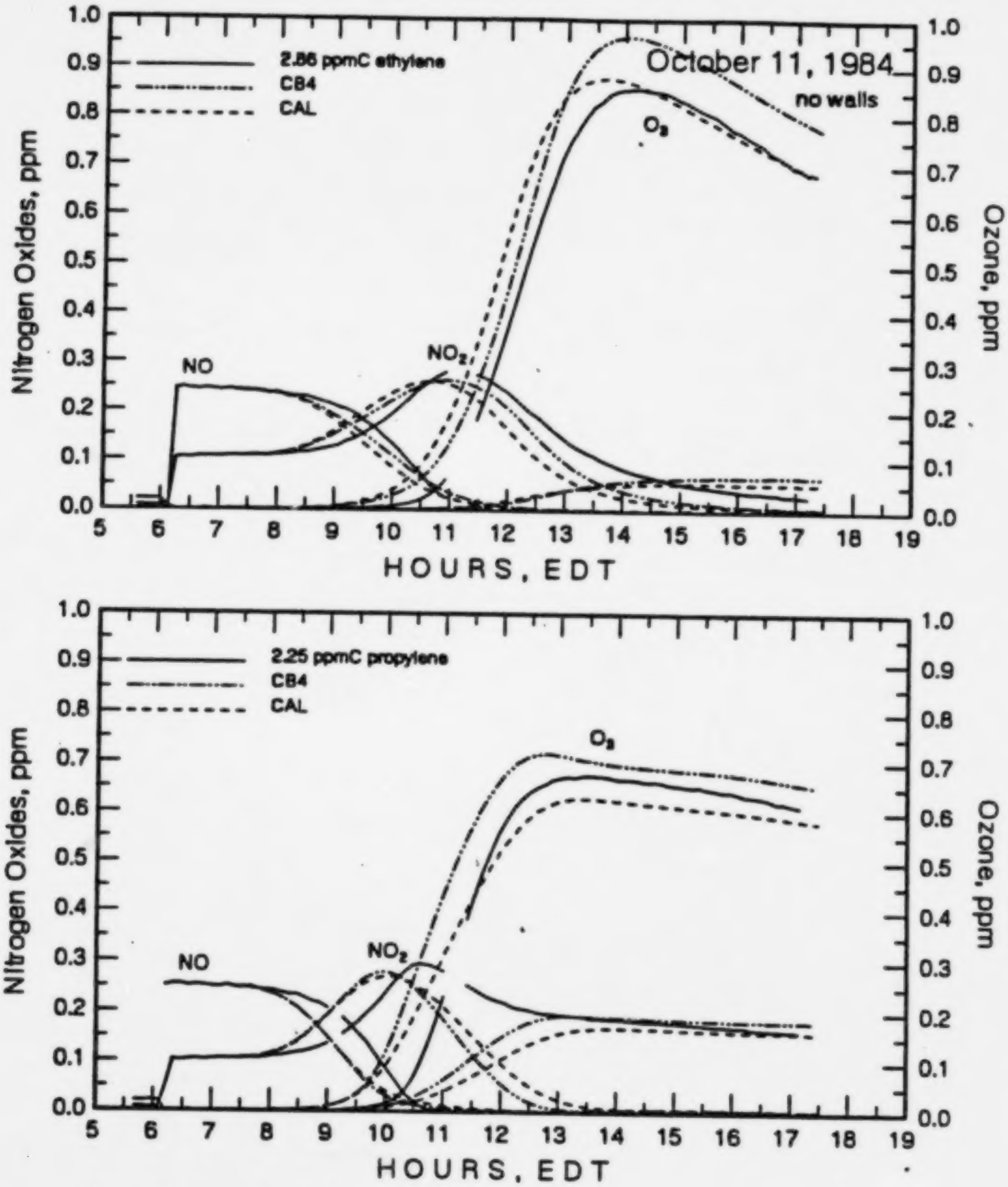

Figure 46. No wall model.

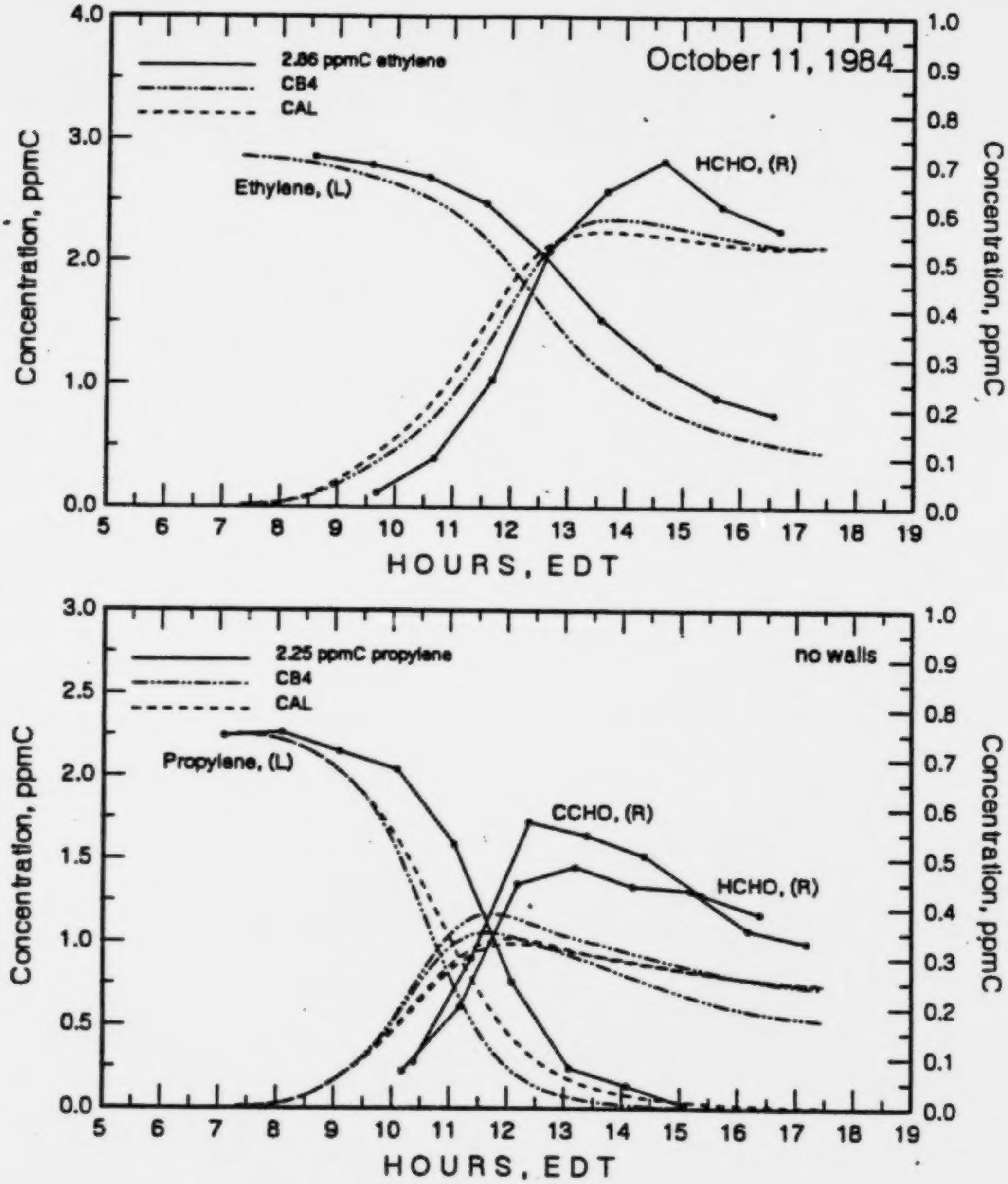

Figure 47. No wall model.

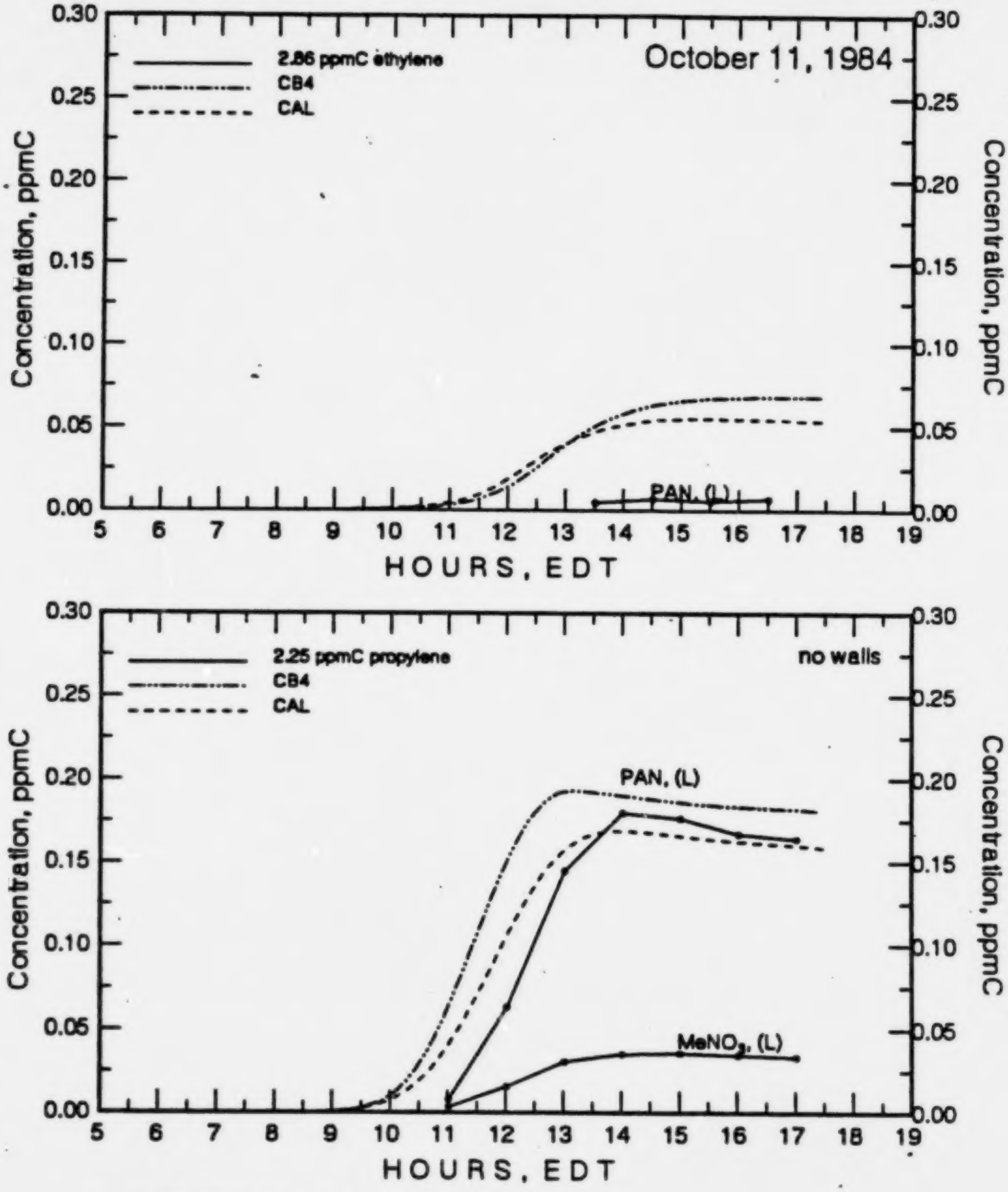

Figure 48. No wall model.

September 27, 1983
1-Butene vs. T-2-butene

Figures 49 to 51 show data and simulations for a relative reactivity experiment with 1-butene and trans-2-butene.

The standard Carter Wall model is too reactive on the 1-butene side of this experiment. Other 1-butene experiments we have simulated also have this problem. A no wall simulation is nearly as fast. September 23, 1983, for example was a near duplicate of September 27, 1983, and it too was over predicted by both mechanisms.

This is the first experiment we have shown in which the two mechanisms diverge significantly on the representation used for a species. CB4 uses two ALD2 to represent one trans-2-butene, whereas CAL has and explicit representation for trans-2-butene. The CAL simulation of this day is quite good, including reproducing the strange shape of the NO_2 peak and the little lag in O_3 production between 1000 and 1100 EDT. CB4's simulation is fairly poor for timing, with cross over being nearly two hours late and O_3 production starting nearly three hours late. The final O_3 value, however, is converging with the observations near the end of the experiment.

Both mechanisms over predict HCHO in 1-butene and both under predict HCHO in trans-2-butene.

This experiment confirms the developers statistists in the beginning of this chapter: both mechanisms appear to have poor representations for 1- butene.

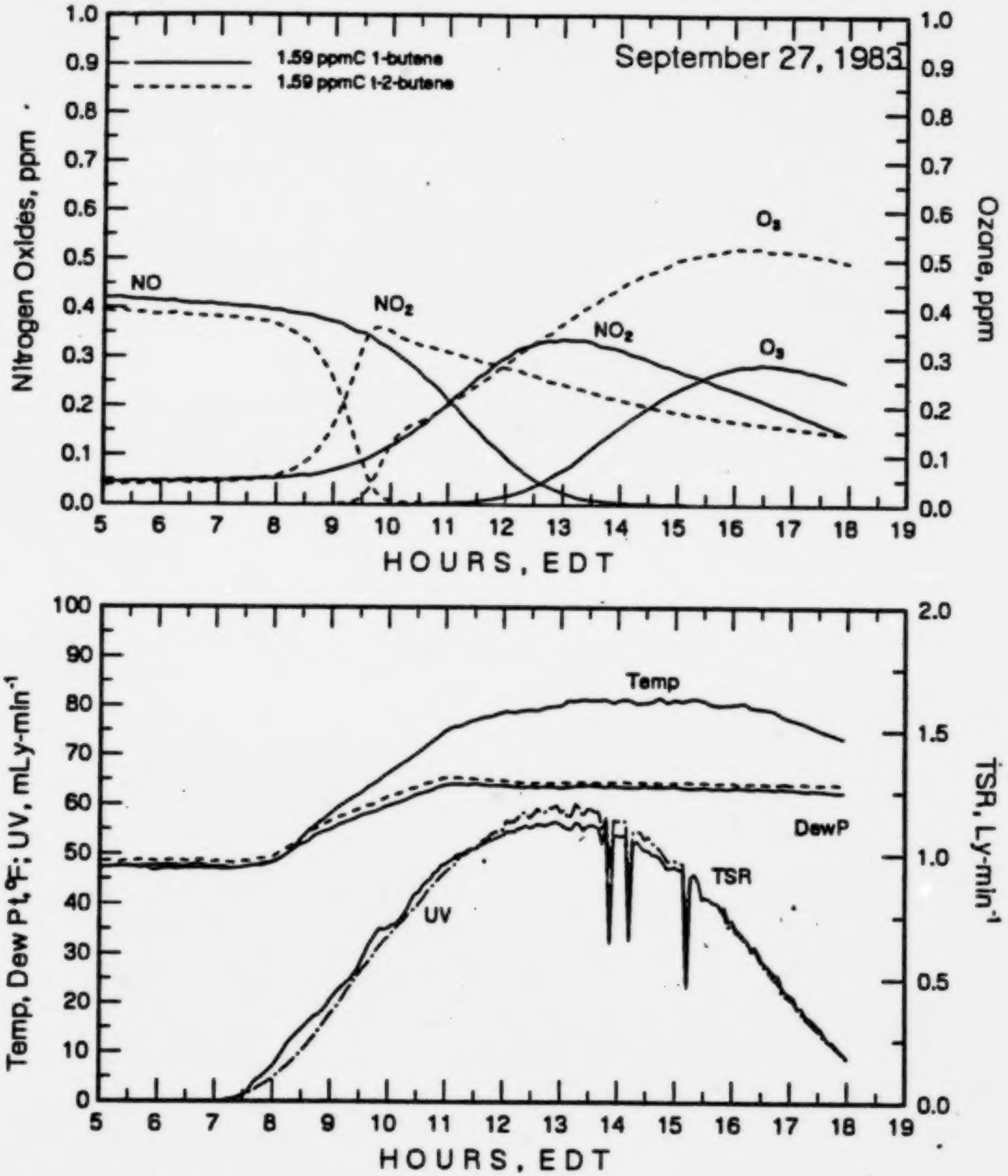

Figure 49. Relative HC reactivity experiment.

Table 27. September 23, 1983 Initial Condition Simulation File.

```
#if RED
Sept. 27, 1983 (R) 1.59 1-butene
#end
#if BLUE
Sept. 27, 1983 (B) 1.59 T-2-butene
#end
#if CB4
c:\pkss\mech\CB42chm.pks
CONC=
@c:\pkss\mech\CBckCB4.icx
#end
#if CAL
c:\pkss\mech\CALchm.pks
CONC=
@c:\pkss\mech\CBckCAL.icx
#end

#if RED
 NO  =0.405,
 NO2 =0.049,
#end
#if BLUE
 NO  = 0.381,
 NO2 = 0.046,
#end

#if RED
#if CB4
 OLE = 0.40, (1-butene)
 PAR = 0.80,
#end

#if CAL
 PRPE= 0.40,
 (MISS=0.10)
#end
#end

#if BLUE
#if CB4
 RCHO = 0.80, (2 ALD2 = t-2-butene)
#end

#if CAL
 TBUT = 0.40,
#end
#end

  HONO  =         0.0034,
 CO    =         0.36;

@e:\segfiles\finalseg\83\ST2783.lix
@e:\segfiles\finalseg\83\ST2783.twd

FINISH;
```

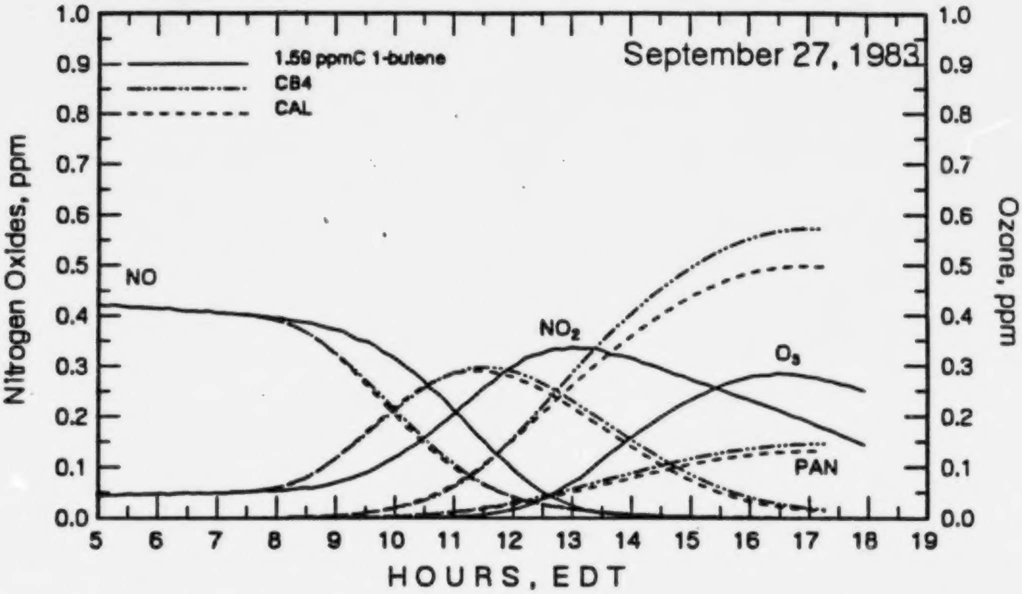

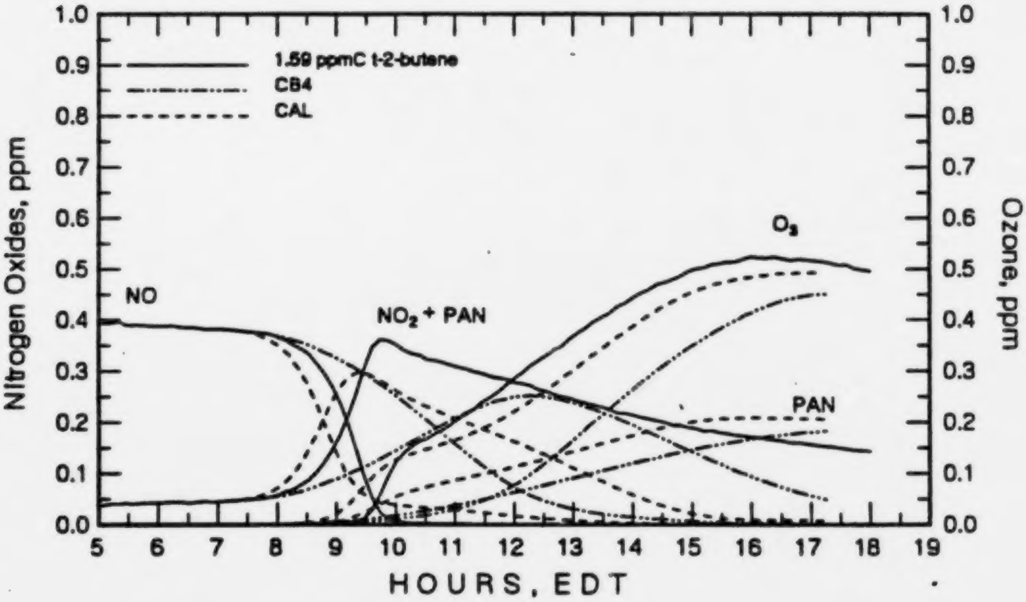

Figure 50. Standard Carter wall model.

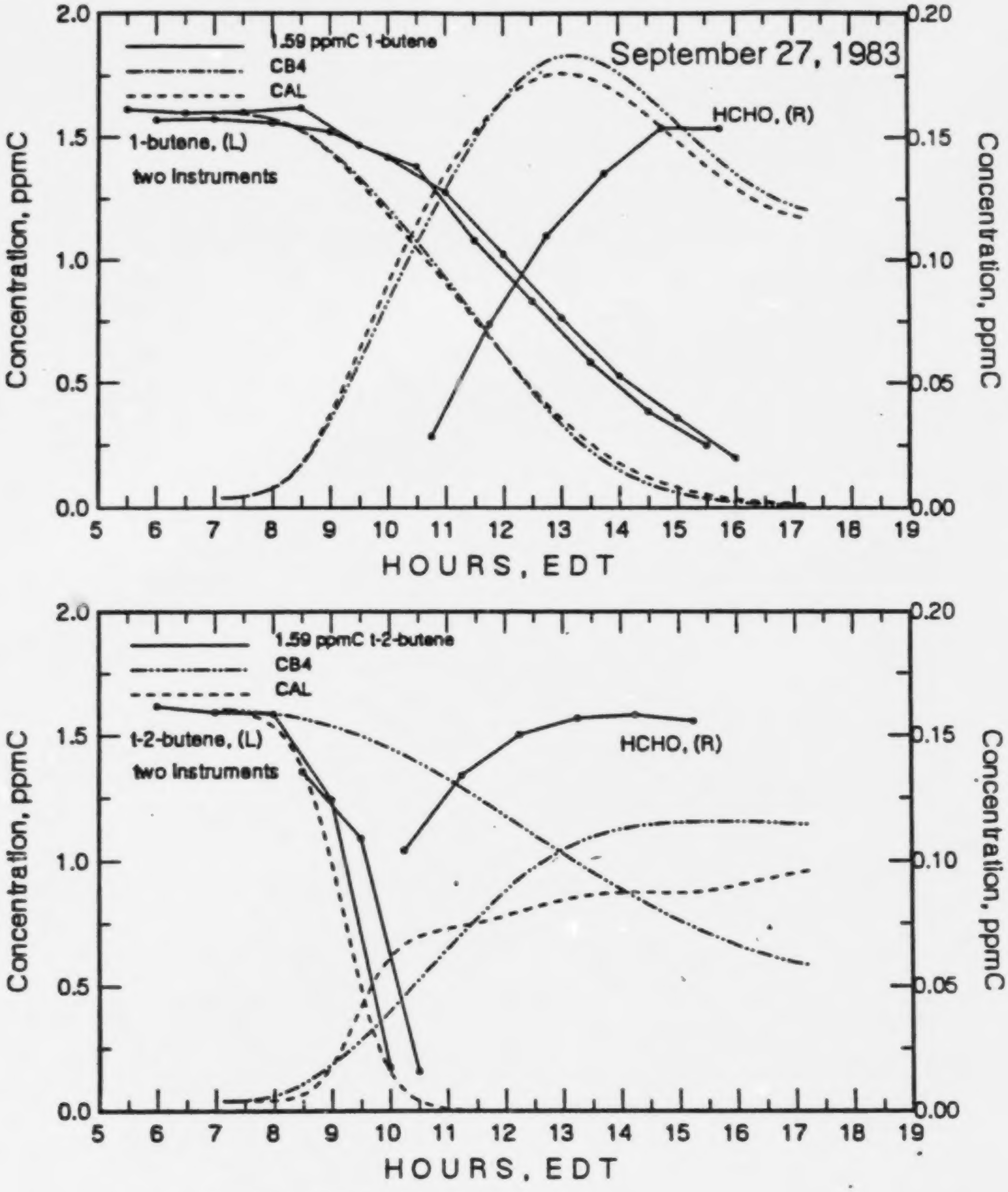

Figure 51. Standard Carter wall model.

June 27, 1984
Toluene vs. m-Xylene

Figures 52 to 55 show data and simulations for a reactivity comparison experiment with toluene and m-xylene. With the standard Carter Wall model, both sides are slightly too fast.

CB4

is better at simulating ozone yields in toluene than is CAL and CAL is better at simulating ozone yields in m-xylene than CB4. Both mechanisms stop consuming toluene after the NO_2 has reached a low value and thus both miss the final toluene by nearly 1 ppm.

Both mechanisms over predict the HCHO by more than a factor of two in xylene and by about a factor of two in toluene. Recent measurements using different HCHO methods have confirmed the HCHO yields in this experiment.

Both mechanisms predict the peak PAN well for xylene, but CB4 follows the temperature decay better. In toluene, CB4 is better at predicting the PAN peak, while CAL over predicts PAN by a large amount.

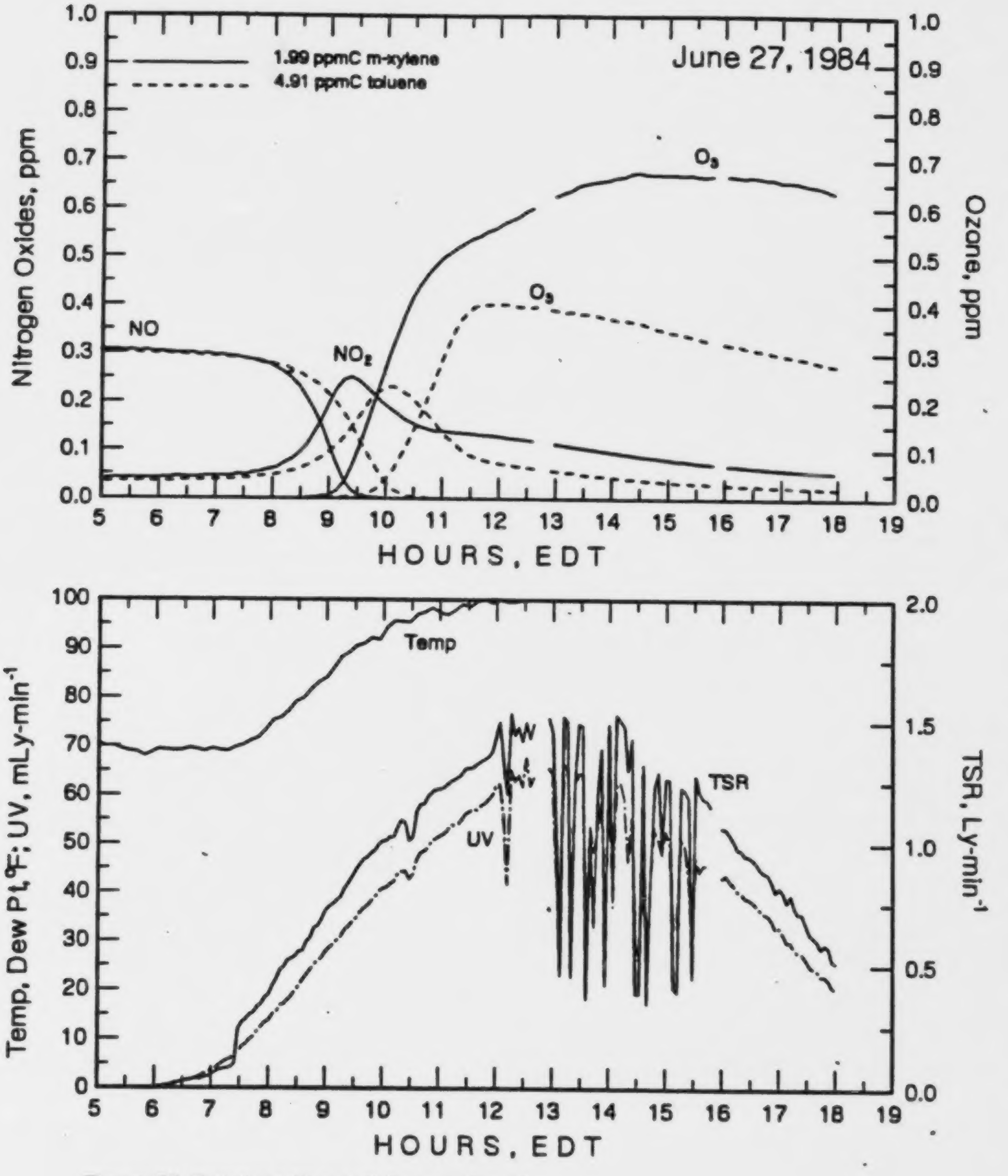

Figure 52. Relative HC reactivity experiment.

Table 28. June 27, 1984 Initial Condition Simulation File.

```
#if RED
June 27, 1984 2 ppmC m-Xylene (RED)
#end
#if BLUE
June 27, 1984  5 ppmC Toluene (BLUE)
#end
#if CB4
c:\pkss\mech\CB42chm.pks
CONC=
@c:\pkss\mech\CBckCB4.icx
#end
#if CAL
c:\pkss\mech\CALchm.pks
CONC=
@c:\pkss\mech\CBckCAL.icx
#end
#if RED
 NO  =  0.303,
 NO2 =  0.041,
#end
#if BLUE
 NO  =  0.300,
 NO2 =  0.035,
#end
#if RED
#if CB4
 XYL =  0.249,
 ETH =  0.13, (contamination)
#end
#if CAL
 XYLE =  0.249,
 ETHE =  0.13, (contamination)
#end
#end
#if BLUE
#if CB4
 TOL  =  0.702,
 ETH  =  0.122, (contamination)
#end
#if CAL
 TOLU =  0.702,
 ETHE =  0.122, (contamination)
#end
#end
 HONO  =  0.002,
 CO    =  0.3;

@e:\segfiles\finalseg\84\jn2784.lix
@e:\segfiles\finalseg\84\JN2784.twd
FINISH;
```

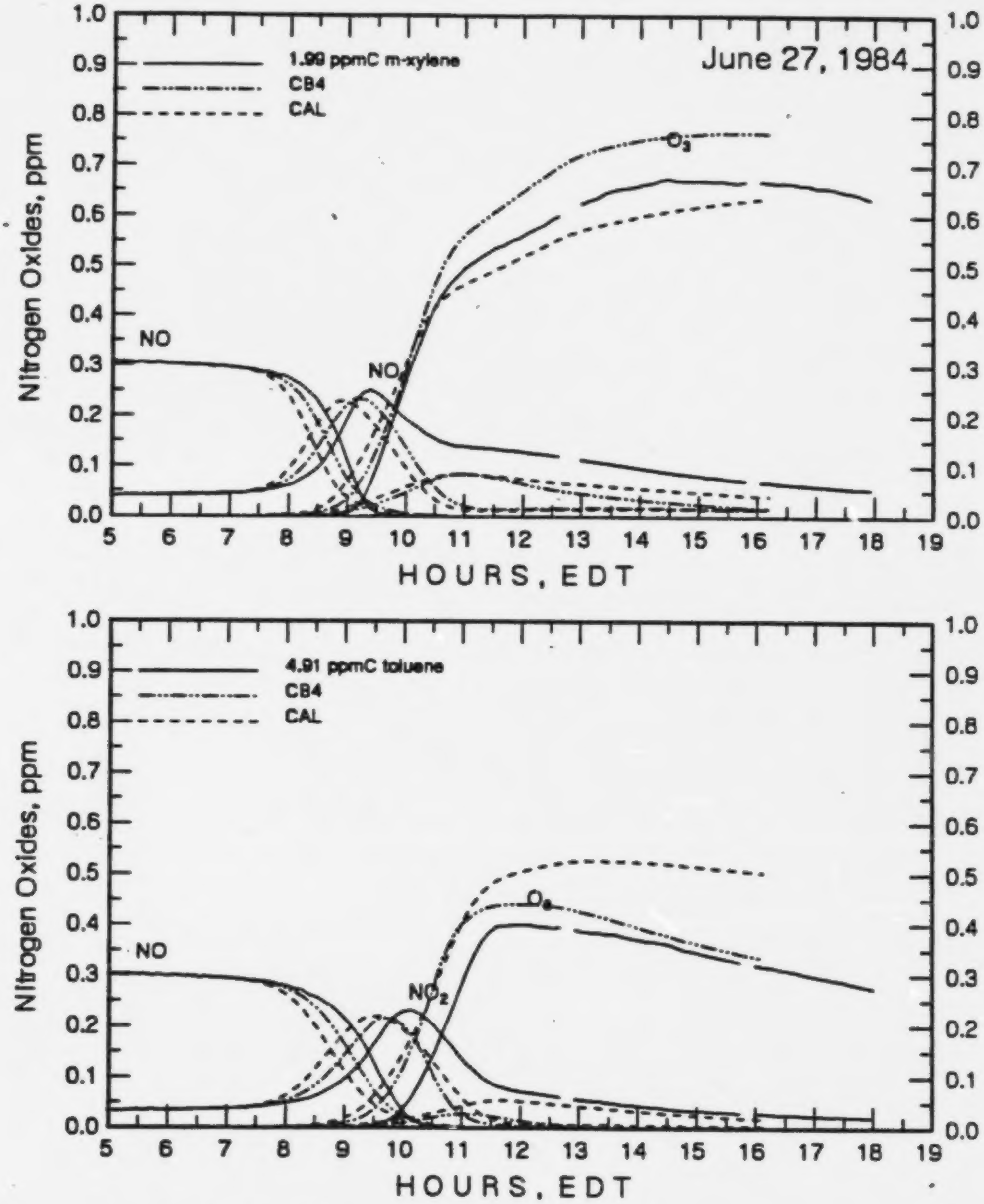

Figure 53. Standard Carter wall model.

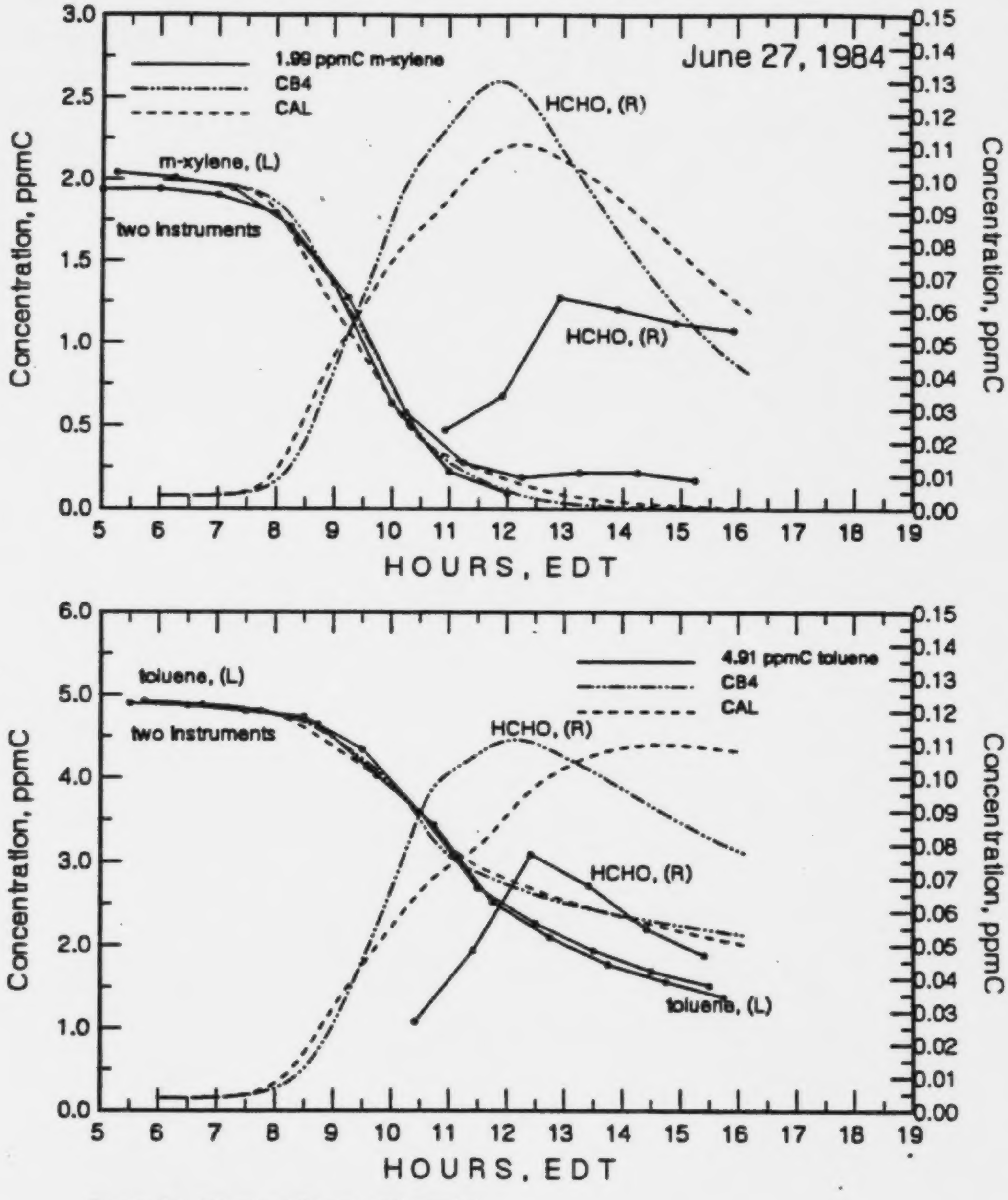

Figure 54. Standard Carter wall model.

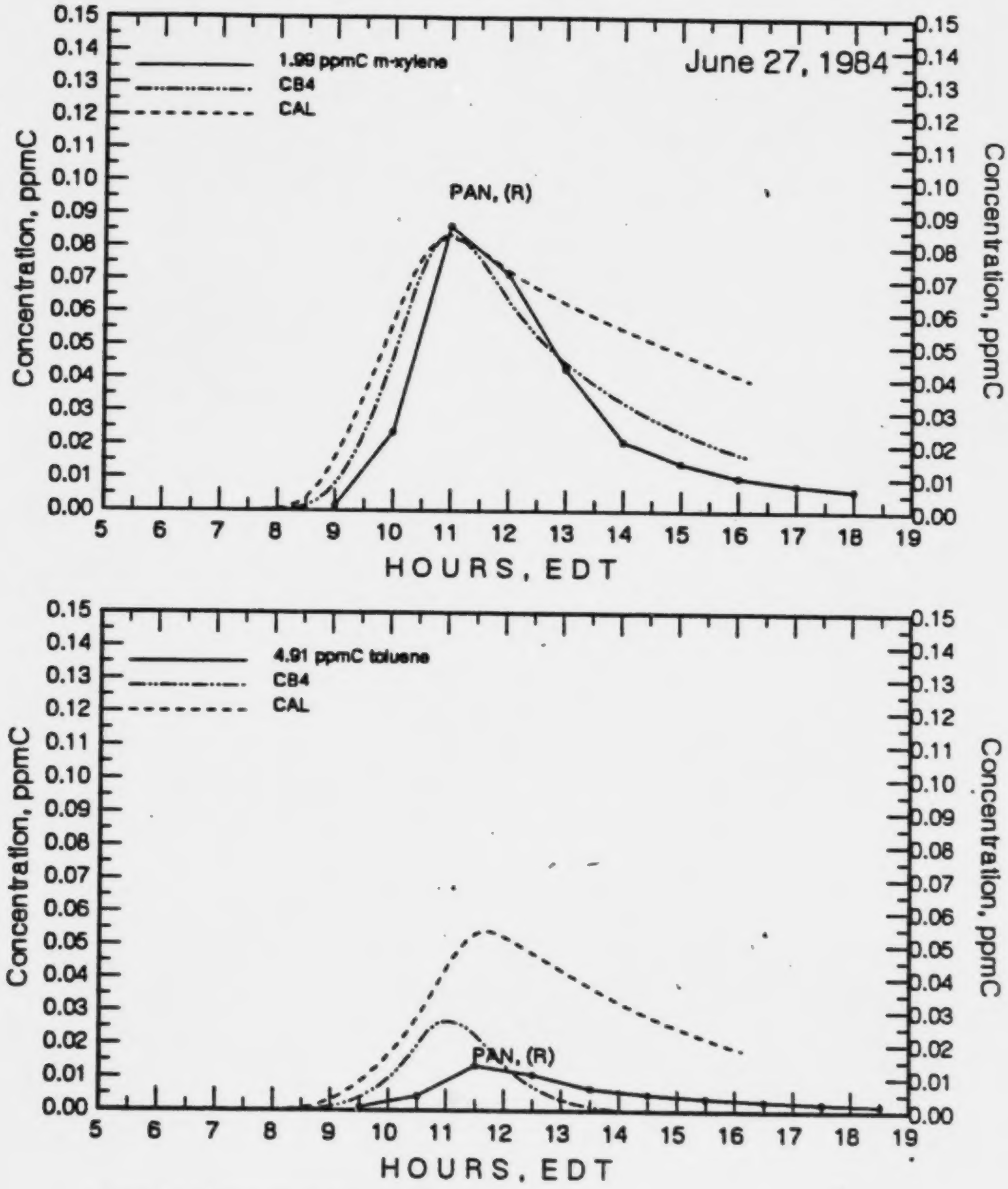

Figure 55. Standard Carter wall model.

June 26, 1984
o-Xylene vs. m-Xylene

Figures 56 to 59 show data and simulations for a reactivity comparison experiment using o-xylene and m-xylene. Again the standard Carter wall model is a little too reactive for this day. In the m-xylene side, initially CAL gives a better fit to the O_3 peak, but as the PAN decays (see Figure 59), CB4's prediction reaches an exact agreement with the O_3. In the o-xylene side, both mechanisms are too reactive in terms of time, and CB4 over predicts the O_3 peak, while CAL under predicts. Both mechanisms fail to predict the PAN, both as measured by PAN itself and by the chemiluminescent NO_x meter reading after 1200 EDT.

CB4 predicts a peak HCHO that is close to the data, but the time is wrong by three hours. Both mechanisms also under predict the CO by a large amount.

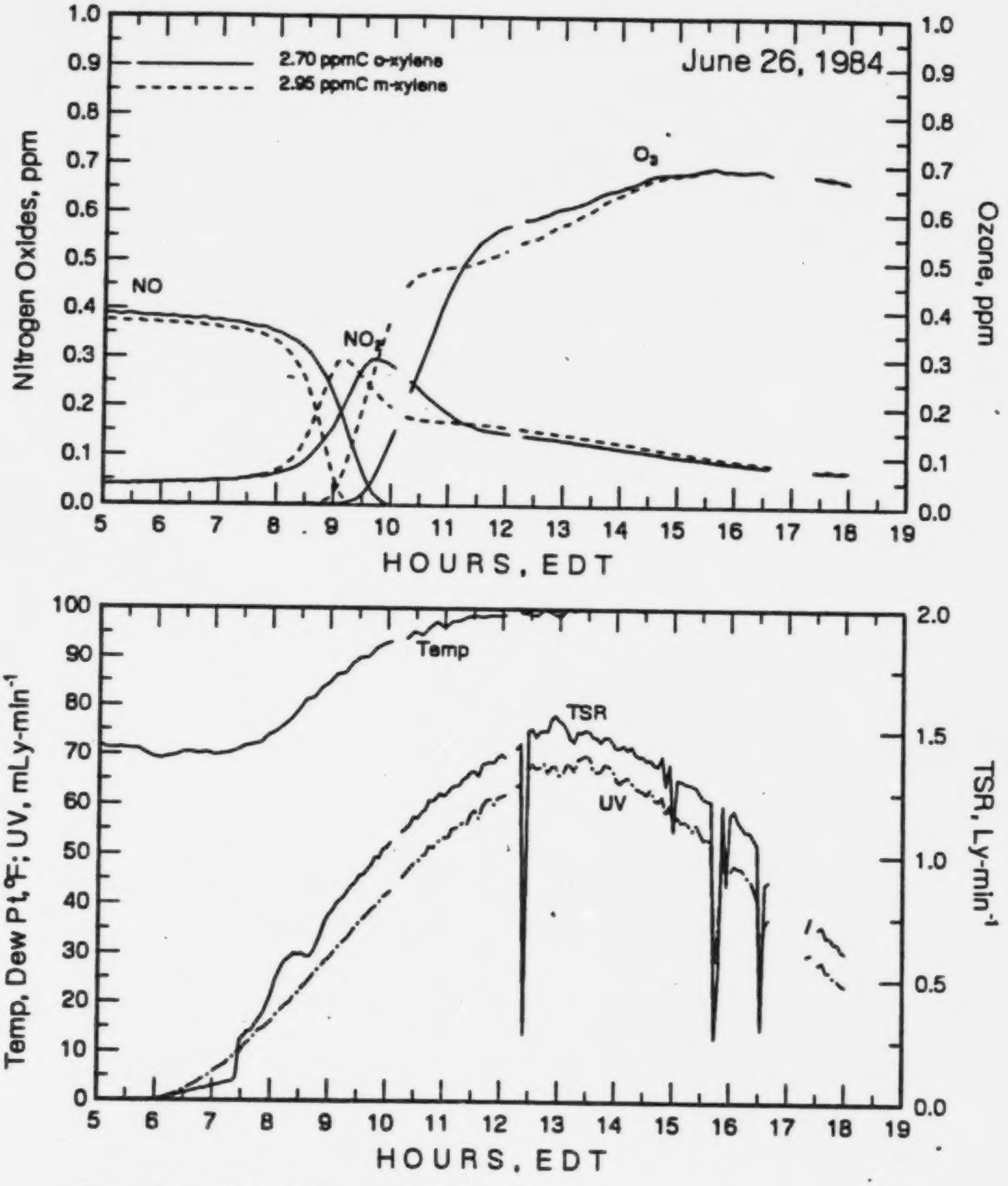

Figure 56. Relative HC reactivity experiment.

Table 29. June 26, 1984 Initial Condition Simulation File.

```
#if RED
June 26, 1984  2.70 ppmC o-Xylene (RED)
#end
#if BLUE
June 26, 1984  2.95 ppmC m-Xylene (BLUE)
#end
#if CB4
c:\pkss\mech\CB42chm.pks
CONC=
@c:\pkss\mech\CBckCB4.icx
#end
#if CAL
c:\pkss\mech\CALchm.pks
CONC=
@c:\pkss\mech\CBckCAL.icx
#end

#if RED
 NO  =   0.384,
 NO2 =   0.044,
#end
#if BLUE
 NO  =   0.371,
 NO2 =   0.043,
#end

#if RED
#if CB4
  XYL    =   0.338,
#end

#if CAL
  XYLE  =   0.338,
#end
#end

#if BLUE
#if CB4
  XYL    =   0.369,
#end

#if CAL
  XYLE  =   0.369,
#end
#end

HONO  =          0.003,
CO    =          0.3;

@e:\segfiles\finalseg\84\JN2684.lix
@e:\segfiles\finalseg\84\JN2684.twd

FINISH;
```

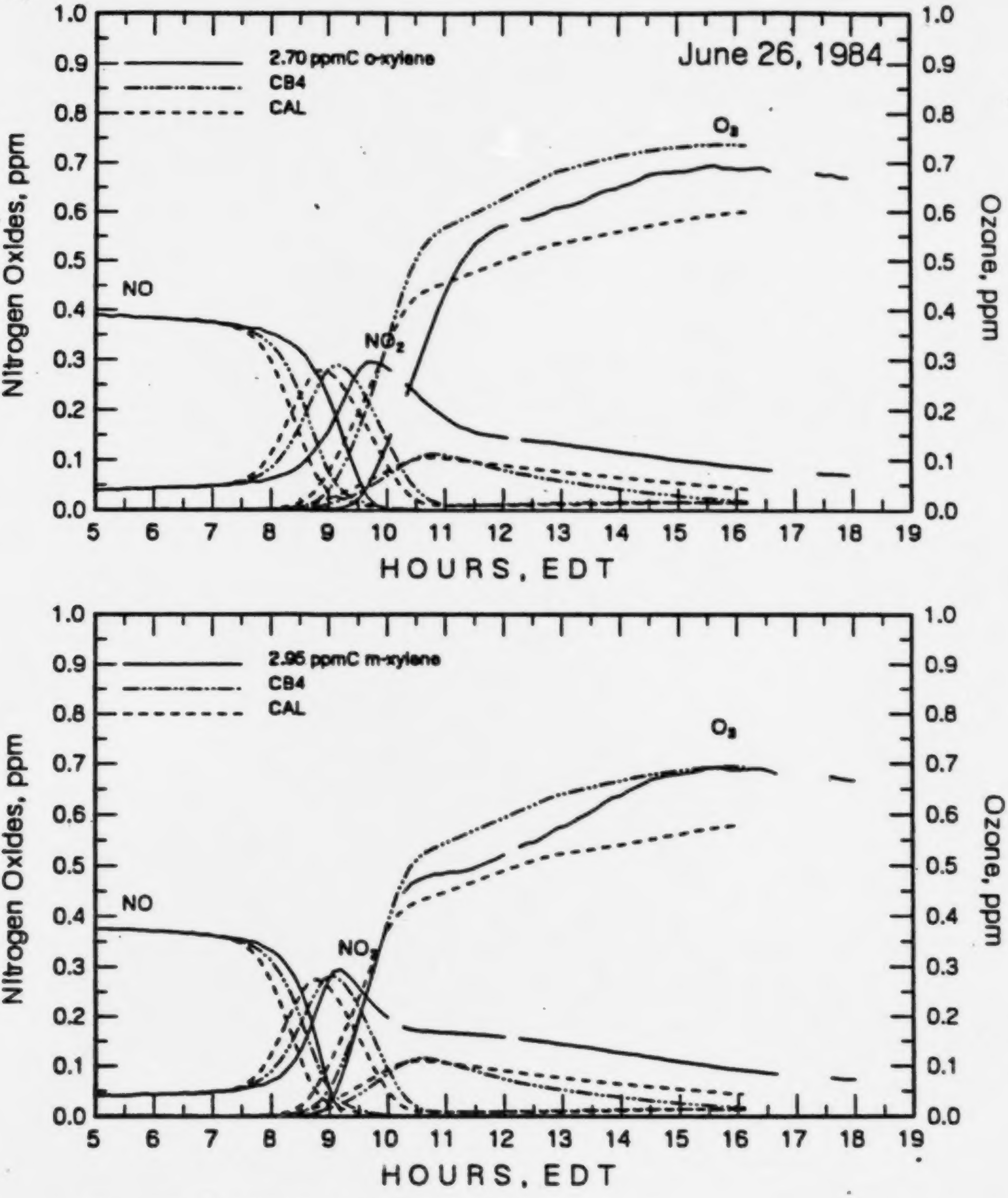

Figure 57. Standard Carter wall model.

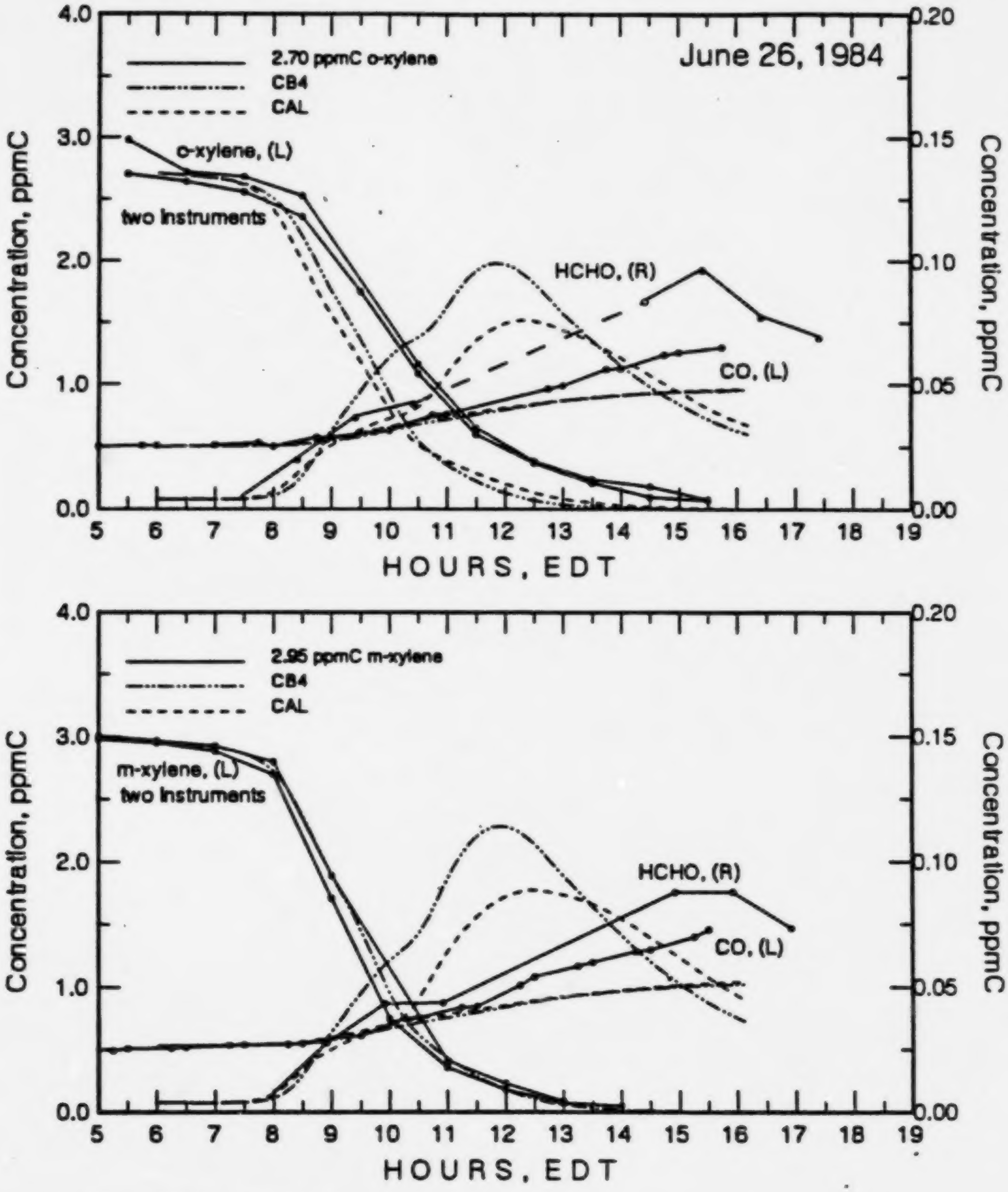

Figure 58. Standard Carter wall model.

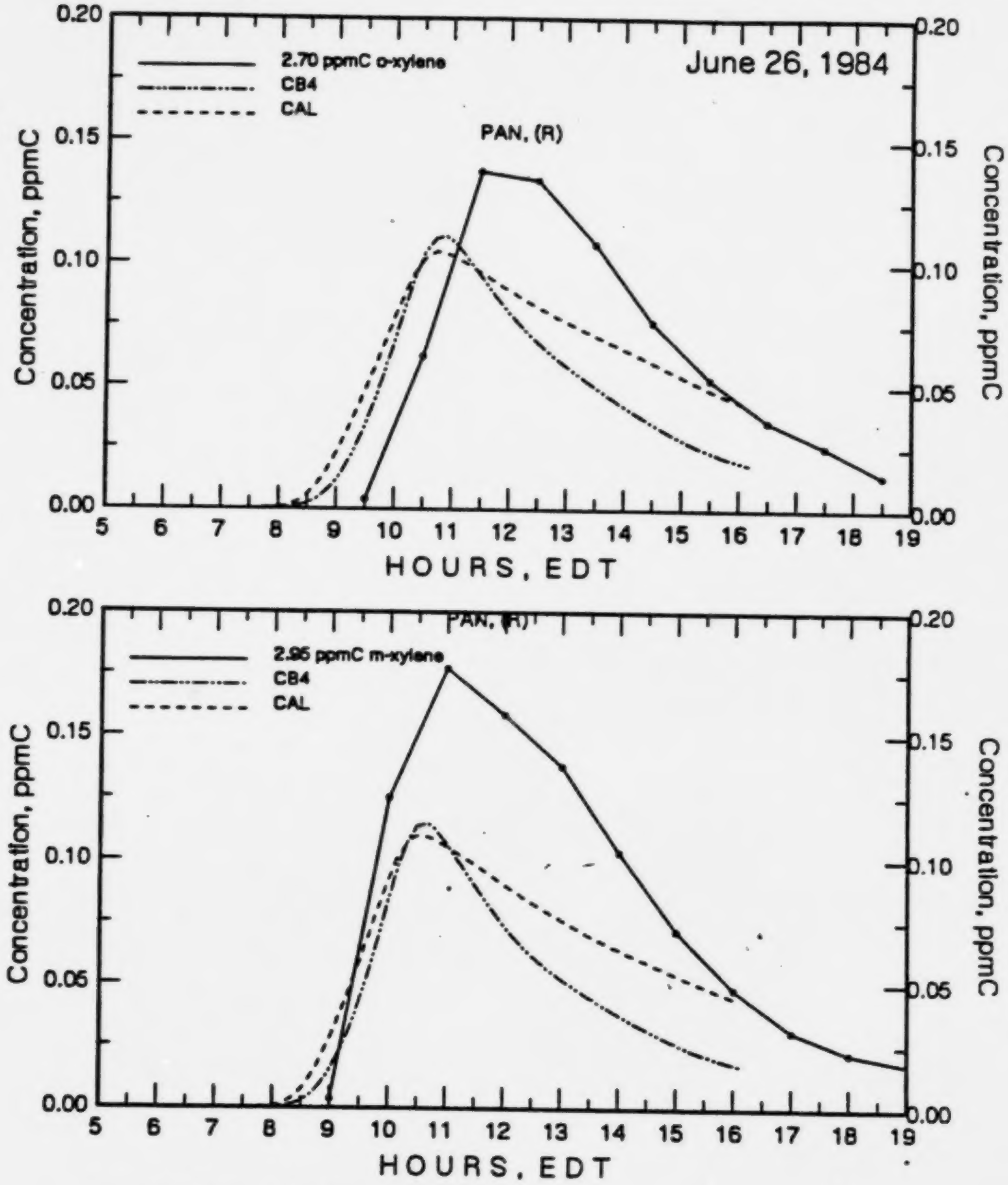

Figure 59. Standard Carter wall model.

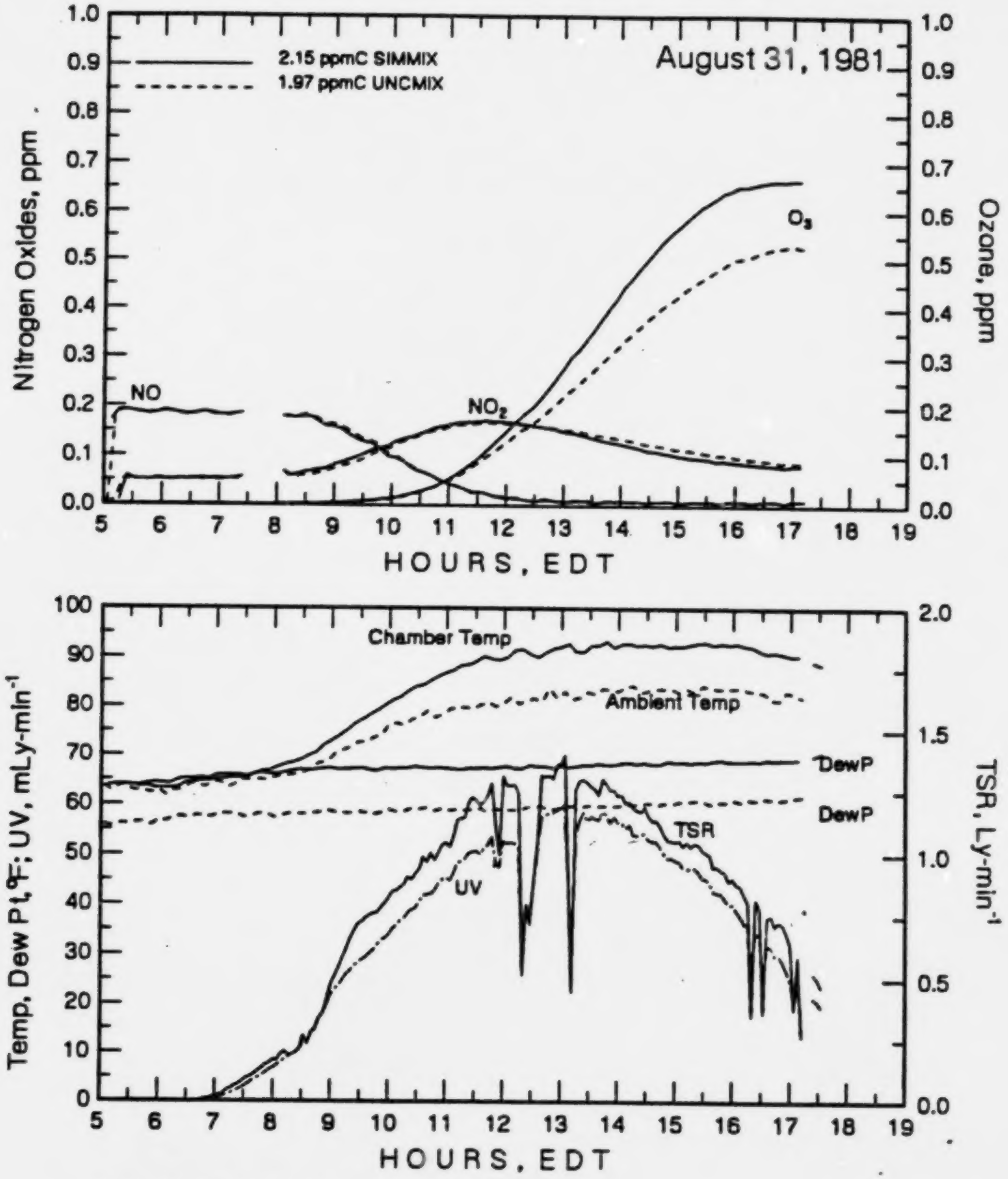

Figure 60. Relative HC reactivity experiment.

August 31, 1981
SIMMIX vs. UNCMIX

Figure 60 to 62 show data and simulations for a four component mixture vs. the 11 component paraffin-olefin UNCMIX.

Both mechanisms do well on both runs, but the UNCMIX simulation is a little too reactive. Neither mechanism simulates the HCHO profiles well.

Table 30. August 31, 1981 Initial Condition Simulation File.

```
 #if RED
 August 31, 1981 2.15 ppmC SIMMIX1 (RED)
 #end
 #if BLUE
 August 31, 1981 2.0 ppmC UNCMIX (BLUE)
 #end
 #if CB4
 c:\pkss\mech\CB42chm.pks
 CONC=
 @c:\pkss\mech\CBckCB4.icx
 #end
 #if CAL
 c:\pkss\mech\CALchm.pks
 CONC=
 @c:\pkss\mech\CBckCAL.icx
 #end
 #if RED
  NO  =    0.186,
  NO2 =    0.053,
 #end
 #if BLUE
  NO  =    0.185,
  NO2 =    0.051,
 #end
 #if RED
 #if CB4
  ETH  =   0.1752 ,
  OLE  =   0.0849 ,
  PAR  =   0.0849 ,
  PAR  =   1.5444 ,
 #end
 #if CAL
  ETHE  =  0.1752 ,
  PRPE  =  0.0849 ,
  ALK4  =  0.2151 ,
  ALK7  =  0.1368 ,
  (MISS =  [4.0-4.5]*0.2151+[5.0-7.0]*0.1368 = -0.3812 ppmC)
 #end
 #end
 #if BLUE
 #if CB4
  ETH   =  0.1267 ,
  OLE   =  0.0631 ,
  PAR   =  1.4879 ,
  RCHO  =  0.0514 ,
 #end
 #if CAL
  ETHE  =   0.1267 ,
  PRPE  =   0.0631 ,
  TBUT  =   0.0257 ,
  ALK4  =   0.1616 ,
  ALK7  =   0.0807 ,
  (MISS =   0.1325 ,)
 #end
 #end
   HONO =   0.0036,
  CO   =   0.3;
@e:\segfiles\finalseg\81\au3181.lix
@e:\segfiles\finalseg\81\au3181.twd
FINISH;
```

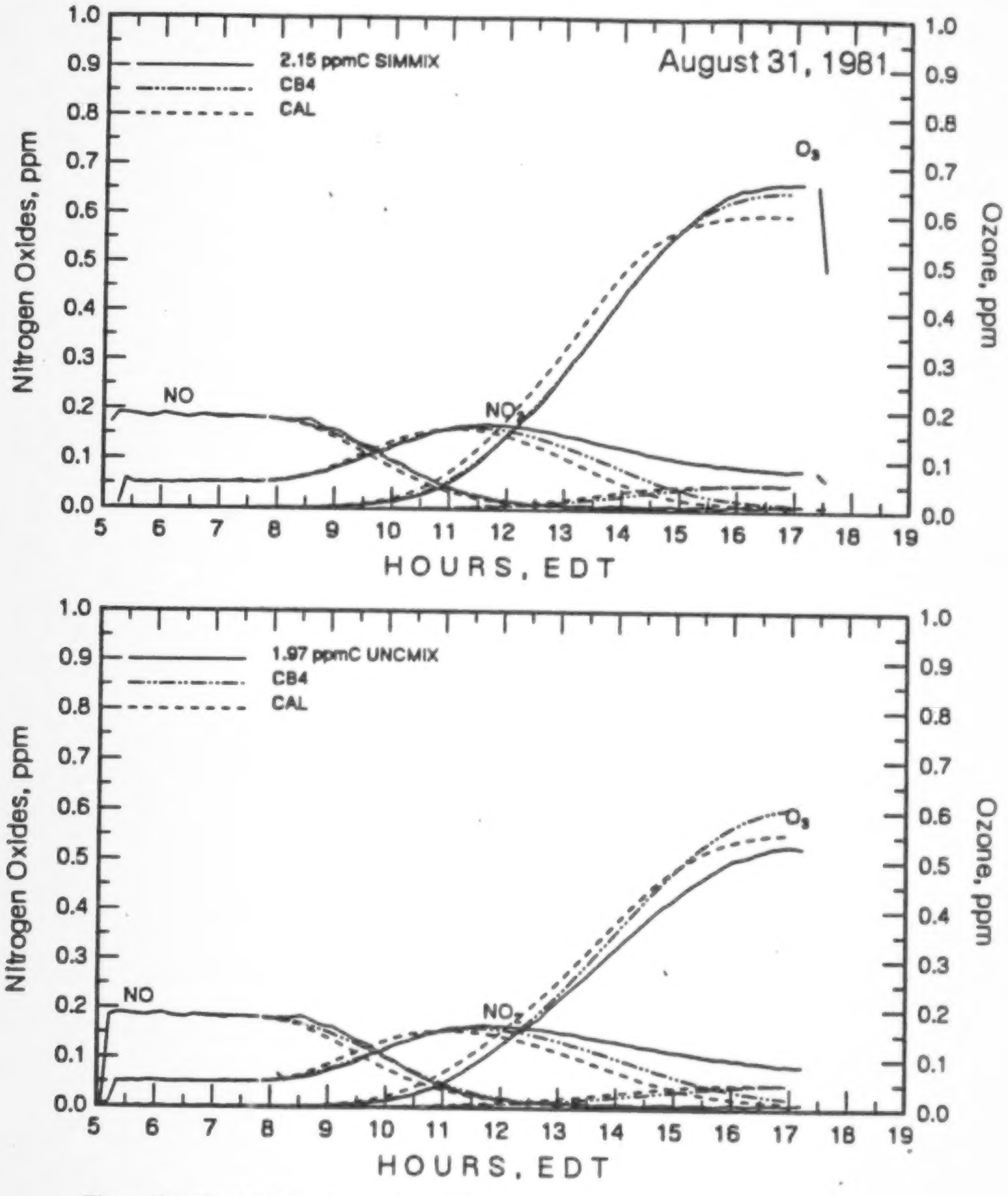

Figure 61. Standard Carter wall model.

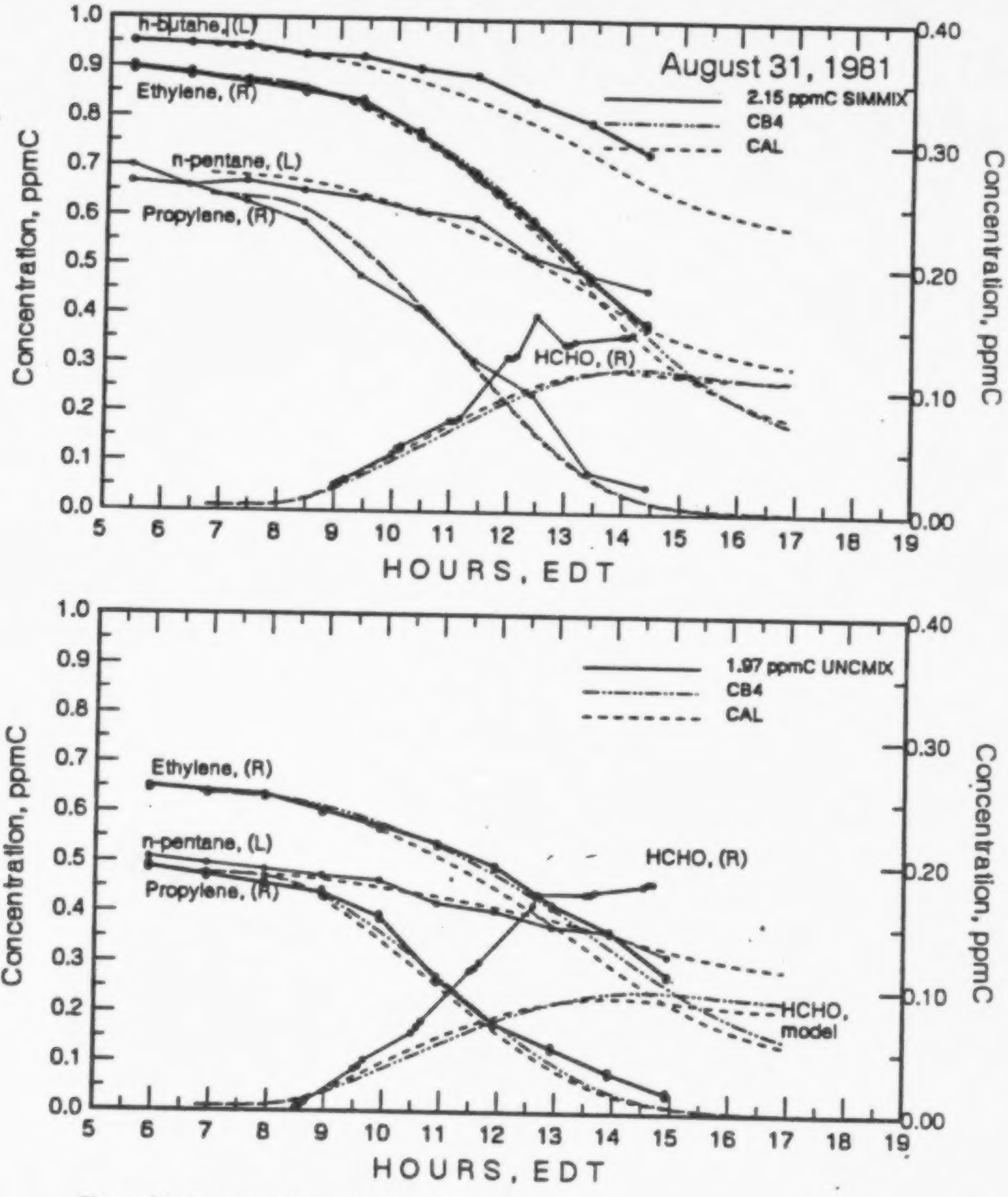

Figure 62. Standard Carter wall model.

August 5, 1984
Delta HC SynAuto

Figure 63 to 65 show data and simulations for a delta HC SynAuto experiment.

Both models are slow to cross over and slow to consume the HC with only the standard Carter wall model. This run, however, because of the early morning dew point rise and like July 30, 1978, needs initial HONO off gasing.

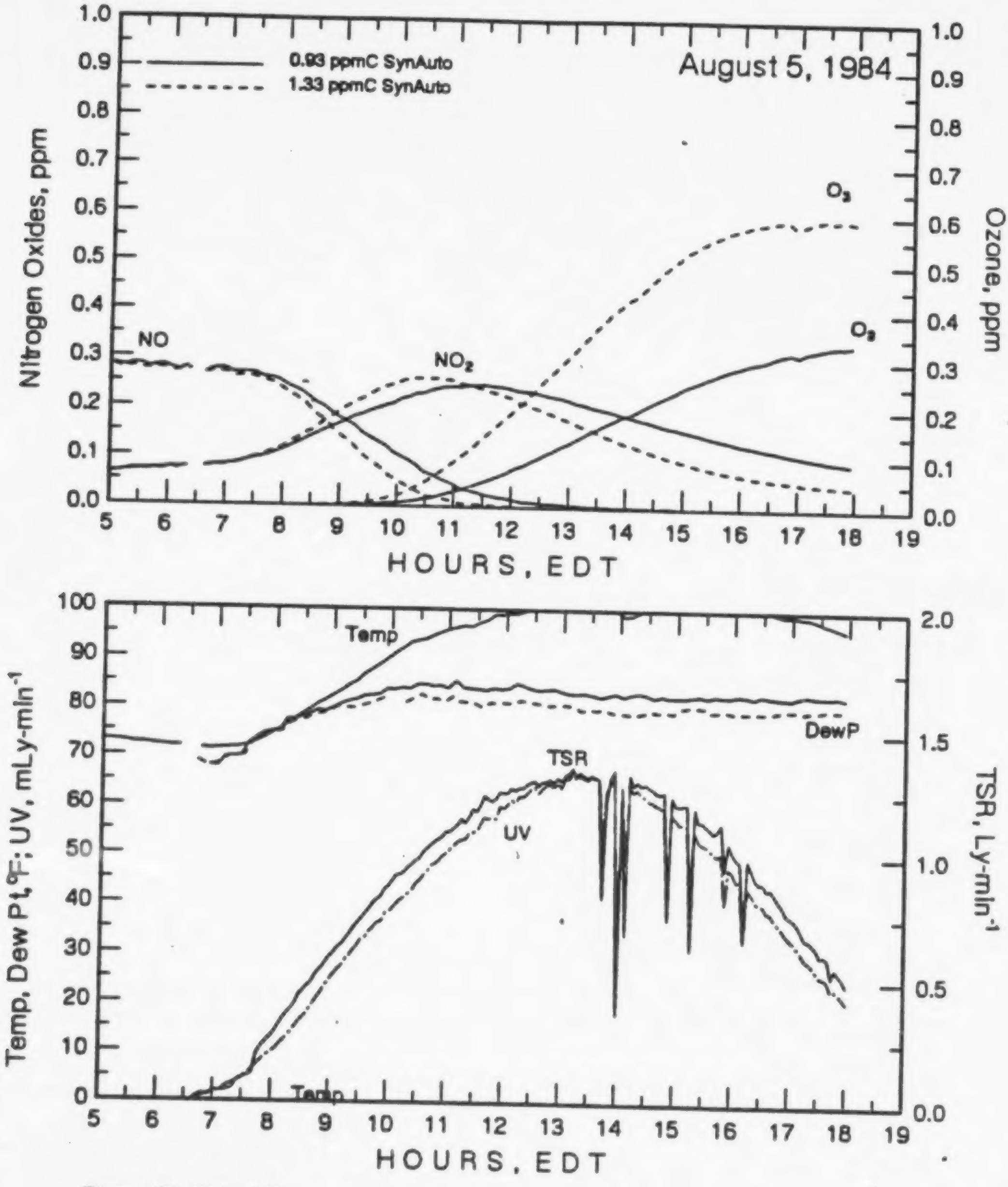

Figure 63. Delta HC experiment.

Table 31. August 5, 1984 Initial Condition Simulation File.

```
 #if RED
 Aug 5, 1984 0.9 ppmC SYNAUTO (RED)
 #end
 #if BLUE
 Aug 5, 1984 1.3 ppmC SYNAUTO (BLUE)
 #end
 #if CB4
 c:\pkss\mech\CB42chm.pks
 CONC=
 @c:\pkss\mech\CBckCB4.icx
 #end
 #if CAL
 c:\pkss\mech\CALchm.pks
 CONC=
 @c:\pkss\mech\CBckCAL.icx
 #end
 #if RED
  NO    =         0.272,
  NO2   =         0.079,
 #end
 #if BLUE
  NO    =         0.268,
  NO2   =         0.077,
 #end
 #if RED
 #if CB4
  PAR       =       0.2269,
  ETH       =       0.1326,
  OLE       =       0.0195,
  TOL       =       0.0246,
  XYL       =       0.0195,
  HCHO      =       0.0124,
  RCHO      =       0.0105,
 #end
 #if CAL
  ALK4      =       0.0201,
  ALK7      =       0.0144,
  ETHE      =       0.1326,
  PRPE      =       0.0195,
  TBUT      =       0.0053,
  TOLU      =       0.0246,
  XYLE      =       0.0145,
  TMBZ      =       0.00502,
  HCHO      =       0.0124,
 #end
 #end
 #if BLUE
 #if CB4
  PAR   =         0.3214,
  ETH   =         0.1946,
  OLE   =         0.0290,
  TOL   =         0.0345,
  XYL   =         0.0281,
  HCHO  =         0.0188,
  RCHO  =         0.0155,
 #end
```

```
        #if CAL
         ALK4  =        0.0293,
         ALK7  =        0.0197,
         ETHE  =        0.1946,
         PRPE  =        0.0290,
         TBUT  =        0.0078,
         TOLU  =        0.0345,
         XYLE  =        0.0210,
         TMBZ  =        0.00705,
         HCHO  =        0.0188,
        #end
        #end
         HONO  =        0.0054,
         CO    =        0.3;
        @e:\segfiles\finalseg\84\au0584.lix
        @e:\segfiles\finalseg\84\au0584.twd
FINISH;
```

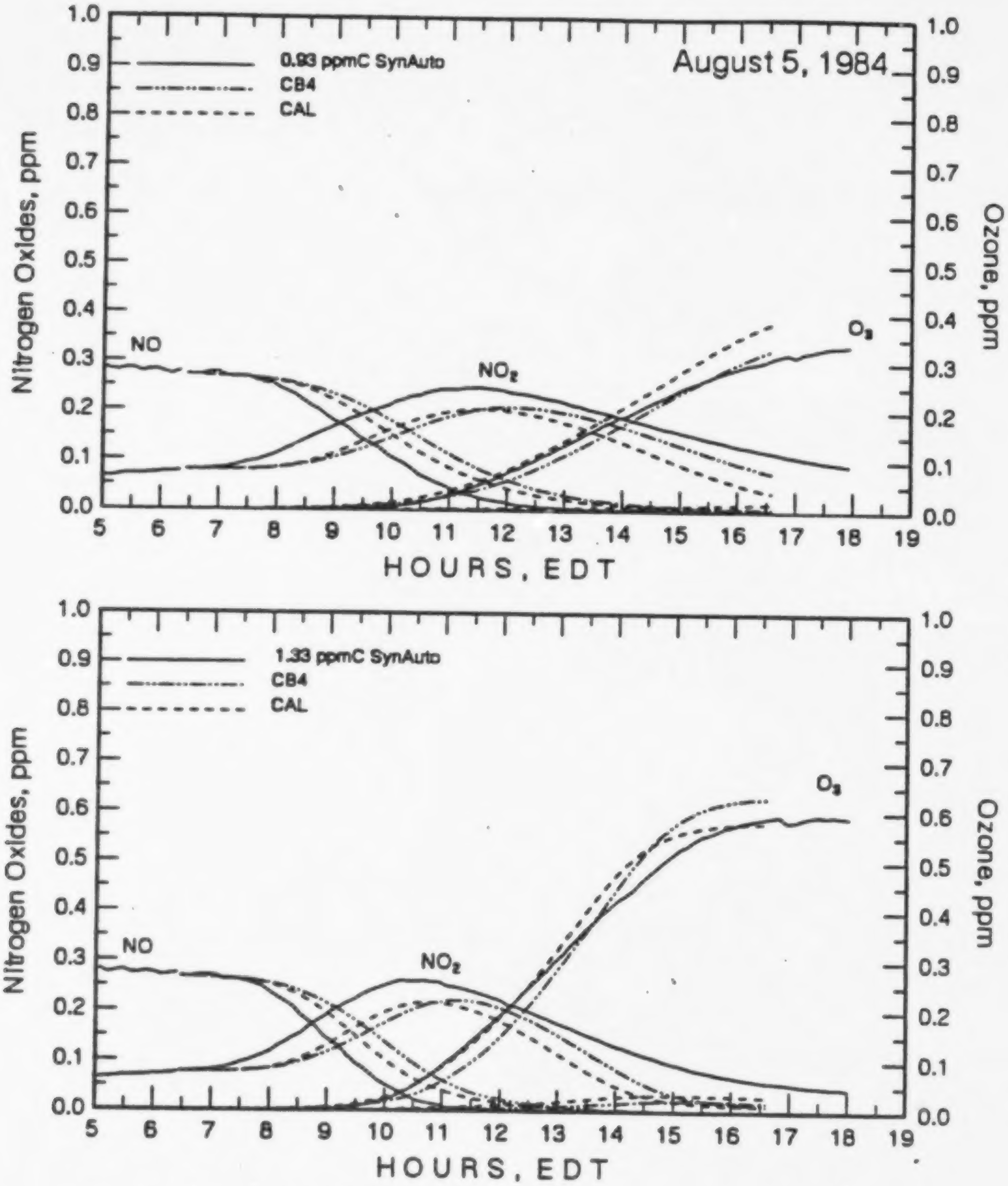

Figure 64. Standard Carter wall model.

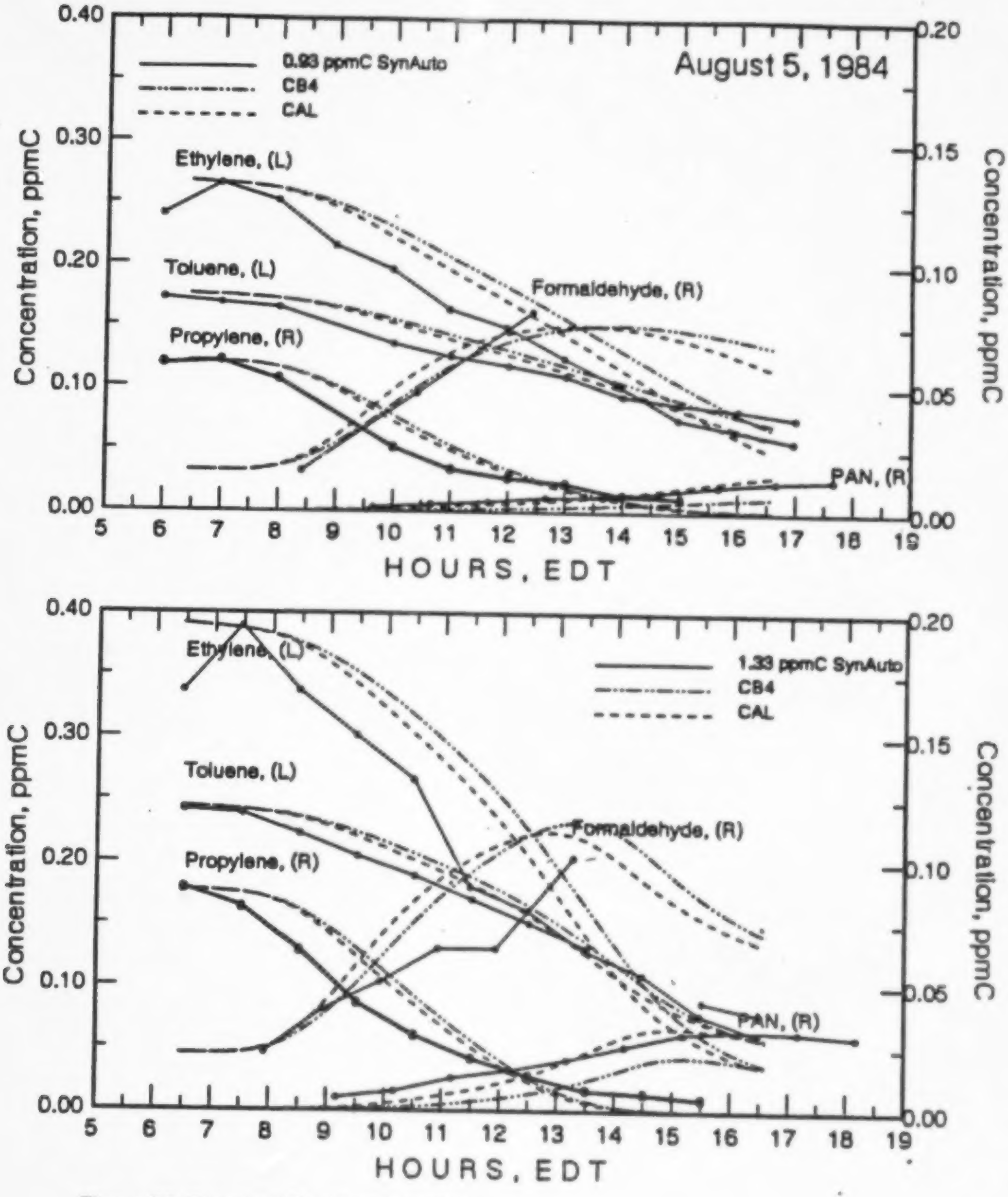

Figure 65. Standard Carter wall model.

August 6, 1984
Delta HC SynAuto

Figure 66 to 68 show data and simulations for another delta HC SynAuto experiment.

The results are similar to August 5, 1984.

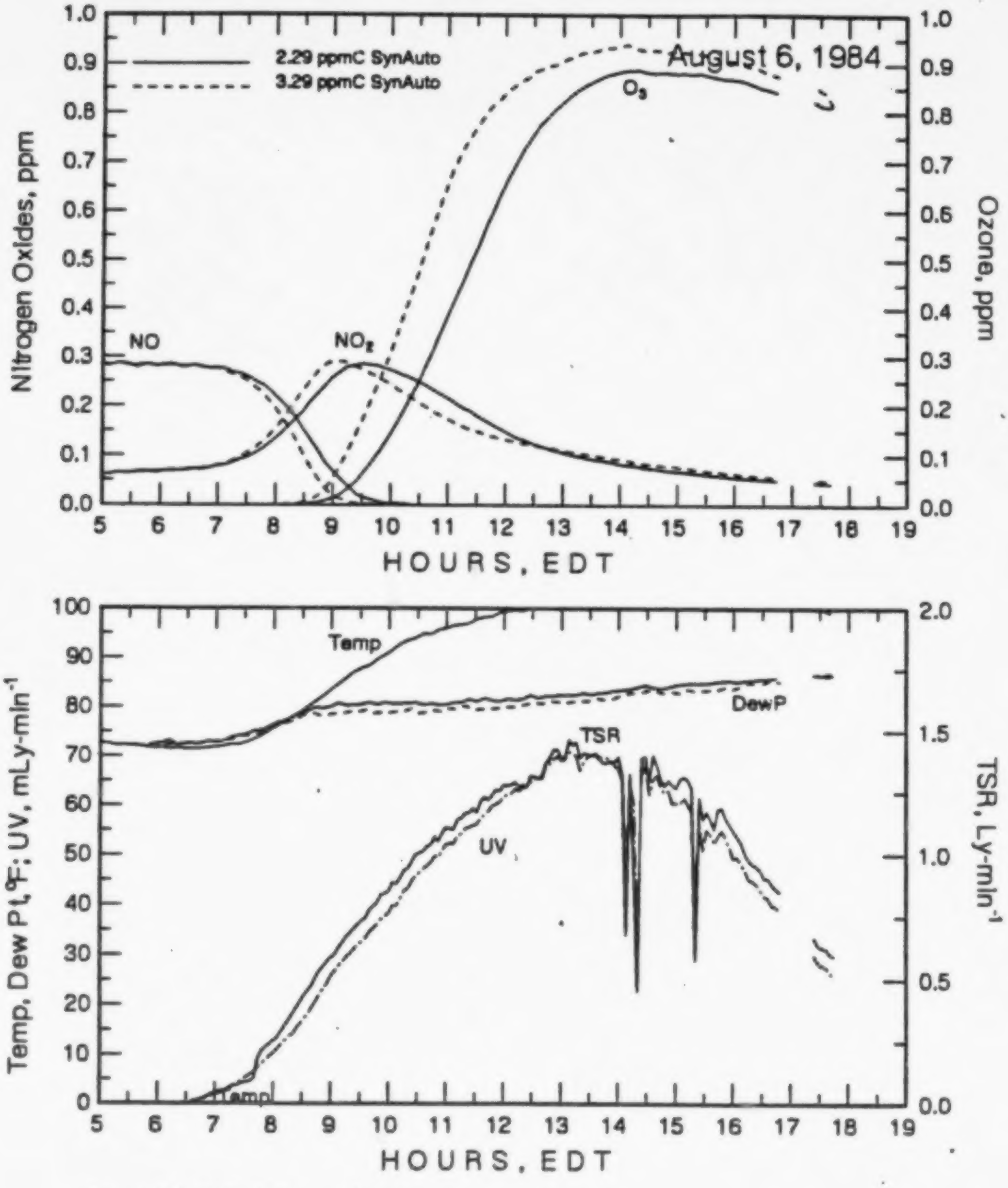

Figure 66. Delta HC experiment.

Table 32. August 6, 1984 Initial Condition Simulation File.

```
#if RED
August 6, 1984 2.3 ppmC SYNAUTO (RED)
#end
#if BLUE
August 6, 1984 3.3 ppmC SYNAUTO (BLUE)
#end
#if CB4
c:\pkss\mech\CB42chm.pks
CONC=
@c:\pkss\mech\CBckCB4.icx
#end
#if CAL
c:\pkss\mech\CALchm.pks
CONC=
@c:\pkss\mech\CBckCAL.icx
#end

#if RED
 NO       =      0.279,
 NO2      =      0.072,
#end
#if BLUE
NO        =     0.283,
NO2       =     0.072,
#end
#if RED
#if CB4
 PAR      =      0.5434,
 ETH      =      0.3330,
 OLE      =      0.0493,
 TOL      =      0.0602,
 XYL      =      0.0494,
 HCHO     =      0.039,
 RCHO     =      0.0260,
#end
#if CAL
 ALK4     =      0.0502 ,
 ALK7     =      0.0325 ,
 ETHE     =      0.3330 ,
 PRPE     =      0.0493 ,
 TBUT     =      0.0130 ,
 TOLU     =      0.0602 ,
 XYLE     =      0.0366 ,
 TMBZ     =      0.0128 ,
 HCHO     =      0.0390 ,
#end
#end
#if BLUE
#if CB4
 PAR   =         0.7879,
 ETH   =         0.4813,
 OLE   =         0.0710,
 TOL   =         0.0860,
 XYL   =         0.0700,
 HCHO  =         0.057,
 RCHO  =         0.0395,
#end
#if CAL
 ETHE    =        0.4813 ,
 PRPE    =        0.0710 ,
 TBUT    =        0.0197 ,
 ALK4    =        0.0711 ,
 ALK7    =        0.0481 ,
 TOLU    =        0.0860 ,
 XYLE    =        0.0520 ,
 TMBZ    =        0.0180 ,
 HCHO    =        0.0570 ,
#end
#end
  HONO  =         0.0054,
 CO    =          0.3;
@e:\segfiles\finalseg\84\au0684.lix
@e:\segfiles\finalseg\84\au0684.twd
FINISH;
```

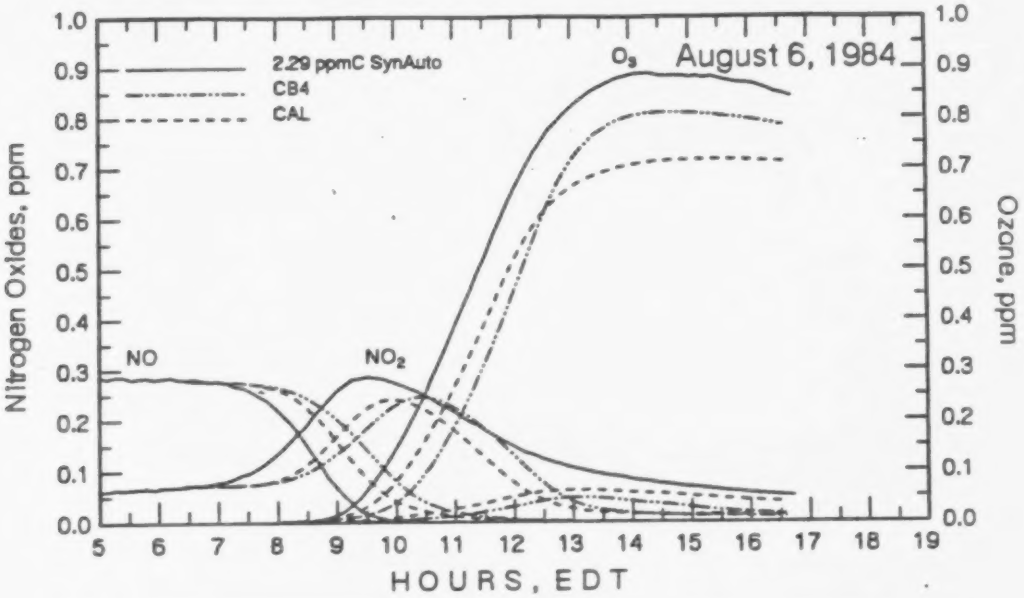

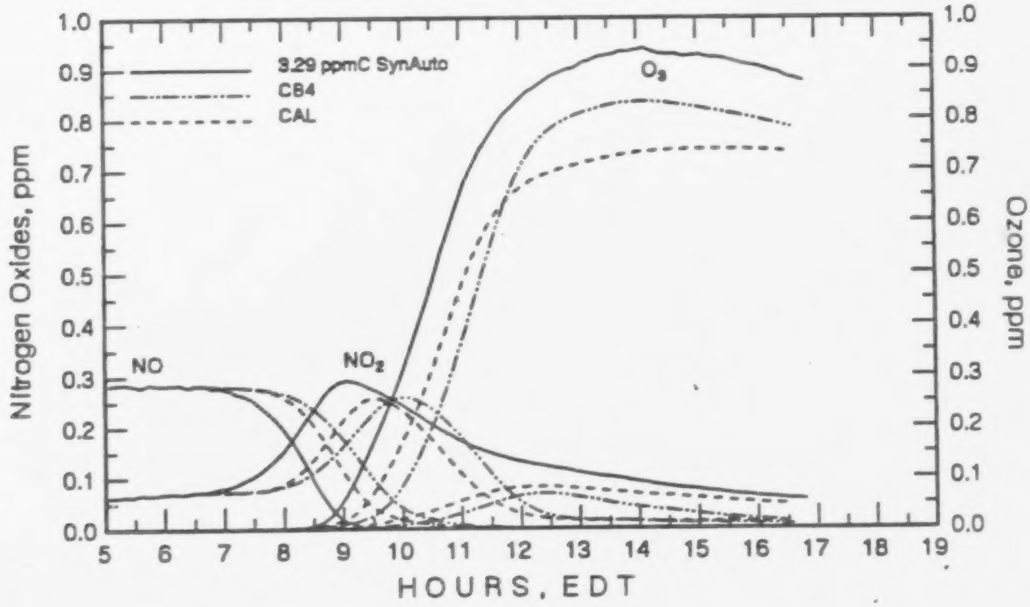

Figure 67. Standard Carter wall model.

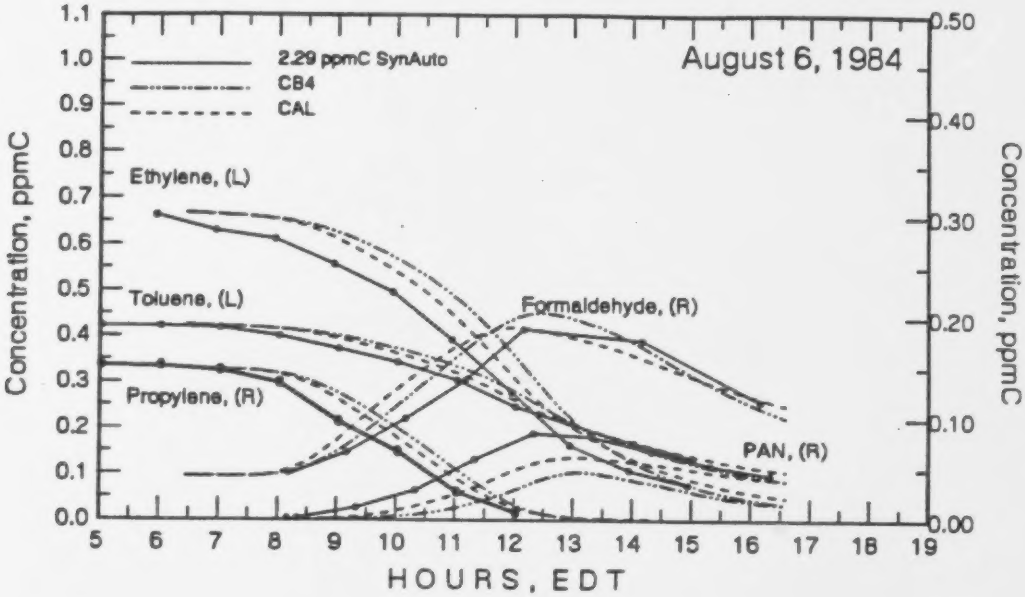

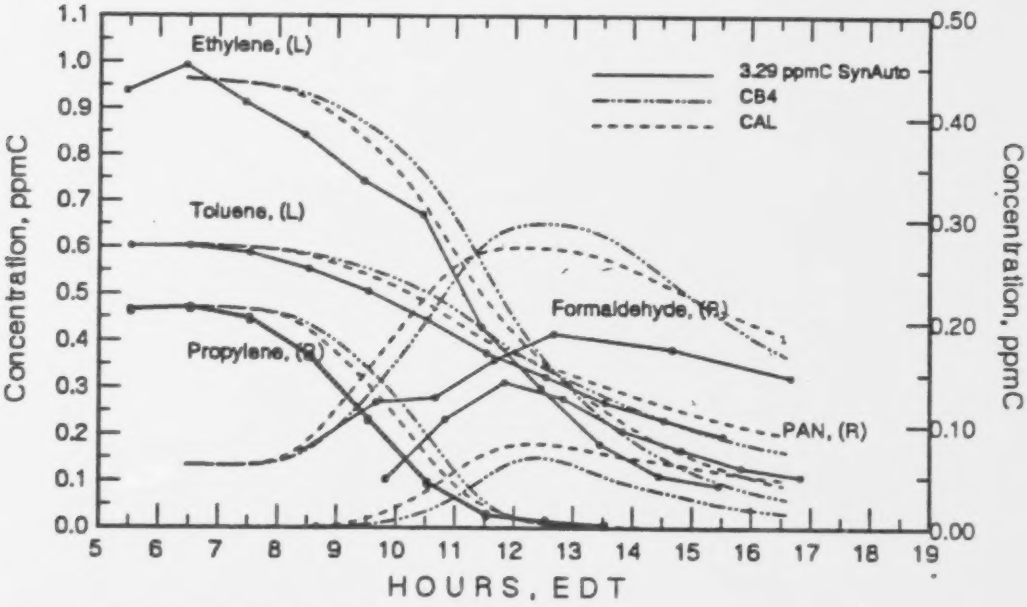

Figure 68. Standard Carter wall model.

August 7, 1984
SynAuto/SynMeth Substitution

Figure 69 to 70 show data and simulations for a 1/3 substitution of synthetic methanol exhaust into the SynAuto mixture.

Both mechanisms simulatate this compositional change well.

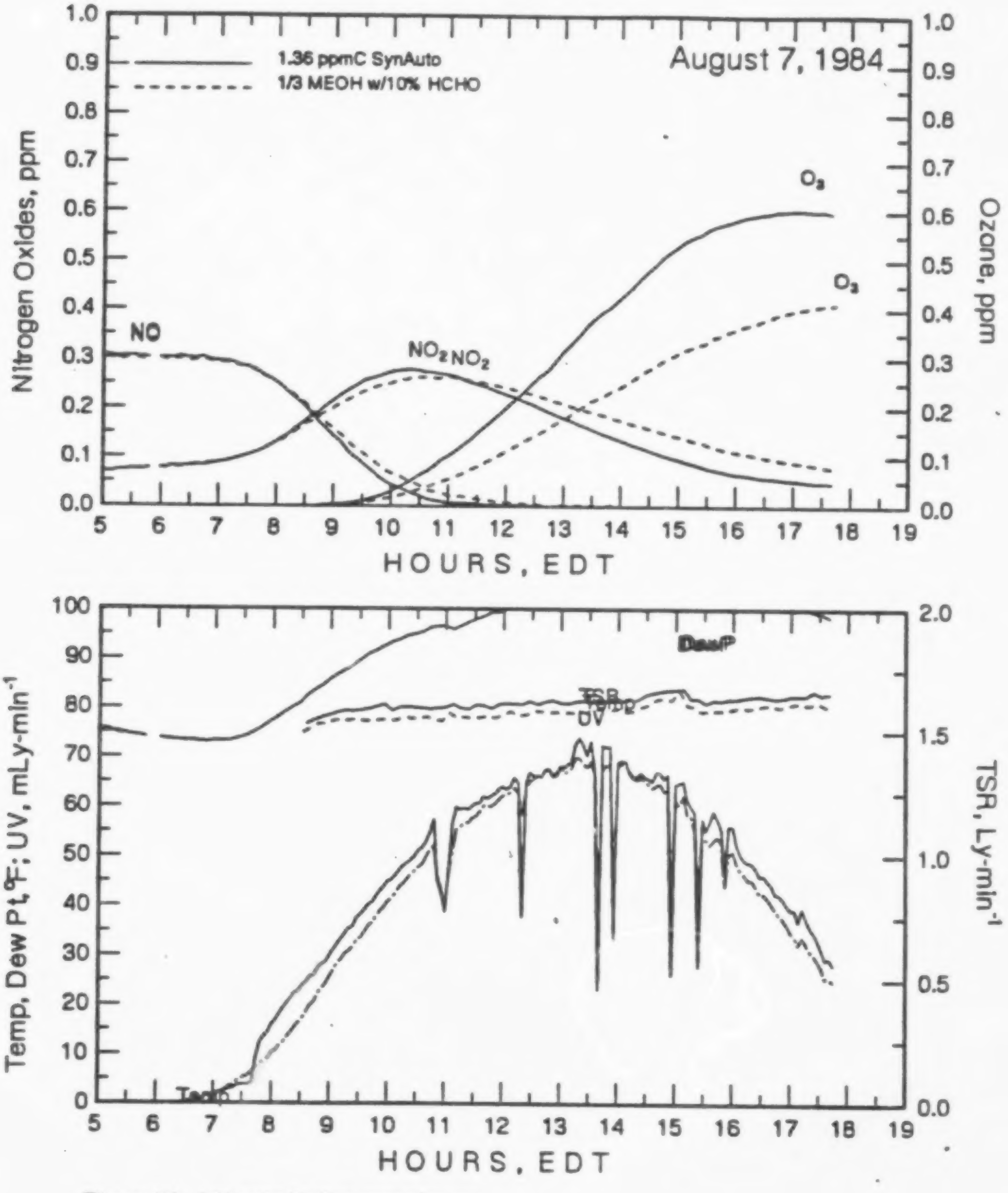

Figure 69. HC substitution experiment.

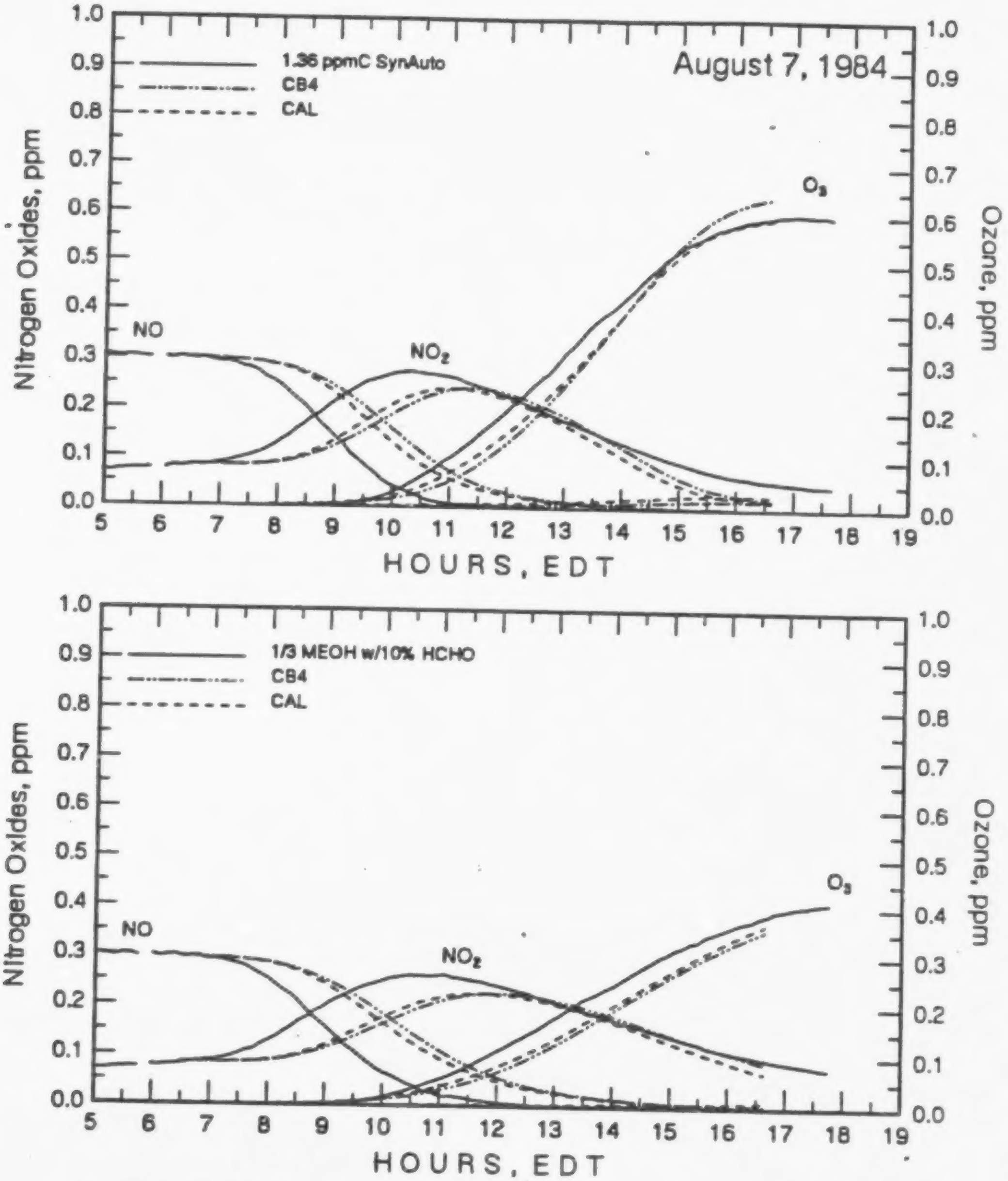

Figure 70. Standard Carter wall model.

August 8, 1984
SynAuto vs. SynAuto/SynMeth

Figure 71 to 73 show data and simulations for 1/3 substitution of SynMeth into SynAuto.

As in the August 6 simulation, CB4 does better at predicting the peak O_3. Both mechanisms simulated the composition change well. HCHO is reasonably well predicted in this mixture.

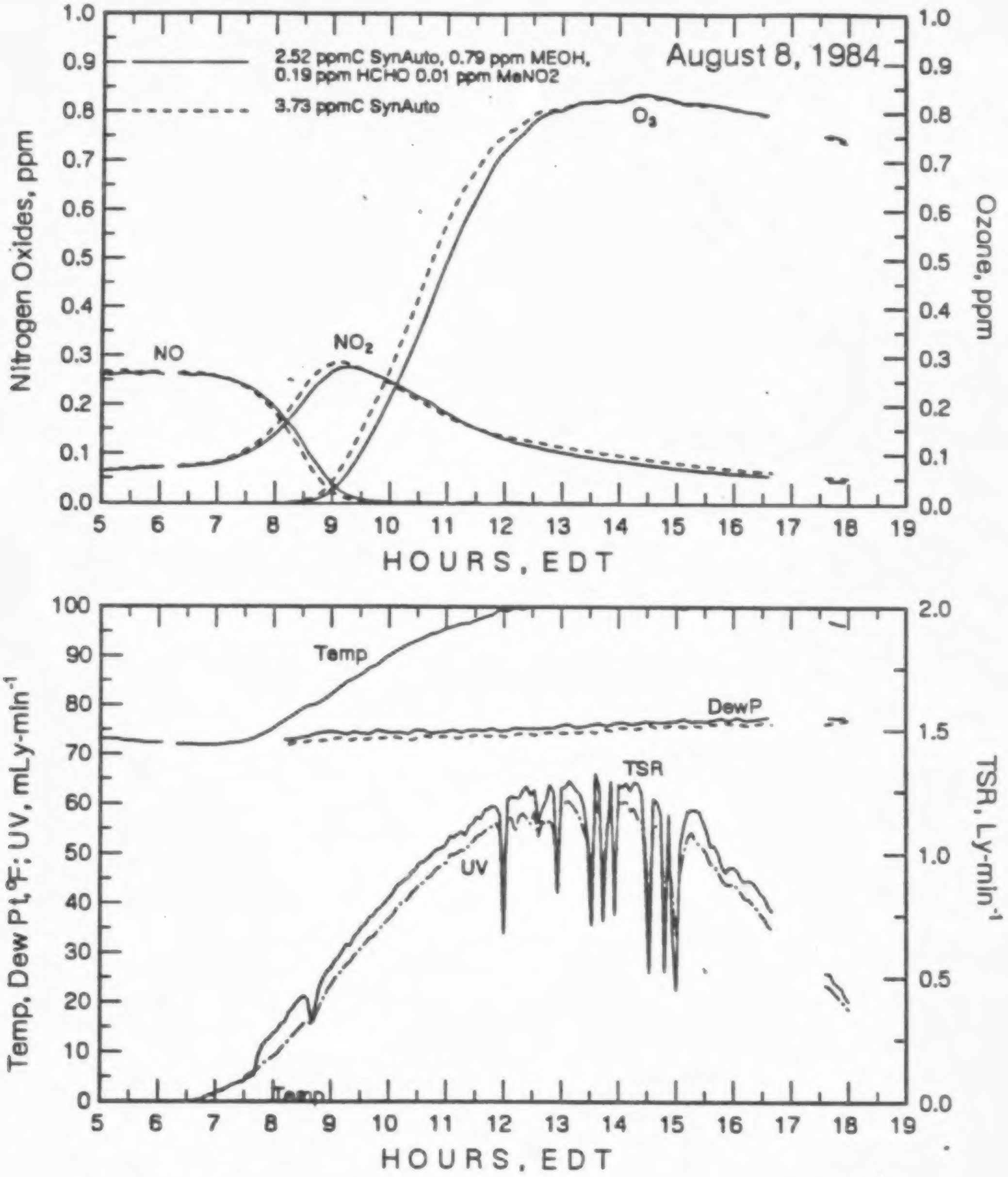

Figure 71. Delta HC experiment.

Table 34. August 8, 1984 Initial Condition Simulation File.

```
#if RED
August 8, 1984 2.5 ppmC SYNAUTO, 0.79 ppm MeOH, 0.23 ppm HCHO (RED)
#end
#if BLUE
August 8, 1984 3.7 ppmC SYNAUTO (BLUE)
#end
#if CB4
c:\pkss\mech\CB42chm.pks
CONC=
@c:\pkss\mech\CBckCB4.icx
#end
#if CAL
c:\pkss\mech\CALchm.pks
CONC=
@c:\pkss\mech\CBckCAL.icx
#end
#if RED
 NO    =        0.262,
 NO2   =        0.076,
#end
#if BLUE
 NO    =        0.265,
 NO2   =        0.075,
#end
#if RED
#if CB4
 ETH     =       0.3523 ,
 OLE     =       0.0521 ,
 PAR     =       1.3884 ,
 TOL     =       0.0686 ,
 XYL     =       0.0541 ,
 HCHO    =       0.2280 ,
 RCHO    =       0.0289 ,
 MEOH    =       0.7850 ,
#end
#if CAL
 ETHE    =       0.3523 ,
 PRPE    =       0.0521 ,
 TBUT    =       0.0145 ,
 ALK4    =       0.0524 ,
 ALK7    =       0.0388 ,
 TOLU    =       0.0686 ,
 XYLE    =       0.0401 ,
 TMBZ    =       0.0140 ,
 HCHO    =       0.2280 ,
 MEOH    =       0.7850 ,
#end
#end
#if BLUE
#if CB4
 ETH     =       0.5252 ,
 OLE     =       0.0763 ,
 PAR     =       0.8888 ,
 TOL     =       0.1021 ,
 XYL     =       0.0803 ,
 HCHO    =       0.0570 ,
 RCHO    =       0.0445 ,
#end
#if CAL
 ETHE    =       0.5252 ,
 PRPE    =       0.0763 ,
 TBUT    =       0.0223 ,
 ALK4    =       0.0779 ,
 ALK7    =       0.0569 ,
 TOLU    =       0.1021 ,
 XYLE    =       0.0594 ,
 TMBZ    =       0.0209 ,
 HCHO    =       0.0570 ,
#end
#end
  HONO  =        0.0053,
 CO    =         0.3;
@e:\segfiles\finalseg\84\au0884.lix
@e:\segfiles\finalseg\84\au0884.twd
FINISH;
```

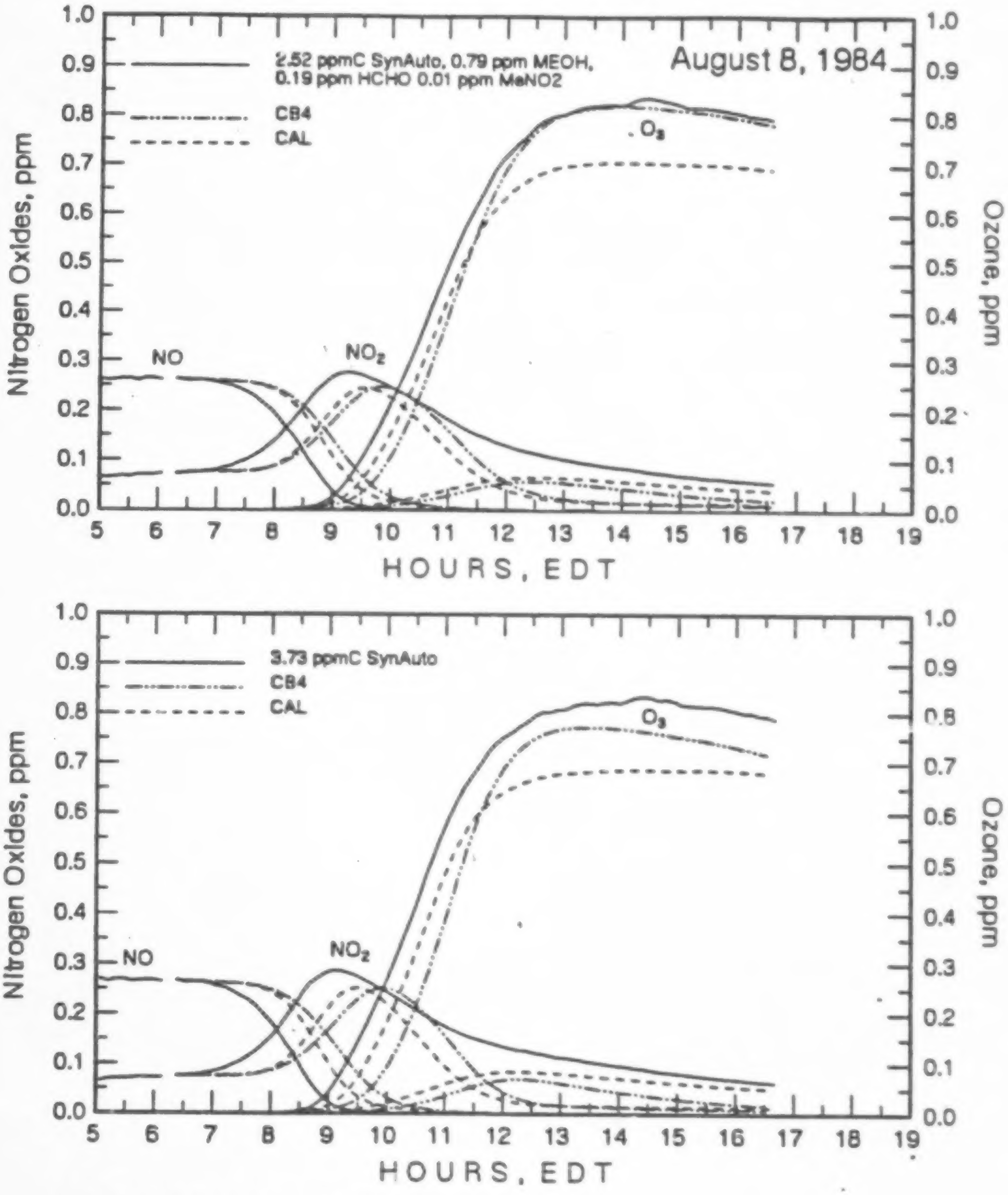

Figure 72. Standard Carter wall model.

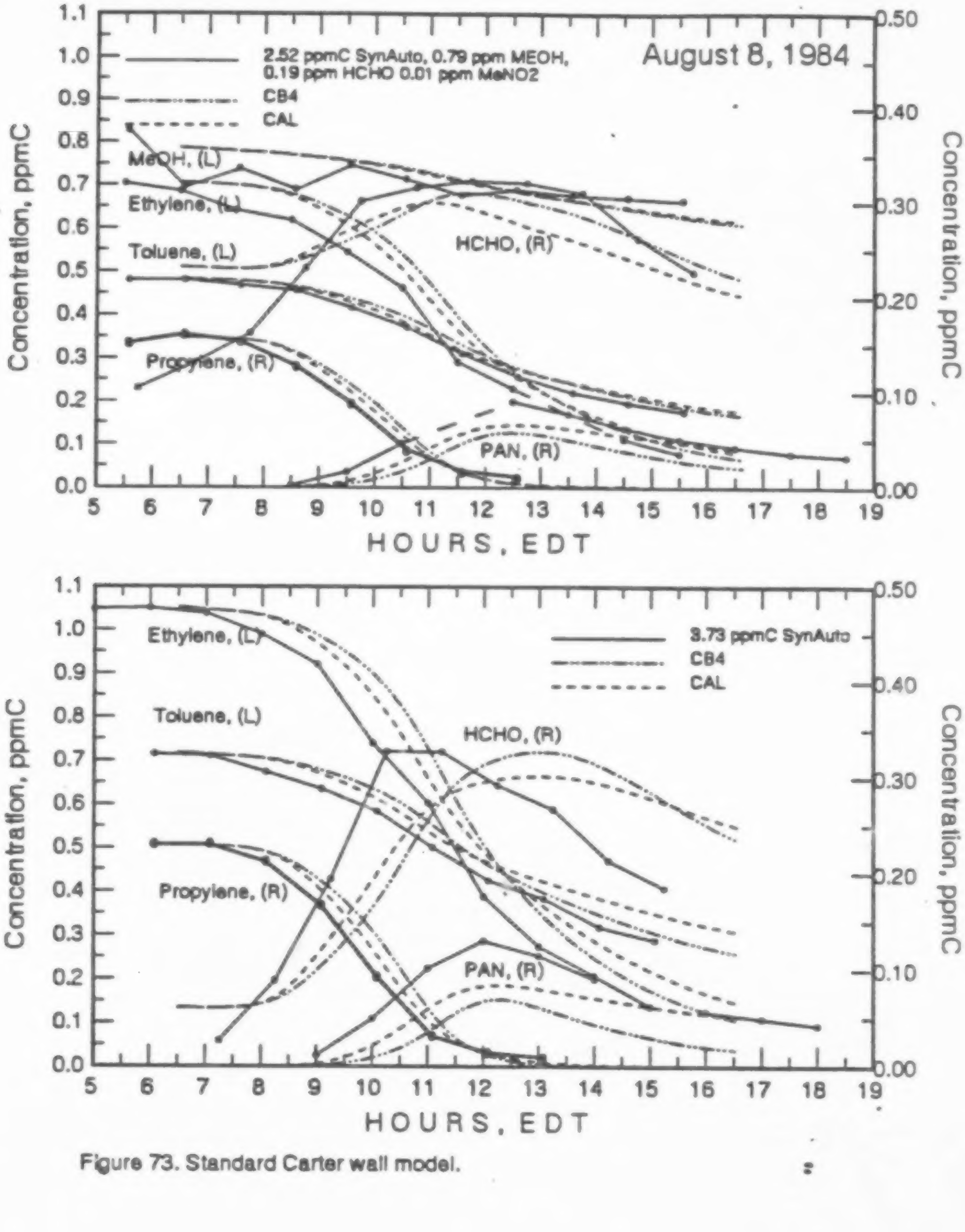

Figure 73. Standard Carter wall model.

August 9, 1984
SynAuto/SynMeth Substitution

Figure 74 to 75 show data and simulations for a 1/3 substitution of SynMeth into SynAuto at a low HC-to-NO_x ratio.

Both mechanisms do well for this condition.

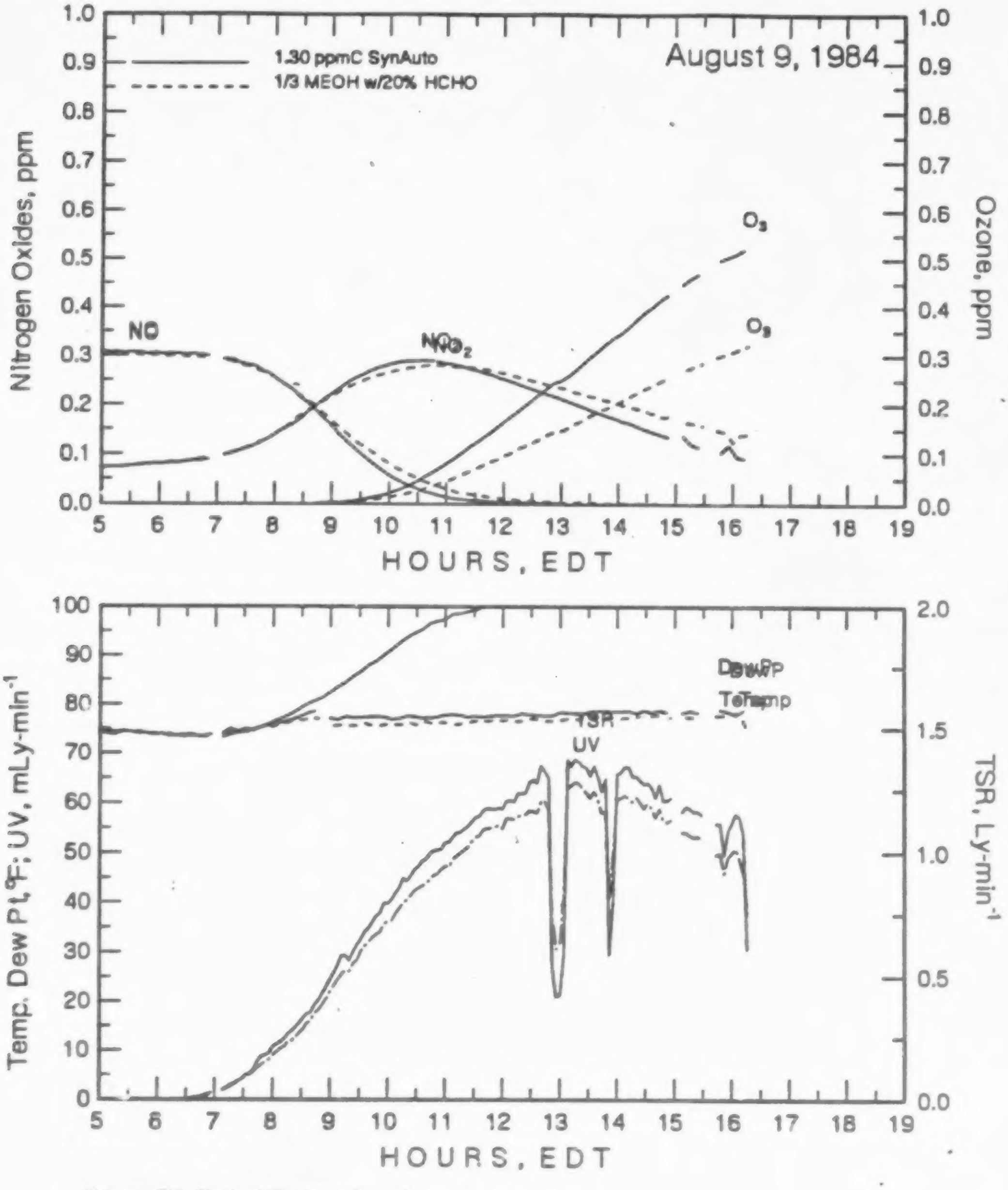

Figure 74. Delta HC experiment.

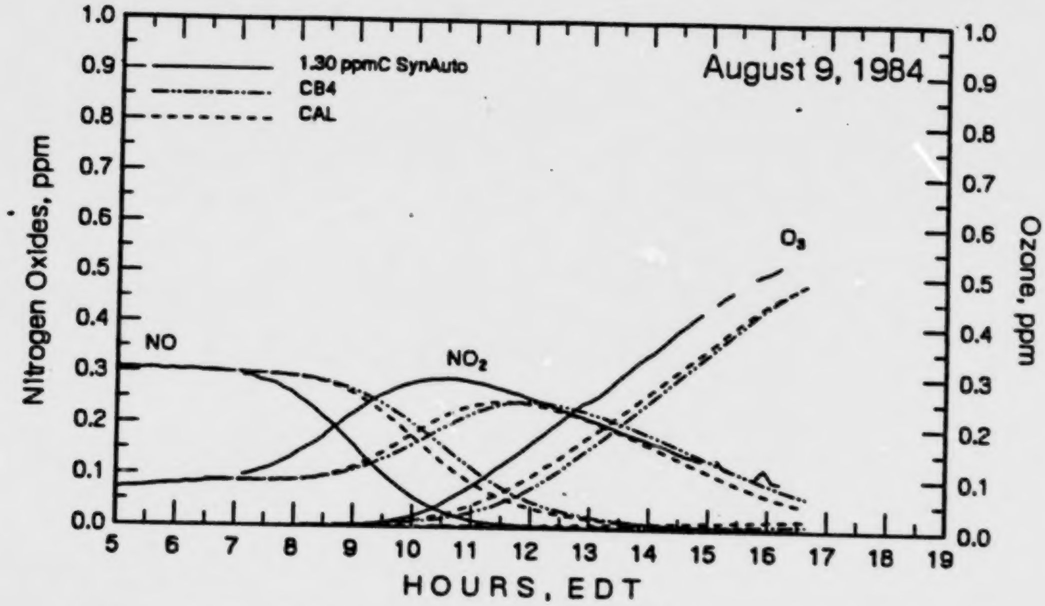

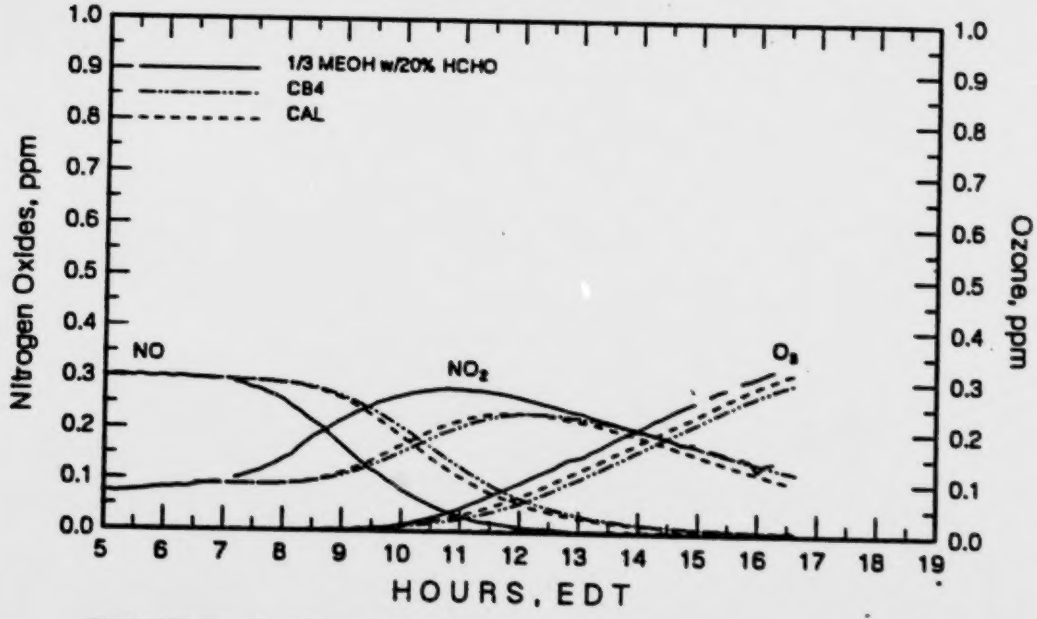

Figure 75. Standard Carter wall model.

June 26, 1985
Delta HC SynUrban

Figure 76 to 77 show data and simulations for a delta HC SynUrban mixture.

Compared to the SynAuto simulations, these simulations are over reactive.

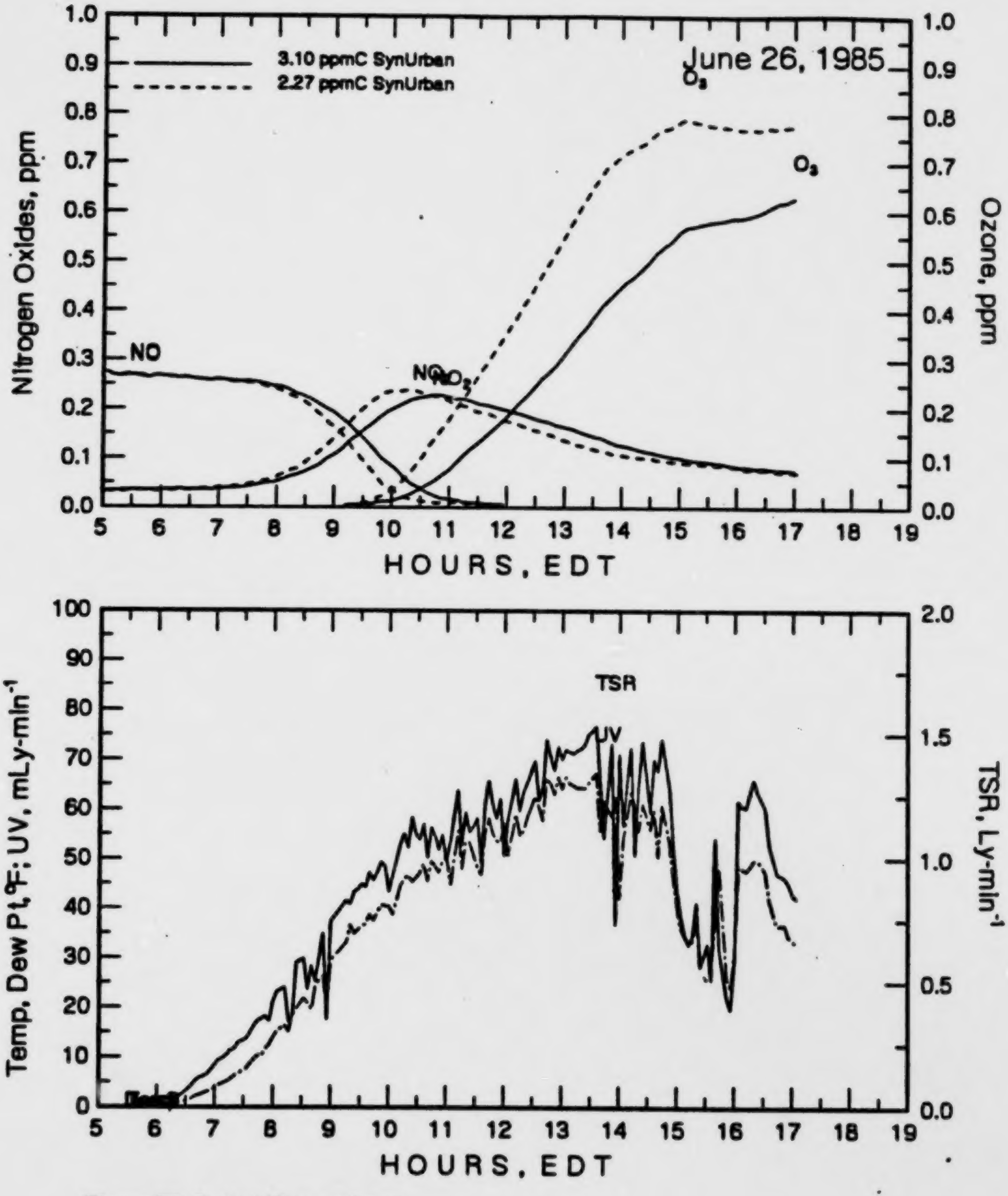

Figure 76. Delta HC experiment.

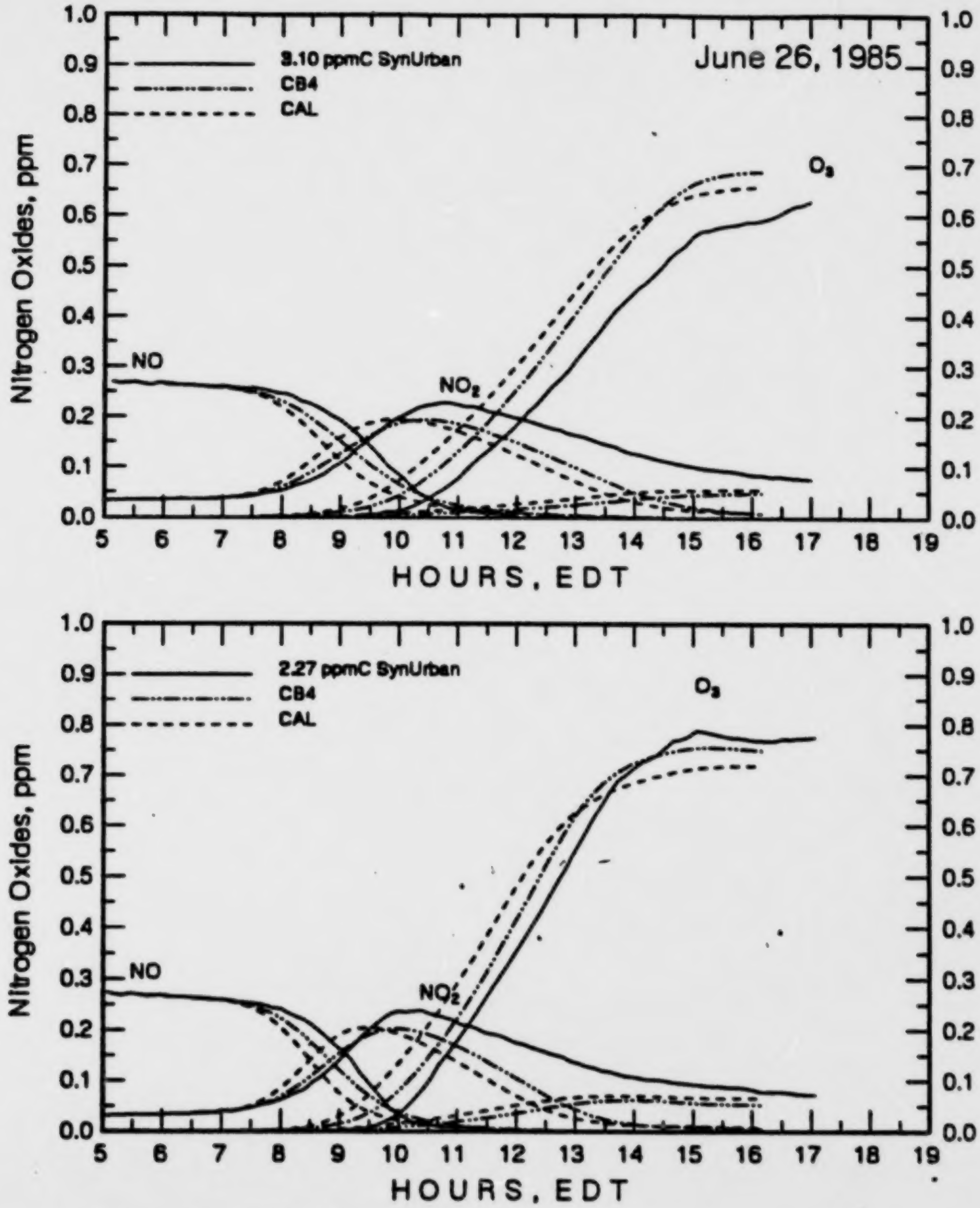

Figure 77. Standard Carter wall model.

August 22, 1984
SynUrban vs. SynUrban/SynMeth

Figure 78 to 81 show data and simulations for a delta HC SynUrban mixture.

Even though the initial cross time is correct and the HC decays are very good, these simulations are over reactive for O_3. That is, there were too many NO to NO_2 conversions per HC molecule consumed.

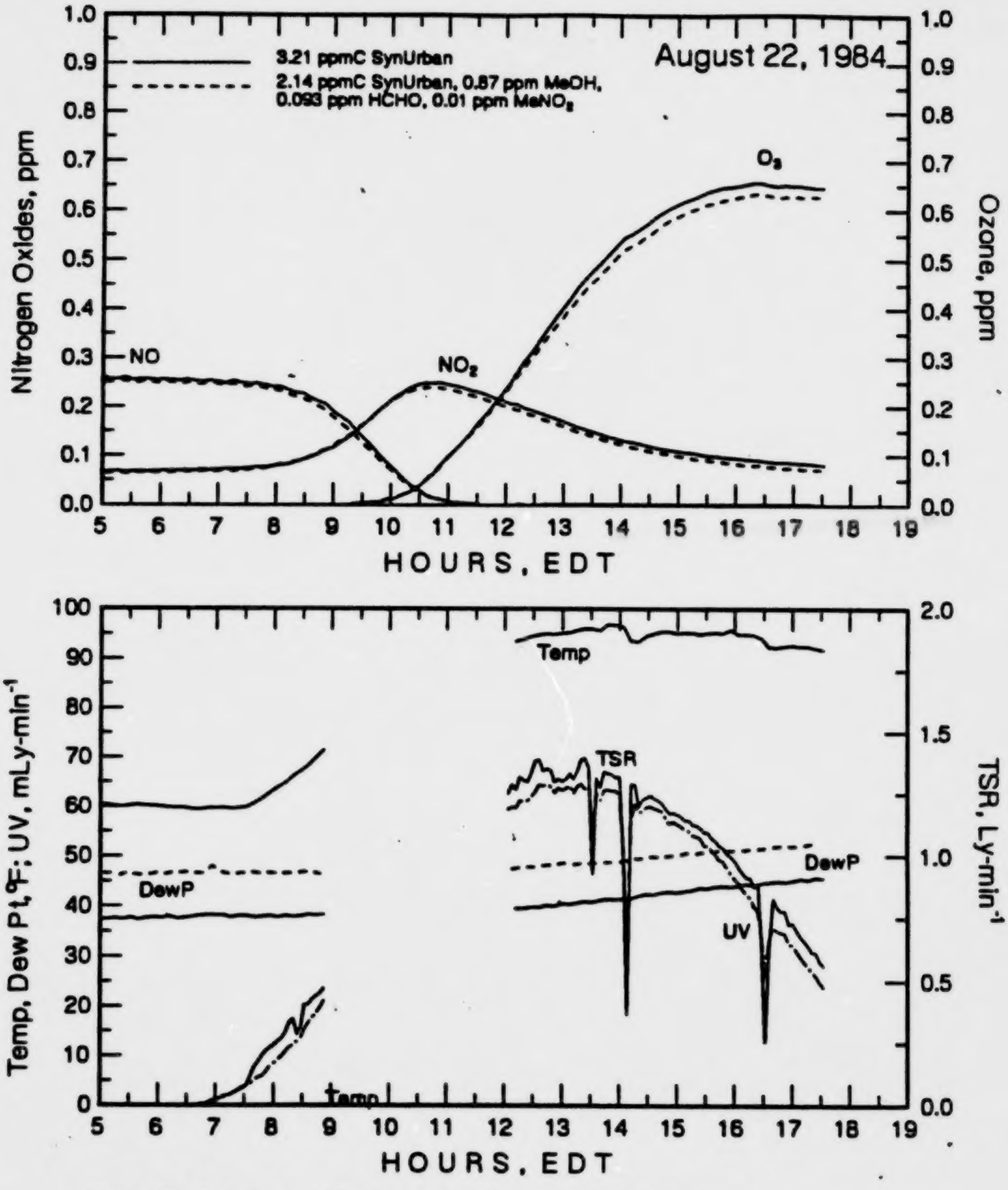

Figure 78. Relative hydrocarbon reactivity experiment at 0.35 NO_x.

Table 37. August 22, 1984 Initial Condition Simulation File.

```
#if RED
Aug 22, 1984 3.2 ppmC SYNURBAN (RED)
#end
#if BLUE
Aug 22, 1984 2.1 ppmC SYNURBAN, 0.87 PPM MEOH, 0.13 HCHO (BLUE)
#end
#if CB4
c:\pkss\mech\CB42chm.pks
CONC=
@c:\pkss\mech\CBckCB4.icx
#end
#if CAL
c:\pkss\mech\CALchm.pks
CONC=
@c:\pkss\mech\CBckCAL.icx
#end

#if RED
 NO    =        0.254,
 NO2   =        0.070,
#end
#if BLUE
 NO   =         0.254,
 NO2   =        0.070,
#end
#if RED
#if CB4
 ETH     =      0.1104 ,
 OLE     =      0.0557 ,
 PAR     =      1.8811 ,
 TOL     =      0.0576 ,
 XYL     =      0.0513 ,
 HCHO    =      0.0556 ,
 RCHO    =      0.0318 ,
#end
#if CAL
 ETHE   =      0.1104 ,
 PRPE   =      0.0557 ,
 TBUT   =      0.0202 ,
 ALK4   =      0.1166 ,
 ALK7   =      0.1973 ,
 TOLU   =      0.0576 ,
 XYLE   =      0.0364 ,
 TMBZ   =      0.0149 ,
 HCHO   =      0.0556 ,
#end
#end
#if BLUE
#if CB4
 ETH     =      0.0704,
 OLE     =      0.0344,
 PAR     =      1.2377,
 TOL     =      0.0396,
 XYL     =      0.0357,
 HCHO    =      0.1301,
 MEOH    =      0.8661,
 RCHO    =       0.0237,
#end
#if CAL
 ETHE   =       0.0704,
 PRPE   =       0.0344,
 TBUT   =       0.0151,
 ALK4   =       0.0769,
 ALK7   =       0.1302,
 TOLU   =       0.0396,
 XYLE   =       0.0262,
 TMBZ   =       0.0095,
 HCHO   =       0.1301,
 MEOH   =       0.8661,
#end
#end
  HONO  =        0.0049,
 CO    =         0.3;
@e:\segfiles\finalseg\84\au2284.lix
@e:\segfiles\finalseg\84\au2284.twd
FINISH;
```

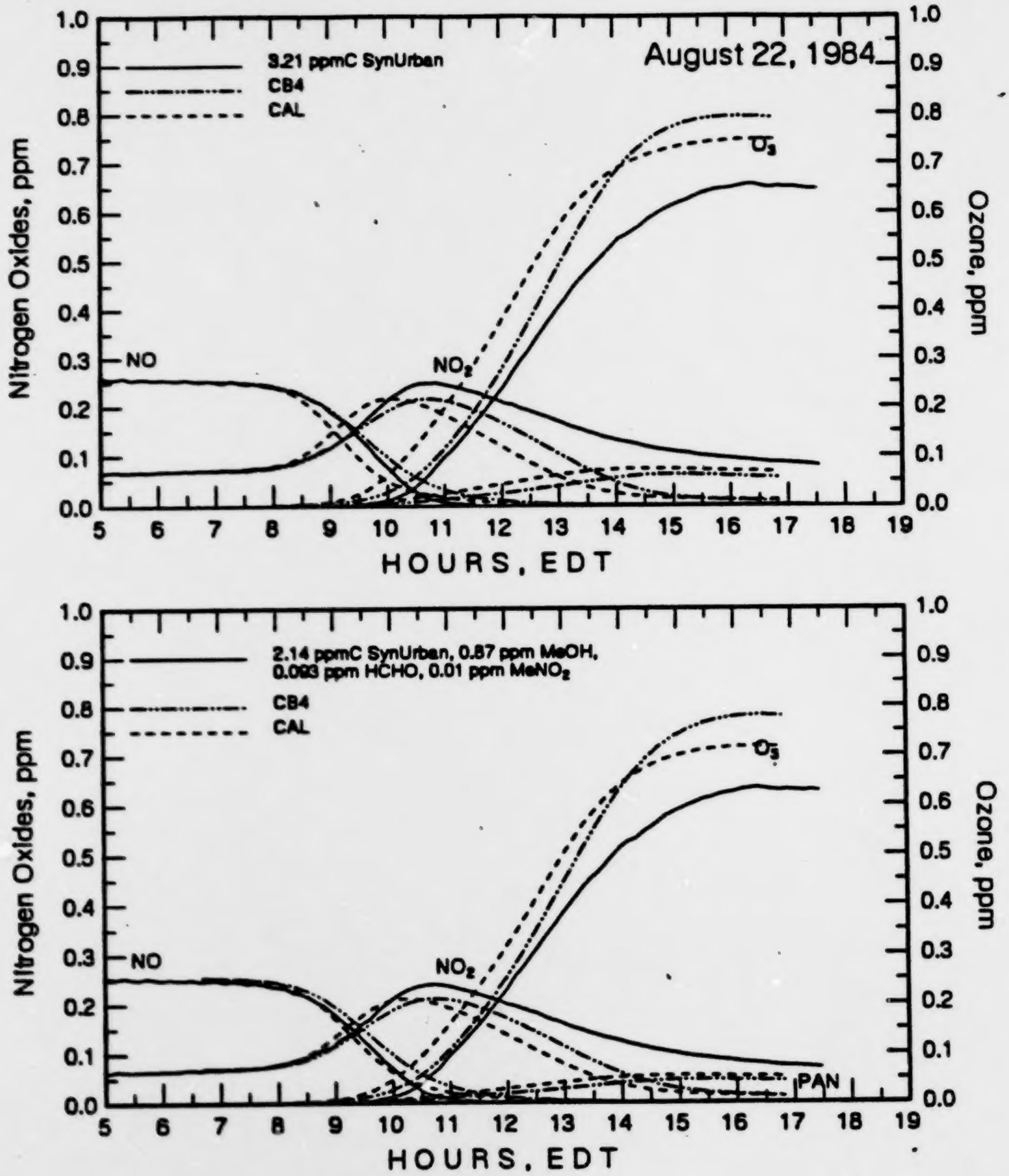

Figure 79. Standard Carter wall model.

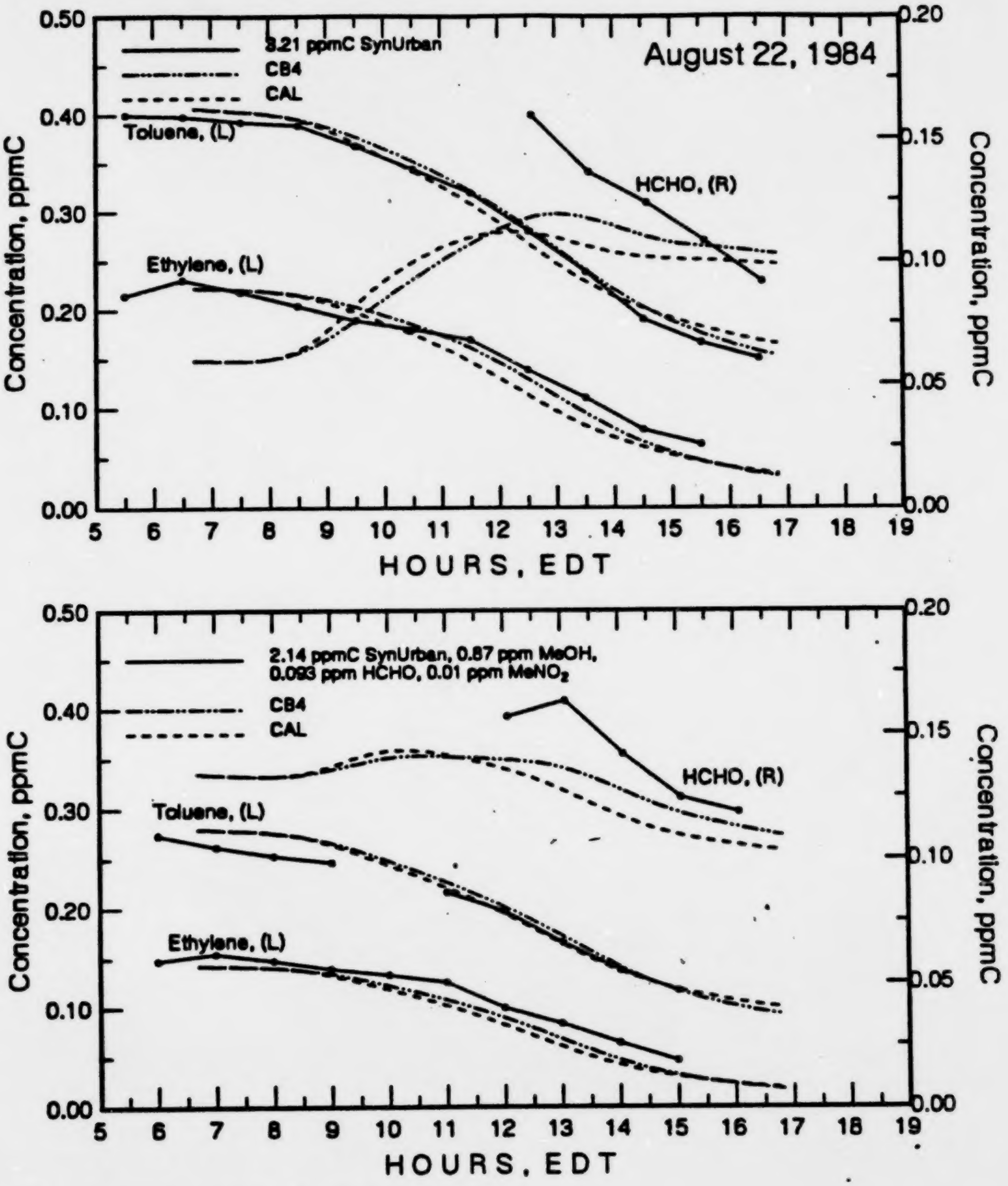

Figure 80. Standard Carter wall model.

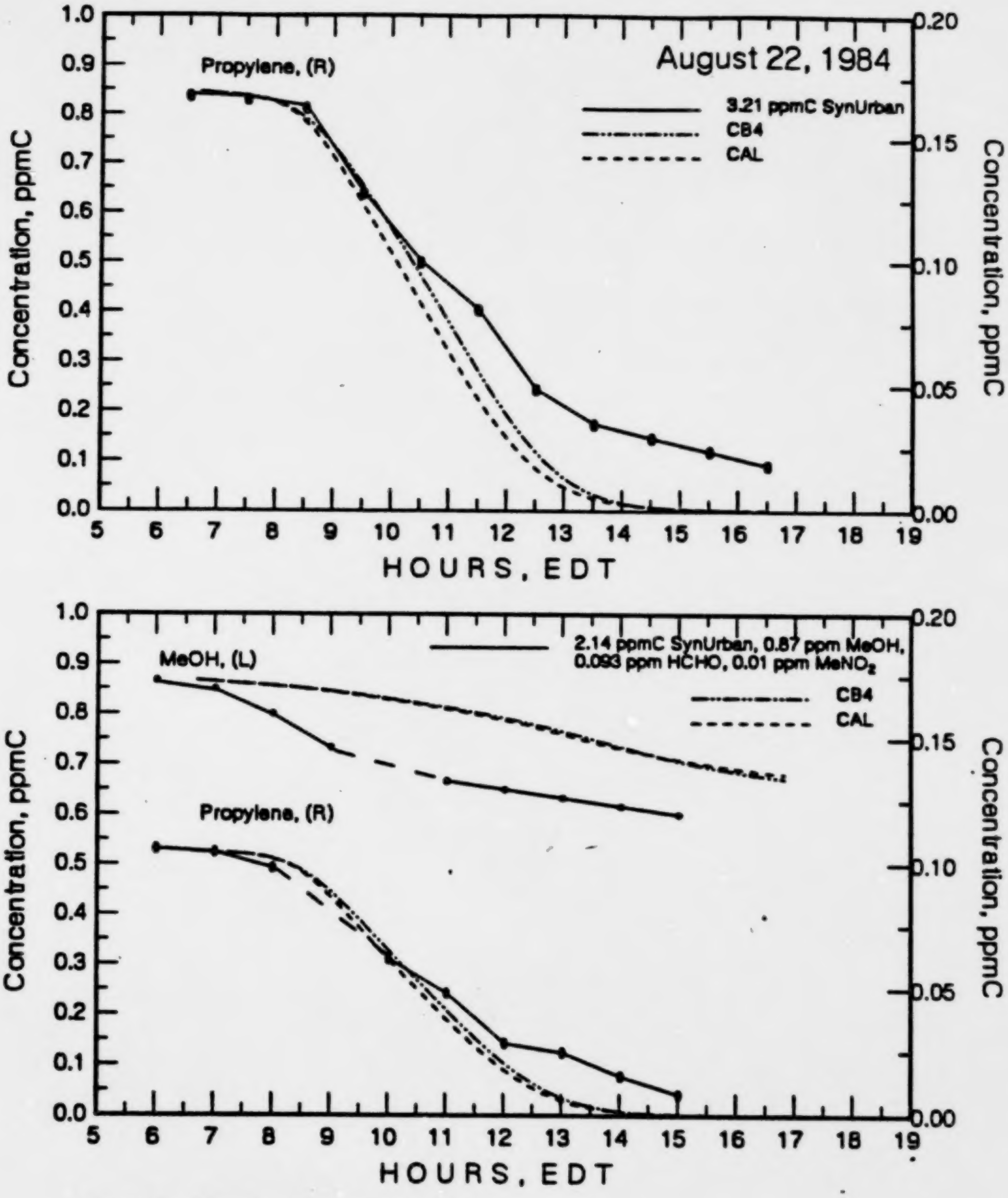

Figure 81. Standard Carter wall model.

September 1, 1984
SynUrban vs. SynUrban/SynMeth

Figure 82 to 83 show data and simulations for 1/3 substitution of SynMeth into SynUrban.

Both mechanisms are too reactive for these conditions.

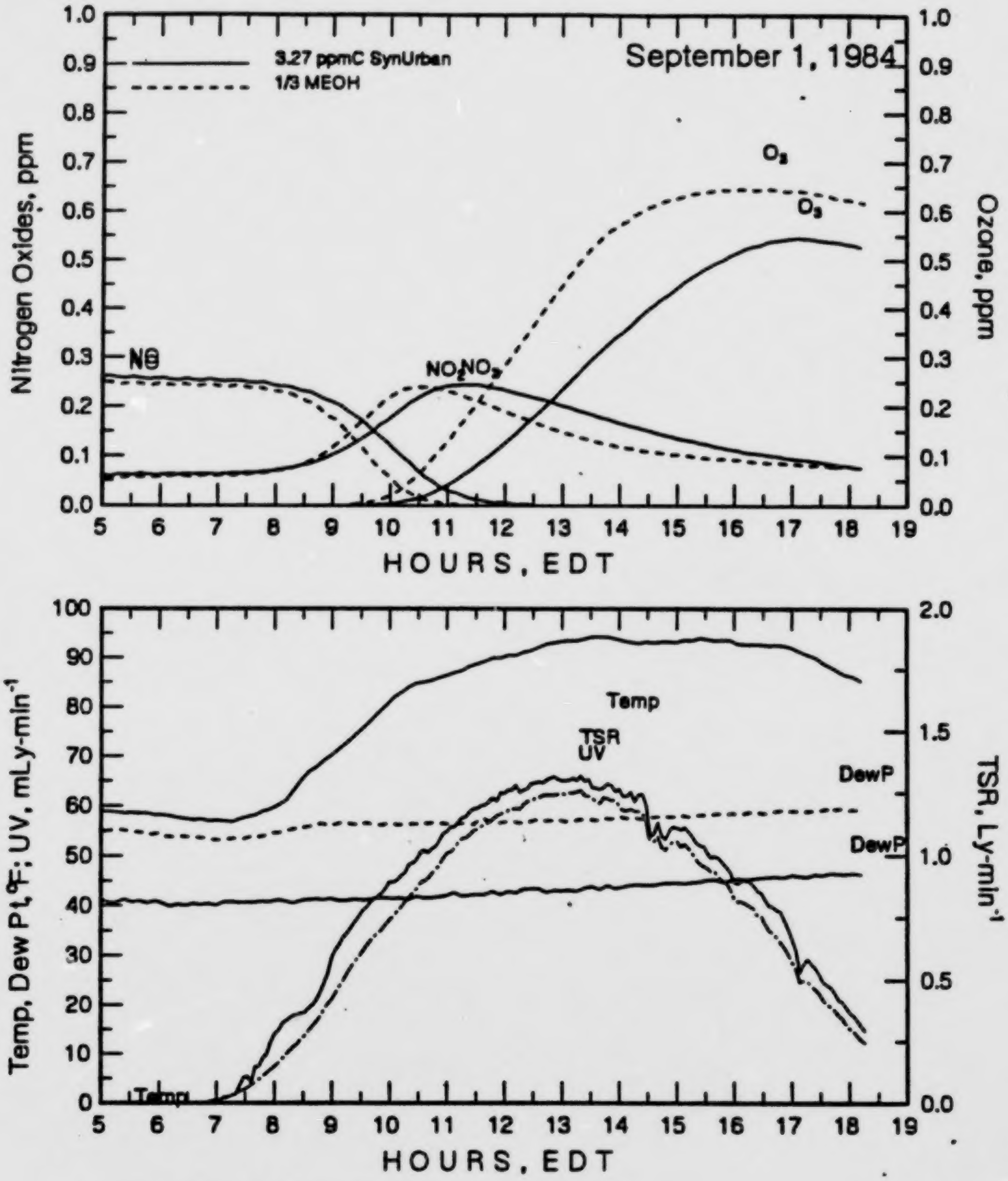

Figure 82. Delta HC experiment.

Table 38. September 1, 1984 Initial Condition Simulation File.

```
#if RED
September 1, 1984 2.68 ppmC SYNURBAN, 0.97 ppmC MeOH (RED)
#end
#if BLUE
September 1, 1984 3.26 ppmC SYNURBAN (BLUE)
#end
#if CB4
c:\pkss\mech\CB42chm.pks
CONC=
@c:\pkss\mech\CBckCB4.icx
#end
#if CAL
c:\pkss\mech\CALchm.pks
CONC=
@c:\pkss\mech\CBckCAL.icx
#end
#if RED
 NO    =  0.252,
 NO2   =  0.062,
#end
#if BLUE
 NO    =  0.243,
 NO2   =  0.059,
#end
#if RED
#if CB4
ETH   =  0.0804,
OLE   =  0.0358,
PAR   =  1.7838,
TOL   =  0.0392,
XYL   =  0.0341,
HCHO  =  0.0370,
MEOH  =  0.9660,
RCHO  =  0.0202,
#end
#if CAL
ETHE   =  0.0804,
PRPE   =  0.0358,
TBUT   =  0.0132,
ALK4   =  0.2034,
ALK7   =  0.1377,
TOLU   =  0.0392,
XYLE   =  0.0256,
TMBZ   =  0.0086,
HCHO   =  0.0037,
MEOH   =  0.9660,
#end
#end
#if BLUE
#if CB4
ETH   =  0.1080,
OLE   =  0.0509,
PAR   =  1.9587,
TOL   =  0.0590,
XYL   =  0.0495,
HCHO  =  0.0550,
RCHO  =   0.0299,
#end
 #if CAL
#end
 ETHE    =        0.1080,
PRPE    =        0.0509,
TBUT    =        0.0192,
ALK4    =        0.1427,
ALK7    =        0.1954,
TOLU    =        0.0590,
XYLE    =        0.0373,
TMBZ    =        0.0122,
HCHO    =        0.0550,
#end
  HONO  =          0.0043,
 CO    =           0.3;
@e:\segfiles\finalseg\84\st0184.lix
@e:\segfiles\finalseg\84\st0184.twd
FINISH;
```

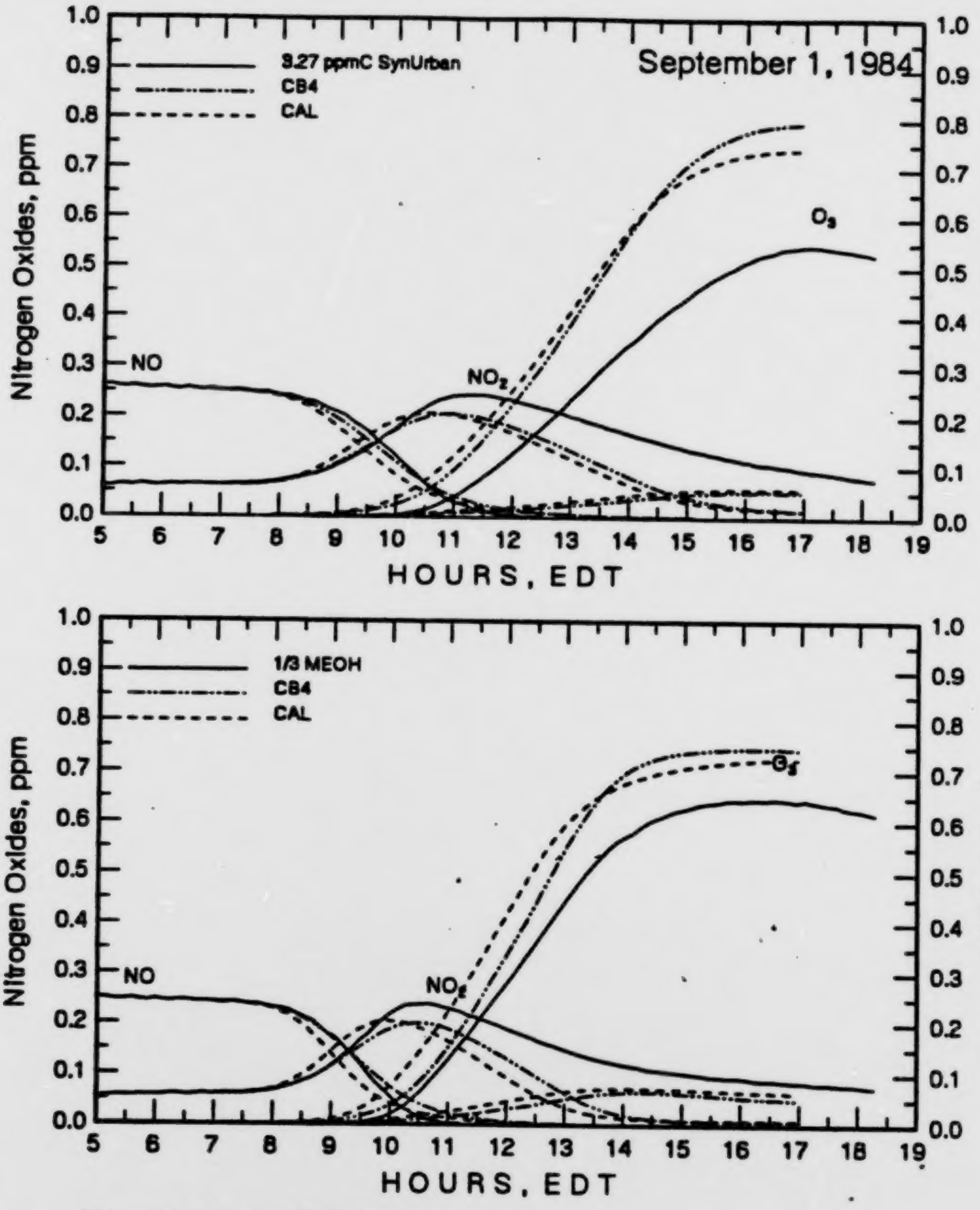

Figure 83. Standard Carter wall model.

September 2, 1984
Delta HC SynUrban

Figure 84 to 85 show data and simulations for a delta HC SynUrban at a low HC to NO_x ratio.

Both mechanisms are too reactive for these conditions.

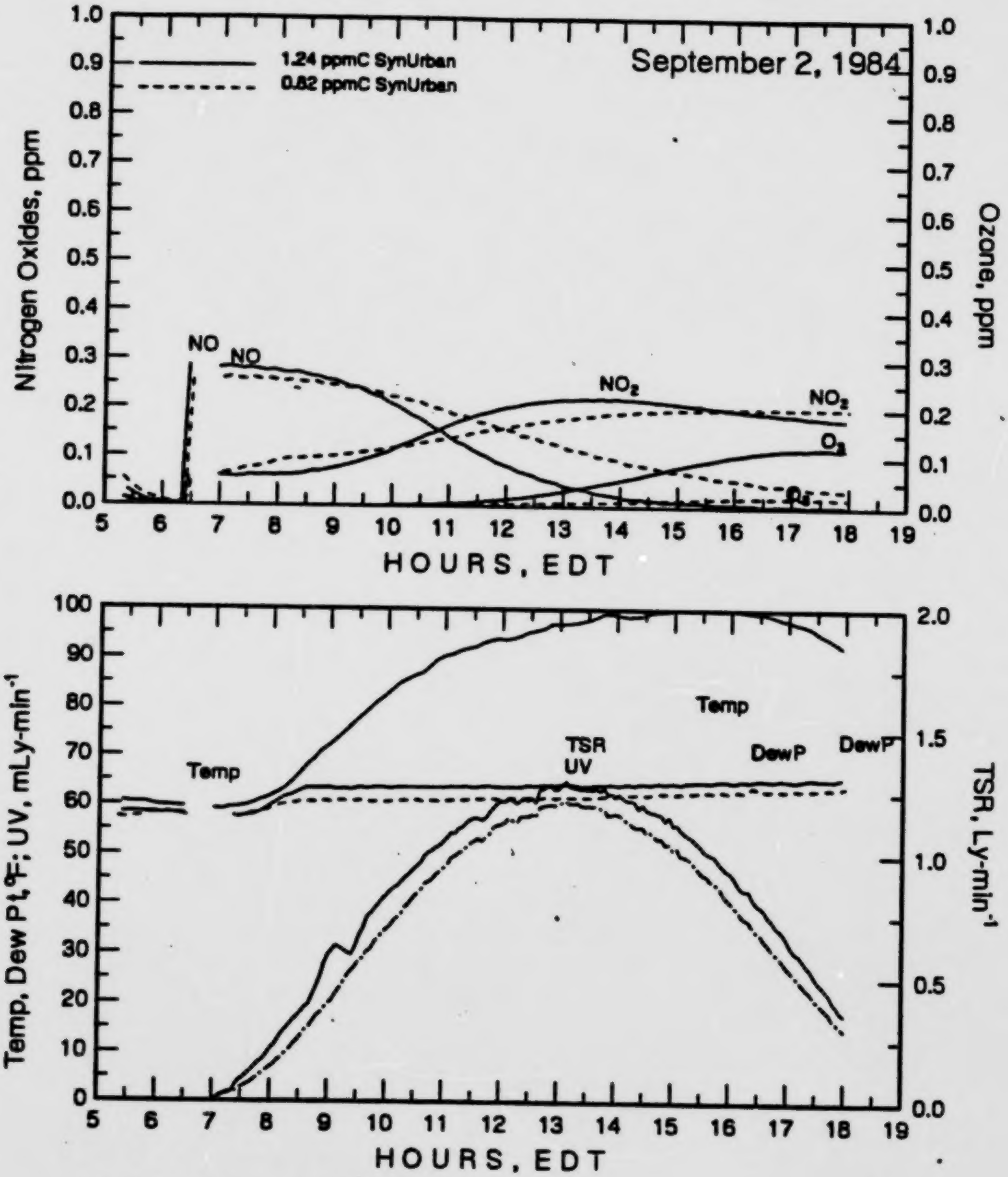

Figure 84. Delta HC experiment.

Table 39. September 2, 1984 Initial Condition Simulation File.

```
#if RED
September 2, 1984 1.24 ppmC SYNURBAN (RED)
#end
 #if BLUE
September 2, 1984 0.90 ppmC SYNURBAN (BLUE)
#end
#if CB4
c:\pkss\mech\CB42chm.pks
CONC=
@c:\pkss\mech\CBckCB4.icx
#end
#if CAL
c:\pkss\mech\CALchm.pks
CONC=
@c:\pkss\mech\CBckCAL.icx
#end

#if RED
 NO   =            0.284,
 NO2   =           0.060,
#end
#if BLUE
 NO   =            0.259,
 NO2   =           0.063,
#end
#if RED
#if CB4
ETH      =      0.0444,
OLE      =      0.0211,
PAR      =      0.7560,
TOL      =      0.0190,
XYL      =      0.0182,
HCHO     =      0.0184,
RCHO     =      0.0129,
#end
#if CAL
ETHE     =      0.0444,
PRPE     =      0.0211,
TBUT     =      0.0081,
ALK4     =      0.0519,
ALK7     =      0.0760,
TOLU     =      0.0190,
XYLE     =      0.0124,
TMBZ     =      0.0058,
HCHO     =      0.0184,
#end
#end
 #if BLUE
#if CB4
ETH      =      0.0278,
OLE      =      0.0144,
PAR      =      0.5816,
TOL      =      0.0129,
XYL      =      0.0119,
HCHO     =      0.0121,
RCHO     =      0.0085,
#end
 #if CAL
ETHE    =       0.0278,
PRPE    =       0.0144,
TBUT    =       0.0054,
ALK4    =       0.0539,
ALK7    =       0.0504,
TOLU    =       0.0129,
XYLE    =       0.0082,
TMBZ    =       0.0038,
HCHO    =       0.0121,
#end
#end
 HONO  =         0.0042,
 CO    =         0.3;
@e:\segfiles\finalseg\84\st0284.lix
@e:\segfiles\finalseg\84\st0284.tud
FINISH;
```

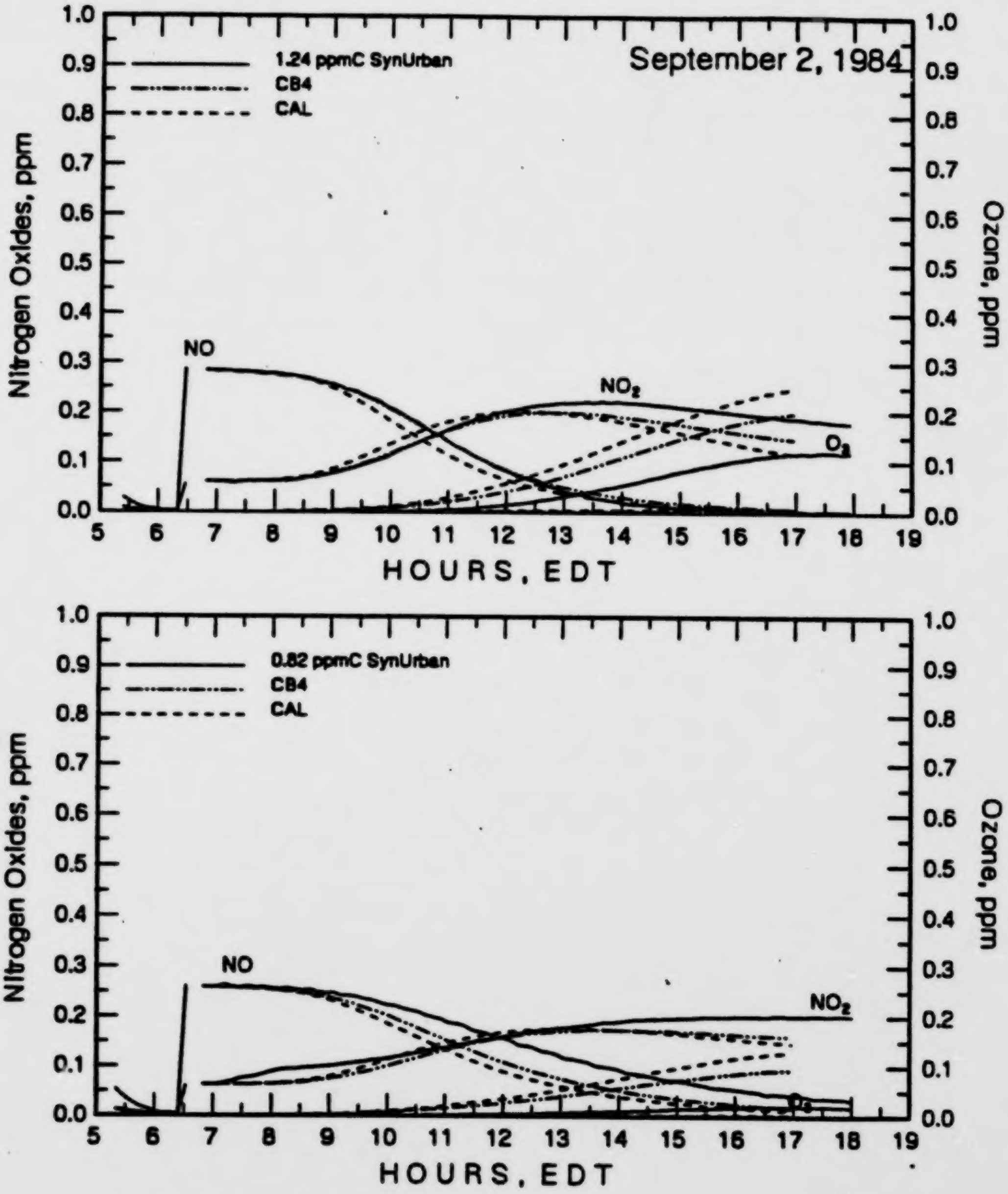

Figure 85. Standard Carter wall model.

Summary

1. Both mechanisms show excellent agreement with experimental data for HCHO-NO_x systems. This fit is only slightly effected by a choice of a wall radical model.
2. While the standard Carter wall model give the best overall fit to data, it is clear that specific experiments have additional morning wall-related processes associated with evaporation of water off the chamber walls. The magnitude of this morning radical process, when needed, is about 2/3 of the total radical input by the standard Carter wall model, but the input occurs in about 30 minutes instead of 10 hours. On the other hand, the simulations of fall experiments using the standard Carter wall model tended to be slightly fast, and in some case, even using no wall radical model still resulted in too reactive a simulation.
3. In ethylene experiments, both models show good fits to NO, NO_x, O_3, and ethylene decay profiles, if the standard Carter wall model is used. The models still under predict HCHO as a product, as well as under predicting CO as a product.
4. CB4 and CAL have the same $HO^{\cdot}$+ETH and O_3+ETH chemistry, but differ in the predictions of O_3 and ethylene loss at the end of ethylene simulations; CB4 agrees better with the data. This difference is due to differences in radical termination treatment between the two mechanisms.
5. CB4 and CAL have different lumped $HO^{\cdot}$+propylene and O_3+propylene chemistries. When CB4 and CAL agree well with the ethylene side of an experiment, CB4 tends to be too reactive for the propylene side of a dual experiment and CAL tends to be a little too un-reactive, but closer to the data. Both fail to predict the measured HCHO , and both tend to under predict the CO.
6. For a cool, and dry, ethylene-propylene experiment, the standard Carter wall radical model is much too reactive. The models were also too reactive for NOwall model, however. The prediction of ozone for propylene was good, again with CB4 being high and CAL being low. On the ethylene side, however, both models were too fast, but the rise rate for ozone was excellent. CAL 's ozone maximum prediction was perfect, and CB4 's was too high. Based on the fit for other days, however, this means that CAL was also too reactive for this cool condition. HCHO was much better predicted in the ethylene side, but both acetaldehyde and formaldehyde were under predicted almost by a factor of two. PANwas over predicted by CB4 and reasonably predicted by CAL .

7. Neither mechanism does well for 1-butene in cool conditions, being much too reactive in producing ozone. At the same time, however, CAL produces an excellent fit to t-2-butene on the other side of the chamber. CB4 's surrogate of two ALD2s shows too little reactivity throughout the simulation, but does begin to converge towards the correct ozone near the end of the experiment. When used in mixtures, this behavior of very reactive olefins in the two mechanisms would probably tend to make CB4 slow to start, but, because more ALD2 would be available later to result in an increase reactivity near the end.
8. CB4 is better than CAL in simulating toluene; CAL is better than CB4 in simulating xylene. In contrast to the olefin situtation, both mechanisms over predict HCHO by nearly a factor of two or three (these HCHO yields have recently been confirmed by new measurements with a new HCHO instrument in toluene and xylene experiments). Both mechanisms predict PAN fairly well in xylene, but both over predict PAN in toluene, CAL predicting nearly twice as much PAN as CB4. Both models over estimate the reactivity of o-xylene compared to m-xylene and both under predict the CO produced in these systems.
9. In a HC mixture with no aromatics, both mechanisms demonstrated excellent fits to NO, NO_2, and O_3, as well as to propylene, ethylene, n-pentane, n-butane decays. HCHO was under-predicted, however (and in the case of UNCMIX, by 50
10. In the cases of SynAuto HC mixture, both mechanisms demonstrated excellent fits to NO, NO_2, and O_3, and to propylene, ethylene, toluene decays. HCHO predictions tend to be much closer suggesting a compensation between the over production in the aromatics chemistry and an under production in the olefin chemistry. At the higher SynAuto concentrations, CB4 demonstrated a better fit to the ozone peak than did CAL . Both models also reproduced the relative effects of 1/3 methanol substitution into the SynAuto mixture quite well.
11. Both mechanisms were uniformily too reactive in making ozone for the SynUrban hydrocarbon mixture experiments, even though the propylene, ethylene, and toluene decays were well fitted. HCHO was also better fitted in these experiments. Both mechanisms were also too reactive to the 1/3 methanol substitution in SynUrban mixtures.

5

EKMA Comparisons

A Detailed Example EKMA Simulation

For an example comparing the two mechanisms in a control calculation scenario, we used a set of conditions similar to an actual SIP case in the Philadelphia area.[30] These included the following:

Initial Conditions

Item	Value	Units
Latitude	39.93	degrees
Longitude	75.10	degrees
Date	6/24/80	mm/dd/yy
Initial Mixing Ht.	250	meter
Final Mixing Ht.	1235	meter
Initial NMOC	1.100	ppmC
Initial NO_x	0.120	ppm
Initial CO	1.000	ppm
Surface NMOC	0.038	ppmC
Surface O_3	0.010	ppm
Aloft NMOC	0.040	ppmC
Aloft O_3	0.070	ppm
Aloft CO	0.500	ppm
Temperature	303	K
Water Vapor	25000	ppm
Basecase O_3	0.171	ppm
Basecase HC-to-NO_x	9.5	ppmC/ppm
Future NO_x	10.5	percent higher

Emissions Fractions

Hour	1	2	3	4	5	6	7	8
NMOC	0.17	0.17	0.17	0.10	0.02	0.02	0.02	0.02
NO_x	0.35	0.35	0.35	0.19	0.03	0.03	0.03	0.07

Hydrocarbon Composition

Species	PAR	ETH	OLE	TOL	XYL	HCHO	RCHO	NR
CB4	0.564	0.037	0.035	0.089	0.117	0.021	0.052	0.084
Species	ALK4	ALK7	ETH	PREP	TBUT	TOL		
CAL	0.214	0.280	0.037	0.048	0.029	0.080		
Species			XYL	TMB	HCHO	ALD	RCHO	NR
CAL			0.079	0.042	0.02	0.037	0.000	0.141

A simple trajectory calculation is shown in Figure 86. As can be seen in Figure 86b, c, and d, the two mechanisms classify compounds slightly differently, and therefore toluene is used as a surrogate for different compounds in the two mechanisms resulting in a difference in initial concentrations. Likewise, CB4 uses ALD as a surrogate for internal olefins while CAL has TBUT, so, again the two simulations differ in initial ALD. The slightly higher initial reactivity of CAL, is probably due to the differences in the initial reactivity of the TBUT verses ALD as was shown in the September 27, 1983 experiment in Chapter 4. This resulted in CAL's NO-to-NO_2 conversion being slightly greater than CB4's initially. This produced slightly more O_3 in the first 400 minutes of the simulation. This larger reactivity also lead to more HNO_3 earlier because there was more $HO^{\cdot}$. In the last 200 minutes, however, CB4's O_3 reactivity increased, probably because of the higher HCHO and ALD and CB4's O_3 exceeded that of CAL in the last 150 minutes.

Figure 87 shows a three-dimensional representation of the ozone surfaces for both mechanisms, and shows a surface for their difference. Ozone isopleths for both mechanisms are ploted in the bottom of Figure 88; the top shows CB4 O_3 minus CAL O_3 isopleths. The CAL mechanism is more reactive at higher ($> 10:1$) HC-to-NO_x ratios and is slightly more reactive at lower ($\approx 5:1$) HC-to-NO_x ratios than is CB4The maximum positive difference (CB4 being higher) occurred at near the basecase HC-to-NO_x ratio of 9.5:1 for this calculation.

The solid heavy lines on the difference surface and isopleths indicate the pathway traversed by the OZIPM4 program in the EKMA procedure to find the needed hydrocarbon control. The program starts at a point where NMHC = 1.00 and uses

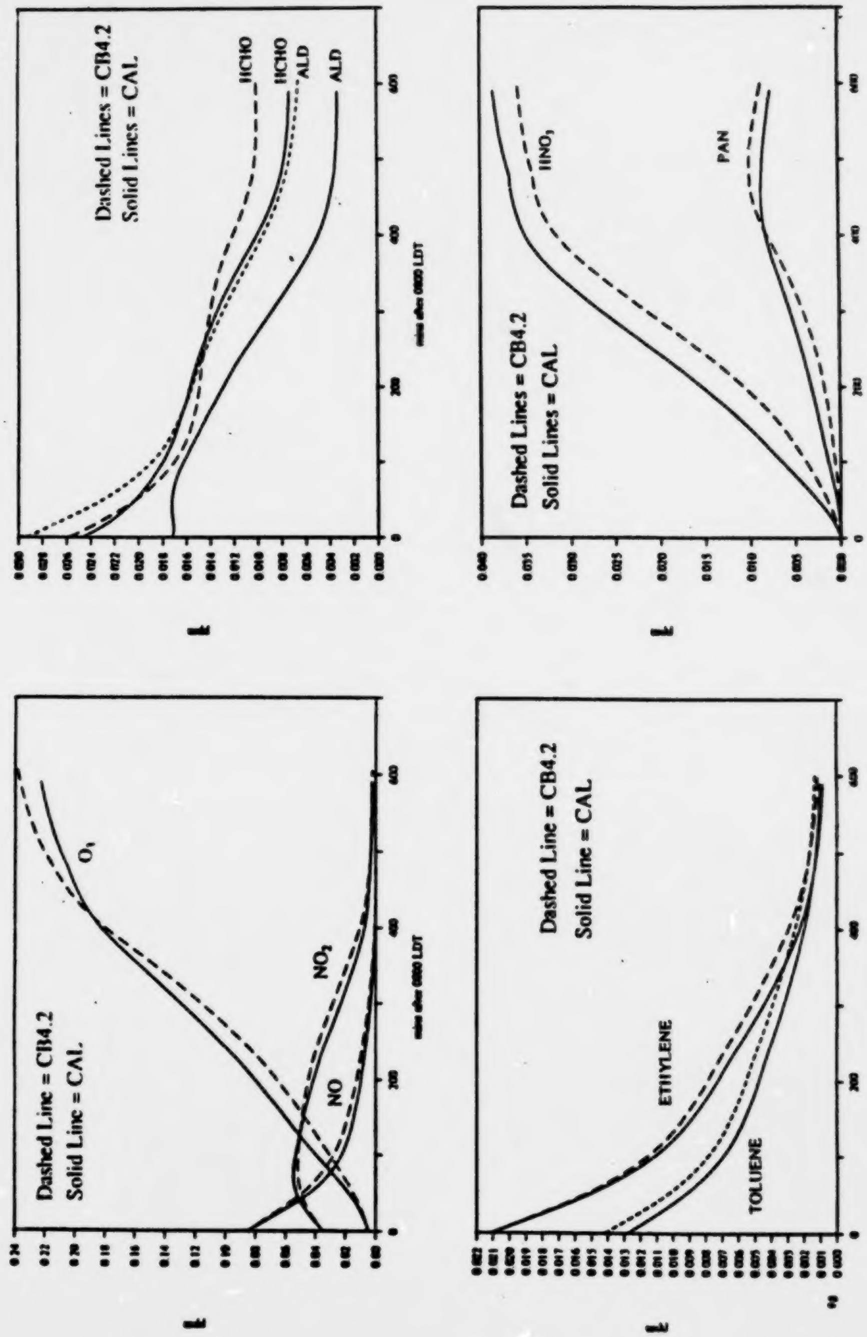

Figure 86. Base Case Philadelphia SIP Trajectory Calculation.

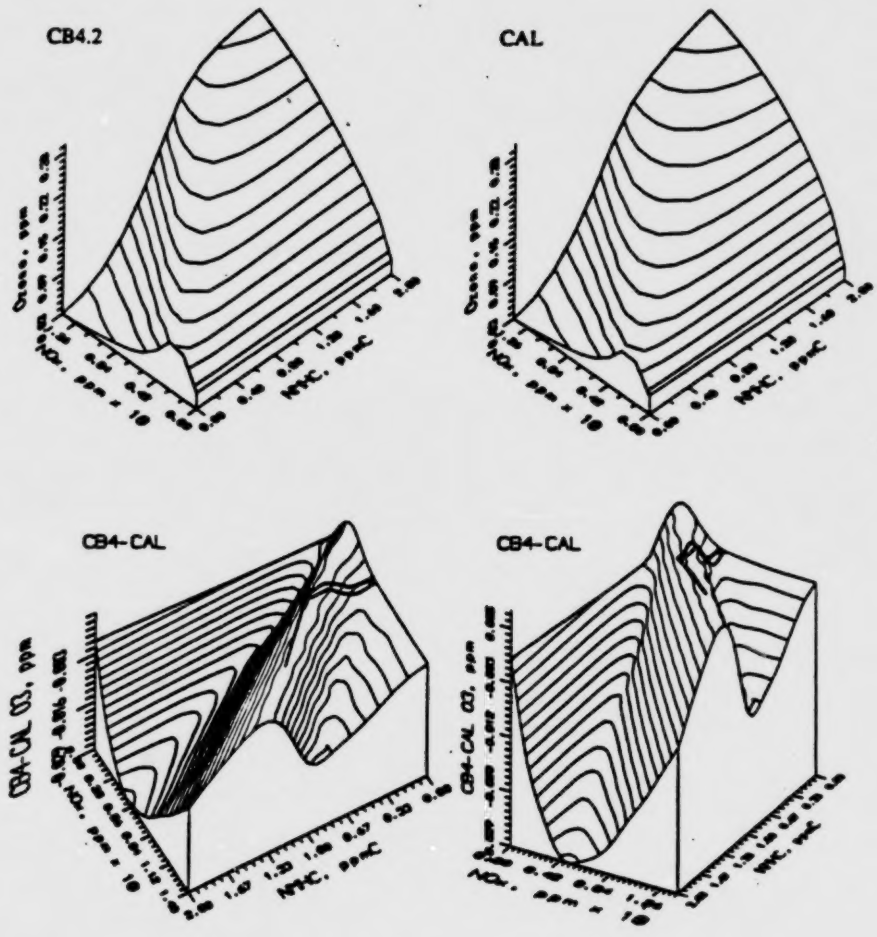

Figure 87. CB4 and CAL Ozone Surfaces (Top) and Two Views of Their Difference Surface (Bottom).

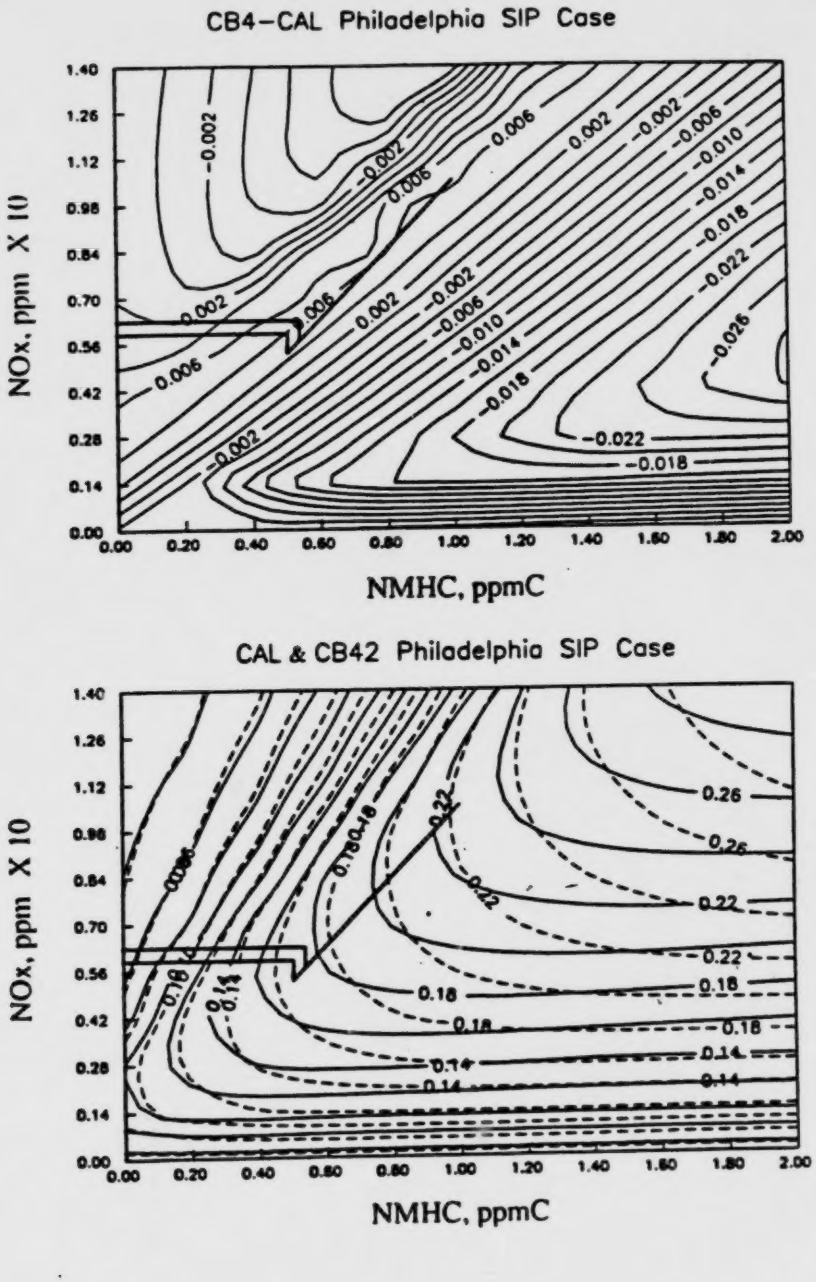

Figure 88. CB4 and CAL Isopleths (bottom) and CB4- CAL (top).

the HC-to-NO_x ratio to find the starting NO_x; it then moves along the HC-to-NO_x ratio line seeking the NMHC that will produce the basecase O_3 of 0.171. In this case, both NMHC and NO_x had to be reduced to find O_3=0.171. This occurred at two slightly different levels in the two mechanisms. Then the NO_x is increased by 10.5% and the NMHC is further reduced until 0.12 ppm O_3 is reached. The percent difference in NMHC between where the NO_x was increased and where O_3 is 0.12 ppm is the control requirement.

Ozone along this heavy solid line for both mechanisms is shown in Figure 89 for three NMHC compositions: the middle line is for the all-city average composition as given in the table above. For this case, the two mechanisms give control requirements that agree within 3.5% reduction. The Cluster 1 composition was for the group of cities with the highest aromatic fraction (27%) and lowest alkane fraction (50%), and the Cluster (3,6) composition was for the group of cities with the lowest aromatic (13%) and highest alkane fraction (60%). The effect of this range in NMHC reactivity is a difference of about 10% in needed reduction.

Two other baseline cases at the all-cities HC composition were simulated: (1) a 25:1 HC-to-NO_x ratio with a baseline O_3 of 0.26 ppm, which placed the EKMA starting point at the biggest difference between the two mechanisms; and (2) a 6.25:1 HC-to-NO_x ratio with a baseline O_3 of 0.14 ppm, which placed the EKMA starting point at the other negative difference between the two mechanisms. The calculated control requirements were:

HC-to-NO_x	CB4	CAL	Diff.
6.5	17.8%	13.1%	4.7%
9.5	48.7%	45.5%	3.5%
25	84.5%	84.5%	0.0%

At least for this typical SIP case, hydrocarbon composition had a larger effect on calculated control requirements than did the choice of which chemical mechanisms to use.

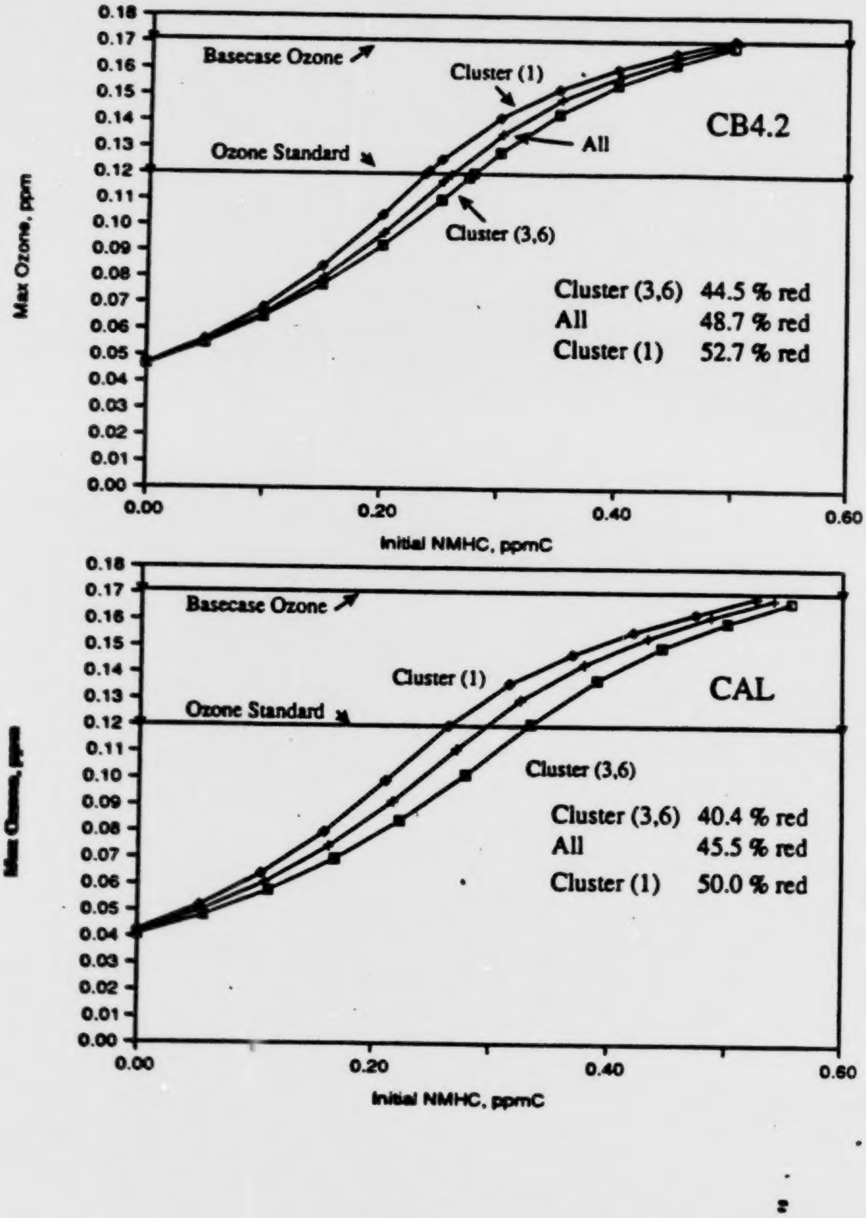

Figure 89. Ozone As A Function Of HC For CB4 and CAL For Three HC Compositions.

SIP Simulations using CB4 and CAL mechanisms

This section presents the results of our comparison of the CB4 and CAL mechanism for several selected real SIP conditions and for variations (or sensitivity tests) on a single SIP case. These are presented as a series of tables, bar graphs, and isopleths.

The CB4 mechanism used was the version SAI included in the OZIPM4 program as of 6-Jan-1988 and is identified internal to the OZIPM4 code as version 4.3 (but is really CBM4.2). The CAL mechanism used was the mechanism listed in March 1987 final report,[7] Table 3.2 "SAPRC/ERT Ozipm Chemical Mechanism," with two exceptions. These exceptions were:

- the rate constant for the second reaction was reduced by a factor of 10 because it was incorrectly listed in the table; and
- a pseudo-reaction of OH and methane was added because independent sensitivity analysis by both Dodge and Jeffries showed that it affected the control calculations by contributing reactivity for the reduced future NMOC conditions.

Because of its large background concentration and the unspecified magnitude of the urban source, the methane concentration was treated as constant at 1.85 ppm resulting in a reaction rate constant of $6.52 \times 10^3 \exp(-1710/T)$ min^{-1} or (21.0 min^{-1} at 298 K).

The photolysis rates used for CB4 were the ones build into the OZIPM4 computer code. These were described in detail in Jeffries *et al.*[31] The photolysis rates used for the CAL mechanism were based upon the absolute values computed by Lurmann,[7] but were scaled to the higher NO_2 photolysis rates built into OZIPM4. This is essentially the way Lurmann computed the rates he used in the adapation report.[7] It should be noted that the kinetics data base for the values used in the OZIPM program and the values recommended by Lurmann for CAL are very similar. Neither of these sets of rates, however, are up to date, and, in some cases are quite different than the absorption cross sections and quantum yields used in computing the new in-chamber photolytic rates which were used in Chapter 4.

The emissions fractions used for CB4 were those included in the OZIPM4 program. These were based upon the work described in Volumn 2 of this report. As described in that volume, "HC-splits" were derived from analysis of 46 city-years of detailed gas chromatographic HC data. The emissions fractions used for CAL were also described in Volume 2.

The implementation of both mechanisms and of OZIPM4 was verified by exchanging input and output files with Dr. Marcia Dodge and independently reproducing each other's results for several sets of conditions.

The SIP Conditions

The OZIPM input conditions were supplied by Micheal Gery, SAI, from previous SIP cases that SAI had collected for several projects. In his study of the effects of increased UV-B on urban ozone, Gery started with 57 initial basecase conditions in 10 cities; the conditions were described in the final report for that project.[32] Gery selected 15 of these cases for detailed study. He supplied us 14 OZIPM inputs for seven cities, and these are identified here in Table 40. The important input conditions are described in Tables 40 to 42. The cases cover a range of basecase ozone, HC-to-NO_x ratios, emission profiles, light intensities, final mixing heights, aloft ozone, temperature profiles, and show some variation in initial mixing height and aloft NMOC.

SIP Simulation Results

The last three columns of Table 42 give the calculated control requirements (these are shown in Figure 91) and the difference for the two mechanisms. Note that the calculated control requirements varied from 2.8% to 57.2% depending upon the city and case. Over this range of control requirements, the two mechanisms differed by at most 7% control required (*e.g.*, 29.3% vs. 22.7%) and sometimes CB4 predicted more control required and sometimes CAL predicted more. We are not able to discern any pattern as to when one will predict higher than the other. While Dodge[33] has suggested that temperature is responsible for the differences, we will show in the next section that although there may well be a temperature effect, the direct correlation between temperature and control differences may be spurious and other equally valid relations can be shown (*e.g.*, cases 3,1, and 12 verses cases 10, 9, 13, 5, 11, 6). Similarly, at first inspection it might appear that CB4 predicts less control than CAL when the basecase ozone is higher than in cases where the CB4 predicts more control, but cases 10,11,12 suggest that this is not always true: in case 12, with an intermediate basecase ozone, CB4 predicted more control, whereas CAL predicted slightly more control at both higher and lower basecase ozone. The relationship between the two mechanisms is not even the same within a given city: see cases 3 and 4.

The maximum differences between the predicted control requirements for the two mechanisms, however, appear to be bounded by approximately 1/5 of the control required (*e.g.*, predicted controls of 18% and 22% or a difference of 4% in about

Table 40. SIP Cases: Basic Meterological Input Conditions

Comparison of CAL and CB4 for Selected SIP Conditions

Case	*Date*	*Place*	*Site*	*Lat.*	*Long.*	*Tz*	*MHo*	*MHf*	*Tf*
1	1-Aug-80	Nashville	Health Center	36.2	86.81	5	250	1845.0	1500
2	1-Aug-80	Nashville	Hendersonville	36.2	86.81	5	250	1845.0	1500
3	6-Aug-82	Tulsa	Site 137	36.1	96.00	5	250	1953.7	1800
4	1-Jul-81	Tulsa	Site 127	36.1	96.00	5	250	1671.1	1800
5	7-Aug-80	Puget	Sumner	47.6	122.34	7	250	579.2	1800
6	11-Aug-81	Puget	Sammanish	47.6	122.34	7	250	769.1	1800
7	7-Aug-80	Washington DC	Tokoma	38.9	77.05	5	420	1714.3	1800
8	7-Aug-80	Washington DC	Tokoma	38.9	77.05	5	420	1714.3	1800
9	21-Jul-80	Washington DC	Tokoma	38.9	77.05	5	160	2217.4	1800
10	31-Aug-84	Phoenix		33.5	112.07	7	250	3300.0	1800
11	14-Sep-84	Phoenix		33.5	112.07	7	250	2400.0	1800
12	5-Jul-84	Phoenix		33.5	112.07	7	250	2400.0	1800
13	13-Jul-79	Philadelphia		39.9	79.15	4	250	1017.8	1800
14	24-Jun-80	New York	Middletown	40.7	74.10	4	300	1700.0	1800

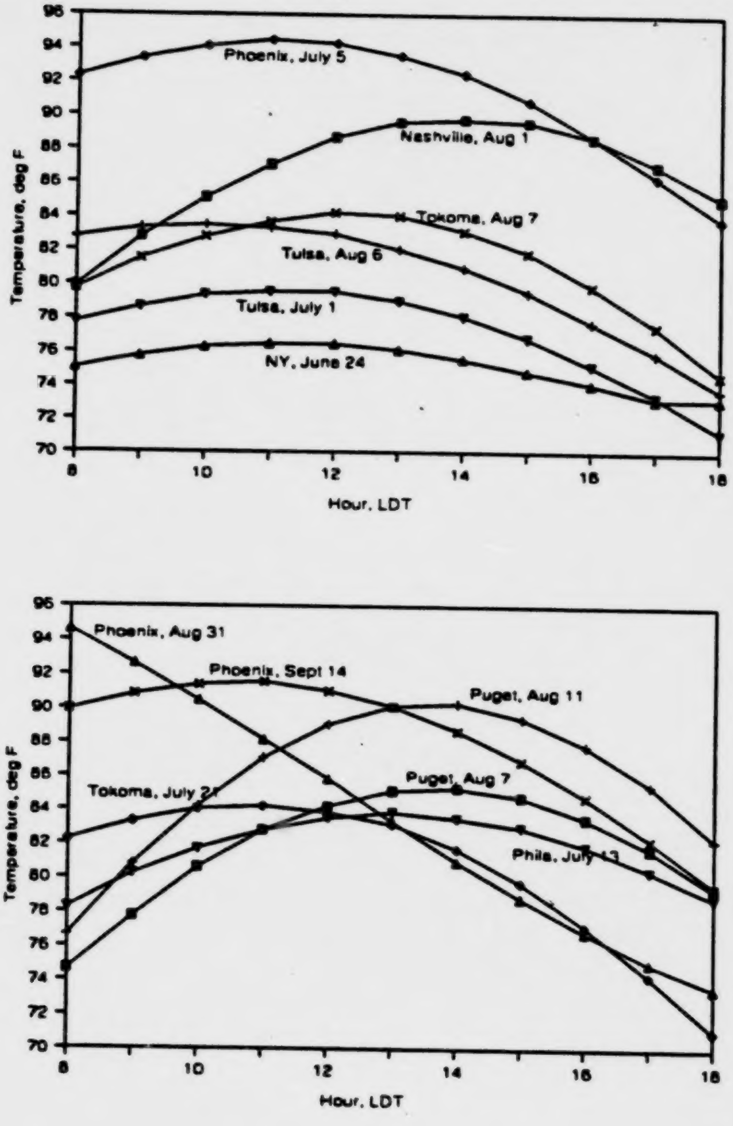

Figure 90. SIP Cases: Surface Temperature Profiles

Table 41. SIP Cases: Basic Chemical Input Conditions

Case	Date	Place	Ozone		NMOC		CO		VOC emiss		NOx emiss	
			Surf	Aloft	Surf	Aloft	Surf	Aloft	Init	Final	Init	Final
1	1-Aug-80	Nashville	0.010	0.013	0.038	0.090	1.20	0.50	0.016	0.016	0.017	0.017
2	1-Aug-80	Nashville	0.010	0.013	0.038	0.090	1.20	0.50	0.054	0.048	0.052	0.052
3	6-Aug-82	Tulsa	0.000	0.051	0.038	0.040	1.20	0.50	0.020	0.008	0.039	0.001
4	1-Jul-81	Tulsa	0.000	0.046	0.038	0.040	1.20	0.50	0.019	0.019	0.033	0.033
5	7-Aug-80	Puget	0.000	0.000	0.038	0.040	1.20	0.50	0.045	0.090	0.045	0.090
6	11-Aug-81	Puget	0.000	0.000	0.038	0.040	1.20	0.50	0.124	0.101	0.124	0.101
7	7-Aug-80	Wash. DC	0.000	0.056	0.038	0.040	1.20	0.50	0.095	0.095	0.168	0.168
8	7-Aug-80	Wash. DC	0.000	0.056	0.038	0.040	1.20	0.50	0.095	0.095	0.168	0.168
9	21-Jul-80	Wash. DC	0.000	0.065	0.038	0.040	1.20	0.50	0.200	0.200	0.400	0.400
10	31-Aug-84	Phoenix	0.000	0.062	0.038	0.040	1.20	0.50	0.129	0.183	0.178	0.194
11	14-Sep-84	Phoenix	0.000	0.040	0.038	0.040	1.20	0.50	0.093	0.105	0.238	0.144
12	5-Jul-84	Phoenix	0.000	0.025	0.038	0.040	1.20	0.50	0.173	0.154	0.361	0.254
13	13-Jul-79	Philadelphia	0.004	0.105	0.038	0.040	1.20	0.50	0.120	0.120	0.160	0.160
14	24-Jun-80	New York	0.004	0.102	0.038	0.040	1.20	0.50	0.185	0.020	0.680	0.073

Table 42. SIP Cases: Control Predicted

Case	Date	Place	Ozone Base	VOC/NOx	%NOx change	CB4 Control	CAL Control	Diff
1	1-Aug-80	Nashville	0.130	4.73	5.3	21.6	16.7	4.9
2	1-Aug-80	Nashville	0.130	4.61	5.3	19.3	13.6	5.7
3	6-Aug-82	Tulsa	0.128	8.50	1.6	29.3	22.7	6.6
4	1-Jul-81	Tulsa	0.148	8.50	0.0	41.1	44.6	-3.5
5	7-Aug-80	Puget	0.130	5.23	0.0	2.8	3.7	-0.9
6	11-Aug-81	Puget	0.150	9.50	0.0	35.8	35.3	0.5
7	7-Aug-80	Wash. DC	0.180	8.00	0.0	18.0	22.3	-4.3
8	7-Aug-80	Wash. DC	0.180	8.00	10.0	17.0	20.7	-3.7
9	21-Jul-80	Wash. DC	0.140	10.25	0.0	30.0	30.8	-0.8
10	31-Aug-84	Phoenix	0.130	10.67	0.0	14.4	14.8	-0.4
11	14-Sep-84	Phoenix	0.160	13.77	0.0	42.8	43.1	-0.3
12	5-Jul-84	Phoenix	0.148	15.27	0.0	40.4	36.5	3.9
13	13-Jul-79	Philadelphia	0.183	6.90	10.5	57.2	57.1	0.1
14	24-Jun-80	New York	0.234	9.50	0.0	33.6	38.7	-5.1

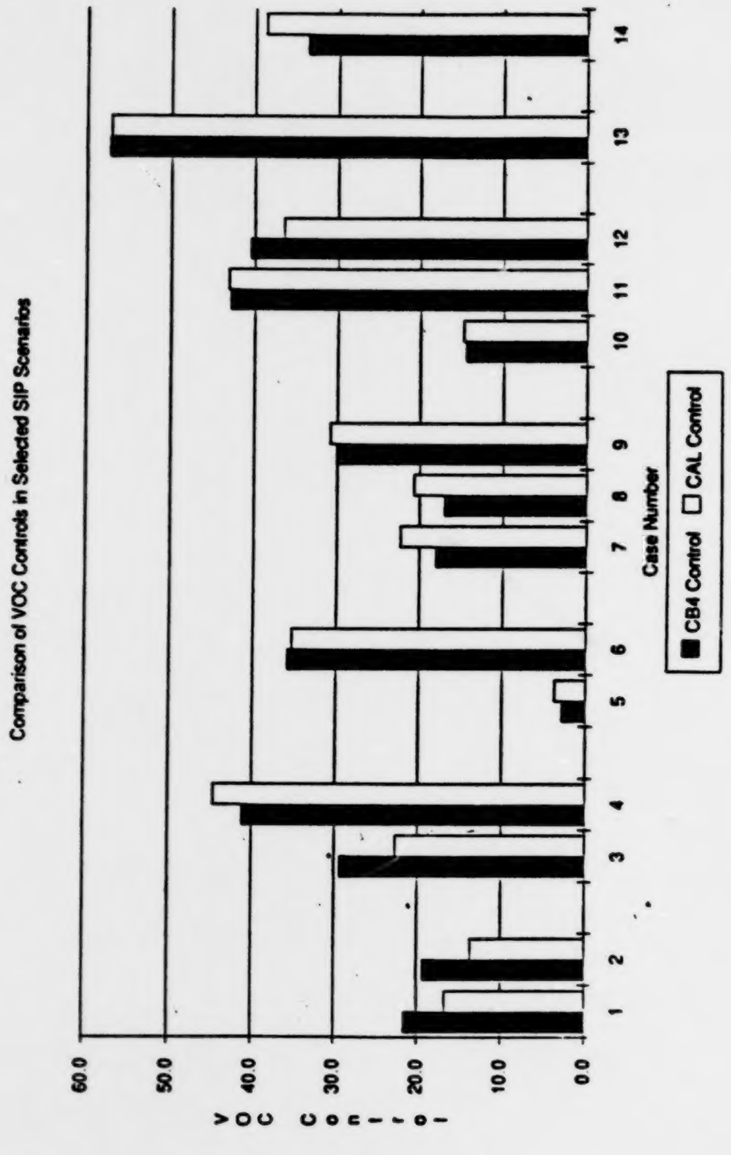

Figure 91. Comparison of VOC Controls in Selected SIP Scenarios

20% or 1/5). To gain insight into the differences, isoploths were produced for O_3, NO_x, PAN, and HCHO for the four days with the largest differences: two negative and two positive. These are shown in Figures 92 to 95. One pattern that emerges here is that the two positive differences occurred in those cases in which the O_3 isopleth lines crossed, while the negative differences occurred for O_3 isopleths that did not cross. In all four cases the NO, NO_2, and HCHO isopleths are very similar. Only the PAN isopleths show major difference between the two mechanism's predictions. Chamber simulations showed that the two mechanisms had very different PAN predictions from aromatic compounds. This coupled with the difference in the temperature treatment of PAN formation may be a factor in the predicted control calculation differences.

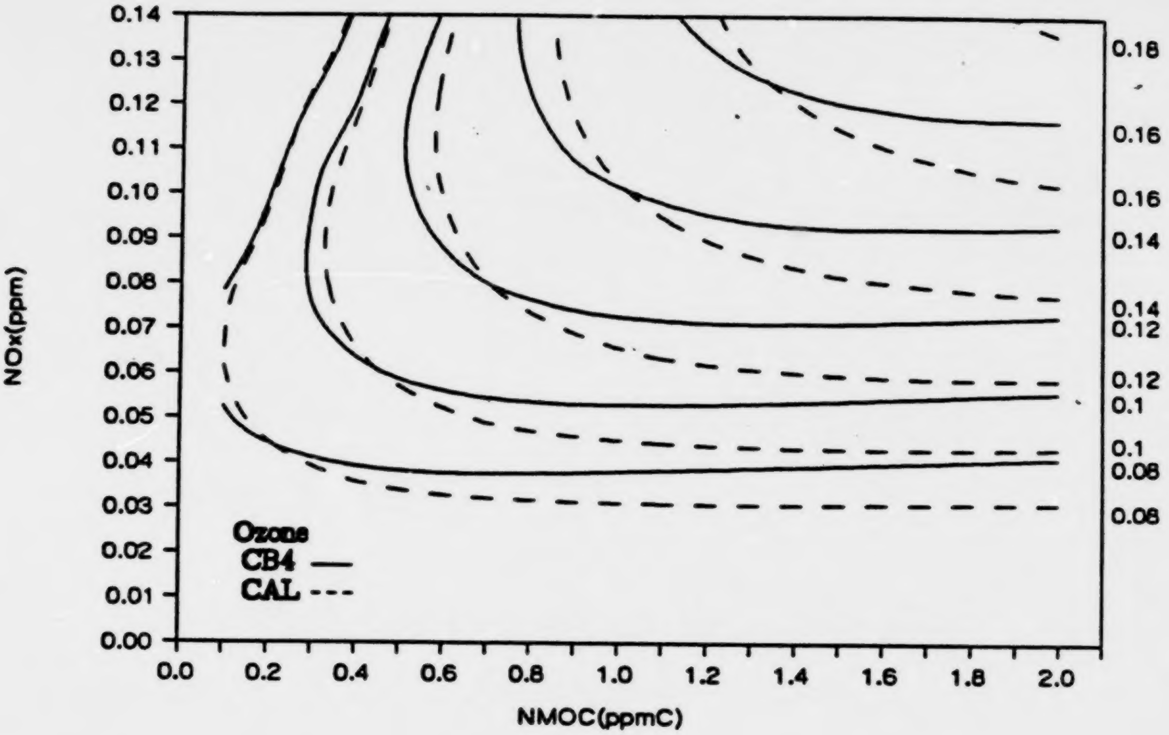

Figure 92a. Ozone Isopleth for Nashville.

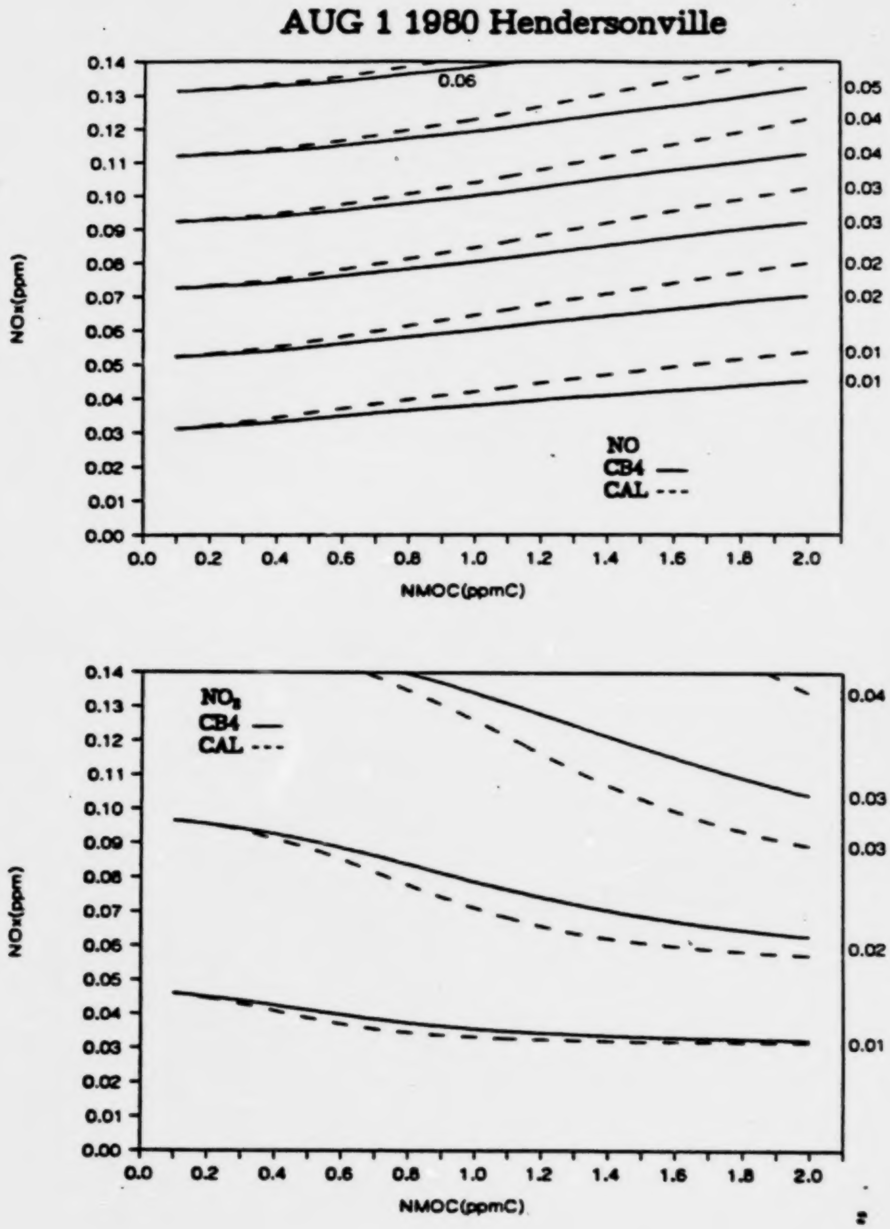

Figure 92b. NOx Isopleth for Nashville.

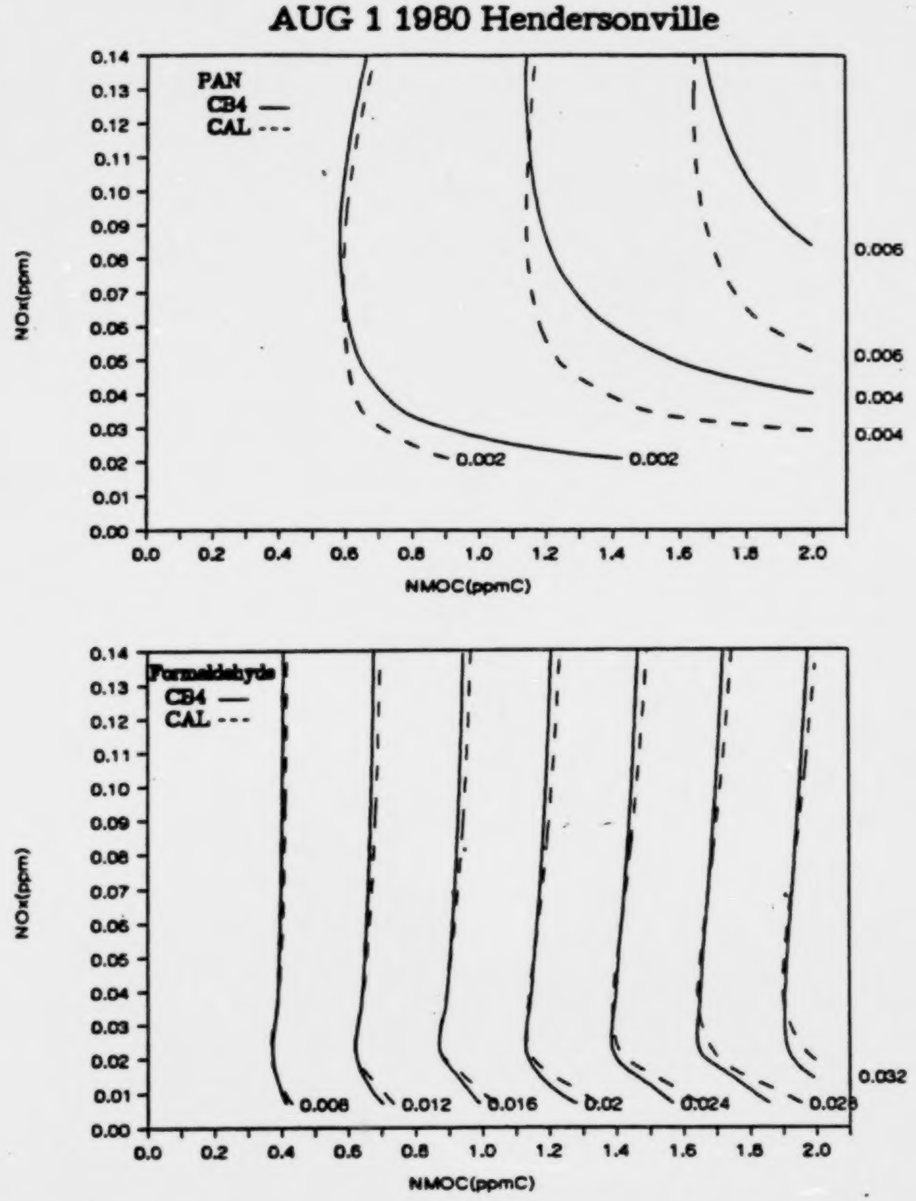

Figure 92c. PAN and HCHO Isopleth for Nashville.

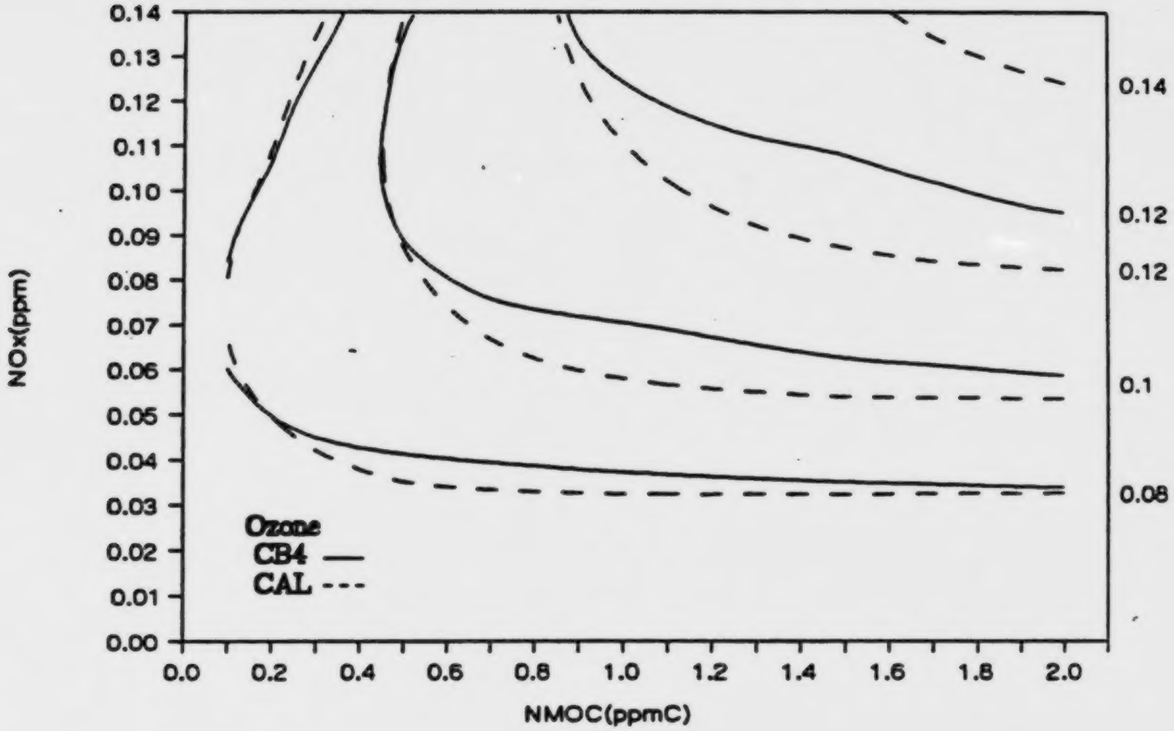

Figure 93a. Ozone Isopleth for Tulsa.

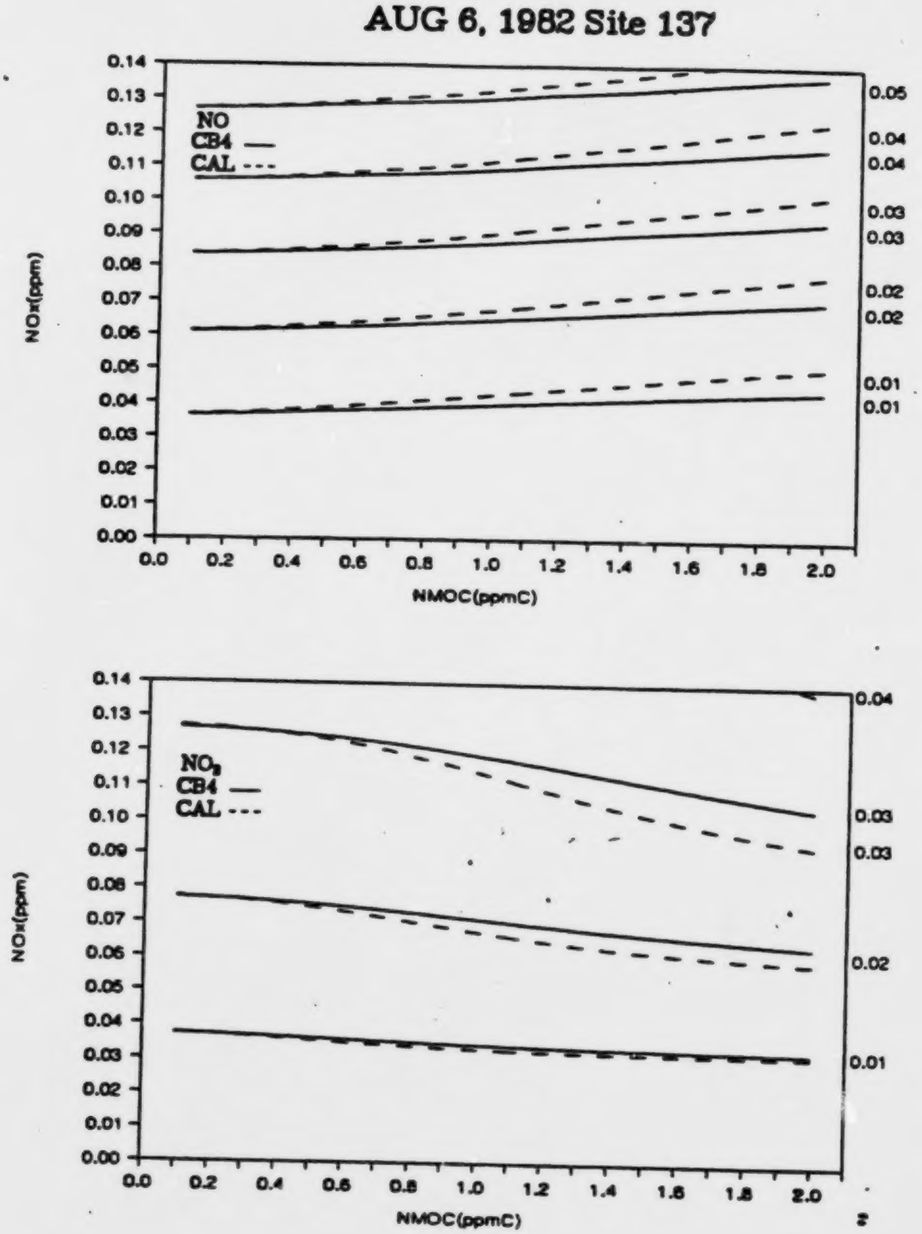

Figure 93b. NO_x Isopleth for Tulsa.

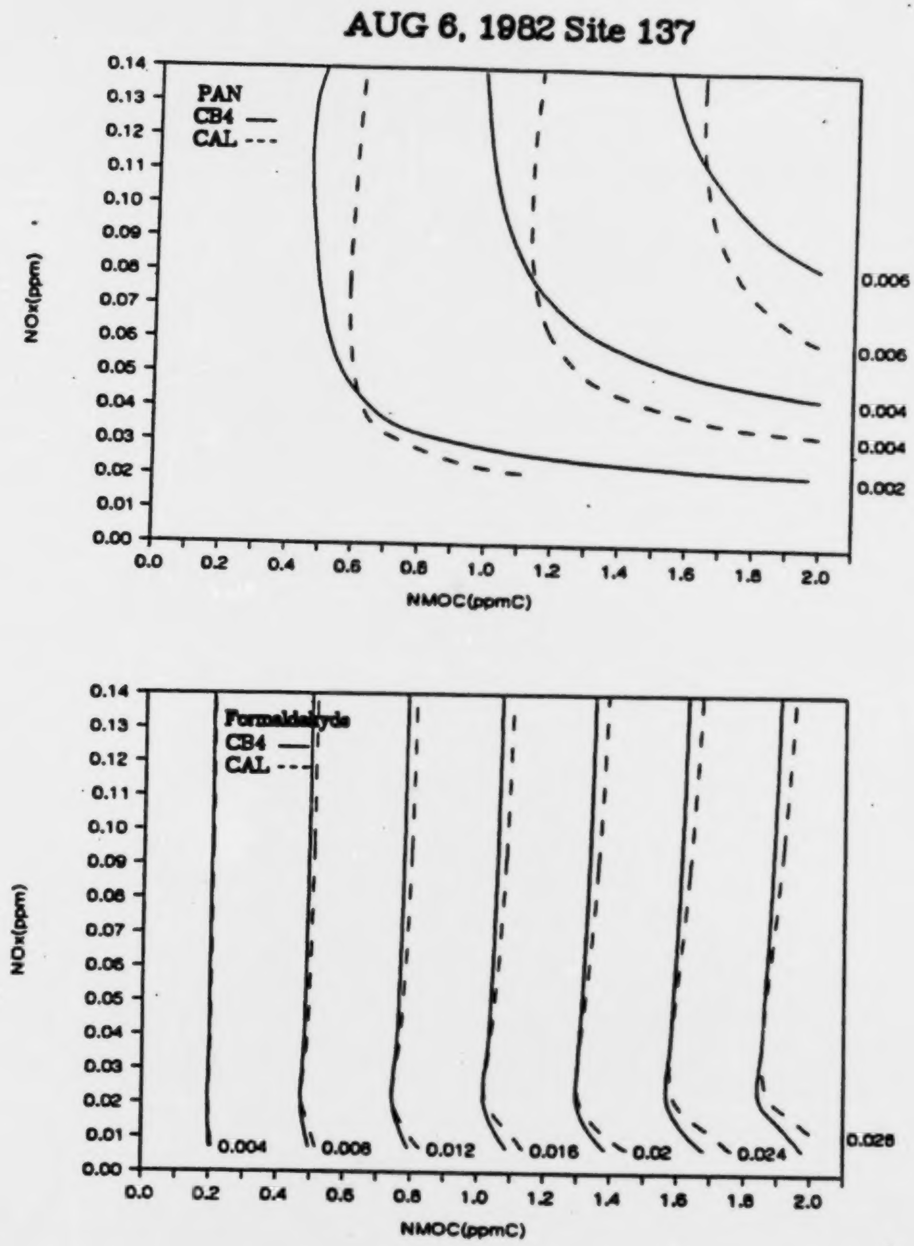

Figure 93c. PAN and HCHO Isopleth for Tulsa.

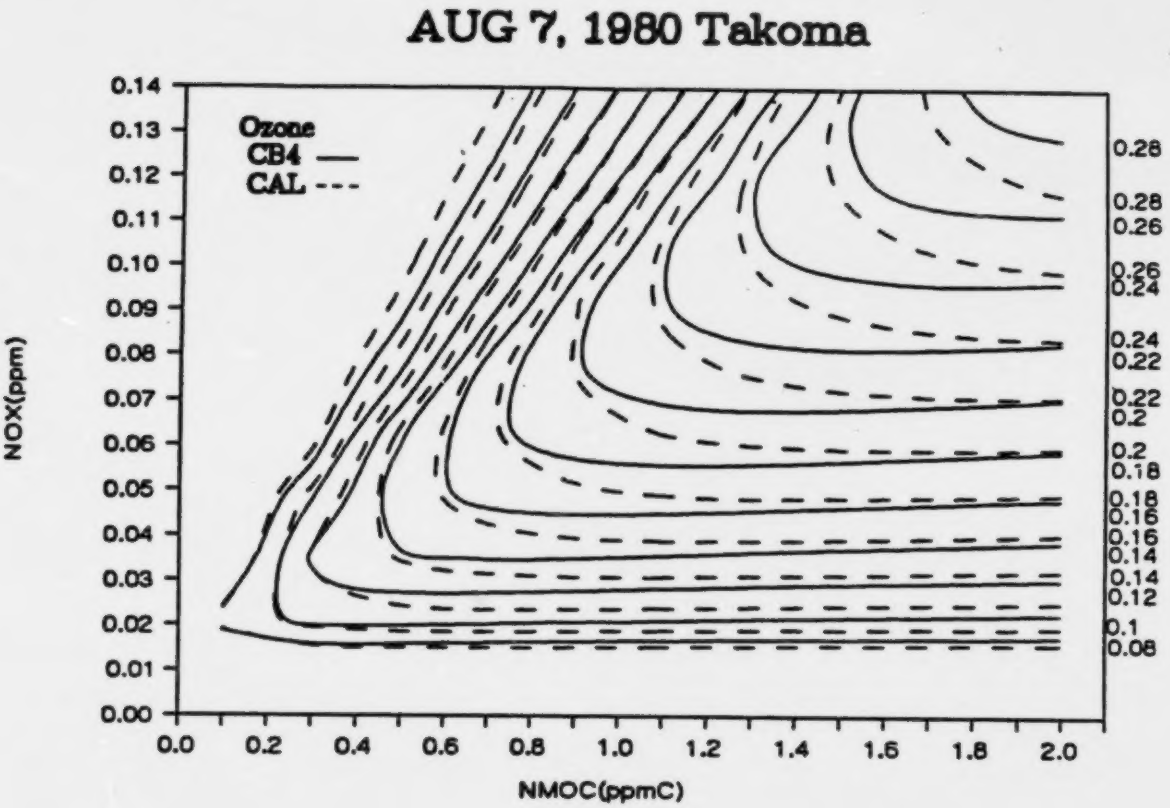

Figure 94a. Ozone Isopleth for Washington.

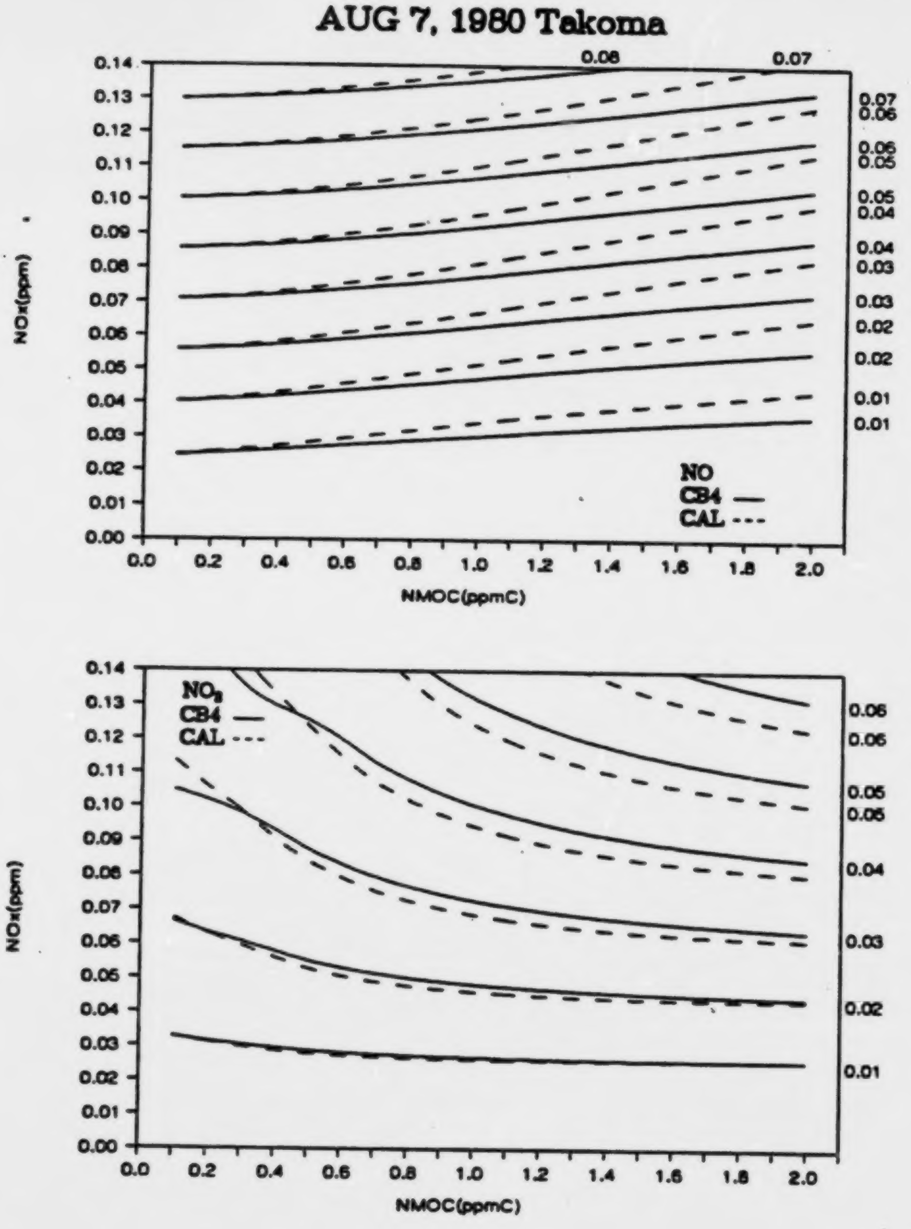

AUG 7, 1980 Takoma

Figure 94b. NO_x Isopleth for Washington.

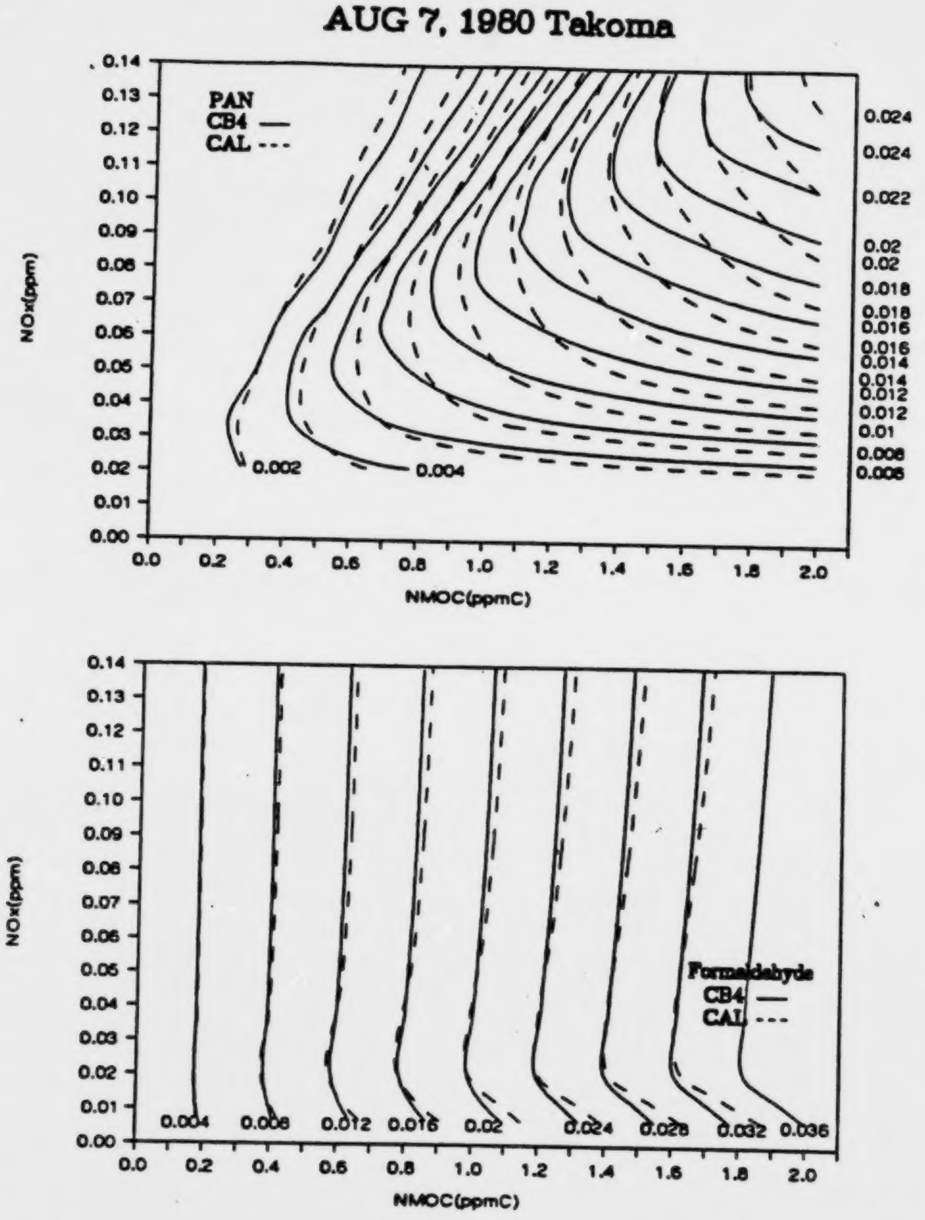

Figure 94c. PAN and HCHO Isopleth for Washington.

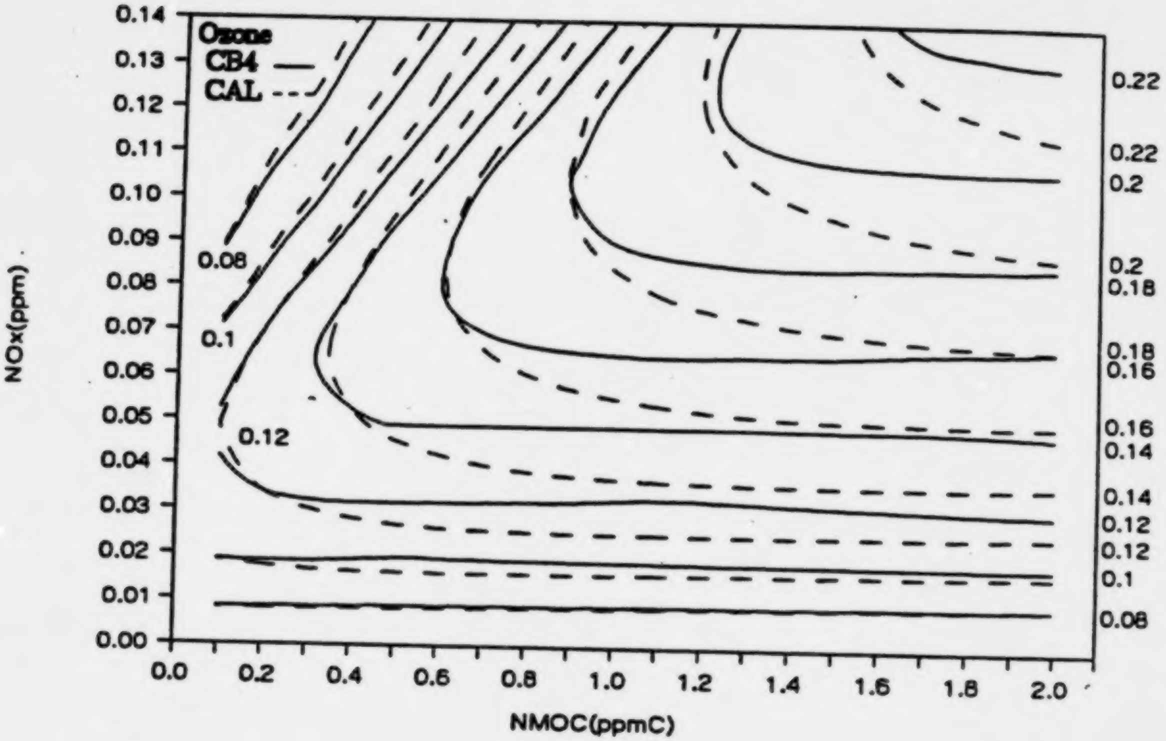

Figure 95a. Ozone Isopleth for New York.

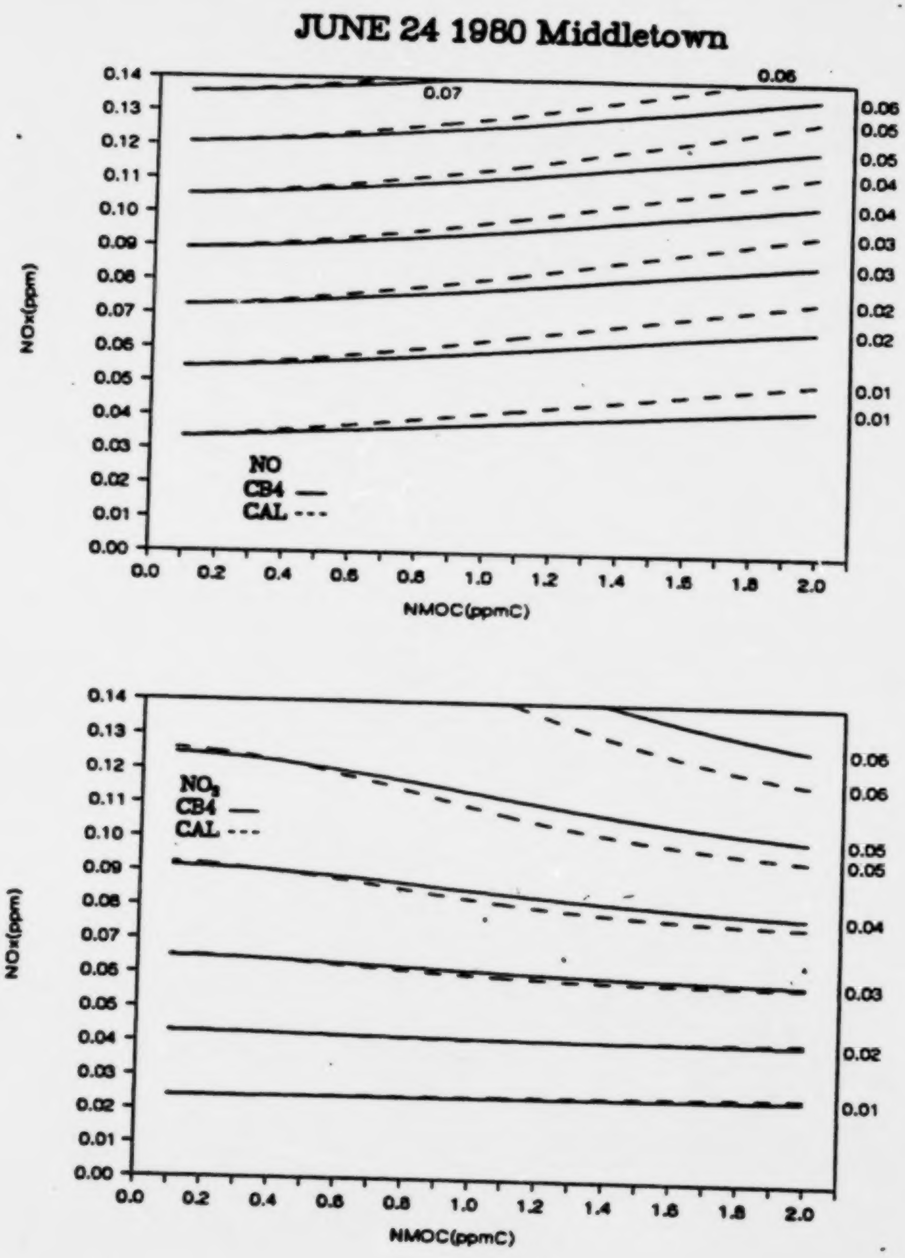

Figure 95b. NO$_x$ Isopleth for New York.

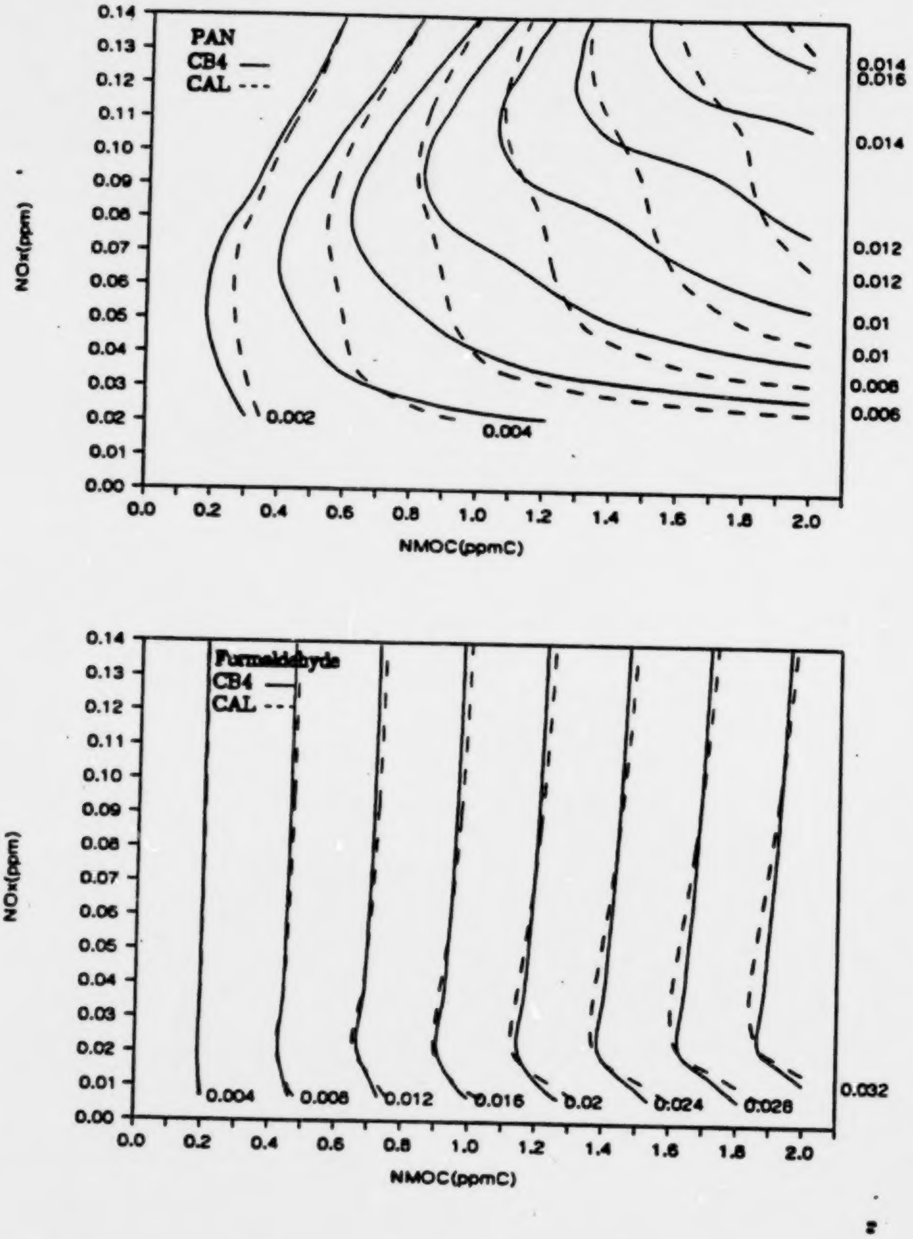

JUNE 24 1980 Middletown

Figure 95c. PAN and HCHO Isopleth for New York.

Sensitivity of Single SIP Case

Sensitivity to Reactivity Changes

A second Philadelphia SIP day was chosen to explore the effects of HC reactivity and HC-to-NO_x ratio on the agreement between the two mechanisms. These test conditions and results are shown in Tables 43 to 45 and in Figures 96 and 97. Here the emissions HC composition was changed from the recommended default value to the highest and to the lowest average reactivity for any of the 66 city-years used to compute the default. In addition, the future change in NO_x was first increased by 10.7% and then decreased by 10.7%. The biggest difference in predicted control required between the two mechanisms was 2.4% at the lowest reactivity for reduced NO_x where the requirement was 59.2% (CB4) and 56.8% (CAL). Two extreme sets of HC-to-NO_x ratios for these isopleths were also simulated: 6.25:1 and 25.7:1. Although the predicted control requirements for these cases ranged from 13% to 85%, in a given case, the two mechanisms predicted control requirements differed from each other by less than 1.3%.

Sensitivity to Aloft Material

A second variation on the Philadelphia SIP is shown in Table 45. In the first five cases in this table, the sensitivity of each mechanism's predicted control requirement to assumptions of ozone and HC aloft were investigated. In the last four cases, the sensitivity of each mechanism's predicted control requirement to the temperature profile (and maximum temperature) was investigated. In these tests, a clear pattern of differences between the two mechanisms does emerge.

As shown in cases 1–5 of Table 45, CB4 exhibits a greater sensitivity to external radical sources (*e.g.*, aloft HC and aloft O_3) than does CAL. That is, when a significant portion of the future condition's reactivity was attributable to the boundary conditions (*i.e.*, aloft material), then the two mechanisms predicted similar control requirements, and the two mechanisms required similar levels of HC to produce the basecase 0.171 ppm O_3. The extra radicals from the aloft material were not very important, because the system was basically NO_x-limited at the basecase condition. When the boundary conditions are stepwise reduced, however, CB4's reactivity falls more rapidly than CAL's reactivity–that is, CB4's $\Delta O_3/\Delta HC$ is larger than CAL's for lower levels of external radicals–resulting in CB4's needing a smaller change in HC for the same change in O_3. Put another way, CAL has slightly more internal reactivity at lower HC than does CB4. Nevertheless, the difference in predicted control required between the two mechanisms is small: less than 4% in 30% required.

Table 43. Conditions in the SIP Sensitivity Cases.

Lat:=39.933, Long =75.10, Time zone =4
Mixing: 250 @ 0800--1235 @ 1600
Ozone (surf,aloft)=0.010, 0.070
HC(surf, aloft)=0.038, 0.040
VOC Emiss(init, final)=0.17--0.02
NOxEmiss (init, final)=0.35--0.03

Table 44. Reactivity Variations on a SIP Case.

Variations on a SIP Case: Philadelphia

Case	*Date*	*HC reactivity*	*Ozone Base*	*VOC / NOx*	*%NOx change*	*CB4 Control*	*CAL Control*	*Diff*
1	24-Jul-80	standard	0.171	9.50	10.7	46.5	46.6	-0.1
2	24-Jul-80	high	0.171	9.50	10.7	50.8	51.4	-0.6
3	24-Jul-80	low	0.171	9.50	10.7	42.5	41.3	1.2
4	24-Jul-80	standard	0.171	9.50	-10.7	61.6	59.8	1.8
5	24-Jul-80	high	0.171	9.50	-10.7	64.6	62.7	1.9
6	24-Jul-80	low	0.171	9.50	-10.7	59.2	56.8	2.4
7	24-Jul-80	standard	0.156	6.25	0.0	13.6	13.0	0.6
8	24-Jul-80	standard	0.210	25.70	10.7	84.1	85.3	-1.2
9	24-Jul-80	standard	0.171	9.50	0.0	53.7	54.6	-0.9

Table 45. Temperature Variations on a SIP Case.

Variations on a SIP Case: Philadelphia

Case	*Date*	*Temp Profile*	*Max Temp*	*Sur/Aloft NMOC*	*Ozone Base*	*VOC/NOx*	*CB4 Control*	*CAL Control*	*Diff*
1	24-Jul-80	Default	'303 86F	0.040	0.171	9.50	54.6	53.7	0.9
2	24-Jul-80	Default	'303 86F	0.020	0.171	9.50	45.0	45.4	-0.4
3	24-Jul-80	Default	'303 86F	0.010	0.171	9.50	40.3	41.4	-1.1
4	24-Jul-80	Default	'303 86F	0.000	0.171	9.50	35.8	37.5	-1.7
5	24-Jul-80	Default	'303 86F	0.000	0.171	9.50	25.8	29.1 *	-3.3
6	24-Jul-80	Tulsa	'299 80F	0.040	0.171	9.50	35.6	43.4	-7.8
7	24-Jul-80	Wash.DC	'302 85F	0.040	0.171	9.50	45.2	48.9	-3.7
8	24-Jul-80	Default	'303 86F	0.040	0.171	9.50	54.6	53.7	0.9
9	24-Jul-80	Puget	'306 90F	0.040	0.171	9.50	58.5	56.2	2.3

* Cases 1-4 and 6-9 had 0.070 ppm O3 aloft, Case 5 had 0.040 ppm O3 aloft

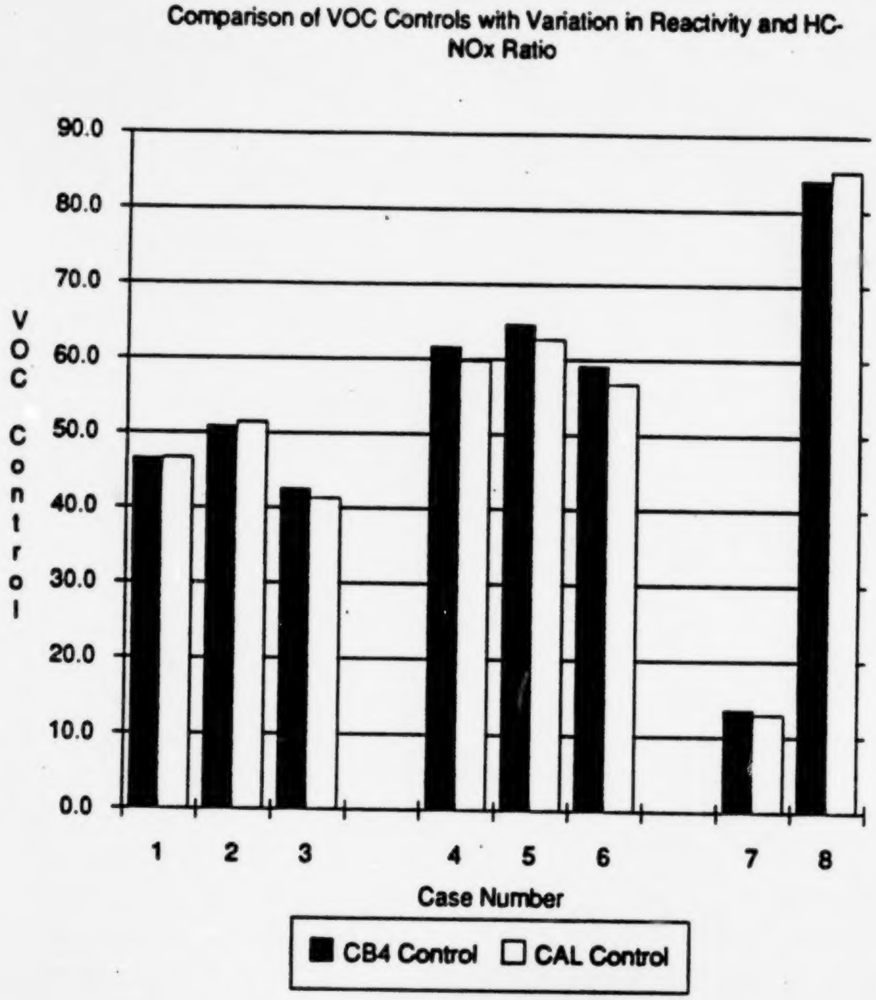

Figure 96. Reactivity Variations on a SIP Case.

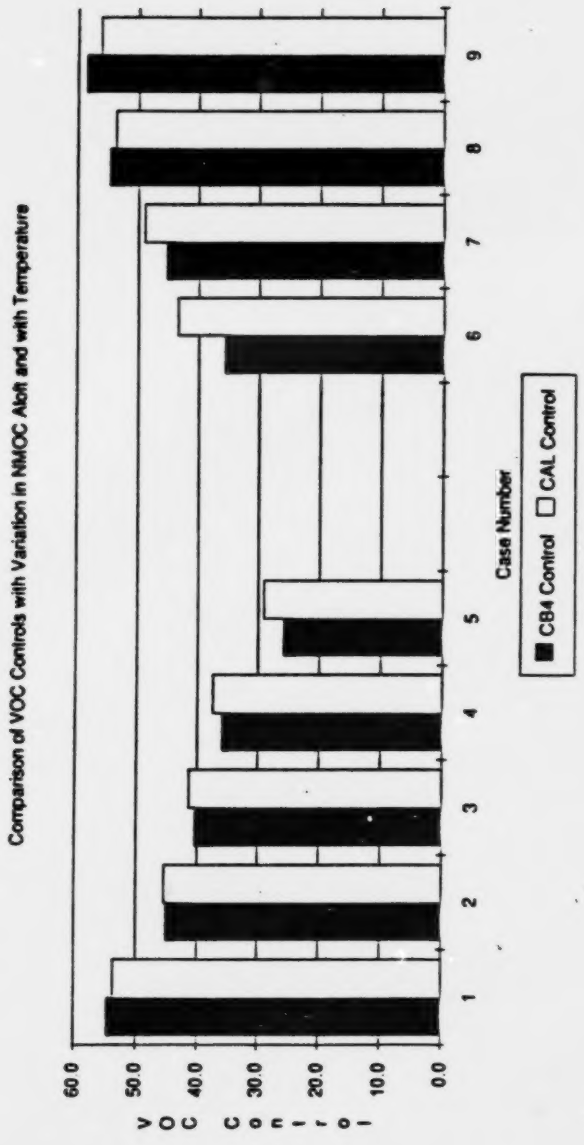

Figure 97. Temperature Variations on a SIP Case.

Given the sensitivity of the control requirement to small changes in boundary conditions, *e.g.*, the presence of 40 ppb HC and 70 ppb O_3 essentially doubles the controls needed, one might question the manner in which OZIPM4 represents these boundary conditions. For example, in the Phoenix case (see case 10, first table), which had a final mixing height of 3300 meters, 40 ppbC HC aloft is equivalent to an initial condition of 0.49 ppmC HC (at the 250 meter initial mixing height) and 70 ppb O_3 is equivalent to an initial condition of 0.85 ppm O_3! In the Puget case (number 5), on the other hand, with its final mixing height of 580 meters, the same 40 ppb HC and 70 ppb O_3 aloft is only equivalent to an initial condition of 0.052 ppm HC and 0.092 ppm O_3—ten times as much material is being added to Phoenix by external sources as was added to Puget. Given the system sensitivity, the approximation of the entrainment process in OZIPM4 seems crude at best. A better method would be to specify a profile of concentration verses altitude, especially for HC material aloft. The present method essentially describes an unlimited mass of material.

Sensitivity to Temperature

As shown in cases 6–9 of Table 45, CB4 also exhibits a greater sensitivity of predicted control requirements to changes in temperature than does CAL. In these scenarios, we substituted the temperature profiles from the SIP cases listed in Table 40 for temperatures in the Philadelphia SIP case. These profiles were shown in Figure 90. The Tulsa case for example, had a maximum temperature of 299 K or 80°F, the Washington, DC SIP had a maximum temperature of 85°F and the Puget SIP had a maximum temperature of 90°F. CB4 exhibited a 10% change in predicted control requirement for a 5°F change in temperature while CAL showed a 5% change in predicted control requirements for the same change. The differences in these cases can be significant at lower temperatures, *e.g.*, CAL requires 8% more needed control in 35% or about 1/5 of the control requirement at 80°F.

This sensitivity to temperature and difference in predictions can be directly traced to a difference in the treatment of the temperature dependance of the PAN chemistry in the two mechanisms. As part of the final work on the CB4 mechanisms, SAI, re-fitted the RCO3+ NO and RCO3+ NO_2 reaction rate constants using data from fall and winter UNC chamber experiments with large PAN formation and from having re-evaluated the kinetics data in the literature. Their re-assessment resulted in much more temperature dependence for ozone formation in the CB4 mechanism because the removal of NO_x to PAN is greater at lower temperatures in the CB4 mechanism. Carter and Atkinson used the earlier sources of information and did not attempt to model the cold UNC chamber experiments. The CB4 simulations do fit the existing chamber data quite well, something that has not been achieved before. The proper before. The proper resolution of this problem, however, will require new laboratory kinetics data on the temperature dependence of the ratio of peroxyacyl radicals with NO and NO_2.

It has been suggested by Dodge[34] that the differences between the two mechanisms' control requirements shown in Table 42 were caused by the mechanisms differential responses to temperature. That is, she suggested that the difference was negative for Case 5 (Puget, Aug 7) because the maximum temperature was only 85°F; it was positive in Case 6 (Puget, Aug 11) because the maximum temperature was 90°F. In her sensitivity analysis, Dodge showed that it was the afternoon temperature, when PAN is formed, that was the important factor.[33] In Figure 98 we plot the control requirement difference verses the 1400 LDT temperature. While two apparent correlations of control with temperature can be drawn as in the top of Figure 98, other strong correlations, independent of temperature can also be produced as in the bottom of Figure 98. Thus we are un-convinced that temperature alone is responsible for most of the differences in Table 42.

OZIPM's Representation of Temperature

Previously the effect of temperature on the predictions of control requirements has been largely ignored and essentially no guidance has been given on how to specify the simulation temperature. Now that the mechanisms show significant temperature sensitivity (the sensitivity of CAL is also significant), new questions about OZIPM as a calculation tool must be asked.

The reason EPA recommends that a mathematical modeling tool like OZIPM be used is to provide a "working" (but imperfect) replica of the system under study, one that mimics the happenings in the atmosphere. Various questions about the imperfections and the acceptability of the replication of the real system have been asked in the past.[35] The thrust of a "city-specific" EKMA method is to account better for the effects of local conditions on the relationship between oxidant precursors and ozone, presumably to produce a more correct answer for how much control is needed. The model, of course, is a compromise of costs, easy of use, and accuracy. If more accurate answers are desired, then the EPA recommends the use of the Air Shed Model. Nevertheless, it is important that OZIPM not have fundamental flaws.

The conceptual model implemented in OZIPM is that of a moving box which extends from the surface to the "mixing height" and this box is well mixed throughout its volume. Thus mass added at the bottom of the box through emissions is immediately converted into a box concentration by dividing the mass by the box volume

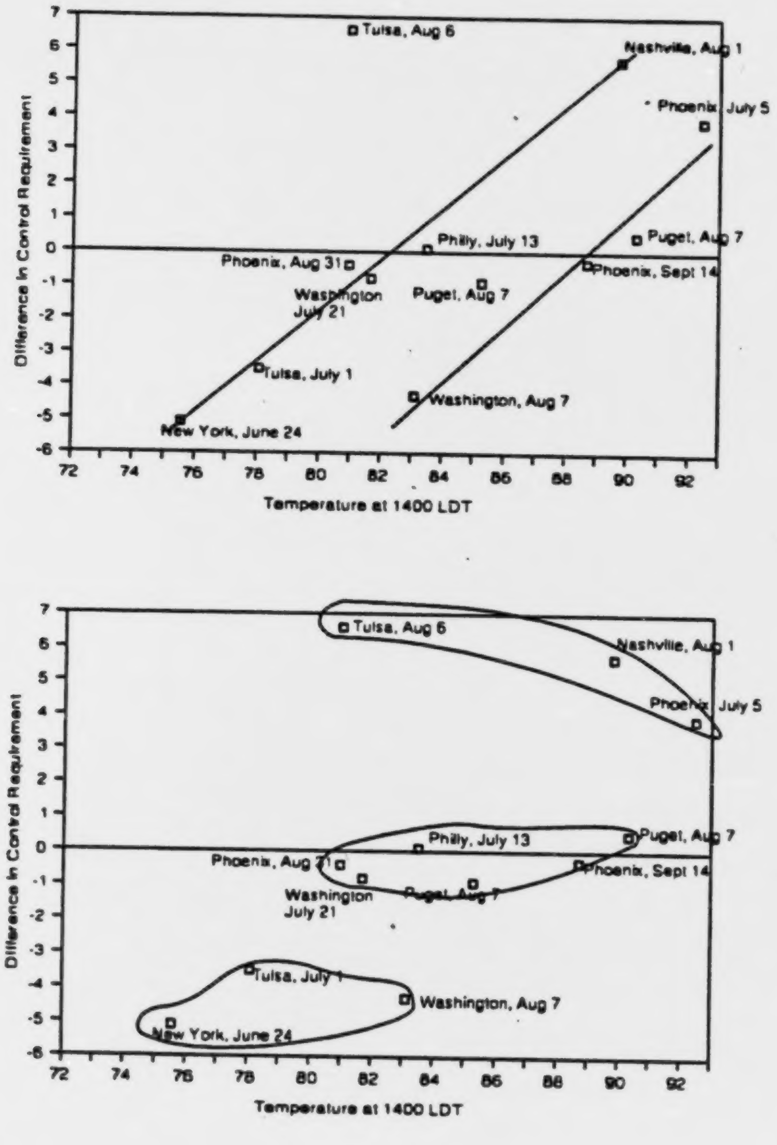

Figure 98. Differences in Control Predictions vs. 1400 LDT Temperature

(for a unit area box, this is the box height). Actually this is not true: because in the atmosphere pressure is decreasing with altitude, the concentration (mass/volume) *decreases* with altitude. Because *mixing ratios*, or ppm, are unaffected by temperature and pressure, however, they can be the same at the top and bottom of the well mixed box. In spite of the fact that we use ppm units in the OZIPM program, however, the actual chemical rates are controlled by concentrations–molecules per cc, which are pressure and temperature sensitive. When the program is using ppm units, there *must* be a temperature and pressure adjustment to the reaction rate constants to account for the real change in concentration as a function of temperature and pressure. The ppm values remain the same, the rate constants change.

The adequacy of the boundary layer representation in some of EPA's modeling tools has been investigated in a Cooperative Agreement between the American Meteorological Society and EPA. In a paper reporting on findings, Weil[36] said "Most diffusion models currently used in air quality applications are substantially out of date with the understanding of turbulence and diffusion in the planetary boundary layer." In this review, the convective boundary layer (CBL) was described as:

- The CBL extends from the ground to the base of an elevated stable layer and is characterized by strong vertical mixing driven by upward heat flux. Two parameters that characterize the CBL are z_i, the depth, and w_*, the convective velocity scale:

  $$w_* = \left(\frac{gQ_o z_i}{\rho C_p T}\right)^{1/3}$$

  where

  g gravitational acceleration,
  Q_o the surface heat flux,
  ρ the air density,
  C_p the specific heat at constant pressure,
  T the air temperature.

- For simplicity, the CBL can be considered to be horizontally homogeneous and to have a vertical structure comprising three layers:
  - ▷ surface layer: ($z < 0.1z_i$), the mean wind and potential temperature exhibit strong gradients;
  - ▷ mixed layer : ($0.1z_i < z < 0.8z_i$) the mean wind, potential temperature, and turbulence components show relatively little height variation;

  - ▷ the entrainment layer : ($0.8z_i < z < 1.2z_i$) the variables gradually approach their values above the CBL.

- The convective elements in the CBL consists of thermal plumes or updrafts surrounded by large downdrafts; both extend from near the surface into the interfacial layer. For sufficiently unstable conditions, the elements are randomly distributed and long-lived, having time scales of z_i/w_* of approximately 10 minutes.

Potential temperature is the temperature an air parcel at altitude z would have if brought to the surface. It is computed by :

$$T_* = T_z + \gamma_d z$$

where γ_d is the adiabatic lapse rate (10 K/1000 meter).

The OZIPM model assumes no vertical structure to the CBL, essentially assuming only the middle or mixed layer. This is necessary to have only one "cell" of chemistry, otherwise, three coupled cells, each with their own set of species would be needed and the computational effort would increase by more than an order of magnitude. So the approximation of the whole CBL by only the mixed layer is a reasonable compromise. The effects of this approximation are probably to over-estimate the concentration of some reactive species in the mixed layer which would have been partially reacted in the surface layer, to perhaps under-estimate the mixed layer NO-to-NO_2 ratio, because more NO could be oxidized to NO_2 in the higher concentration surface layer before the vertical transport moves the NO_x into the mixed layer. OZIPM also uses the full height of the mixing depth for the box size, not just the volume of the mixed region (*e.g.*, upper limit of $0.8z_i$), and therefore OZIPM may under-estimate the CBL concentrations resulting from emissions. The extent to which these errors may off-set each other is unknown.

Two areas in the representation of the CBL in OZIPM, however, are harder to justify given the discussion above: at present, the OZIPM model ignores pressure, and it assumes that the input temperature applies to the whole box volume. This is true even when the program accepts mixing height inputs as high as 2.2 kilometers. Given that convective mixing maintains the properties of the mixed layer in a uniform state, the mixing ratio of reactant species will be constant with altitude, ***but the pressure and temperature will not be constant with altitude.*** Therefore the *rate* of chemical reaction at the top of the well-mixed region will not be the same as the rate at the surface, ***even if the chemical mechanism has no temperature dependence.*** The rate calculation algorithms in OZIPM make no adjustment other than the standard Arrhenius calculations, therefore, OZIPM ***over-estimates*** the chemical transformation rate because it is solving the system as if the surface pressure existed throughout the whole box. Being a single cell model, however, OZIPM must use only one pressure. There is a simple compromise for this condition: use a pressure for the altitude at which half the reactant mass is above and half the reactant mass is below.

In the case of the photolytic rates, Whitten,[2] recognizing that the actinic flux is greater higher in the atmosphere, has already proposed that the single set of photolysis rates included in the OZIPM model should be at some average altitude. Therefore, he suggested that the rates should be given at 640 meters. Jeffries, *et al.*,[31] in calculating these rates for inclusion in the OZIPM4 program, found Whitten's argument compelling and did calculate the values at 640 meters. These values are presently included in the version of OZIPM4 distributed by EPA.

The case of temperature is more complex than either simple pressure corrections or average height photolysis rates. Potential temperature in the mixed-layer "shows relatively little height variation"[36] and therefore the actual temperature must decrease with height at approximately the adiabatic lapse rate of 10 K/1000 meter. A clear example of this is shown in Figure 99 in which four helicopter soundings of O_3, NO_x, and temperature over St. Louis at 6, 7, 8, and 9 am LDT are presented. These data were part of the EPA intensive study in RAPS and were analyzed by Roy Evans.[37] As shown in the plot for 9 am, the temperature inversion has been completely removed and there is already a temperature gradient of 2°C in 300 meters this early in the morning.

Another way to visualize the temperature situation is shown in Figure 100. These data are taken from Stern's Air Pollution and are from a diagram of average two-month average isotherms. This plot clearly shows temperature decreasing–up to 20°F–with altitude (after the morning inversion is gone at 830 LDT) even though the surface is warming considerably.

Because the OZIPM program has no vertical structure in the mixed region, a single temperature must be used. Clearly, a physically correct representation of temperature in the OZIPM program could not use the surface temperature to represent the whole mixed layer temperature, the top of which may exhibit as much as a 20°F difference with the surface. A compromise representation, then, would be to use some type of average temperature, probably a mass-weighted temperature, in which the amount of material at a given temperature would determine how much weight to accord to the material's temperature in computing the average. This first-order approximation would not be too difficult to compute given the surface

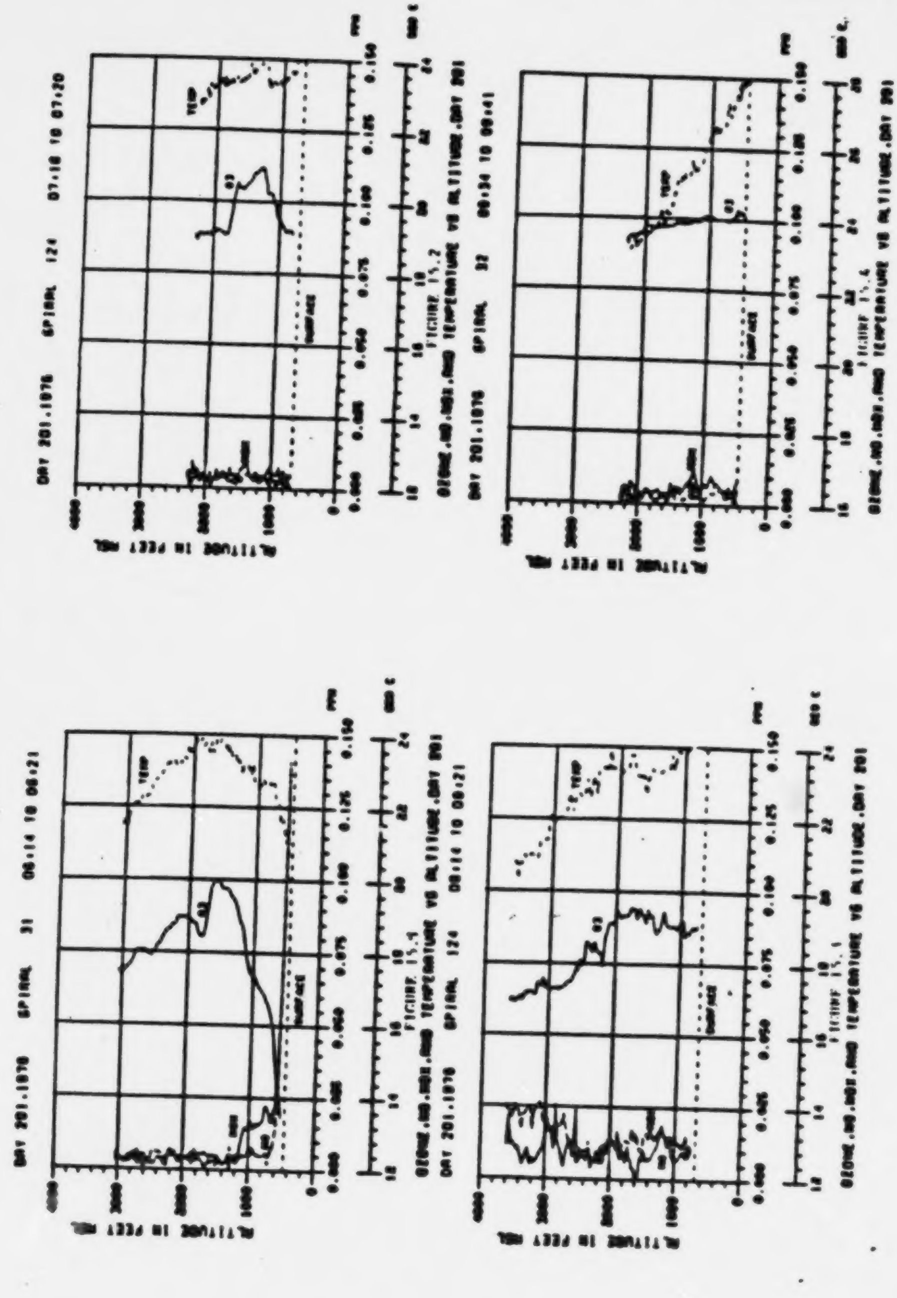

Figure 99. Helicopter soundings above St. Louis (after Evans[37])

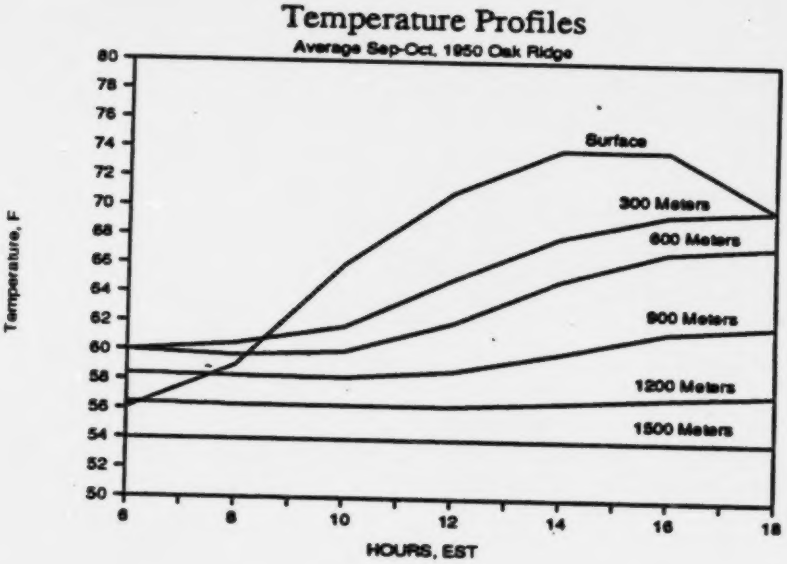

Figure 100. Average Temperature profiles over Oak Ridge as a function of Altitude.

temperature and the mixing height profile, and certainly would not represent much of a computational burden.

Now that these problems have been recognized and now that the chemical mechanisms are showing sensitivity to temperature, it would be prudent to move ahead in up-dating and revising OZIPM to correct its inaccurate physical representation of such fundamental properties of the convective boundary layer as pressure and temperature vertical profiles.

Impact of More Physically Correct Temperature

To estimate the impact that a more physically correct temperature representation might have on control calculations, we will use a zeroth-order approximation. That is, we will estimate the average box temperature using a linear or mid-height approximation. This is probably an 'upper-limit'-type approximation in that a true mass weighted temperature would be weighted more toward the bottom of the box than is our estimate. We will use the standard US atmosphere at 40°N latitude which has a lapse rate of about 3.5°F/1000 feet as an estimate of the lapse rate in the mixed box.

The mixing heights in SIP cases were sometimes quite large and these will result in large changes in the average box temperatures. The Washington DC, SIP (case 9), for example, had a mixing height of 2217 meters (7300 feet). If we assume an average mixing height of 1233 meters (accounting for the minimum of 250 meters), the average reaction temperature would be 14°F cooler at the maximum mixing height, but the morning temperature would change very little. In fact, the morning temperature becomes the maximum simulation temperature. The surface temperature profile and the zeroth-order estimated average mixed layer temperture are shown in Figure 101. The original SIP scenario with CB4 predicted that 30% HC reduction would be needed to meet the standard. The basecase O_3 of 0.140 ppm was achieved at a HC level of 0.881 ppmC NMOC and NO_x of 0.085 ppm; the O_3 standard was reached with 0.616 ppmC NMOC. We re-ran case 9 with a modified temperature profile using the estimated average mixing height temperature at each hour instead of the original temperature data. The results were that only 10.7% control was needed to meet the standard. The reactivity of CB4 was much lower: 1.45 ppmC NMOC and 0.141 ppm NO_x were needed to produce the basecase O_3 of 0.140 ppm and the O_3 standard was reached with 1.29 ppmC NMOC. We repeated the whole calculation with CAL which predicted a new control requirement of 24% (compared to the original 31%). While CB4 may be too sensitive to temperature, the effects of pressure in the OZIPM box, which would have lowered the reactivity of both mechanisms, also were not included in this calculation.

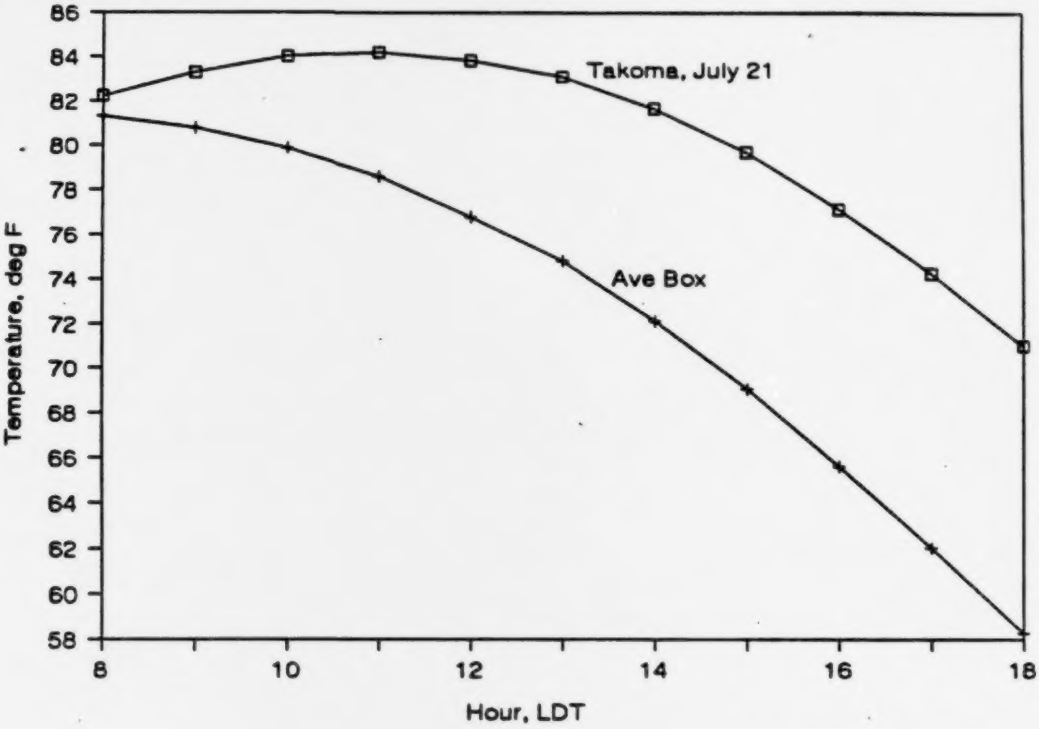

Figure 101. Washington DC SIP Temperature Profile and Average Box Temperature.

Conclusions

The mechanisms, with a new, consistent set of hydrocarbon default carbon fractions, produced very similar hydrocarbon control requirements for a wide range of HC-to-NO_x in a typical SIP situation. Control differences arising from the possible range of NMHC composition may be greater than those arising from the use of one or the other of the two mechanisms.

If methane concentrations are higher than 1.85 ppm in an urban area they will increase the calculated control requirement above the values shown here. We suggest that the present and future levels of urban methane be assessed and that a another series of sensitivity tests be conducted using these values.

In the city SIP cases, and over the range 3% to 57% predicted control requirements, the two mechanisms differed by at most 7% control required (*e.g.*, 29.3% vs. 22.7%). In some cases, CB4 predicted more control required and in others CAL predicted more. The biggest disagreements were bounded by a maximum difference of about 1/5 of the control requirement. Based on our tests, we can not recommend one mechanism over the other for use in SIPs.

Differences resulting from varying the HC composition for either mechanism within the range found in the 66-city-year study were greater than the differences between CB4 predictions and CAL predictions for the same composition.

A clear pattern of difference between the two mechanisms did appear when external radical sources were varied. CB4 showed more sensitivity to external radical sources (lower ozone for lower radicals) than does CAL, and thus CB4 predicted slightly less needed controls. Because of uncertainties in the chamber radical sources in both the UNC and UCR chambers, we can not, at this time, distinguish between the two mechanisms in this regard. The differences, however, are small, about 4% out of 28% or about 1/7 of the control requirements.

Likewise, CB4 showed more sensitivity to maximum temperature than did CAL. CB4 exhibited a 10% change in predicted control requirement (35% to 45%) for a 5°F change in temperature while CAL showed a 5% change in predicted control requirements (43% to 48%) for the same change. Thus CB4 showed a 1/4 change for a 5°F change, while CAL showed a 1/9 change.

Some of the sensitivity of SIPs to boundary conditions might be reduced if the boundary conditions were more correctly represented in the OZIPM4 model. For example, if a profile of aloft HC and aloft O_3 were used instead of the presently used constant concentration (*i.e.*, independent of height). The present representation provides an inexhaustible supply of material.

We believe that the representation of the convective boundary layer in the OZIPM4 model is incomplete, especially with regard to the physically correct representation of pressure and temperature in the vertical. Because OZIPM is a cost-effective, relative simple model, there must be compromises in the accuracy of it representations; major shortcommings in representing the physical situation, however, may lead to scientifically unsupportable predictions. Because of the complexities of the chemistry used, the model is clearly limited to a single cell that represents the entire mixed region of the convective boundary layer. This layer, however, can extend vertically several kilometers (as shown in the SIP conditions) and, because both pressure and temperature decrease with altitude, there can be significant differences in the top portion of the mixed region compared to the bottom protion. Currently OZIPM uses surface pressure and temperature to represent the entire mixed region, even when the mixing height is 2000-3000 meters. Not only is this physically inaccurate, it is not difficult, within the framework of the OZIPM4 model, to produce a better representation of the mixing layer conditions.

Both chemical mechanisms exhibit temperature sensitivities, and when estimated average mixing layer temperatures are used in SIP simulations, both mechanisms predict smaller control requirements, the CB4 mechanisms predicting quite small reductions. The CAL mechanism showed a smaller, but significant, decrease in the control requirement for this condition. The temperature sensitivity in CB4 is, in part, due to a highly speculative kinetics value and this highlights the fact that, because little kinetics data exists in this temperature region, predictions below 75°F may be very wrong, not only for CB4, but also for CAL. More work is needed on this subject.

6

Formaldehyde and Hydrogen Peroxide Study

Introduction

During the summer of 1986 EPA sponsored a two-part study to compare hydrogen peroxide and formaldehyde (HCHO) instruments designed and operated by five different research groups. The first part of the study was a blind-intercomparison using laboratory samples and was conducted by Northrop Services Inc. (NSI) at the Research Triangle Park. UNC did not participate in the NSI part of the study. The second part of the study was a comparison of concentration-time profile measurements from HC-NO_x irradiation experiments in the UNC dual outdoor smog chamber. This was needed because modelers had questioned the accuracy of earlier HCHO data and previous H_2O_2 collected by UniSearch in 1984. The first part of this chapter discusses the HCHO portion of the study and the last part describes the hydrogen peroxide results.

Formaldehyde measurements were taken by:

- University of North Carolina (UNC);
- National Center for Atmospheric Research (NCAR);
- Texas Tech University (Texas);
- Unisearch Associates (Unisearch); and
- Environmental Protection Agency (EPA).

Formaldehyde Measurement and Calibration Methods

UNC Method

The standard UNC formaldehyde method is an automated colormetric instrument manufactured by CEA Corp. (Westwood, NJ). This system uses a reverse West and Gaeke technique[38,39] and hence requires a continueous supply of wet chemicals which include highly purified pararosanaline, mercuric chloride, sodium chloride, and sodium sulfite.

The minimum detectable concentration for the CEA instrument is about 20 ppb and the normal sensitivity is about 185 ppb per inch chart deflection. We have observed a 5% positive interference from acetaldehyde in the concentration range 0.1–1 ppmV acetaldehyde (*i.e.*, 5% of the acetaldehyde concentration appears as HCHO concentration). We have also determined that the instrument exhibits no response to other carbonyls such as acetone, propionaldehyde, ketones, and glycoaldehyde as well as to formic acid, all at ppm levels.

Three different HCHO standards were used to calibrate this instrument:

- liquid HCHO standards, prepared by serial dilution of 37% formaldehyde solution to produce standards of about 1 mg/liter (equivalent to about 300 ppb in air given the instrument liquid and air flowrates);
- a dynamic HCHO standard (375 ppb) generated in an airstream by a commercial permeation tube system (Metronics Corp., Santa Clara, CA); and
- static or batch HCHO standards, produced by subliming precision weighted quantities (50–200 mg) of > 95% pure paraformaldehyde into the dehumidified 150,000 liter chambers (the majority of these standards were near 1000 ppb HCHO).

The liquid standards were prepared by serial dilution of commercial (Fisher ACS grade) methanol-stabilized 37% formaldehyde solutions. The liquid injections were accomplished by letting the CEA reagent pump pull the sample directly from a sample flask. The UNC certified HCHO permeation tube emits 293 ng/min at the calibrator's 76°C (this temperature is held to within ±0.05°C), into an air flow of 187 cc/min. This stream is diluted to a total flow of 636 cc/min to give a very stable mixing ratio of 375 ppb HCHO in the air stream. The paraformaldehyde (Baker Chemical) for chamber injections was weighted on an 6-place, stabilized analytical balance at the site and was injected by heating air passing over the solid in a U-tube directly under the chamber. The line from the U-tube to the chamber was less than 6-inches of Teflon tubing. The chamber volume was determined previously by three independent strapping operations which agreed to within 0.5%.

We routinely cross-check the calibration methods and we generally find that they are consistent with each other within a standard deviation of less than 10%. One factor that affects the CEA span is the stability of the sample air flow, which is controlled by a needle valve and rotometer system. When this changes, the flow usually drifts downward, resulting in an under-reporting of the true concentration. The instrument also has a 30–50% zero drift over a 3–4 hour period, which requires that the instrument sample a zero air source every few hours to allow the baseline to be established; a clock timer is used to switch the inlet valve to a zero HCHO stream about every three hours. If a zero baseline can not be well established, then the HCHO concentrations would most likely be over-reported; this occasionally happens due to failure of the zeroing clock.

The NCAR Formaldehyde System

The NCAR HCHO analytical technique[40] was based on the aqueous oxidation of HCHO to formic acid, catalyzed by formaldehyde dehydrogenase enzyme. The concurrent reduction couple was NAD+/NADH. The resulting NADH was fluorescent with an exication wavelength of 350 nm and an emission wavelength of 450 nm. The method used a Technicon peristaltic pump and coil system to provide a continuous gas-liquid contactor. The system output at UNC was recorded on an NCAR IBM XT computer with a Tecmar A/D converter.

The NCAR system was calibrated by the use of liquid standards made from a single stock formaldehyde solution brought from NCAR. Several determinations of the stock solution were made during the course of the study. Lind *et al.*[41] say that the accuracy of the NCAR HCHO measurements were dominated by the uncertainty in the concentration of the stock HCHO used in the instrument calibrations and this may have been true in the very low concentration portion of the study conducted at Northrop Services. At the UNC chamber, however, the accuracy of the NCAR HCHO measurements appear to be dominated by the NCAR system becoming non-linear due to enzyme saturation at the higher chamber concentrations (*e.g.*, > 500 ppb HCHO). NCAR choose to use a calibration curve of the from of Michaelis Menton kinetic equation

$$y = \frac{ax}{(b+x)}$$

for enzyme catalyzed reactions to fit the non-linear, daily calibration data. We will show that small variations in the fit of this equation to the calibration points can have a large effect on the NCAR HCHO values.

The Texas Tech University Formaldehyde System

The Texas HCHO analytical system used a porous membrane diffusion scrubber to collect the HCHO in water. HCHO was detected in the water solution by addition of acetylacetone-amonium acetate and the formation of dihydrodiacetyllutidine which was detected by a fluorescence system. A heated bath speeds up the formation reaction.

In the Texas Tech Final Report,[42] Dasgupta said that the diffusion scrubber used on the HCHO instrument did not collect gaseous HCHO quantitatively, and therefore the instrument had to be calibrated with an on-board membrane-based calibration source. This calibration source was similar to that described in Hwang and Dasgupta[43] and in Dong and Dasgupta[44] and was based on humidified air flowing through a porous Teflon tube immersed in its entirety in a formaldehyde solution in a constant temperature bath system. The output of this source was diluted again by a second airstream to establish two lower concentrations. In the UNC study, the system was operated as 2-minutes of measure, 2-minutes of zero, and calibrations were performed once or twice a day.

Dasgupta suggests[42] that the constant temperature baths used for the calibration systems in this study were not entirely satisfactory. He said, "Calibration uncertainty therefore was the largest error source in our measurements both for HCHO and H_2O_2." We will show that the Texas calibration source was indeed unsatisfactory which lead to problems with the Texas HCHO data.

The EPA Aldehyde System

This system used commercial silica gel cartridges coated *in situ* with acidified 2,4-dinitrophenylhydrazine.[45] Air was drawn through the cartridges at a flowrate of 1 liter/minute for 15 minutes. The cartridges were returned to EPA for extraction with acetonitrile (ACN) and analysis by gradient liquid chromatography. The standards used in the chromatography were made by dissolving weighted quantities of pure hydrazone derivatives of the aldehydes in ACN. The hydrazone derivatives were prepared by reaction of individual carbonyl compounds with saturated DNPH solution in 2 N HCl. Purity was determined by melting point measurement and HPLC analysis.

We will show that concentrations of ozone above 200 ppb cause sever loss of response for this method. In the absence of ozone, the method showed excellent agreement with several other groups and calibration sources.

Unisearch Associates Formaldehyde Method

This system was a tunable diode laser absorption spectrometer (TDLAS). An air sample is drawn into a White cell operated at a total pressure of about 25 torr. The White cell provides a path length of 40 meters. A tunable lead salt diode laser provides a highly monochromatic source to determine the absorption from single rotational-vibrational lines in the mid-infrared spectrum of a given molecule. The TDLAS was contained in its own van and was parked near the chamber. A small diameter Teflon sample line was inserted into each chamber and connected to a two-way Teflon valve with a Teflon line leading into the van and to the White cell inlet.

The calibration source was a formaldehyde permeation system designed by Unisearch that was operated in the van. Chromotropic acid bubblers were used to determine the permeation rate in the laboratory before the study and ten determinations using chromotropic acid bubblers were made during the field program. Because of the location of this calibration source in the van which was located on the opposite side of the chamber from the laboratory where all other methods were operated, no cross-checking of the Unisearch permeation system was performed. As will be shown below, Unisearch consistently read below other groups and therefore their permeation system may not have been calibrated correctly, or the system was designed for use below 100 ppb and most of the conditions at the UNC chamber site were at 500—1000 ppb.

Calibration Statistics

UNC Calibration Factor Statistics

Figure 102 shows the standard UNC QA plot of the UNC HCHO calibration factor (ppm HCHO/inch chart deflection) for the time period of the intercomparison study. Various statistics for these data are shown below the figure. Calibration factors from all three sources are included in the plot. The regression equation shows extremely small negative slope and an intercept of 0.189 ppm HCHO per inch chart deflection. The standard deviation for the intercept was 8.6% and the probable error was 0.010 ppm HCHO per inch or about 5%.

Figure 103 shows in separate symbols the permeation tube calibration points, the chamber calibration points, (that is, those based upon injection of weight samples of paraformaldehyde into the chamber), and the liquid standards calibration points. Below the plot are statistics for each source.

These data show that not only was the CEA's response to HCHO stable (standard deviation of about 8%), but also that three different sources were consistent over the whole time of the study. In addition, the individual calibration factors were applied to the respective data, thereby decreasing the actual calibration uncertainty to that of the calibration factors. A number of previous tests have demostrated that the CEA is linear in response. If during an experiment the sample flow rate was stable, and if there were an adequate number of zero baseline determinations, then the uncertainty of the experimental data should be less than the calibration factor variation, provided *there were no interferences.*

NCAR Calibration Statistics

Figure 104 shows a QA plot for the determination of the NCAR HCHO stock solution used in making the liquid standards used daily to calibrate the NCAR HCHO system. The uncertainty in the HCHO value is dominated by the single chromotropic acid determination on June 20. The values determined during the UNC portion of the study are 4% lower than the average value adopted by NCAR and exhibit a much smaller scatter. Thus the uncertainty in the NCAR calibration source is probably less than the UNC sources (*e.g.*, about 8%).

Unfortuately the satuation of the enzyme system leading to a non-linear response degrades the accuracy of the NCAR data. This is shown in Figure 105 which shows the calibration curves for a number of days in the UNC portion of the study. In the early part of the study the calibration curves were very similar (July 3, 4, and 5) and, below 500 ppb were nearly identical. The curves, however, fit the

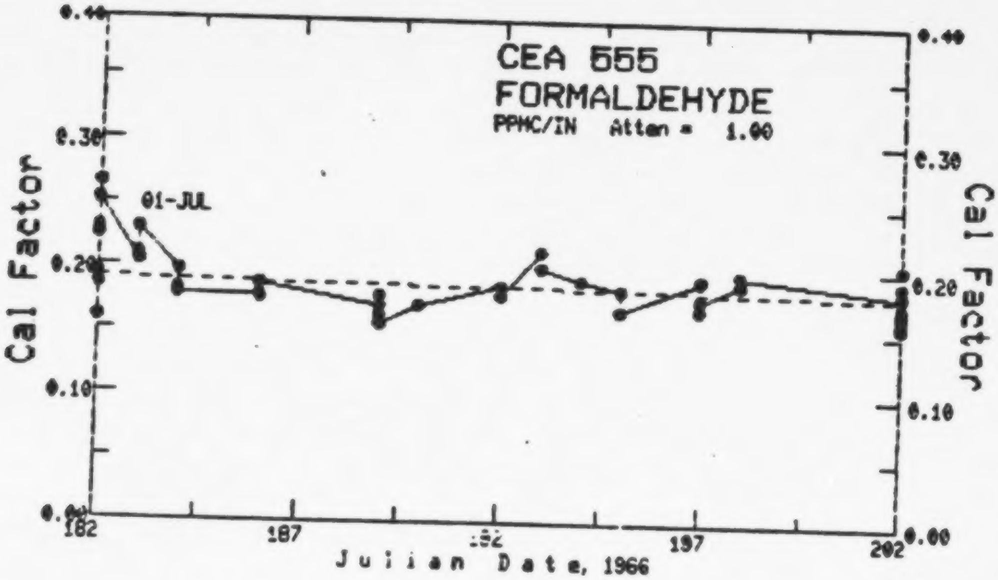

Figure 102. CEA Calibration Factors from Three UNC Sources

```
For the species FORMALDEHYDE and the instrument CEA 555:

Beginning Caldate:            30-JUN-86
                        Day:  182
Ending    Caldate:            25-OCT-86
                        Day:  299
Upper CalFactor Limit            0.75000
Lower CalFactor Limit            0.00000

The number of data points        47
The number included  was         39
The slope of this fit  is -1.919712E-004
       with a std dev of 9.3331656E-005   rel. dev = -48.6 %
The intercept is          2.2428774E-001
       with a std dev of 1.9264764E-002   rel. dev = 8.6 %
The std dev of the fit is 1.5725477E-002   PE =  0.01048
The correlation coeff is  -0.32033

The min, mean, max are        0.15750,    0.18500,    0.26790
The standard deviation is  0.01638   rel. dev = 8.9 %

Cal = -0.00019 X (Julian Date - 182) +  0.18935

                    ...press RETURN-key when ready...
```

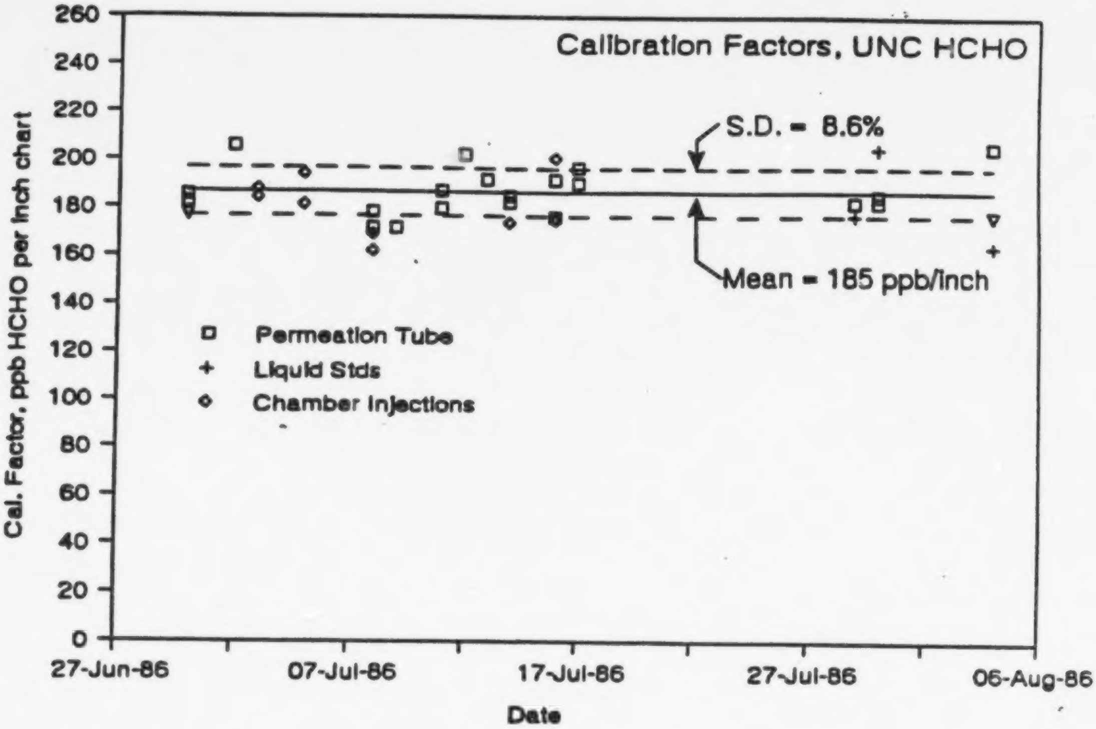

Table 103. Separate Calibration Factors from Three UNC Sources.

Item	Perm. Tube	Liquid Stds.	Chamber Inj.
Mean	187.2	182.2	181.4
Std. Dev.	9.9	16.8	11.6
% Std. Dev.	5.3%	9.2%	6.4%
Number	19	3	9
Ratio	1.00	0.97	0.97

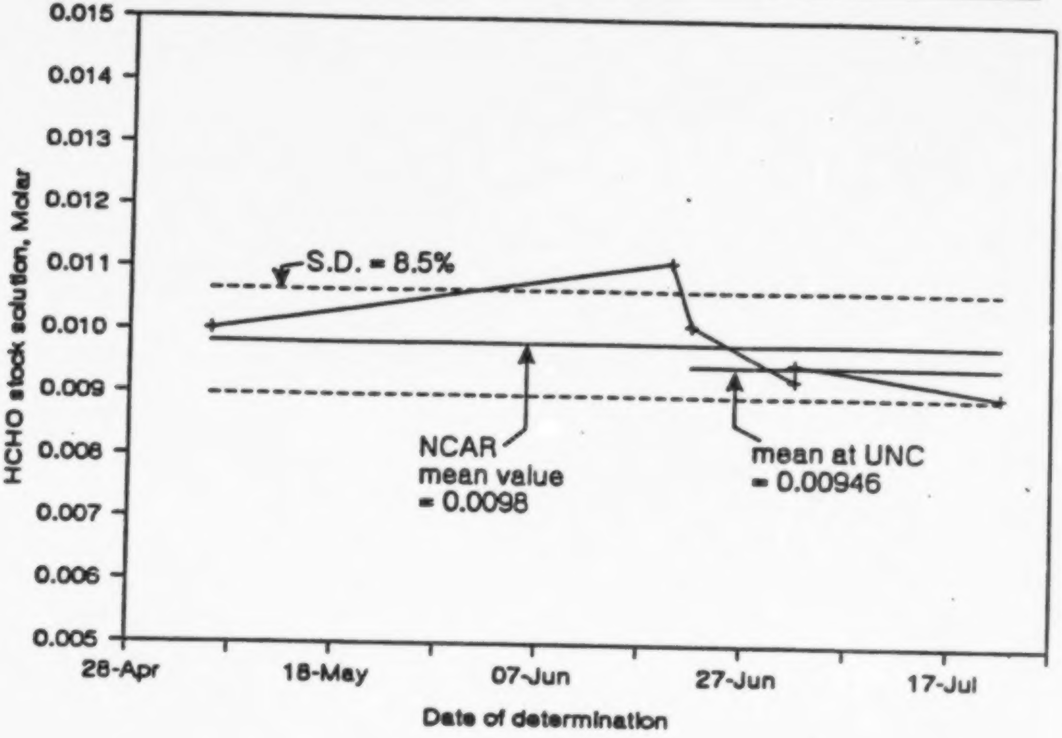

Figure 104. NCAR determinations of standard HCHO stock solution concentration.

points near 1000 ppb poorly. The July 8 calibration curve shows an especially poor fit to both the 500 and 1000 ppb points. After July 8 there were large swings in calibrations and an increase in non-linearity as shown by the July 9 and July 16 curves.

Figure 106 shows the effect of small changes in the July 8 fit of the calibration curves to the measured calibration points and the subsequent impact on the agreement with other HCHO measurements in the chamber experiments. In the top plot of Figure 106 the HCHO profiles from the UNC CEA instrument are compared with profiles produced by NCAR using the calibration curve fitted in their final report. This curve is shown as dashed lines in the bottom plot of Figure 106. We adjusted the *a* and *b* values in NCAR's fit slightly to improve the agreement near 1000 ppb, while coming as close as NCAR did at 500 ppb, just slightly below the point instead of above the calibration point. The impact on the agreement of the NCAR measurement with the UNC measurement is quite significant as shown in the top plot. Because many of the NCAR calibration curves tend to be above the 500 ppb calibration points, the NCAR chamber profiles during the middle of experiments tend to be under the other group's chamber profiles, while still showing reasonable agreement with the higher and lower values at the beginning and end of experiments. In addition, NCAR lost a RED/BLUE sample valve in the middle of the program, and, as will be shown later, on July 9, it appears that not only was there a very strong non-linear calibration problem on this day, there appeared to be a bad sampling valve on the RED chamber that greatly reduced the sample.

Texas Tech Calibration Data

Shen Dong determined[46] that the low level output of the Texas Tech calibration system was 456 ppb HCHO, and that the high level output was 792 ppb HCHO using a bubbler method described in reference 44. No additional determinations of the Texas calibration source output were made by Texas during the NSI or UNC study. Several group determinations were made, however, and these will be described below.

In the Texas Final Report,[42] Dasgupta commented on the operation of this calibration source:

> "the gas cylinders were placed outside and inlet air temperature to the generation source varied significantly during the course of a day, from early morning to early evening. While all our calibration was based on the set temperature of the box, it is more than likely that the actual generation temperature varied during the day. ... On the other hand, the

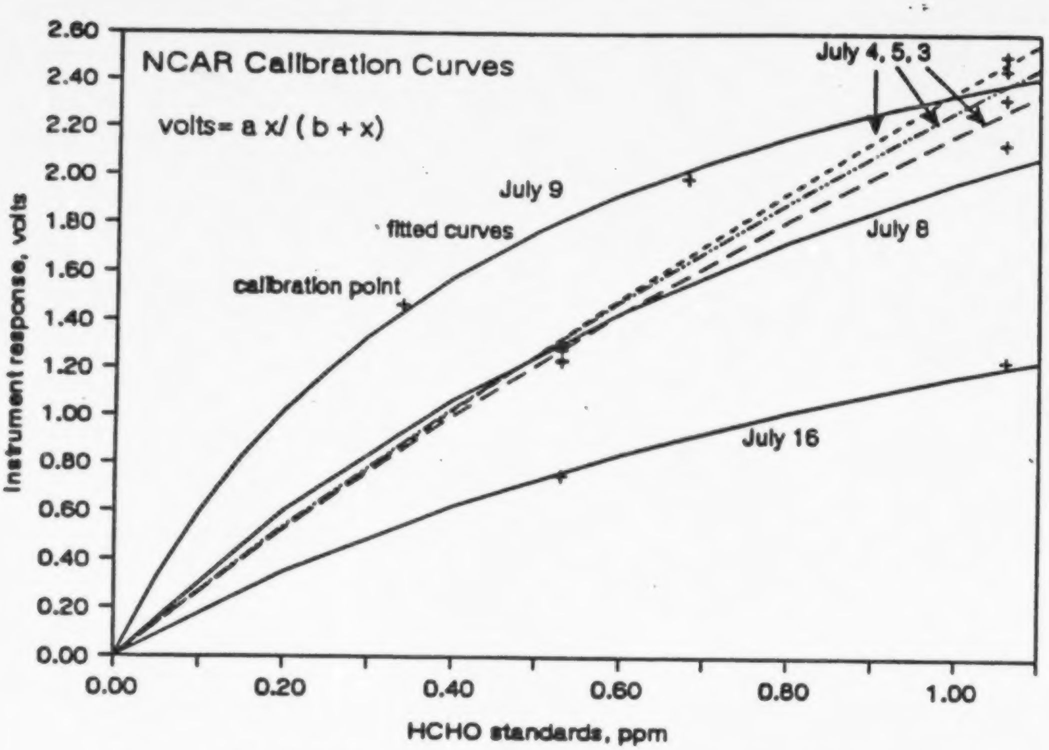

Figure 105. NCAR calibration curves for selected days in the UNC study.

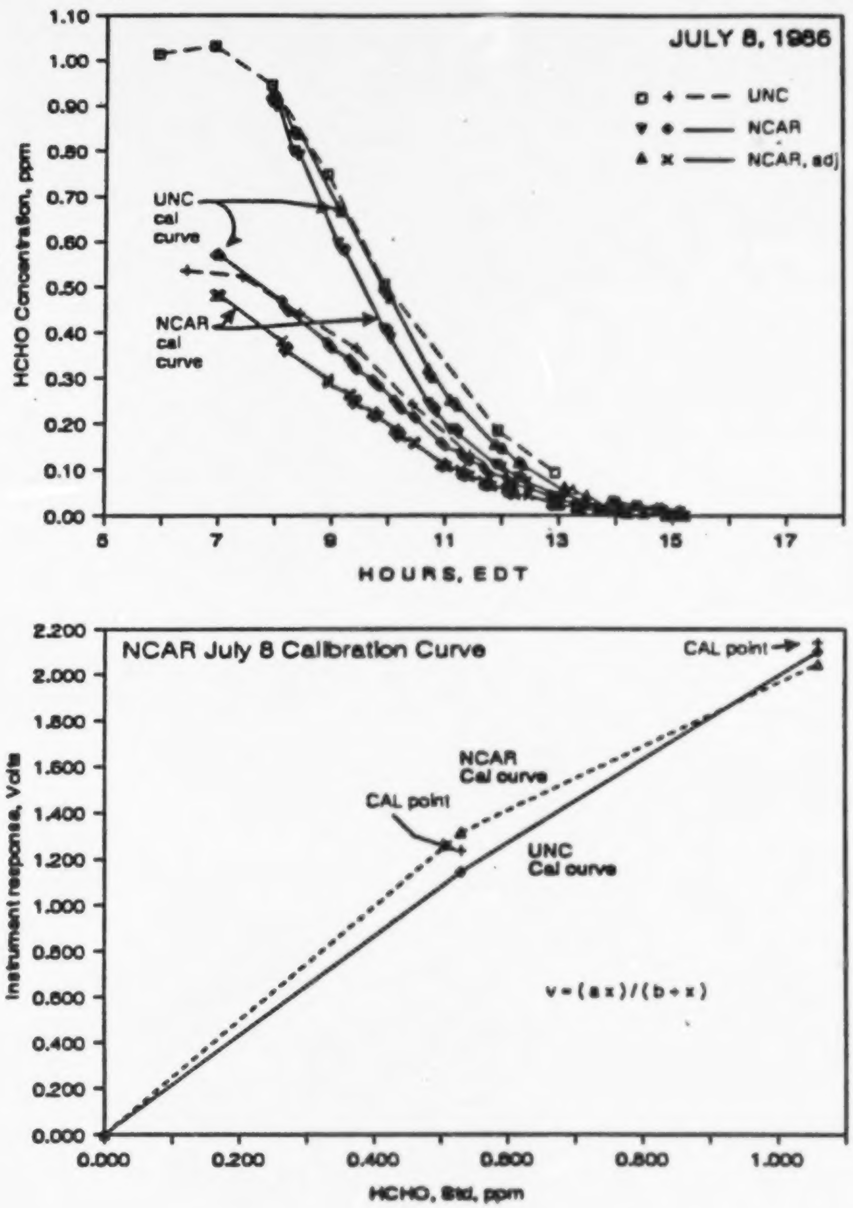

Figure 106. Effect of small changes in fitted non-linear calibration curve on NCAR HCHO measurements.

data reported are based on the implicit assumption that the calibration concentration remains constant"

Unisearch Calibration Data

In their final report,[47] Mackay and Schiff reported that the permeation rate for their HCHO source was 185 ± 5 ng/min as determined by chromotropic acid in the laboratory before the study. During the field study, 10 determinations using chromotropic acid gave a value of 183 ± 8 ng/min.

The permeation source was used to supply a continueous HCHO calibration stream to a sample–calibrate valve located near the sample line inlet to the TDLAS. The computer system could switch the valve to obtain a calibration signal. According to the description in the final report, the TDLAS sampled at 12.0 liters/minute. If the whole permeation source was added to zero air at 12.0 liters/minute, then the calibration signal would have been 12.3 ppbV of HCHO. This value was close to the test values of 0–50 ppb during the NSI portion of the study, but was 40–80 times less than the morning injections into the chamber.

Calibration Sources Intercomparison

July 2 Measurement of Calibration Sources

Approximately two days after all groups had set up at the UNC chamber, a first intercomparison of calibration sources was performed. The values were not reported until a meeting held about one week after the program was underway. In addition to the intercomparisons of calibration sources on July 2 there also had been a number of before sunrise chamber injections of HCHO that could be treated as gravimetric standards. These data are shown in Table 46 and are plotted in Figure 107. Delays in setting up some sampling equipment and the location of the Unisearch van on the opposite side of the chamber prevented all groups from sampling all sources.

Table 46.. July 2 Intercomparison of Calibration Sources.
(units are ppb HCHO)

	Source				
Group	UNC375	Tex456	Inj1*	Inj2*	Inj3*
UNC	370	497	1090	556	1010
NCAR	360	520	1044	550	1050
TEXAS	330	456	1040	460	1095
EPA	NA	NA	NA	558	1069
UNISEARCH	NA	NA	677	319	613

* These are 6 AM chamber injections of paraformaldehyde
1) July 3 Red 2) July 8 Red 3) July 8 Blue

UNC, NCAR, and EPA showed close agreement on all sources at all levels. At the 1000 ppb level, UNC, NCAR, Texas, and EPA showed close agreement. At 500 and below, Texas read lower than UNC, NCAR, and EPA. This result will be examined further below. Unisearch reported only about 70% of the average values for 500 and two 1000 ppb calibration points. Unfortuately, no other groups sampled the Unisearch permeation system, and therefore there is no direct way to determine the accuracy of their assigned permeation rate which was based upon bubbler determinations only.[47] Alternatively, there may have been a problem in using a very low calibration value to measure concentrations 80 times higher. Figure 108 shows, in the top plot, the agreement between the Unisearch profile data using their calibration and the UNC profile data. In the bottom plot, the mean value of the injected HCHO as reported in Table 46 was used to adjust the Unisearch reported

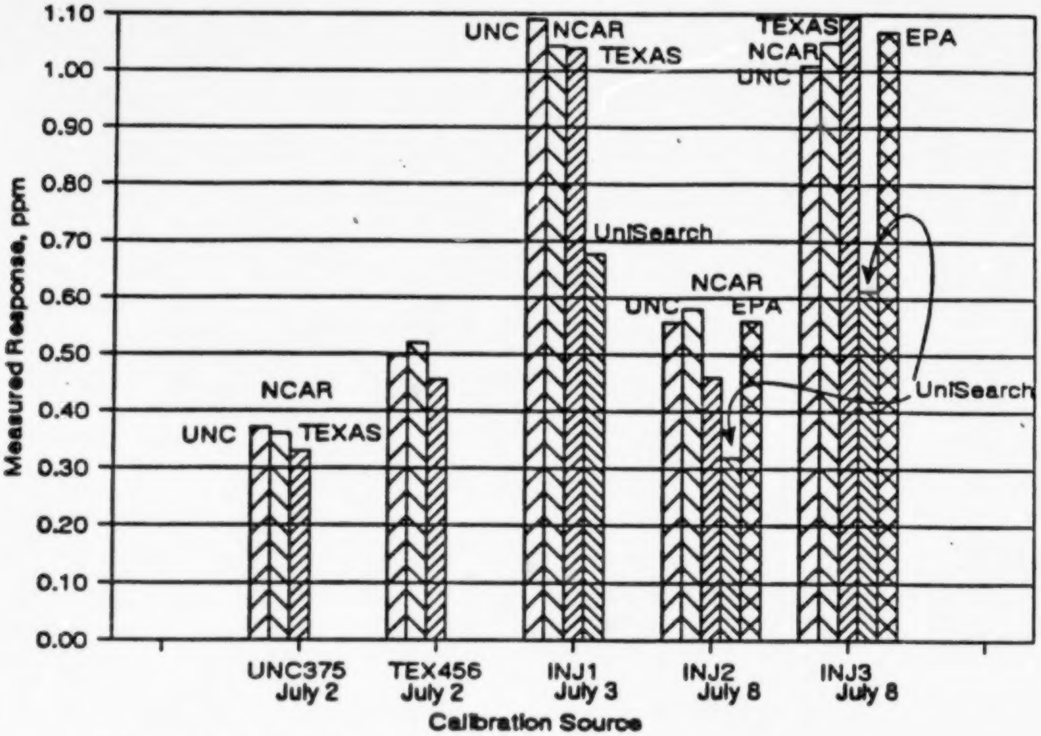

Figure 107. July 2 intercomparison of calibration sources.

data; the agreement is quite good, suggesting that only a difference in values assigned to calibration sources was responsible for the difference in Unisearch data and other groups.

Near the end of the program a special experiment coupled with a simultaneous calibration source intercomparison was designed so as to make as many measurements under different conditions on the same day and, at the same time to include measurements of all the calibration sources by all groups. These tests were conducted on July 16, 1986. Unfortuately, Unisearch had to leave the UNC site before the experiment could be conducted and there is no Unisearch data in the second intercomparison.

July 16 Measurements of the Calibration Sources

The purpose of this test was, first, for each group to measure four calibration sources:

- the UNC permeation tube set to produce 375 ppb HCHO,
- the Texas membrane source at its high dilution setting to produce 456 ppb,
- the Texas membrane source at its low dilution setting to produce 792 ppb, and
- the injection of 197 mg of paraformaldehyde (> 95% purity) into the 150,000 liter chamber at 0600 EDT to produce 1015 ppb.

Secondly, all groups were sampling a side-by-side HCHO and NO_x vs. ethylene and NO_x irradiation experiment. One side of this experiment would have 1000 ppb HCHO initially, which would decay toward zero while making about 0.5 ppm O_3, and the other would have 0 ppb HCHO initially and would produce about 500 ppb HCHO and about 1 ppm of O_3. Finally, we decided to make a second injection of about 350 ppb of HCHO into each side near the end of experiment.

Near the end of the experiment, at about 1430 EDT, NCAR, EPA, and UNC sampled both of the Texas calibration sources, and NCAR, EPA, and Texas sampled the UNC permeation tube calibration source. There were some sample flow problems for the EPA method on the high Texas source that resulted in water being drawn into the sample tube; this sample was lost. UNC and NCAR were successful in measuring the Texas source however. The results of the calibration source measurements are shown in Table 47 and are plotted in Figure 109 and Figure 110.

As was true on July 2, in this July 16 comparison UNC, NCAR, and EPA agreed well on all sources. Also, as on July 2, Texas read the UNC permeation tube lower than everyone else and, of course, calibrated on their 456 ppb source. Recall

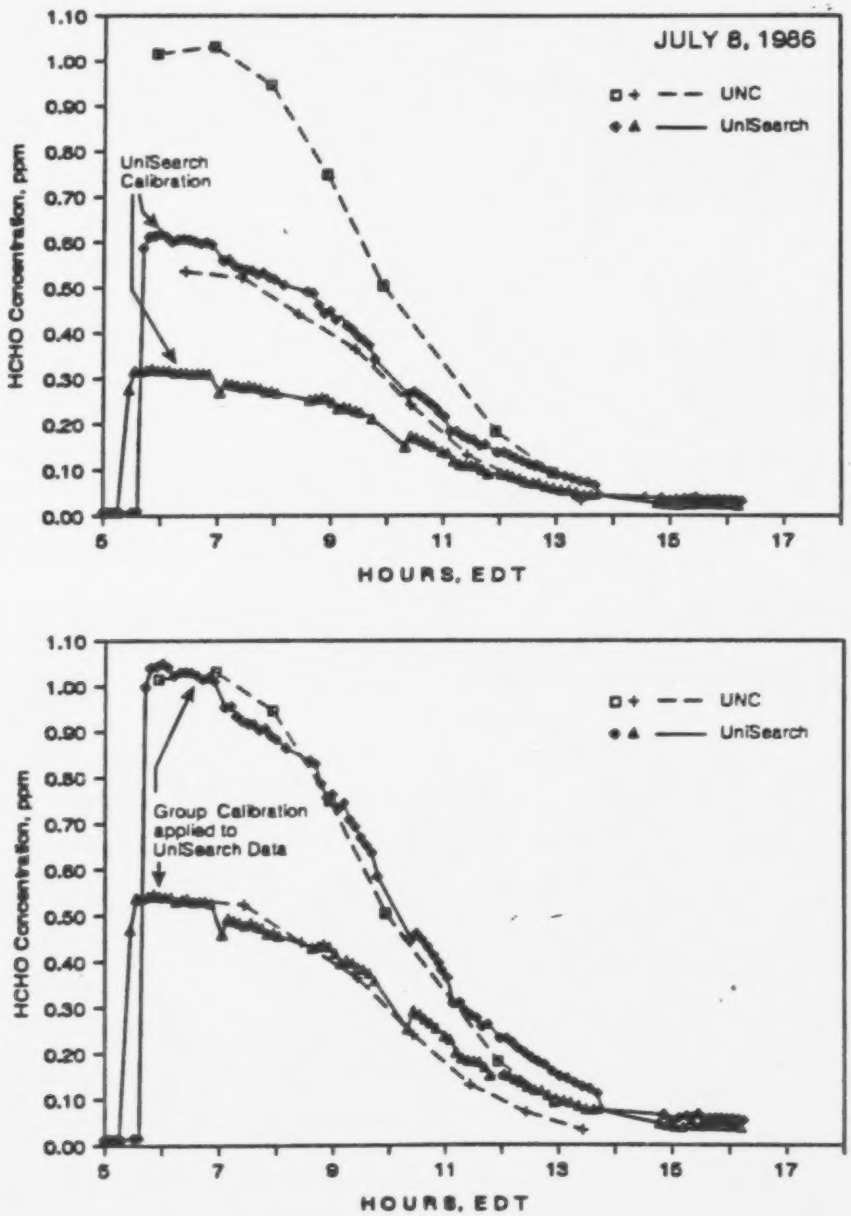

Figure 108. Unisearch calibration and group averaged calibration applied to July 8 HCHO data.

Table 47. July 16 Multi-Group Measurements of Four Calibration Sources.

(units are ppb HCHO)

	Source			
Group	UNC375	Tex456	Tex800	UNC1000
UNC	375	576	861	1025
NCAR	340	600	885	1025
EPA	375	608	NA	1009
TEXAS	280	456	792	1004
Mean 1,2,3	363	595	873	1020

that the NCAR values were based upon their own HCHO stock solution brought from NCAR and subjected to multiple determinations during the study period, that the EPA values were based upon weighted amounts of pure hydrazone derivatives, and the UNC values were based upon a certified permeation tube at a constant temperature and weighted injections into the chamber. It is very unlikely that three independently calibrated methods could agree so close and yet each be wrong.

UNC, NCAR, and EPA all say that the Texas 456 ppb source was most likely 595 ppb, which was 80 ppb higher than NCAR and UNC reported it on July 2. If it is true that the Texas source increased its output by 80 ppb, but Texas still called it 456 ppb, then Texas would have read the UNC permeation tube lower on July 16 than on July 2 by a factor of 0.85 which is what occurred. If the July 16 Texas reading of UNC's permeation tube is corrected by the inverse of this factor, the result is 329 ppb, in good agreement with the 330 ppb value reported by Texas on July 2, strongly suggesting that the Texas membrane calibration source *did* increase its output between July 2 and July 16. In addition, the Texas source was only standardized at Texas three weeks before use at UNC and was not re-standardized during the study. If the mean values of the NCAR, EPA, and UNC measurements are accepted as estimating the values for these four sources, then, as shown in Figure 110, these three methods would show a reasonably linear response, while the Texas method would *appear* to exhibit a non-linear response, being too low in the middle range of HCHO concentrations. What is not clear is why the Texas data agree with the other measurements at 1000 ppb.

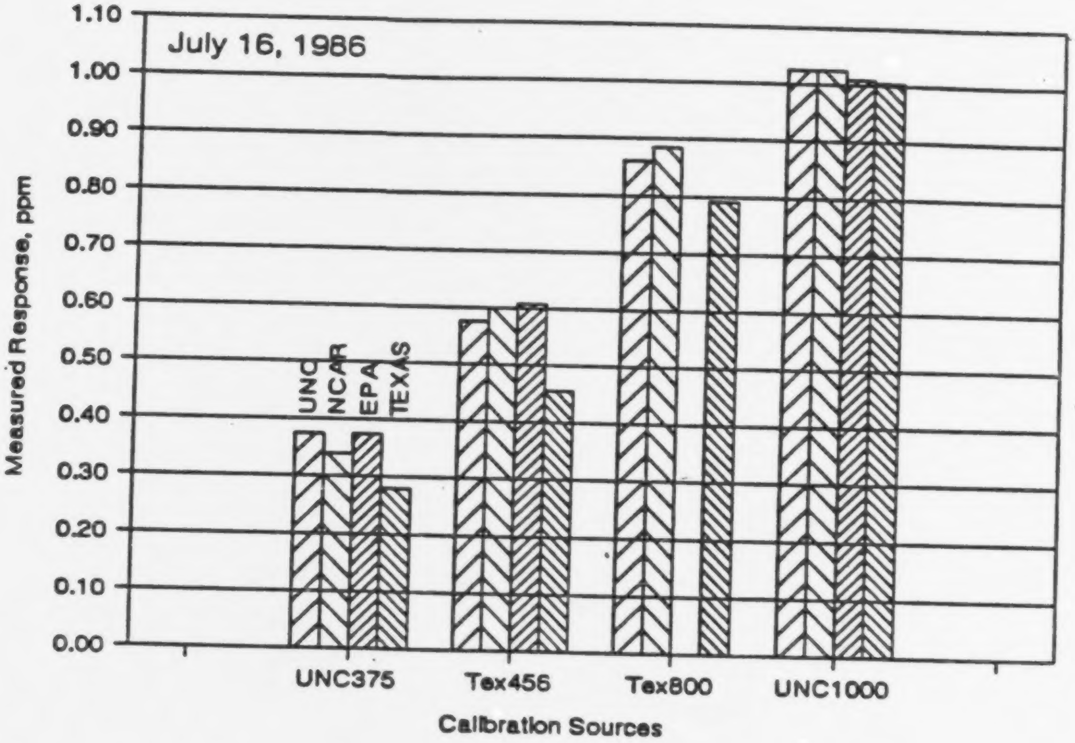

Figure 109. Measurements of Four Calibration Sources

In another program,[48] UNC has build both a Dasgupta diffusion scrubber HCHO instrument and a membrane-based calibration source nearly identical to the one used by Texas at UNC during this study. Our recent tests of this equipment show that the diffusion scrubber instrument is essentially linear in its response up to 1000 ppb when 10-minute sample, zero, and span intervals were used. When operated in the 1986 intercomparison study by Texas, however, much shorter intervals were used. At the high concentrations of the chamber injections, the instrument may not have reached its full response to the high HCHO before switching occurred to the zero source. Thus high concentration samples may not have been comparable to the lower concentration standards and this short sample time might have led to an apparently non-linear response curve.

In the recent UNC tests the membrane-based calibration source was very sensitive to minor pressure changes on its supply and vent lines. For example, if a 3 meter long, 6-mm diameter vent line was used instead of a 50-cm line, the HCHO output changed by more than 20%. In addition if the the air supply was from the clean air generator, then any other use of air from the generator resulted in a shift in calibrator output. The membrane system must have its own tank air supply. Thus we believe that the Texas membrane calibration source shifted its output between the time it was calibrated in Texas using bubblers at 456 ppb and the time it was first used at UNC to produce a value near 500 ppb. This lead to Texas reading the UNC permeation source too low by 456/500, and with correction, Texas would have reported the UNC permeation tube to be $(500/456) \times 330 = 367$ in good agreement (-2%) with UNC and EPA. In addition, the generator was changed from the clean air generator to tanked air during the first week and apparently this resulted in an additional shift in output by 80 ppb to result in an output near 600 ppb for the Texas calibration source. During this whole period and for all of the data processing, Texas used the pre-study value of 456 ppb for this source.

In the rest of this chapter, we will assume that the original assigned values for the Texas sources were incorrect. This assumption means that to meaningfully compare experimental data, the Texas data must be corrected by a non-linear correction curve. Dasgupta's report[42] did not discuss the intercomparison of calibration systems and the data were produced assuming a linear relationship between instrument response and HCHO. A correction curve to account for the apparent non-linear response was obtained by least squares fit to the Texas calibration data and the function is given in Table 48. *All Texas data shown in the rest of this chapter have been corrected by the formula given in Table 48.*

Table 48. Non-linear Correction Curve for Texas Data.

`T^(\prime) = 1.9 + 1.439 T - 0.00043 T^2`

T is the original reported Texas HCHO concentration in ppb

T' is the corrected Texas HCHO concentration in ppb

Values produced by this formula are:

```
   T       T'
 ----    -----
    0      1.9
   50     72.8
  100    141.5
  150    208.0
  200    272.3
  250    334.5
  300    394.5
  350    452.3
  400    508.0
  450    561.5
  500    612.8
  550    661.9
  600    708.9
  650    753.7
  700    796.3
  750    836.8
  800    875.1
  850    911.2
  900    945.1
  950    976.9
 1000   1006.5
```

The Chamber Experiment

The chamber experiment for July 16, 1986 started with 1000 ppb HCHO on one side of the dual chamber and no initial HCHO on the other side. The second side had 2.00 ppmC of ethylene which produced close to 600 ppb HCHO during the irradiation. Both sides had ca. 0.35 ppm NO_x. This resulted in different time of production and formation rates for ozone. When most of the initial HCHO had been consumed and when the ethylene side had reached a maximum value for HCHO produced, the same amount of additional HCHO was injected into both sides at almost the same time.

Thus, in this experiment, HCHO was decreasing while O_3 was increasing, and at the same time HCHO was increasing while O_3 and other products were increasing, and equal amounts of HCHO were injected into systems with different existing levels of HCHO and different levels of potential interfering compounds.

Figure 111 shows the NO, NO_2, O_3 and ethylene profiles for both sides. There was partial cloud cover at different times throughout the day and this was reflected in the non-smooth profiles, especially for the morning NO on the HCHO side and for the afternoon O_3 on the ethylene side. Figure 112 shows, in the top plot, the HCHO profiles for both sides and includes UNC, NCAR, and Texas data; the Texas data have been corrected by the formula in Table HCHO. The bottom plot of Figure 112 shows the HCHO profiles for UNC and EPA only. Table 49 reports the values for all groups at critical times in the experiment. These table values are plotted in bar-graph form in Figure 113.

From the HCHO plot, Figure 112, we can see that all methods agreed before sunrise and until about 1000 EDT, that is, at both high and low values of HCHO. After 1000 EDT, however, the EPA values fall below the group values in the plot. A close examination of Figure 111 shows that the disagreement between the EPA data and the other data is correlated with the rise in O_3 on the two sides. It will become very evident in other data plots that the EPA method showed very good agreement with the others as long as the O_3 levels were below 200 ppb. High values of O_3 cause a sever depression in the EPA response. Subsequent tests conducted by Arnts[49] showed that even O_3 levels of 100 ppb could cause up to a 5% depression in HCHO values; higher levels of O_3 resulted in as much as 80% loss of the HCHO values. The effect is apparently a direct attack on the DNPH.

If the EPA data are rejected after 1000 EDT, when O_3 increases, then the other measurements are seen to cluster fairly tightly on both sides of the chamber, the worst agreement being at the end of the HCHO decay at about 100 ppb (the methods report 143, 107, 110 ppb). The deviation for the fresh HCHO injection on the HCHO

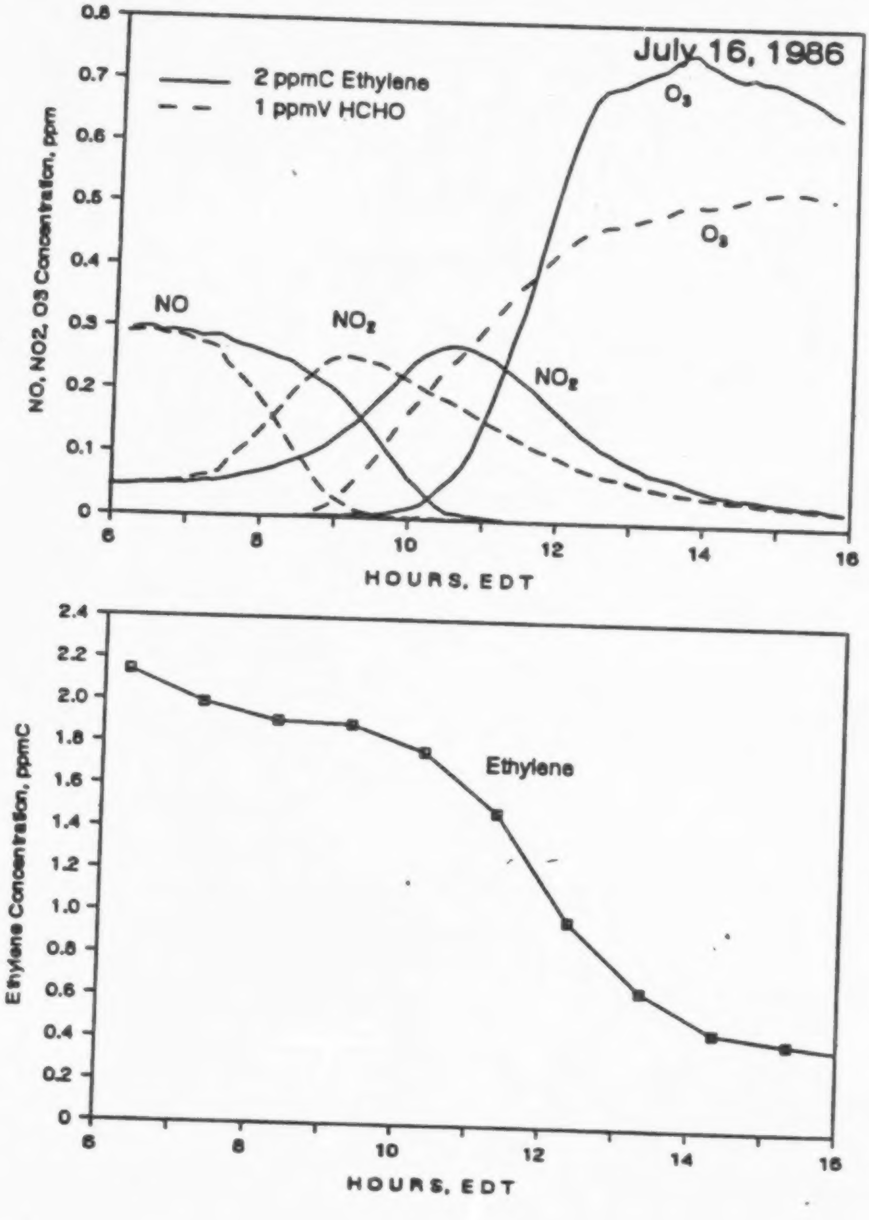

Figure 111. NO$_x$, O$_3$, and Ethylene Profiles For Dual Experiment.

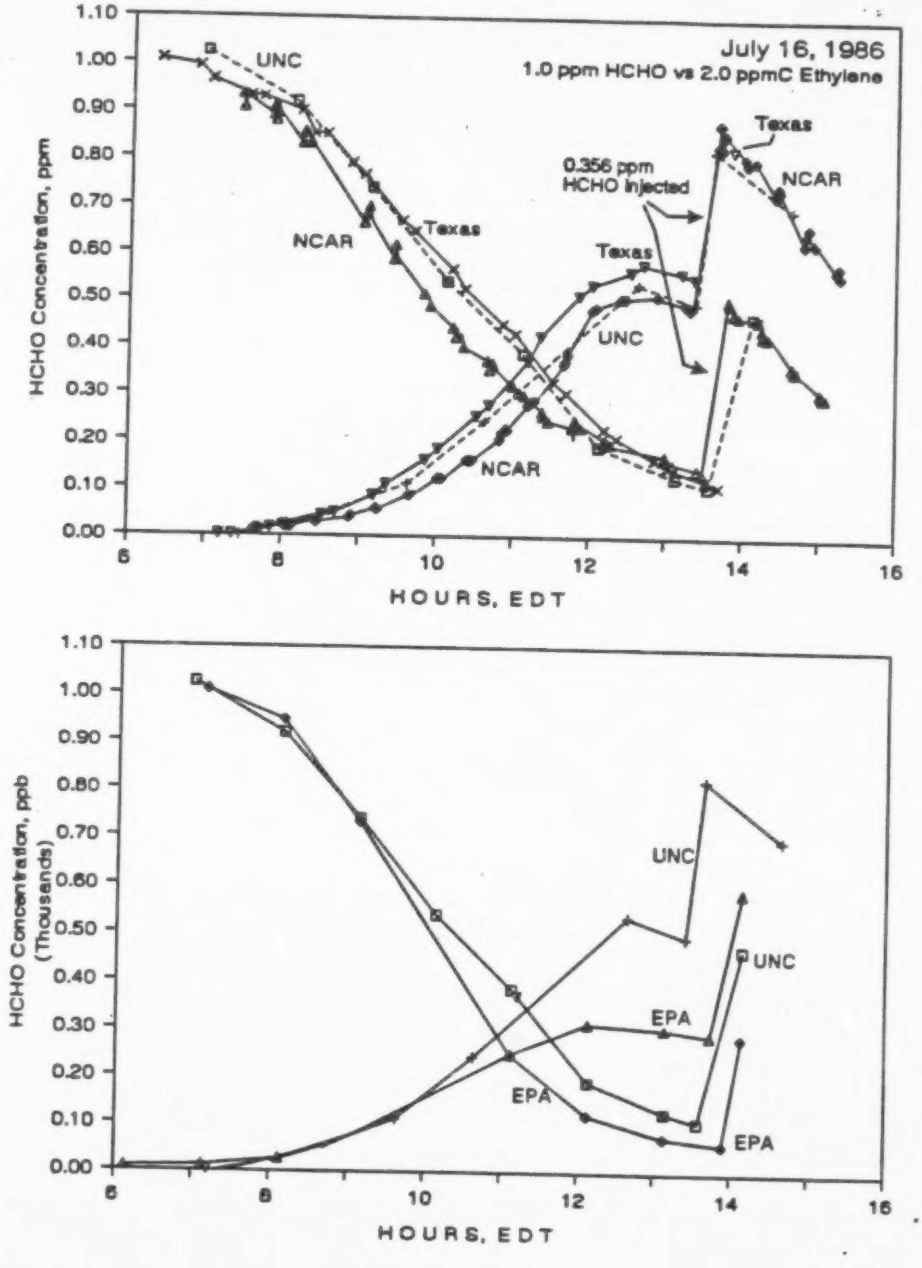

Figure 112. Formaldehyde Profiles For Dual Experiment.

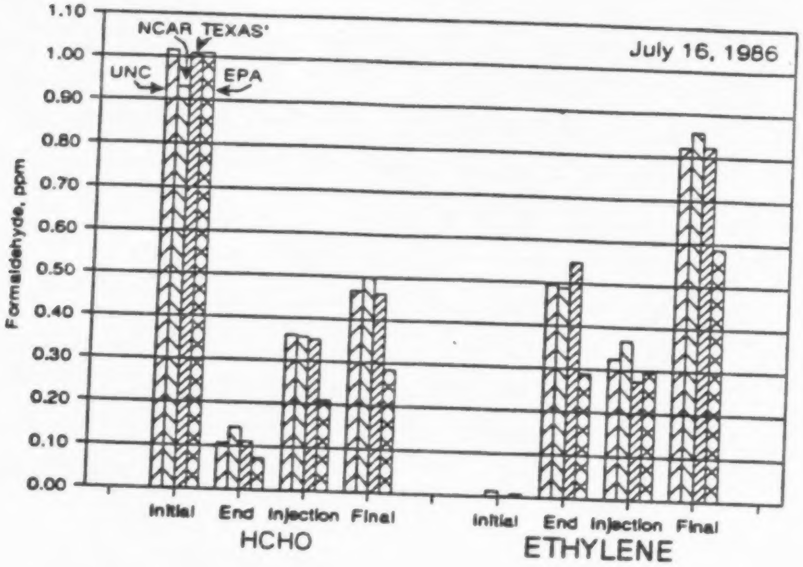

Figure 113. Measurements at key events in July 16 dual experiment.

Table 49.. HCHO Measurements in July 16 Dual Experiment.
(Units are ppb HCHO)

	HCHO				ETHYLENE			
Group	Init	End	Inj	Final	Init	End	Inj	Final
UNC	1015	107	361	468	0	495	326	821
NCAR	930	143	357	500	13	488	369	857
TEXAS'	1009	110	351	461	2	550	274	824
EPA	1010	73	211	284	7	290	297	587
Mean 1,2,3	991	120	356	476	5	511	323	834
Std Dev	40	20	5	21	7	34	47	20
% Std Dev	4	17	1	4	-	7	15	2

side was only 1%, but was 15% on the ethylene side. The latter higher deviation was cause by Texas reporting a higher ending value than either UNC or NCAR before the injection, but reporting a final value within 2% of UNC and NCAR values. While the Texas method may have had mid-scale calibration problems not fully corrected by the non-linear correction curve, the results are still very close. They strongly suggest that none of the three (UNC, NCAR, or Texas) methods were subject to major interference problems for this chemical system because the ozone was at different levels, the HCHO was at different levels, and the ethylene side, which had 0.6 ppmC of ethylene left, was still very active photochemically.

Formaldehyde Data for Other Experiments

The chamber data for July 8, 1986, a 0.5 vs. 1.0 ppm HCHO experiment were shown in Chapter 4. Figure 114 shows four sets of HCHO profiles for this experiment. In producing these plots, the Texas data have been corrected by the non-linear correction given in Table 48, the NCAR data used the slightly adjusted calibration curve shown in Figure 106, and the Unisearch data used the group average data from Table 46 as shown in Figure 108.

The chamber data for July 9, 1986, a 2.0 vs. 1.0 ppmC ethylene experiment were shown in Chapter 4. Figure 115 shows, in the bottom plot, the UNC, Texas, and Unisearch HCHO data for both sides, and in the top plot, the UNC, Texas, and NCAR HCHO data for both sides. Figure 116 shows the UNC, Texas, and EPA data. Here we see that, while there is little O_3, the EPA data are actually a little higher than the UNC data, but as the O_3 increases the EPA data increasingly falls below both the UNC and the Texas data.

Figure 117 shows HCHO data for another 2.0 ppmC ethylene experiment on one side, but a 1.0 ppmC propylene experiment on the other. In this case we have NCAR profile data also. There is more scatter among the methods on this day. This is another example EPA data initially agreeing, in the absence of O_3, but falling below other methods as the O_3 increases. Contrasting the remaining data with those of July 9, it appears that UNC is reading too high on the ethylene side beginning about 1200 EDT. However, this may have been a zero drift problem as the UNC data converge with the NCAR data later in the day. The zero-baseline was determined by linear extrapolation between the morning zero and the evening zero. As the data are closer to one or the other of these, the agreement improves. On this day, Texas also had both an morning and afternoon calibration which may have resulted in a difference in agreement after 1200 EDT. Somewhat surprisingly, there is near perfect agreement between the HCHO profiles on the 1.0 ppmC ethylene side of July 9 and the 1.0 ppmC propylene side of July 12 (just a half-hour difference in timing).

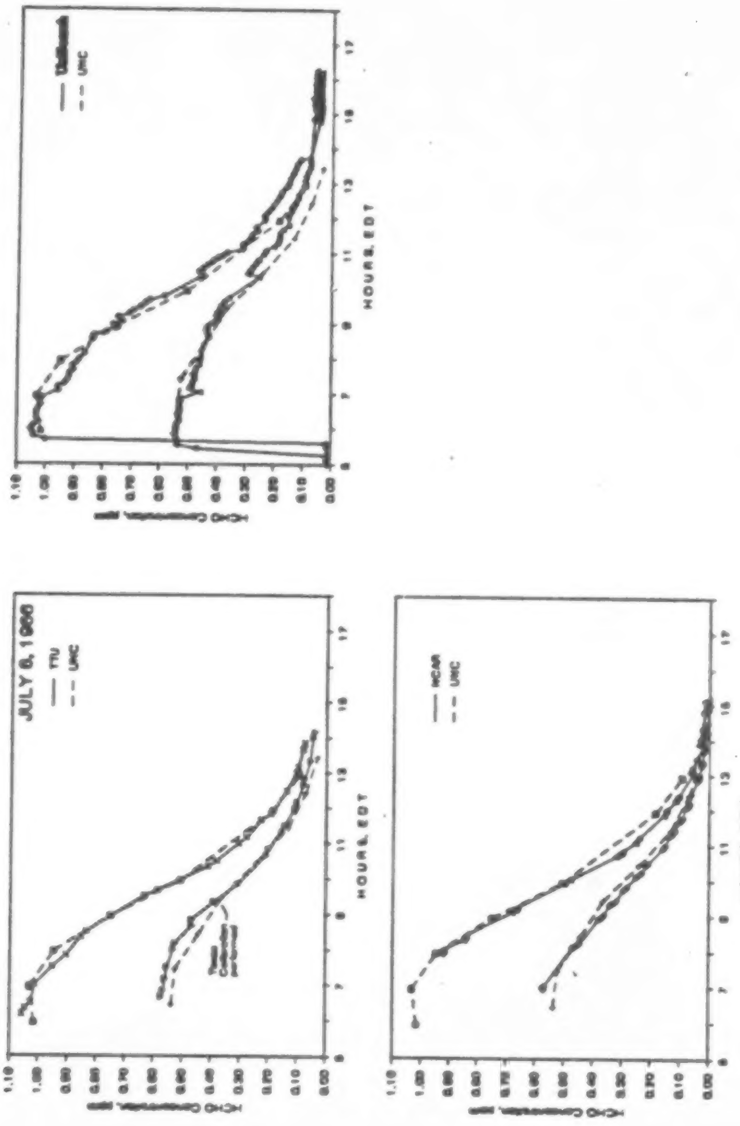

Figure 114. July 8, 1986 Chamber Data.

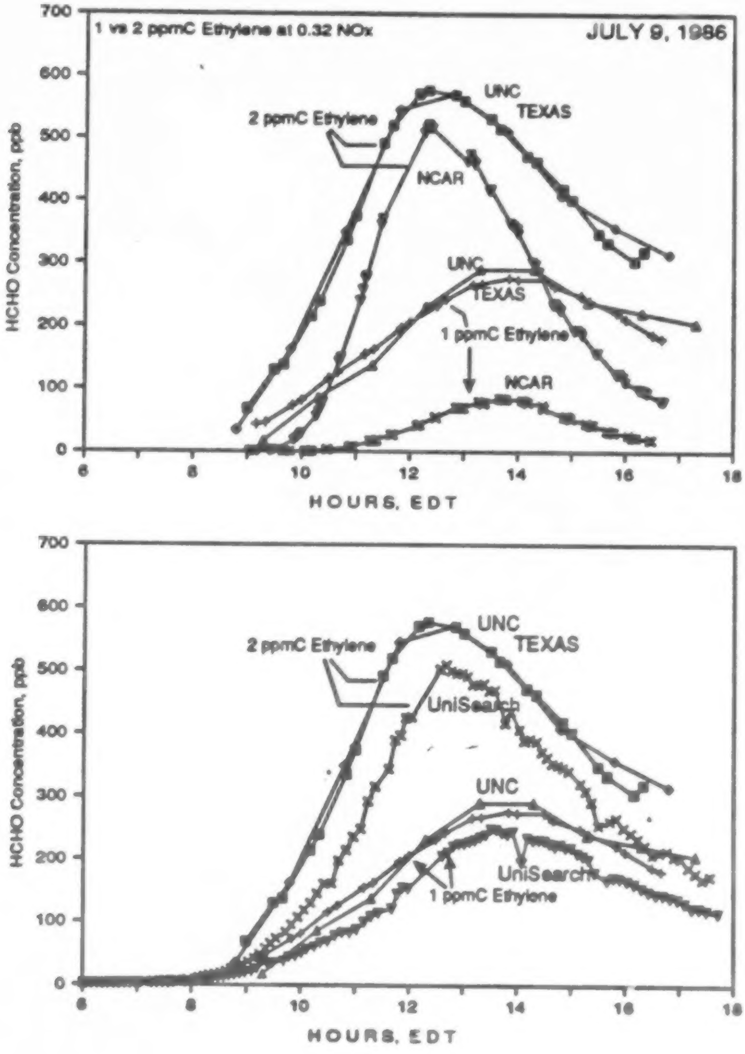

Figure 115. Chamber Data.

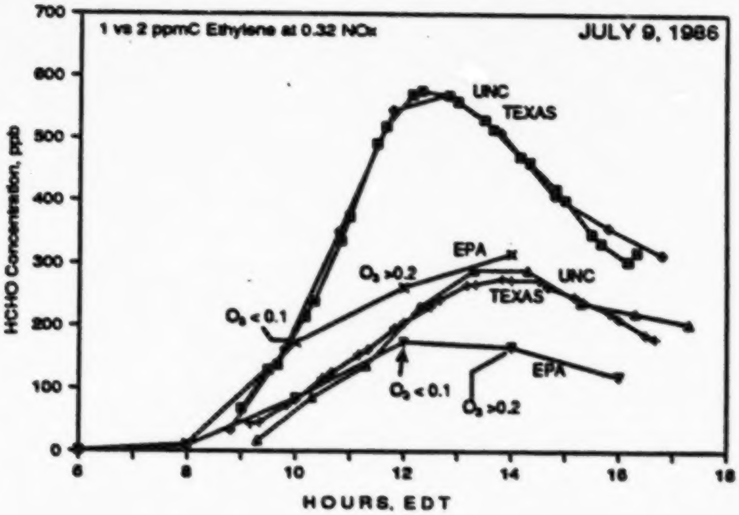

Figure 116. Chamber Data.

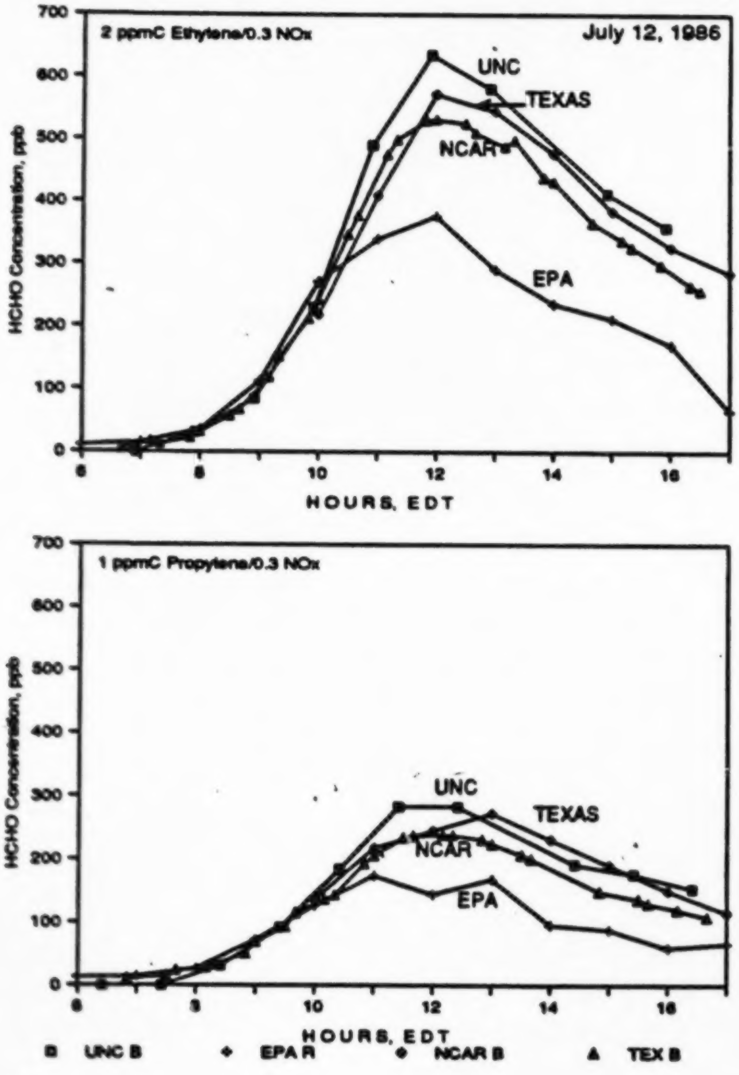

Figure 117. Chamber Data.

Hydrogen Peroxide Tests

While a complete series of experiments were designed to produce H_2O_2 *in situ*, the first experiments were simple injection of H_2O_2 into the chamber in the dark. The first daytime experiments were to be NO_x, H_2O_2, and CO systems. Hydrogen peroxide was injected into the chamber by using an aerosol neublizer to "fog" several cc's of 50% H_2O_2 solution inside the chamber at a height of 2.5 meters.

In an experiment conducted on the afternoon of June 27, a matched injection of H_2O_2 was used. After seeing a rapid decay, we injected CO in one side to see if we could slow the decay. Instead of slowing down, the loss rate increased; there was confusion, however, as to which side of the chamber was being sampled by which H_2O_2 instrument at which time. Another experiment was planned for June 28.

The June 28, 1986 H_2O_2 injection occurred at 0400 EDT and achieved about 300 ppb H_2O_2. Again 345 ppm CO was added to the RED side and background CO of 0.3 ppm was left in the BLUE side. Figure 118 shows the H_2O_2 profile measured in the UNC chamber by UniSearch's laser system (top plot) and by NCAR's wet chemical method (bottom plot). NCAR reported that the first peak was 265 ppb, while the UniSearch laser system measured 345 ppb. The two instruments systems tracked the H_2O_2 with high percision. The curves would exactly overlay each other, except for the difference in calibration.

Figure 119 shows the UniSearch data and the UNC CO and CFC dilution tracer profiles for this 8 hour experiment. The half-life for H_2O_2 in the UNC chamber was short being about 1 hour in the dark. Sunrise was 0602 EDT. Just before sunrise, we injected more H_2O_2 to raise the level back to 300 ppb. In the sunlight, the H_2O_2 loss rate was very large, especially in the chamber with high CO. The addition of CO, at a level of 350 ppm, should increase the half-life by recycling $HO^{\cdot}$ back to $HO_2^{\cdot}$ (in the absence of NO, these should mostly react to make H_2O_2). Most confusing of all, during the accelerated decay of the 350 ppb H_2O_2, there was a loss of 55 ppm CO, while the CFC tracer showed less than a 2% loss. In Figure 119 that when the H_2O_2 was depleted about 0900 EDT, the large rate of decay of CO stopped, but when a new injection was added at 1100 the CO loss became large again. This process was repeatable in the large UNC chamber on several days, but could not be duplicated in new FEP Teflon bags filled with dry, clean air from a generator; adding water to the bags such that there were visible drops did cause a rapid loss of H_2O_2.

Similarly, during experiments designed to produce large quantities of H_2O_2 from chemical reactions of VOC and NO_x, only 4-10 ppb were ever observed. The assumption is that the in-situ produced H_2O_2 also decays rapidly, and therefore a high level never builds up in the chamber.

Speculation as to the mechanism of H_2O_2 loss in the UNC chamber includes: direct absorption on the walls (which did not happen in the much smaller TFE bags); absorption into a thin water film on the walls, this film being maintained by the nitric acid and HCHO and particulate matter absorbed on the well-aged chamber walls (the new bags did not have this material); a catalytic processes involving the absorbed nitrogen species, CO, and H_2O_2 that rapidly consumes H_2O_2 and, by a chain process, CO.

The basic conclusion to be reached from these results is that the chamber walls in the UNC chamber are sufficiently reactive towards H_2O_2 that it is not possible to produce data to test mechanism pathways for making H_2O_2. Based upon the nitric acid data reported by the UniSearch laser system, nitric acid also is probably lost almost as rapidly to the walls.

Further research will be required to determine the mechanism of the loss process and to decide if it is possible to design any chamber operating at near ambient conditions for the testing of H_2O_2 production.

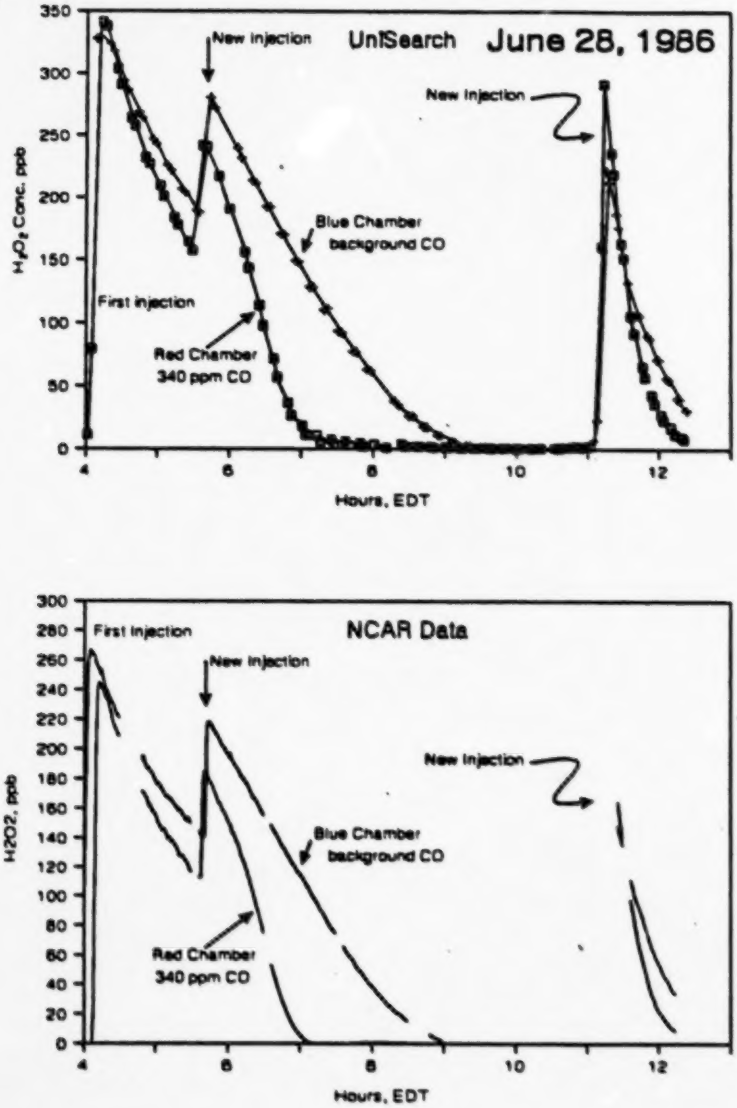

Figure 118. Hydrogen Peroxide Chamber Data.

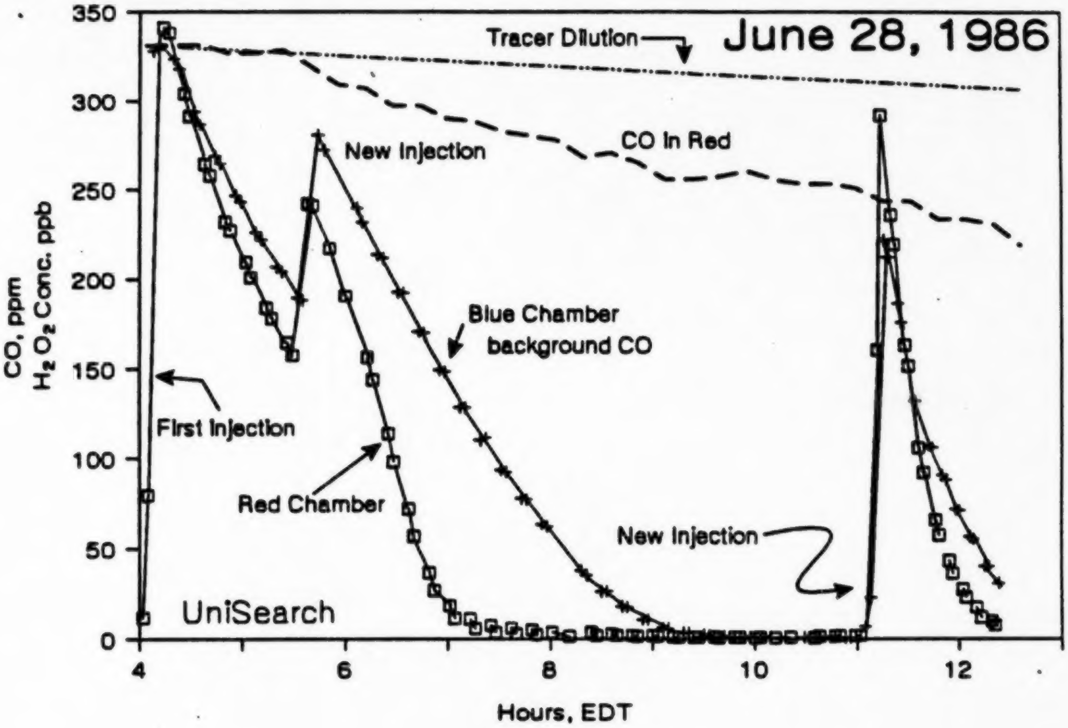

Figure 119. Hydrogen Peroxide Chamber Data.

References

1 Freas W.P., Martinez E.L., Meyer E.L., Possiel N.C., Sennet, D.H., Summerhays J.E., "Procedures for Quantifying Relationships Between Photochemical Oxidants and Precursors:Supporting Documentation," EPA-450/2-77-021b, U.S.M Environmental Protection Agency, Research Triangle Park, North Carolina, 1978.

2 Whitten and Gery."Development of CBM-X Mechanism for Urban and Regional AQSMs" EPA/600/3-86/012, U.S. Environmental Protection Agency, Research Triangle Park, North Carolina, 1986.

3 H. Hogo, M.W. Gery, "Guidelines for Using OZIPM-4 with CBM-IV or Optional Mechanism," EPA/600/8-88/082, U.S. Environmental Protection Agency, Research Triangle Park, North Carolina, 1988.

4 Gery, M.W.,G.Z. Whitten, J.P. Killus, "Development and Testing of the CBM-IV for Urban and Regional Modeling," EPA-600/3-88-012, U.S. Environmental Protection Agency, Research Triangle Park, North Carolina, 1988.

5 Atkinson, R., A.C. Lloyd, L. Winges, "An Updated Chemical Mechanism for Hydrocarbon/Nitrogen Oxides Photoxidations Suitable for Inclusion in Atmospheric Simulation Models, *Atmos. Envir.* **16**, 1341–1345, 1982.

6 W.P. Carter, F.W. Lurmann, R. Atkinson, and A. Lloyd, "Development and Testing of a Surrogate Species Chemical Reaction Mechanism,", EPA/600/3-86/031, U.S. Environmental Protection Agency, Research Triangle Park, NC, 1986.

7 Lurmann, F.W., W.P. Carter, L.A. Coyner, "A Surrogate Species Chemical Reaction Mechanism for Urban Scale Air Quality Simulation Models: Vol I: Adaptation of the Mechanism.", EPA-600/3-87-014a,b, U.S. Environmental Protection Agency, Research Triangle Park, North Carolina, 1987.

8 Carter W.P.L. and Atkinson R. "Evaluation of a Surrogate Species Chemical Reaction Mechanism For Use in Atmospheric Simulation Models," Monthly Technical Report, August 1985, EPA Contract 68-02-4104.

9 Baugues, K., "A Review of NMOC, NO_x, and NMOC/NO_x Ratios Measured in 1984 and 1985," EPA-450/4-86-015, U.S. Environmental Protection Agency, Research Triangle Park, North Carolina, 1986.

10 Lonneman, W.A., "Comparison of 0600-0900 AM Hydrocarbon Compositions Obtained from 29 Cities," Proceedings APCA/US EPA Symposium on Measurements of Toxic Air Pollutants, Raleigh, NC, 1986.

11 Chang *et al.*, NCAR Acid Deposition Modeling Project, Progress report project IAG DW930144-01-2, Project officer John Clarke, U.S. Environmental Protection Agency, Research Triangle Park, North Carolina, 1985."

12 Peterson, J.T., "Calculated Actinic Fluxes for Air Pollution Photochemistry Applications," EPA-600/4-76-002, U.S. Environmental Protection Agency, Research Triangle Park, North

Carolina, 1976.

13 Carter, W.P. personal communication to H.E. Jeffries, August, 1988.

14 Atkinson, R, H.E. Jeffries, G.Z. Whitten, F.W. Lurmann, "Workshop On Evaluation/Documentation of CHemical Mechanisms," EPA/600/9-87-024, U.S. Environmental Protection Agency, Research Triangle Park, North Carolina, 1097.

15 Pua, K.E., H.E. Jeffries, "A Network Testing Strategy for Chemical Mechanisms Used in the EKMA Method,", Paper 11-7, APCA Speciality Conference, Hartford CO, 1988.

16 Lurmann, F., diskette copy of 20-NOV-86 version of Carter, Atkinson, Lurmann mechanism, 1986.

17 Lurmann, F., letter to Marcia Dodge, copy to H. Jeffries, November, 26, 1986.

18 Gery, M., diskette copy of Oct-1987 version of Carbon Bond Four point Two mechanism, 1987.

19 Demore, *et al.*, "Chemical Kinetics and Photochemical Data for Use in Stratospheric Modeling, Evaluation Number 7, JPL Publ. 85-37, 1985.

20 Atkinson, R, and A. Lloyd, "Kinetics and Mechanistic Data for Modeling of Photochemical Smog", *J. Phys. Chem. Ref Data* **13**(2), 315–444, 1984.

21 Atkinson, R., "Kinetics and Mechanisms of the Gas Phase Reactions of the Hydroxyl Radical with Organic Compounds under Atmospheric Pressure," *Chem. Rev.*85, 69–201, 1985.

22 Atkinson, R, W.P. Carter, "Kinetics and Mechanisms of the Gas-Phase Reactions of Ozone with Organic Compounds under Atmospheric Conditions," *Chem. Rev.* **84**, 437–470, 1984.

23 Baulch *et al.*, "Evaluated Kinetics and Photochemical Data For Atmospheric Chemistry", *J. Phys. Chem. Ref. Data*, **9**, 295–379, 1980.

24 Baulch *et al.*, "Evaluated Kinetics and Photochemical Data For Atmospheric Chemistry", *J. Phys. Chem. Ref. Data*, **13**, 1259–1379, 1984.

25 Su *et al.*, *J. Phys. Chem.* **83**, 3185, 1979

26 Vegret, *et al.J. Phys. Chem.* **86** 3424, 1982

27 Barnes *et al.,Chem. Phys. Lett.* **83**,459, 1985

28 Lurmann, F., letter to Marcia Dodge, copy to H.M Jeffries, November 26, 1986.

29 Whitten, G.Z., J.P. Killus, R.G. Johnson, "Modeling of Auto Exhaust Smog Chamber Data For EKMA Development,", EPA-600/3-85-025, 1985

30 G. Gipson, the SIP conditions were supplied by personal communication from Gipson, OAQPS, EPA, Durham NC, to Jeffries in 1985.

31 Jeffries, H.E., K.G. Sexton, "Technical Discussion Related to the Choice of Photolytic Rates for Carbon Bond Mechanisms in OZIPM4/EKMA," EPA-450/4-87-003, U.S. Environmental Protection Agency, Research Triangle Park, North Carolina, 1987.

32 Gery, M.G., "Tropospheric Ultraviolet Radiation, Assessment of Existing Data and Effects on Ozone Formation," EPA/600/3-87/047, 1987.

33 Dodge, M. Memorandum to Keith Baugues, OAQPS,"Effect of Temperature on EKMA control Predictions," April 14, 1988.

34 Dodge, M., letter to H.Jeffries, August 31, 1988

35 Jeffries, H.E., K.G. Sexton, C.N. Salmi, "Effects of Chemistry and Meteorology on Ozone Control Calculations Using a Simple Trajectory Models and the EKMA Procedure," EPA-450/4-81-034, U.S. Environmental Protection Agency, Research Triangle Park, North Carolina, 1981.

36 Weil, J.C., "Updating Applied Diffusion Models,", *J. Climate and Appl. Metero.*, **24**, 1111-1130, 1985.

37 Evans, R. "The Contribution of Ozone Aloft to Surface Ozone Maxima," Ph.D. Thesis, University of North Carolina, Chapel Hill, NC, p 73, 1979.

38 West P.W. G.C. Gaeke, *Anal. Chem.* **28** p 1916, 1956.

39 Lyles, G.R., F.B. Dowling, V.T. Blachard, *JAPCA*20 p 106, 1965.

40 Lazrus, A.L., K. Fong, J.A. Lind, "Automated fluorometric Procedure for Formaldehyde in Air," *Anal. Chem.* **59**, 1987.

41 Lind, J.A., G.L. Kok, B.G. Heikes, J.G. Walega, A.L. Lazrus, "H_2O_2 and HCHO Measurements in the Interlaboratory Intercomparison Study," Final Report submitted to Northrop Services, June 4, 1987.

42 P.K. Dasgupta, "An Intercomparison Study of Gaseous Hydrogen Peroxide and Formaldehyde Measurements," Final Report to Northrop Services, Inc. Research Triangle Park, NC, 1986.

43 Hwang, H., P.K. Dasgupta, "Thermodynamics of the Hydrogen Peroxide–Water System," *Enviro. Sci. Technol.*19, pp 255–258, 1985.

44 Dong, S., P.K. Dasgupta, "Solubility of Gaseous Formaldehyde in Liquid Water and Generation of Trace Standard Gaseous Formaldehyde," *Environ. Sci. Technol.* **20**, pp 637–640, 1986.

45 Tejada, S.B., "Evaluation of Silica Gel Cartridge Coated *In Situ* with Acidified 2,4-Dinitrophenylhydrazine for Sampling Aldehydes and Ketones in Air," 167–185, 1986.

46 Dong, S. personal communication to Jeffries on July 16, 1986 at UNC chamber site.

47 Mackay, G.I., H.I. Schiff,"An Intercomparison Study of Hydrogen Peroxide and Formaldehyde Concentrations: Tunable Diode Laser Absorption Spectrometer Measurements," Final Report

to Northrop Services, February 1987.

48 Jeffries, H.E., "A Chamber and Modeling Study to Assess the Photochemistry of Formaldehyde,", EPA Co-operative Agreement 88888, U.S. Environmental Protection Agency, Research Triangle Park, North Carolina, 1987.

49 R. Arnts, personal communication to H.M Jeffries, 1988.